

Cardiff University

School of Chemistry



**N-FUNCTIONALISED EXPANDED-RING
N-HETEROCYCLIC CARBENES:
SYNTHESIS, STRUCTURE AND CATALYSIS**

by

Abeer A. Binobaid

Submitted in fulfillment of the requirement of degree of

Doctor of Philosophy

School of Chemistry
Cardiff University
Wales, UK

UMI Number: U585351

All rights reserved

INFORMATION TO ALL USERS

The quality of this reproduction is dependent upon the quality of the copy submitted.

In the unlikely event that the author did not send a complete manuscript and there are missing pages, these will be noted. Also, if material had to be removed, a note will indicate the deletion.



UMI U585351

Published by ProQuest LLC 2013. Copyright in the Dissertation held by the Author.
Microform Edition © ProQuest LLC.

All rights reserved. This work is protected against
unauthorized copying under Title 17, United States Code.



ProQuest LLC
789 East Eisenhower Parkway
P.O. Box 1346
Ann Arbor, MI 48106-1346

ACKNOWLEDGEMENTS

First, I would like to thank my supervisor, Professor Kingsley Cavell, for his advice, support and guidance throughout the duration of my PhD, and also Dr. Nancy Dervisi and Dr. Ian Fallis for their help and support.

Special thanks to Dr. Dirk Beetstra for his great ideas and constant help during my three years at the laboratory.

I must also thank Dr. Benson Kariuki for the X-ray structure determinations. I gratefully acknowledge the technical and personal support of all the staff at the department of Chemistry, Cardiff University, especially those working on the NMR machine.

Special thanks go to all my colleagues in Lab. 2.84: Dr. Dave Nielson, Manuel, Tracy, Adrien, Aminue, Emma, Deborah, Mandeep, Gareth, Marcello, Marieke, Mathilde, Sadet, Jay and Wei.

Finally, my eternal gratitude goes to my husband Yasir, for encouraging me to continue my postgraduate studies, and for his patience and support during my PhD.

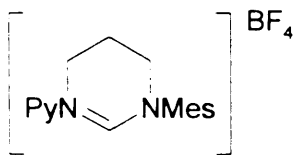
ABBREVIATIONS

acac	Acetylacetonate
Ad	Adamantanone
Ar	Aryl
Atm	Atmosphere
Av	Average
bs	Broad singlet
Bu	Butyl
C _{NHC}	Carbene carbon
COD	1,5-Cyclooctadien
Cy	Cyclohexyl
dbe	Dibenzylideneacetone
DCE	Dichloroethane
DCM	Dichloromethane
DIPP	Diisopropylphenyl
Eq	Equivalent
ES-MS	Electrospray mass spectrometry
Et ₂ O	Diethyl ether
GC-MS	Gas chromatography mass spectrometry
Hz	Hertz
IMes	1,3-bis(2,4,6-trimethylphenyl)imidazol-2-ylidene
ⁱ Pr	<i>iso</i> - propyl
IR	Infrared spectroscopy

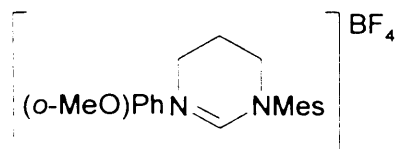
K[HMDS]	Potassium hexamethyldisilazide
Me	Methyl
MeOPh	Methoxyphenyl
Mes	Mesityl (1,3-trimethylphenyl)
MeSPh	2-methyl thio phenyl
nbe	Norbornene
NHC	<i>N</i> -heterocyclic carbene
NMR	Nuclear magnetic resonance
OAc	Acetate anion
ORTEP	Oak-Ridge thermal ellipsoid plot
<i>o</i> -tolyl	<i>ortho</i> -Tolyl group
Ph	Phenyl
R	Alkyl or aryl
^t Bu	<i>Tert</i> -Butyl
THF	Tetrahydrofurane
TMS	Trimethylsilane
TOF	Turnover frequency
TON	Turnover number

New NHC Salts

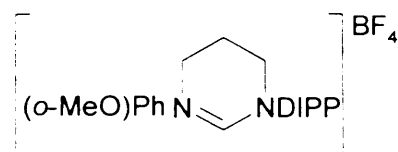
6-Py-Mes



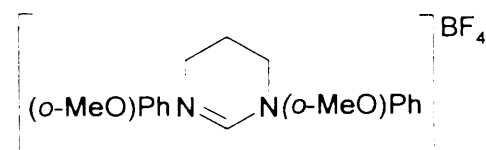
6-*o*-MeOPh-Mes



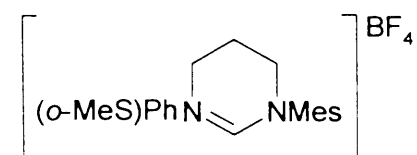
6-*o*-MeOPh-DIPP



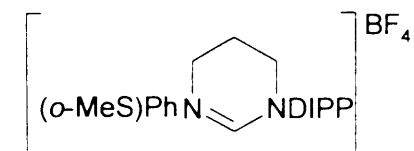
6-*o*-MeOPh



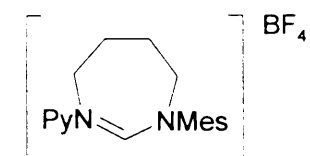
6-*o*-MeSPh-Mes



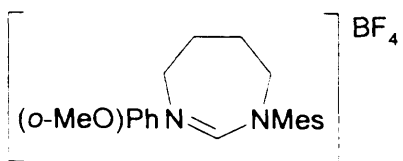
6-*o*-MeSPh-DIPP



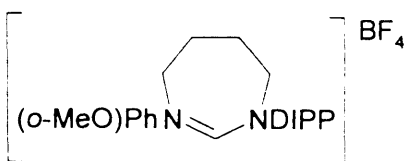
7-Py-Mes



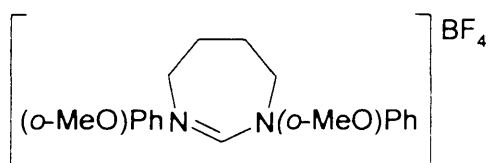
7-*o*-MeOPh-Mes



7-*o*-MeOPh-DIPP

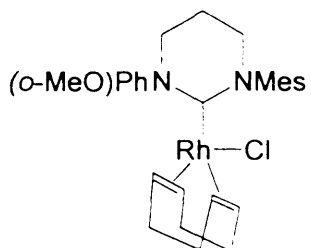


7-*o*-MeOPh

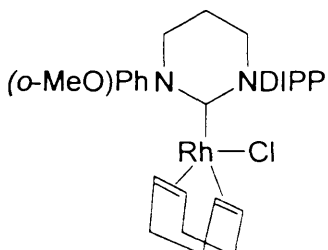


Rh Complexes

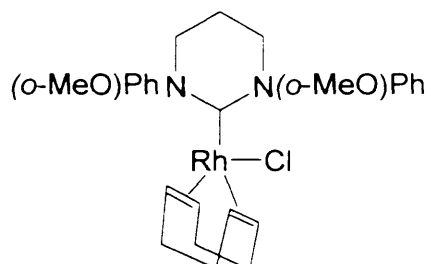
[Rh(6-*o*-MeOPh-Mes)(COD)Cl]



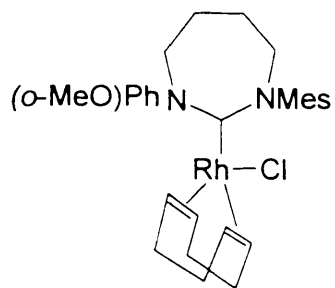
[Rh(6-*o*-MeOPh-DIPP)(COD)Cl]



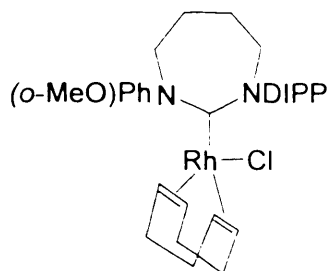
[Rh(6-*o*-MeOPh)(COD)Cl]



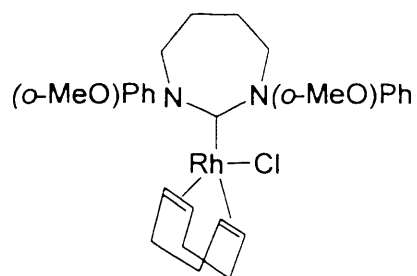
[Rh(7-*o*-MeOPh-Mes)(COD)Cl]



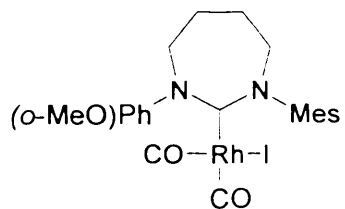
[Rh(7-*o*-MeOPh-DIPP)(COD)Cl]



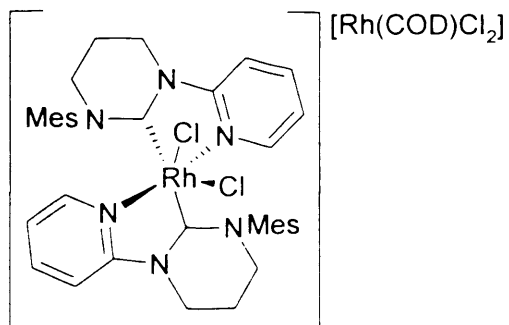
[Rh(7-*o*-MeOPh)(COD)Cl]

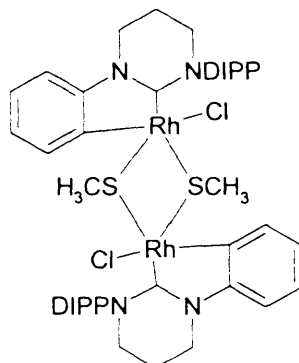
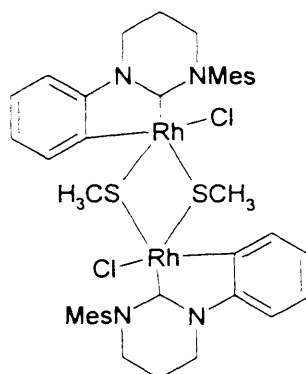


Cis-[Rh(7-*o*MeOPh-Mes)(CO)₂I]

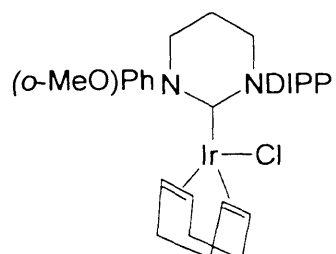
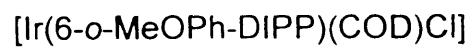
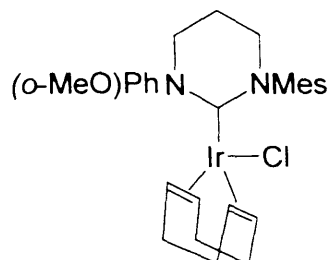
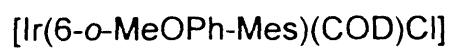


[Rh(6-Py-Mes)₂Cl₂][Rh(COD)Cl₂]

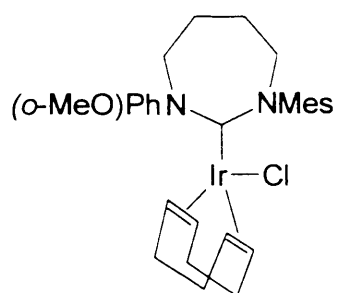




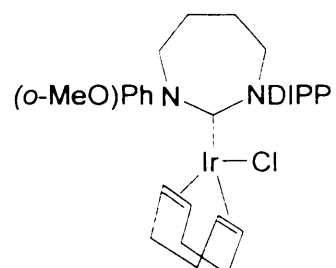
Ir Complexes



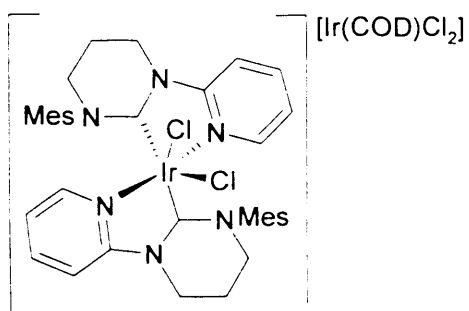
[Ir(7-*o*-MeOPh-Mes)(COD)Cl]



[Ir(7-*o*-MeOPh-DIPP)(COD)Cl]



[Ir(6-Py-Mes)₂Cl₂][Ir(COD)Cl₂]



ABSTRACT

The work presented in this thesis is concerned with the synthesis, metal coordination and applications of expanded (6- and 7-membered) *N*-functionalised heterocyclic carbenes. It is divided into four chapters, which cover the following areas of research.

Chapter One includes the historical and literature review of preparations, reactions, and catalysis applications for different-types of NHC, while in Chapter Two, the syntheses characterisation and solid state properties of new 6- and 7-membered NHC salts (with Mes, DIPP, *o*-MeOPh and *o*-MeSPh *N*-substituents) are discussed. A new method for synthesising saturated NHC salts, using potassium carbonate as a mild base for the deprotonation of the corresponding formamidines reacted with di-electrophiles under aerobic conditions is presented.

Chapter Three describes the syntheses characterisation and solid state structure of rhodium and iridium complexes. Expansion of the ring provides carbenes with $\text{NC}_{\text{NHC}}\text{N}$ angle close to the sp^2 angle (120°), which forces the *N*-substituents to bend closer to the metal center. Furthermore, the expanded carbenes are found to be more basic than their 5-membered analogues. The wide $\text{NC}_{\text{NHC}}\text{N}$ angles and greater donor abilities of the expanded NHC carbenes mean that their catalytic applications are interesting to study.

Chapter Four presents the results of catalytic performance for the 6- and 7-membered NHC rhodium and iridium complexes in olefin hydrogenation reactions with molecular hydrogen. These complexes are also tested as catalysts in the transfer hydrogenation of ketones.

TABLE OF CONTENTS

1. Introduction	2
1.1. Classification of Carbenes	2
1.2. Stable Singlet Carbenes	6
1.3. Methods for the Preparation of Free N-Heterocyclic Carbenes	11
1.4. N-Heterocyclic Carbenes as Ligands	12
1.5. Routes to the Preparation of NHC Complexes	15
1.5.1. In-situ Deprotonation of an Azolium Salt.....	16
1.5.2. Complexes via Free NHCs.....	17
1.5.3. NHC Complexes via Oxidative Addition.....	19
1.5.4. Transmetallation from other NHC-M Complexes.....	20
1.6. Abnormal Carbene Complexes	21
1.7. Six- and Seven-membered NHC Systems	23
1.8. NHC Complexes as Catalysts	25
1.8.1. The Success of NHC Complex Catalysts.....	26
1.8.2. Hydrogenation.....	27
1.8.3. Transfer Hydrogenation.....	28
1.8.4. Catalyst Decomposition.....	29
1.9. Aims and Thesis Overview	30
1.10. References	32
2. Synthesis of New Salt Precursors to Novel Expanded-Ring N-Functionalised Heterocyclic Carbenes	47

2.1. Introduction	44
2.2. Results and Discussion	49
2.2.1. Preparation of Amidine Fragment.....	49
2.2.1.1. Synthesis of New Asymmetrical Formamidines.....	49
2.2.1.2. Synthesis of New Symmetrical Formamidines.....	51
2.2.2. Method of Ring-Closure.....	52
2.2.2.1. Synthesis of Halide Salts.....	52
2.2.2.2. Formation of Tetrafluoroborate salts – Counter- Anion Exchange...	54
2.2.3. Solution NMR Studies.....	56
2.2.4. X-Ray Analysis.....	59
2.2.5. Synthesis of Compounds with Alternative Ring-Closure.....	67
2.3. Experimental	71
2.4. References	98

3. Synthesis of Complexes with Expanded NHCs as

Functionalised Ligands	103
3.1. Introduction	103
3.2. Results and Discussion	107
3.2.1. Attempted Synthesis of Silver (I) Carbene Complexes.....	107
3.2.2. Rhodium (I) and Iridium (I) COD Complexes.....	108
3.2.2.1. Solution NMR Studies of Rh(I) and Ir(I) COD Complexes.....	110
3.2.2.2. Solid State Structures of Rh(I) and Ir(I) COD Complexes.....	112
3.2.3. Rh(I) Biscarbonyl Complex of <i>Cis</i> -[Rh(7- <i>o</i> -MeOPh-Mes)(CO) ₂].....	121

3.2.4. The Reaction of 6-Py-Mes Salt with [M(COD)Cl ₂] (M = Rh or Ir) Unexpected Formation of M(III) Complexes.....	126
3.2.5. Reaction of 6-MeSPh-Mes and 6-MeSPh-DIPP Salts with [Rh(COD)Cl ₂] Unexpected Ar-SMe Cleavage and Synthesis of a Novel Rh(III)NHC Complex.....	132
3.3. Experimental.....	137
3.4. References.....	156
4. Investigation of Catalytic Transfer Hydrogenation and Hydrogenation Reaction Using Expanded Ring NHCs.....	161
4.1. Introduction.....	161
4.2. Results and Discussion.....	165
4.2.1. Catalytic Transfer Hydrogenation of Ketones.....	165
4.2.1.1. Reaction Timescale.....	168
4.2.1.2. Investigation of Catalyst Stability.....	171
4.2.1.3. Temperature Dependence.....	172
4.2.1.4. Catalytic Performance with Different Substrates	173
4.2.2. Catalytic Hydrogenation with Molecular Hydrogen.....	175
4.2.2.1. Reaction Timescale.....	179
4.2.2.2. Catalytic Hydrogenation of Alternative Substrate	182
4.3. Experimental.....	183
4.4. References.....	184
Appendix 1. Publication from this Thesis.....	188
Appendix 2. Table of Bond Distances and Angles.....	189

Chapter One

Introduction

Chapter One

Introduction

1.1. Classification of Carbenes.

Carbenes were first recognized over 100 years ago.^[1] They are “uncharged” compounds featuring a divalent carbon atom with only six electrons in its valence shell.^[2, 3] The carbene carbon is linked to two adjacent groups by a single covalent bond and possesses two, non-bonding electrons^[3] (Figure 1-1).

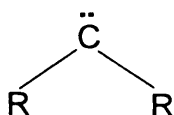


Figure 1-1: A simple carbene.

Because carbenes do not possess an octet of electrons, free carbenes are an electron-deficient and generally highly reactive species. In terms of structure, most free carbenes take on a bent shape to some degree, away from linearity, implying sp^2 -type hybridisation in the carbene carbon with two non-bonding orbitals^[3] (Figure 1-2) .

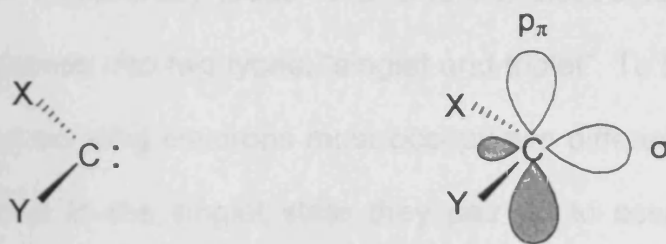


Figure 1- 2: Diagram illustrating the loss in degeneracy of the non-bonding orbitals of free carbenes.

The p_y orbital retains an almost pure p -character with no change and is described as p_π whilst the p_x orbital is stabilised due to the acquisition of some 's' character and is described as σ ^[2, 3](Figure 1-3).

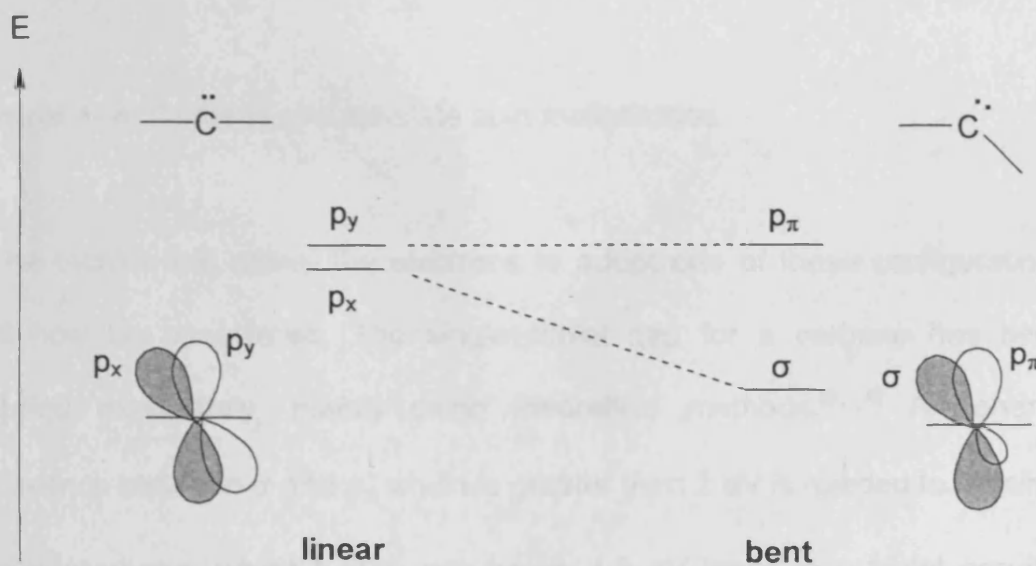
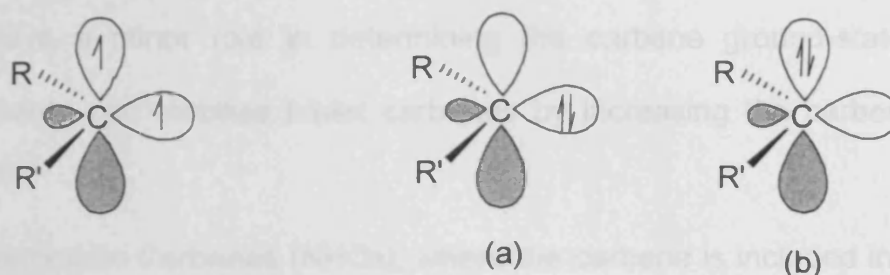


Figure 1-3: Linear and bent carbene geometries and respective energy change.

This break from degeneracy leads to a different electronic configuration which divides carbenes into two types: "singlet and triplet". To form the triplet state, the two non-bonding electrons must occupy two different orbitals with parallel spins, while in the singlet state they pair up to occupy the same orbital with anti-parallel spins (Figure 1-4).^[3, 4]



Triplet

Singlet

Figure 1- 4: Carbene ground-state spin multiplicities.

The factors that cause the electrons to adopt one of these configurations will now be considered. The singlet-triplet gap for a carbene has been studied extensively, mainly using theoretical methods.^[5, 6] An energy difference between σ and p_{π} which is greater than 2 eV is needed to obtain a singlet carbene, whilst a σ - p_{π} gap below 1.5 eV leads to a triplet ground-state.^[7] The substituents surrounding the carbene centre can determine whether a singlet or triplet state is formed through a combination of inductive, mesomeric or steric effects. σ -Electron withdrawing groups (highly electronegative) increase the σ - p_{π} gap by inductively stabilising the σ -

nonbonding orbital through an increase in its 's' character, thus favouring the singlet state since they can stabilise the carbene ion pair.^{[5] [2, 8, 9]} Conversely, σ -electron donating substituents (low electronegativity) will induce a small σ - p_{π} gap and favour the triplet state, whereas most carbenes with π -electron withdrawing groups are predicted to be linear singlet carbenes. The triplet state is favoured by linear molecules. Steric bulk around the carbene centre also plays a minor role in determining the carbene ground-state: bulky substituents can stabilise triplet carbenes by increasing the carbene bond angle.^[8, 9]

N-Heterocyclic Carbenes (NHCs), where the carbene is included in a cyclic structure and where at least one nitrogen atom stabilises the carbene centre, are the most widely studied due to their high stability and excellent performance as ligands for catalytic systems. The stability of these carbenes results from kinetic stabilisation due to the shielding of the carbene centre by bulky *N*-substituents and thermodynamic stabilisation by mesomeric (+M) as well as inductive (-I) effects. A heteroatom donor group in the carbene centre, particularly a nitrogen group, is responsible for the stability of the NHCs through both mesomeric and inductive effects (Figure 1-5).^[2, 3]

Firstly, the nitrogen atom possesses an ion pair which can reduce the electron deficiency of the carbene carbon by electron donation to the empty p carbon orbital, increasing the σ - p_{π} gap (the mesomeric effect). Secondly, because nitrogen atoms are more electronegative than carbon, they can reduce the electron density of the carbon centre through the σ -electron

attraction of two adjacent nitrogen atoms, which serves to stabilise the carbene at an orbital relative to the π orbital (the inductive effect).^[2, 3]

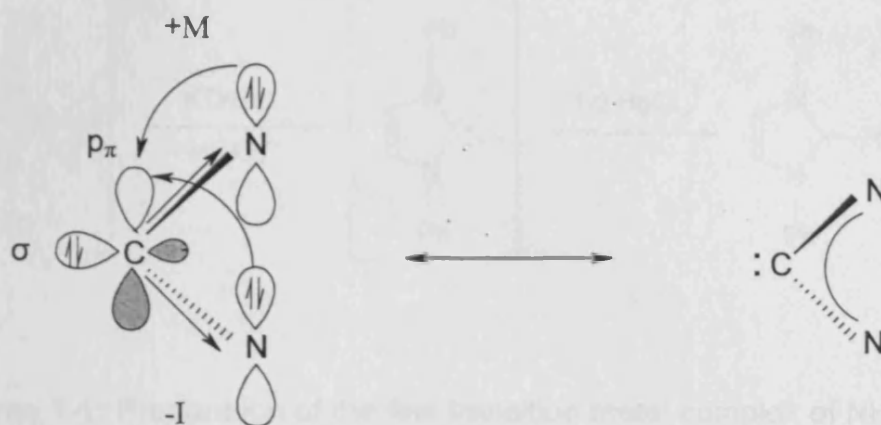


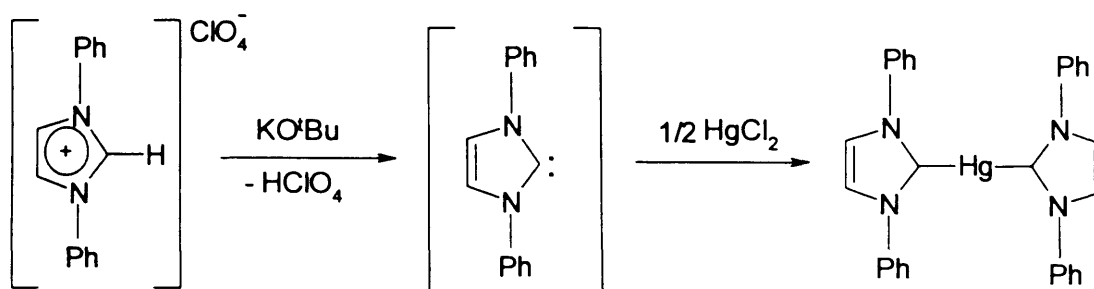
Figure 1- 5: Electronic effects in NHCs.

This results in an increase in the σ - p_{π} gap and, therefore, the two non-binding electrons for the carbene atoms adopt a singlet configuration of paired spins rather than a more reactive triplet arrangement of parallel spins.^[2, 3, 10] Thus, the electronic configuration is critical to the observed stability of NHCs as compared to other carbenes and these species exhibit the properties of singlet carbenes.

1.2. Stable Singlet Carbenes.

Carbenes derived from the imidazole system were first studied in the 1960's by Wanzlick *et al.*^[11-15] Unfortunately, all attempts at that time to isolate free carbenes based on the imidazole ring failed.^[15] Despite the disappointment at

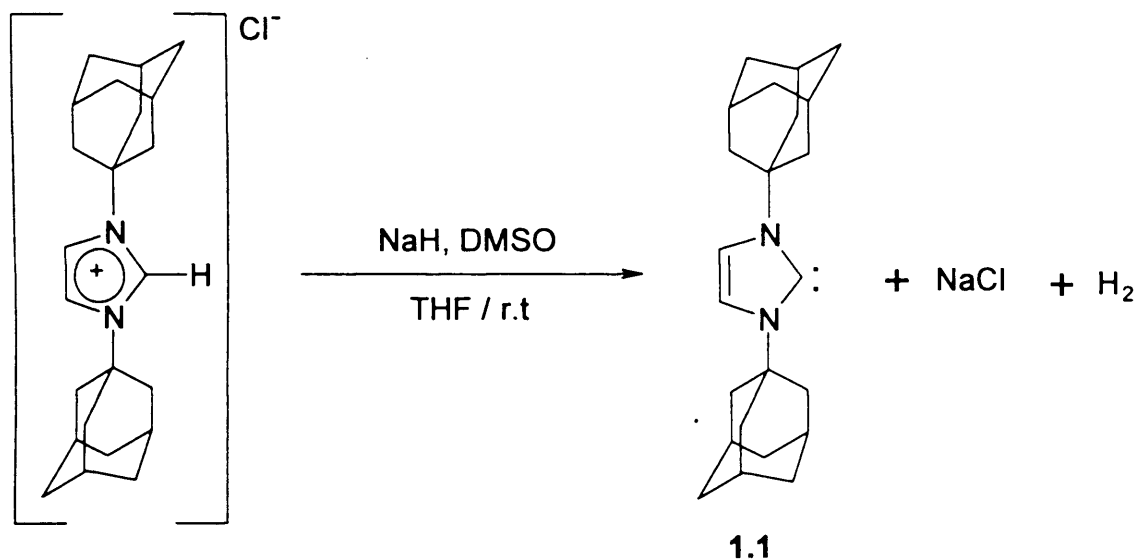
not being able to isolate free carbenes, Wanzlick did manage to trap the carbenes he created in a mercury complex (Scheme 1-1).^[13-18]



Scheme 1-1: Preparation of the first transition metal complex of NHCs.

It was not until 1991 that the first free carbene was isolated. It was based on an imidazole framework. Arduengo and co-workers successfully deprotonated 1,3-bis(1-ad)imidazolin-2-ylidene using sodium hydride under anhydrous, oxygen-free conditions to give the free carbene **1.1** (Scheme 1-2).^[4, 19] The single crystal suitable for X-ray diffraction studies was grown by cooling a toluene solution of the free carbene.

When carbene **1.1** was stored in an inert-atmosphere it was found to be an indefinitely stable, colourless, crystalline solid, which bore an unexpectedly high thermal stability (**1.1** melts at 240 °C without decomposition).^[4, 19]

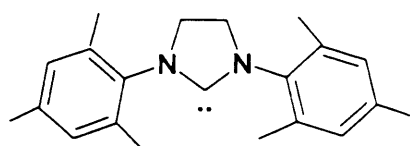


Scheme 1- 2: Preparation of the first isolated, stable, free carbene.

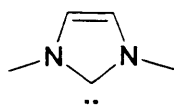
The stability of free carbene **1.1** was initially thought to be due to the steric bulk of the adamantane group preventing nucleophilic attack.^[19] However, isolation of free carbenes with lower steric bulk such as **1.3** and **1.4** (Figure 1-6) confirms that the stability arises from the mesomeric effects of the carbene carbons' adjacent nitrogens.

This groundbreaking discovery has sparked great interest in this field, leading to the isolation of many other stable, free carbenes with extensive variation of the substituents in the two nitrogen atoms (Figure 1-6).

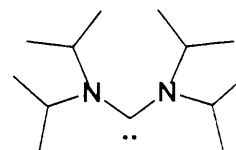
The availability of isolable NHCs has expanded to saturated cyclic (**1.2**),^[20, 21] unsaturated cyclic (**1.3**),^[22] acyclic (**1.4, 1.5**),^[23-26] backbone substituted (**1.6, 1.7, 1.8**)^[27-31] and cyclic diamino-carbene derived from four- (**1.9**),^[32-34] six- (**1.10**),^[32-35] and seven-membered (**1.11**)^[36] compounds.



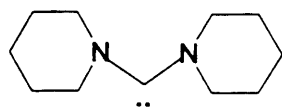
1.2



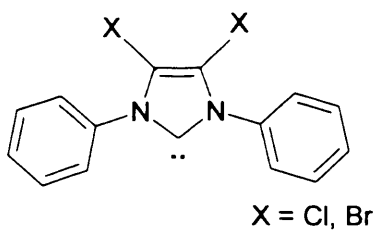
1.3



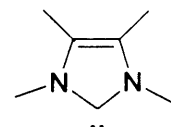
1.4



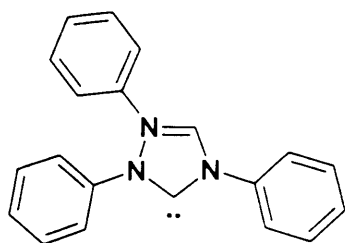
1.5



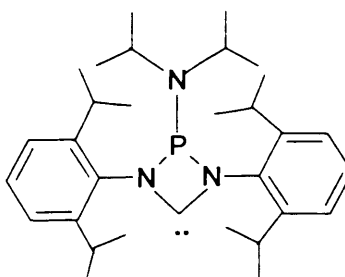
1.6



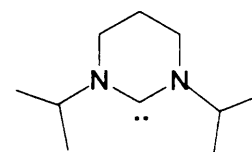
1.7



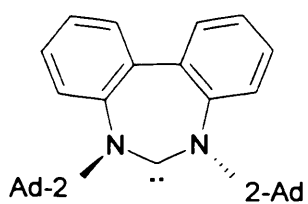
1.8



1.9



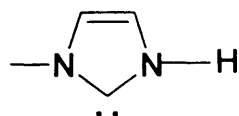
1.10



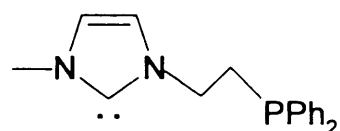
1.11

Figure 1- 6: Examples of isolated, symmetrical, free carbenes.

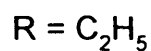
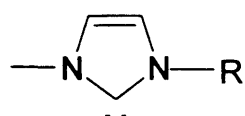
Although in these examples the substituents on the nitrogen atoms are identical, giving symmetrical NHC ligands, unsymmetrical (functionalised) ligands are also accessible,^[37, 38](1.12),^[37] (1.13),^[39] (1.14)^[37] and (1.15)^[40] (Figure 1-7).



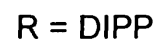
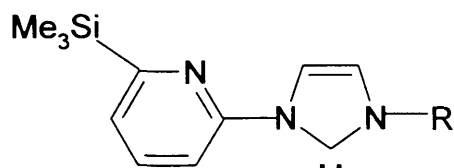
1.12



1.13



1.14



1.15

Figure 1- 7: Examples of isolated, unsymmetrical, free carbenes.

The replacement of one of the nitrogen atoms of imidazol-2-ylidene with a sulphur or oxygen atom gives the corresponding thiazol-2-ylidene^[41] or oxazol-2-ylidene^[42-44] respectively (Figure 1-8).



Figure 1- 8: Isolation of thiazol-2-ylidene and oxazol-2-ylidene carbenes.

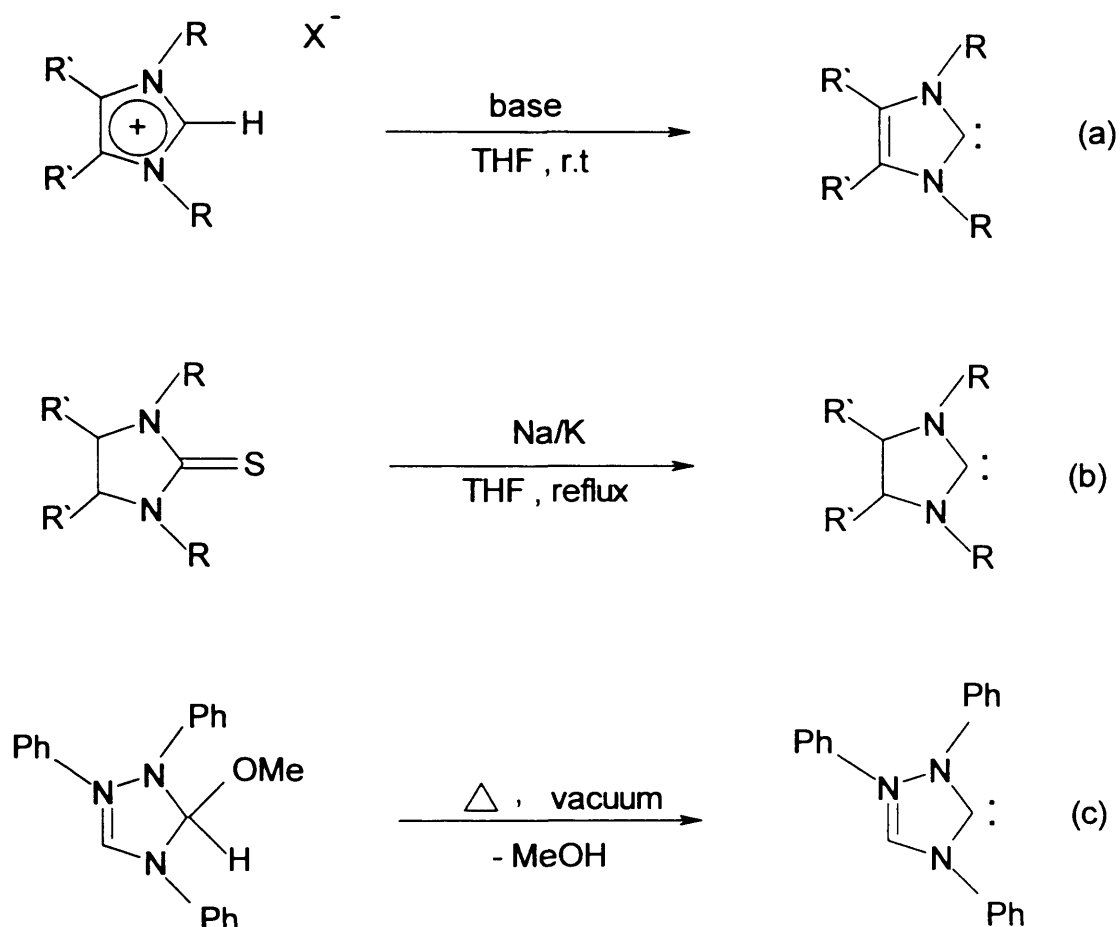
1.3. Methods for the Preparation of Free *N*-Heterocyclic Carbenes.

Most of the common methods of generating free NHCs are based on deprotonation at the C2 position of the corresponding salt with a suitable base.^[19, 45, 46] Strong bases such as KO^tBu or NaH have been used to deprotonate the *N*-alkyl or *N*-aryl substituted azolium salt in THF at room temperature.^[2, 19, 22, 45, 46] Amides such as Li(NⁱPr)₂ or K[HMDS] have also proven useful in the deprotonation of some base-sensitive, functionalised imidazolium salts where the C2 proton may not be exclusively removed due to the presence of other acidic protons (Scheme 1-3a).^[23, 25, 46-50]

Other methods include the reductive desulphurisation of imidazole-2(3H)-thiones (R = alkyl), which on treatment with potassium in boiling THF, yields abundant imidazol-2-ylidenes (Scheme 1-3b).^[29] Using this route, some thermally stable alkyl-substituted NHCs have been prepared, but it is by necessity limited to thermally stable NHCs.^[20]

Finally, the free NHCs may also be formed via the thermal elimination of small stable molecules such as methanol^[31, 51] from imidazolidines,^[13, 52-55] or 5-methoxy-triazol.^[31] This method, however, is limited to thermally stable

NHCs, but has allowed the isolation of the first triazole-based NHCs (which is stable up to 150 °C)^[31] (Scheme 1-3c).



Scheme 1- 3: Methods of preparing free NHCs.

1.4. *N*-Heterocyclic Carbenes as Ligands.

Carbenes as ligands in metal complexes were known long before free carbenes were isolated.^[55] Fischer first introduced carbenes into

organometallic chemistry when he isolated the first carbene complex in 1964.^[56] Carbene complexes are normally classified according to the nature of the formal carbene-metal bond and carbene complexes have been classified as either Fischer- or Schrock-type complexes.^[57]

Fischer carbenes have one stabilising heteroatom containing moiety (OR or NR₂) attached to the carbene carbon. The metal-carbene bond in Fischer-type carbene complexes results from the σ -donation of the carbene electron pair to the metal and π -backbonding from a filled metal d-orbital into the formally empty p _{π} carbene orbital (Figure 1-9). The carbene ligand in these complexes contain a (electrophilic) weakly-donating, singlet carbene,^[57, 58] which accepts backbonding from a low-valent metal (most commonly, middle to late d-block metal).^[2, 3, 59]

The Schrock carbenes lack the heteroatom substituent. These carbenes contain alkyl, aryl or hydrogen substituents. In Schrock-type carbene complexes, the metal-carbene bond can be described as a covalent double bond between a triplet carbene and triplet metal fragment (Figure 1-9).

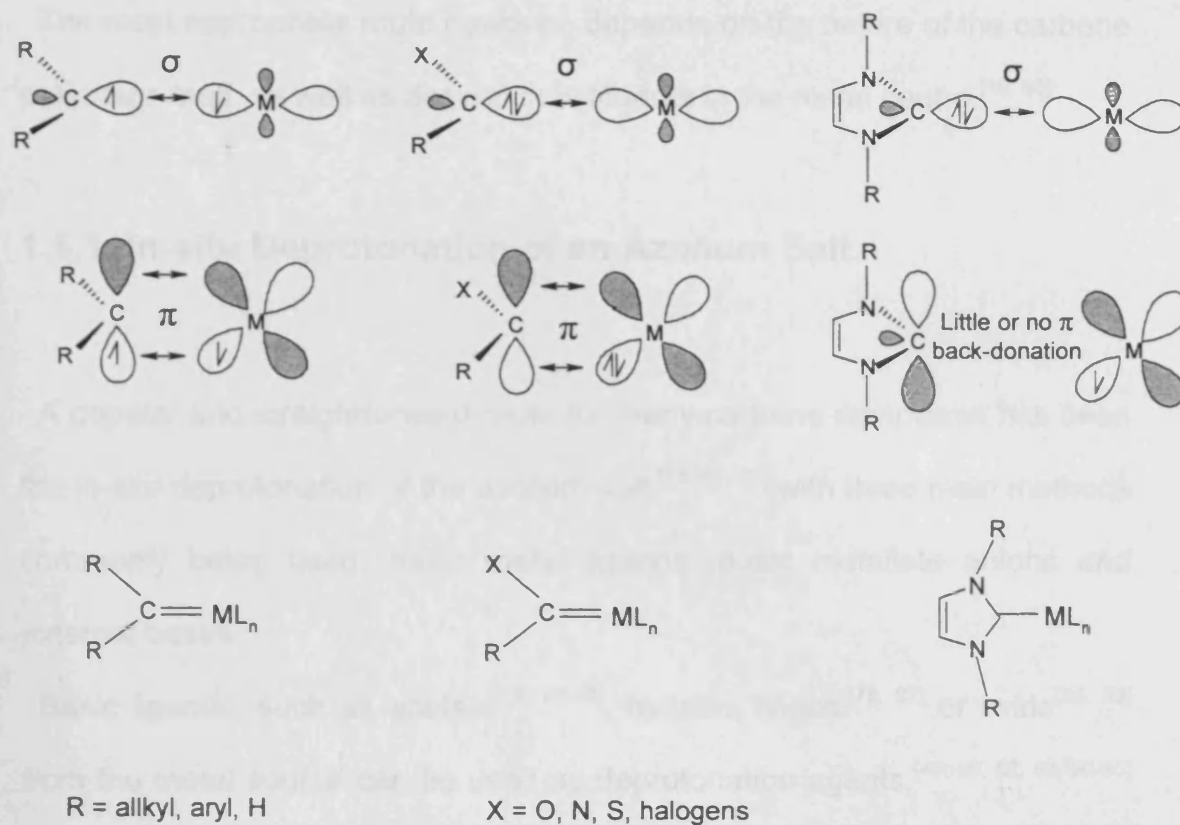
These carbenes are nucleophilic as a result of the greater π -electron density of the carbene and coordinate with high oxidation state metals generally to the left of the d-block.^[57-60]

At first glance, NHCs appear to yield Fischer type carbene complexes on bonding to a metal centre, but the bonding properties actually display entirely different characteristics. Due to the back-donation from the adjacent heteroatom and their strong capacity as σ -donors in metal carbene complexes, the NHCs involve only a single σ -bond to the metal with

negligible π -back-donation^[2, 3] (Figure 1-9) and therefore, heterocyclic carbenes form stable complexes with beryllium and lithium, which have no available electrons for back-donation to the carbene.^[61, 62]

Some experimental studies have confirmed the essentially pure nature of the NHC ligand as a σ -donor to metal complexes.^[63] Other experimental research amongst the CO stretching frequency studies on mixed NHC-Carbonyl complexes have also revealed that NHCs are better σ -donors than trialkylphosphine.^[2, 64, 65] Crystal structure data has shown that M-C bond lengths in NHC complexes are similar to those of the standard M-C alkyl single bond, thus confirming the strong σ -donor properties of these ligands.^[3, 66-68] Due to these particular binding properties, NHCs have been found to form a large range of metal complexes, as the strong C-M σ -bond is sufficient to form stable carbene metal complexes.^[3]

Carbenes are now known to coordinate with a wide variety of metals, ranging from main-group to rare earth metals.^[69-73] Furthermore, electron-rich transition metals have been used to synthesise a variety of interesting and catalytically active carbene complexes.^[66, 68, 73-79] This is in contrast with the Fischer- or Schrock-type carbene where π -backbonding is required to stabilise such complexes i.e. stable bonding occurs only in metals with p- or d-electrons.



Schrock - type

Fischer - type

NHC

Figure 1- 9: Bonding in carbene complexes.

1.5. Routes to the Preparation of NHC Complexes.

A number of different routes exist for the formation of NHC complexes. Many routes have been developed and have permitted the preparation of complexes bearing carbene ligands with a wide variety of electronic and steric properties.^[46]

The most appropriate route however, depends on the nature of the carbene precursor itself, as well as desired substituents in the metal centre.^[16, 80]

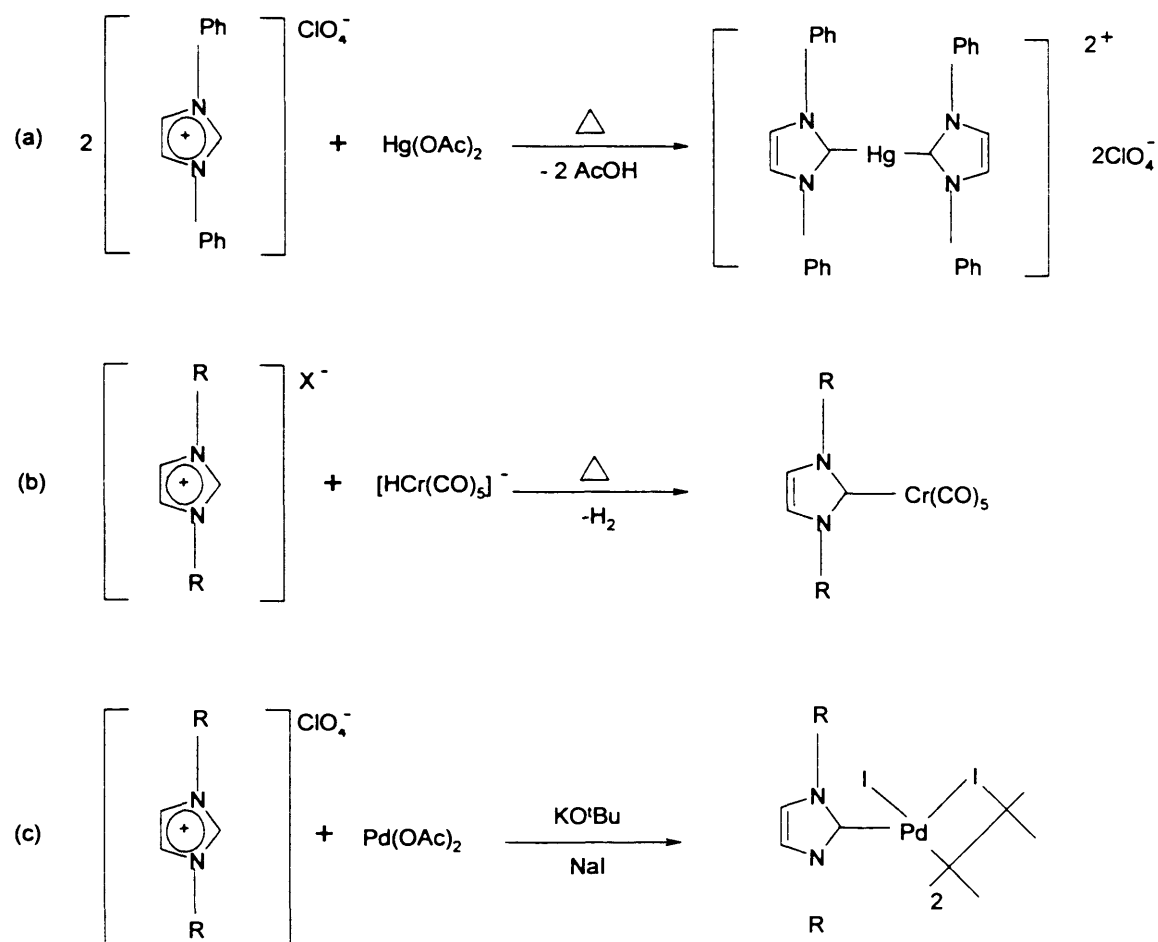
1.5.1. In-situ Deprotonation of an Azolium Salt.

A popular and straightforward route for many carbene complexes has been the in-situ deprotonation of the azolium salt,^[75, 81, 82] with three main methods commonly being used: basic metal ligands, basic metallate anions and external bases.

Basic ligands, such as acetate^[75, 83-86], hydride, alkoxo^[75, 87] or oxide^[88, 89] from the metal source can be used as deprotonation agents.^[46, 80, 82, 88, 90-95] Wanzlick in 1968 made the first reported NHC complexes by using this methodology^[16] (Scheme 1-4a). A significant disadvantage of this method is the limited availability of suitable metal precursors.

The use of basic metallate anions has the advantage that the metal used to deprotonate the azolium salt becomes the ligand acceptor. While this limits the final oxidation state of the metal, a variety of complexes have been successfully created using this method^[91, 96, 97] (Scheme 1-4b).

Another method consists of the addition of an external base for the in-situ deprotonation of the azolium salt in the presence of a metal precursor. Popular bases include potassium,^[98] lithium *tert*-butoxide,^[92] sodium hydride^[64] and butyl lithium^[10, 99] (Scheme 1-4c).



Scheme 1-4: Carbene complexes formed through a basic ligand, basic metallate anion and external base deprotonation.

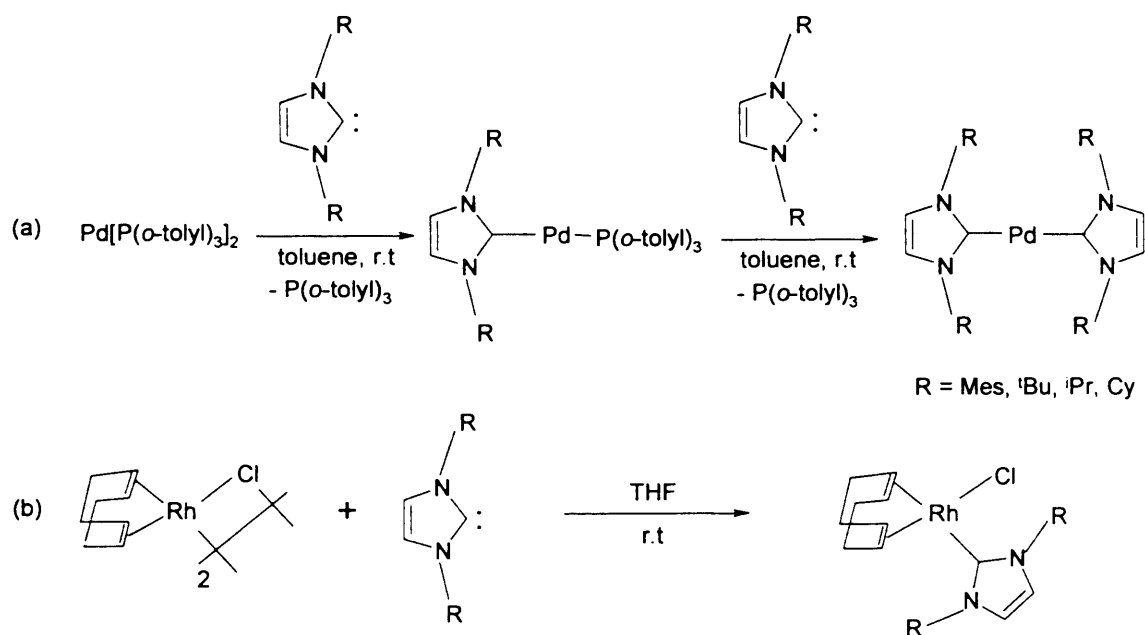
1.5.2. Complexes via Free NHCs.

The most obvious route to the formation of carbene complexes is via free carbene.^[2, 19, 22] The isolation of stable free NHCs has permitted the synthesis of a wide variety of NHC complexes simply through adding the carbene to an appropriate metal precursor.^[64] The strong σ -donor nature of NHCs greatly facilitates the exchange of other donor ligands at the metal

center e.g. carbon monoxide,^[64, 92, 100, 101] or phosphines^[48, 84, 102-104] (Scheme 1-5a).

The use of bulky NHC ligands has allowed the sequential displacement of phosphines and the isolation of mixed NHC-phosphine complexes.^[105] Among the most popular methods are the cleavage of dimeric complexes with bridging ligands, such as halides or carbon monoxide, to form monomeric NHC complexes^[37, 75, 81, 84, 102-104] (Scheme 1-5b).

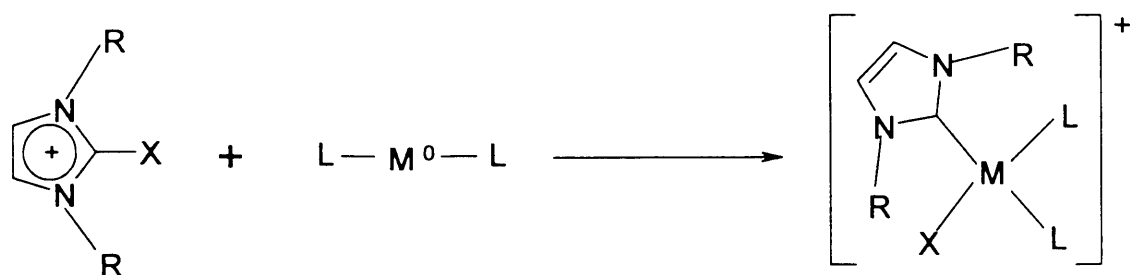
The free carbene route suffers where the high air and moisture sensitivity of the free carbene is concerned, meaning that the generation and manipulation of these species may be problematic.



Scheme 1- 5: The formation of NHC complexes from free carbene and phosphine exchange (a) and dimeric cleavage (b).

1.5.3. NHC Complexes via Oxidative Addition.

Recently the acidity of the C2 proton has been utilised in preparing carbene complexes from the C-H activation of an azolium salt by low-valent metal precursors (Ni^0 , Pd^0 , Pt^0 , Rh^I , Ir^I , Fe^0 , Cr^I) to form the corresponding NHC- M^{+II} -H complexes^[106-116] (Scheme 1-6). Contrary to other methods, the oxidation state of the metal precursor changes during the formation of the NHC-M complexes.

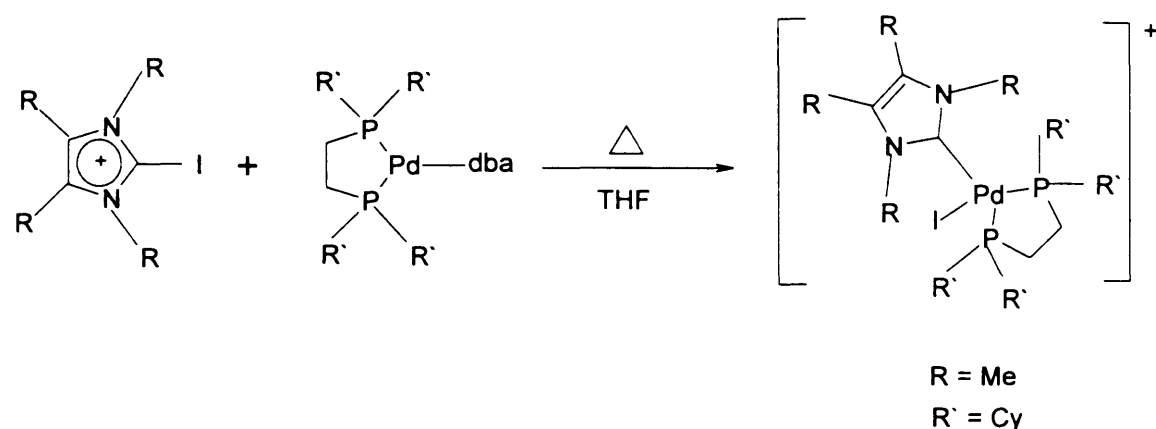


X = H, halogen, CH_3

M = Pt, Pd, Ni, Rh, Ir

Scheme 1- 6: Carbene complex formation via oxidation through the addition of imidazolium salts.

In 2001, Cavell demonstrated the facile formation of NHC complexes via the oxidative addition of 2-haloimidazolium salts to Pd^0 and Pt^0 substrates^[109] (Scheme 1-7).



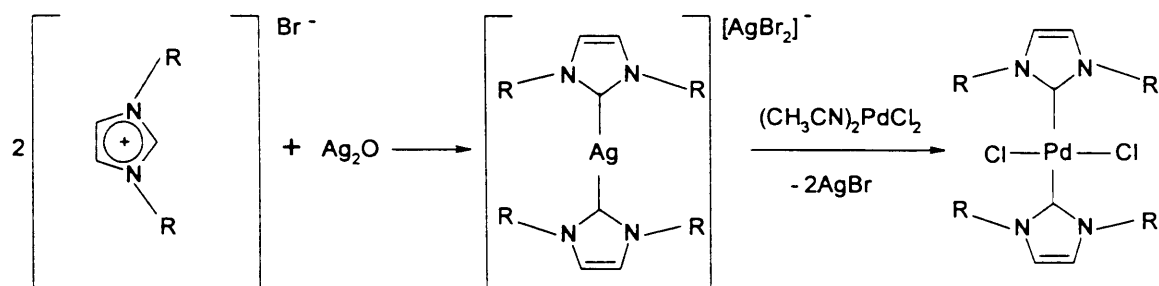
Scheme 1-7: Oxidative addition of 2-haloimidazolium salt to Pd⁰ complex.

The oxidative addition of C2-H bonds, however, is sluggish and no product has been experimentally observed for C2-C_{Alkyl} bonds.^[114, 117, 118] These results have paved the way for the application of oxidative addition as an efficient method of synthesising carbene complexes.

1.5.4. Transmetalation from other NHC-M Complexes.

NHC complexes can be prepared by transferring NHC ligands from one metal complex to another.^[119, 120] The use of Ag (I) NHC complexes, formed by in-situ deprotonation of the azolium salt with silver oxide or silver carbonate,^[119-121] has become particularly useful as a transmetalation agent.^[123, 122]

Transmetalation from Ag (I) NHC complexes is an especially useful method of accessing Pd complexes^[89, 122-128] (Scheme 1-8).



Scheme 1- 8: Preparation of Pd (II) NHC complex via silver transfer reaction.

1.6. Abnormal Carbene Complexes.

The most acidic proton in the imidazolium salt is in the C2 position. C2-coordinated metal imidazol-2-ylidenes are therefore referred to as normal carbenes. It has recently been discovered that the C4- and C5-H bonds of the imidazolium ring are also susceptible to metallation via C-H activation^[129, 130] (Figure 1-10).

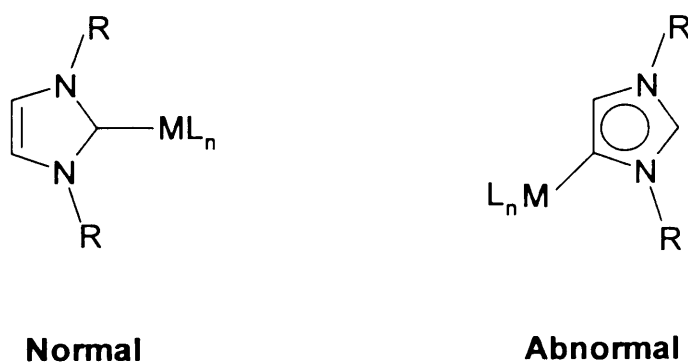
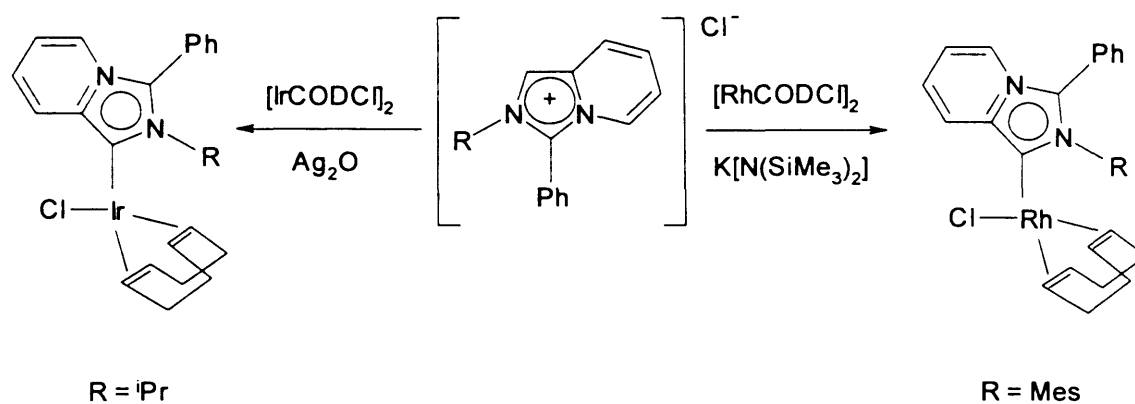


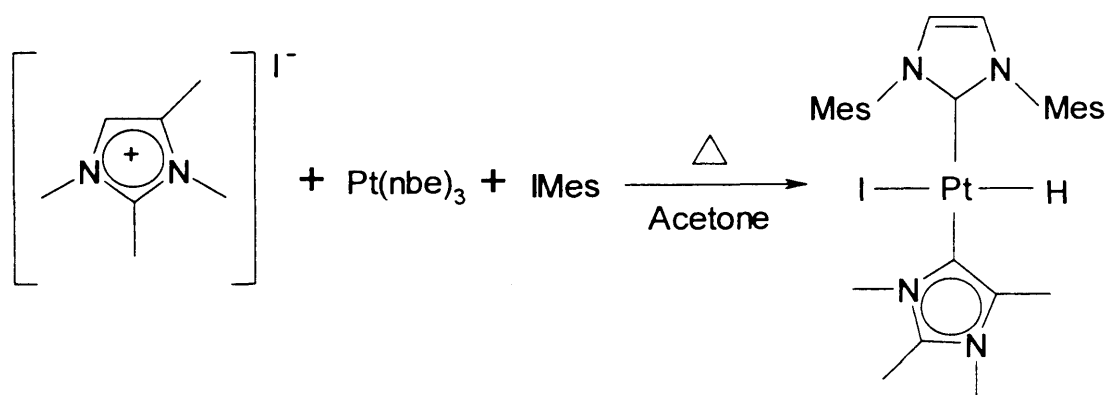
Figure 1-10: Normal and abnormal carbene complexes.

The abnormally bound carbene complex can be obtained selectively by blocking the C2 position, which prevents the formation of C2-coordinated species^[117, 131] (Scheme 1-9).



Scheme 1-9: Synthesis of abnormal carbene complexes.

Cavell and co-workers have demonstrated that the preparation of abnormal carbene complexes can be achieved by oxidative addition of the C4-H bond^[109, 114, 118] (Scheme 1-10).



Scheme 1-10: Synthesis of an abnormal carbene complex by oxidative addition.

1.7. Six- and Seven-membered NHC Systems.

Although five-membered NHCs have been studied in quite some depth as illustrated in the abundance of literature presented throughout this thesis, information on 6- and 7-membered NHCs has only recently been published. The first example of a seven membered ring, from Scarborough and co-workers was as recent as 2005.^[36, 132] Some interesting work has subsequently been carried out regarding these expanded ring systems.

The work presented in this thesis will focus on the synthesis and characterisation of 6- and 7-membered saturated carbene ligands, metal complexes and finally, their experimental application in catalysis.

When expanded to 6- and 7-membered systems, several differences are noticeable, one of which being ring distortion from a planar conformation. It is believed that as the ring size increases, there is an increase in the internal ring strain and the ring twists to alleviate this.^[36, 132-146] It should be noted that the N-C-N bond remains planar even as the ring size increases and torsion occurs in the backbone.^[33]

Although the N-C-N bonds remained strikingly planar in relation to one another and the rest of the ring, the bond angle does show remarkable expansion as the ring increases in size. NCN angles (Figure 1-11) were recorded in the range of 100-110° in 5-membered carbenes, whereas in 7-membered carbenes, this ranges between 115° -125°.^[33, 147]

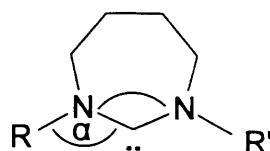


Figure 1-11: Definition of characteristic angles within NHCs.

The good donor ability and large NCN angle featured in expanded carbenes make them very interesting for use as ligands in catalytic systems.^[146]

The conformation of the ring, its NCN angle and ring torsion ultimately have an additive effect upon the conformation of the nitrogen atom substituents. It has been noted by Iglesias and co-workers that the amino substituent angle and planarity deviate (Angle α : Figure 1-10), often resulting in the substituent being forced in and towards the carbene carbon and becoming more planar than in the pre-carbene salt precursors.^[147, 148] This new conformation of the nitrogen substituent adds additional steric hindrance around the carbene carbon which ultimately affects the carbene carbon's availability and stability. When complexing NHCs to metals, the wide NCN angle forces the *N*-substituent to come closer to the metal centre which is likely to be interacting with the metal coordination sphere.^[33-36, 44, 144, 146-149] This additional obstruction around the carbene-metal bond can alter the availability of the metal and thus its potential catalytic properties.^[146]

1.8. NHC complexes as Catalysts.

The following is a brief discussion of NHC as a catalyst. A more comprehensive discussion will be provided in the introductions to the appropriate chapters.

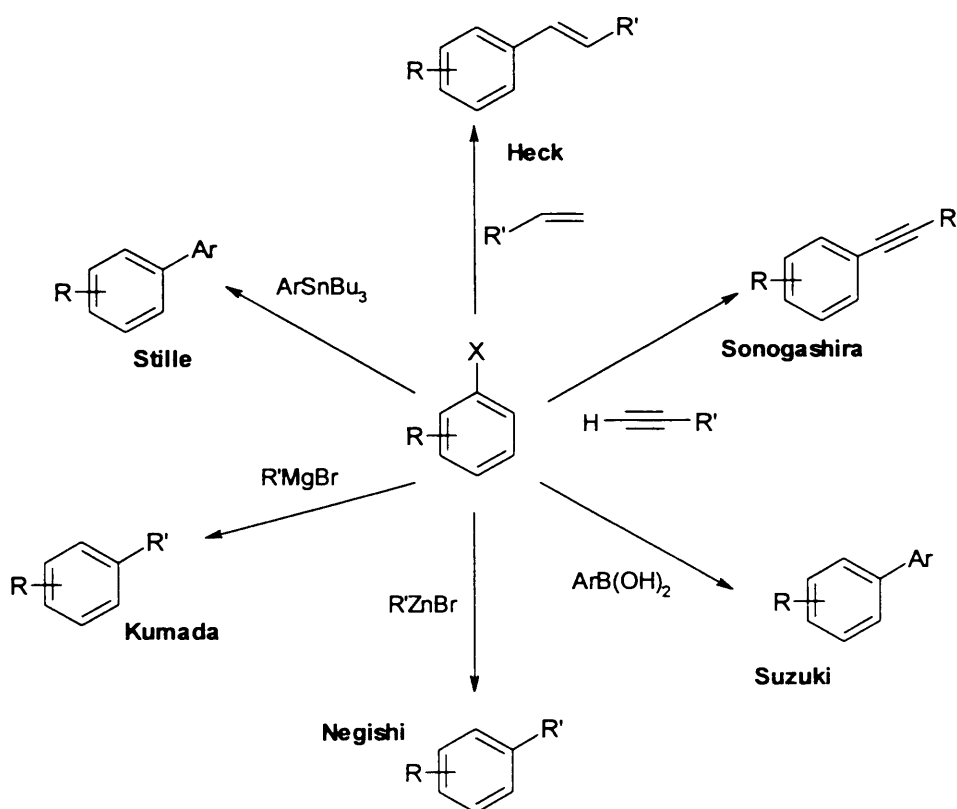
A catalyst is defined as a substance that affect the rate at which a chemical approaches equilibrium. In a catalytic cycle, the catalyst remains unchanged. The importance is that many chemical reactions will not proceed to an appreciable extent in a reasonable time frame without the presence of a suitable catalyst.^[150-152]

Many of the original Fischer- and Schrock-type carbene complexes were trialled in catalytic reactions. They had a tendency to suffer from M-C cleavage, rendering them catalytically inactive.^[2] In contrast, NHCs form stable bonds with metals and can accommodate a wide range of oxidation states, making them suitable for many catalytic cycles.

Since the synthesis and isolation of the first stable NHC by Arduengo *et al.*, these species with strong σ -donor electronic properties have emerged as a new family of ligands for the development of catalysis.^[45] In recent years, NHC-Metal complexes appear to be extraordinarily stable towards air and moisture due to the strong metal-carbon bond^[153] and the use of these complexes as catalysts has increased. Furthermore, a wide variety of routes are available for the synthesis of carbene complexes with diverse steric and electronic properties. Therefore, it is not surprising a substantial amount of effort has been invested in the study of catalytic properties of NHC complexes with success found in numerous important applications.

1.8.1. The success of NHC complex catalysts.

Carbene complexes show a remarkable stability in many catalytic environments, and are often stable to heat, oxygen and moisture. Carbene complexes are also known to catalyse a wide range of organic reactions including hydrogenation,^[154] hydrosilylation,^[155] hydrogen-transfer,^[156] olefin metathesis^[157] and oxidation reaction.^[149] Another area of importance where carbenes have found considerable success is in C-C coupling reactions including the Suzuki,^[158-161] Stille,^[159, 162] Kumada,^[159, 163] Negishi,^[159, 164] and Heck reactions^[165-167] (Scheme 1-11).



Scheme 1-11: A selection of C-C coupling catalytic reactions mediated by Pd.

The real potential of NHC ligands in catalysis has only been realized since the report of Hermann and co-workers in 1995, relating to the use of NHC-Pd complexes as very active catalysts for the Heck reaction (Figure 1-12).^[168]

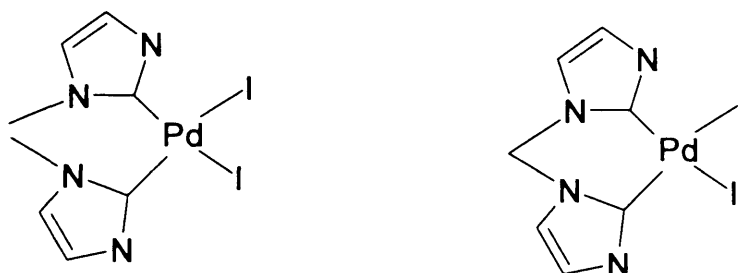
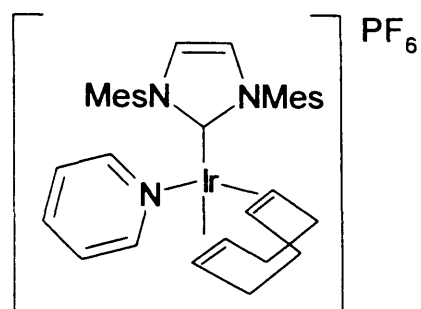


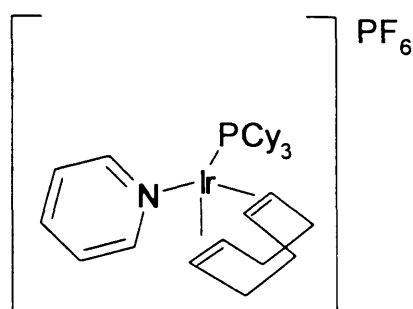
Figure 1-12: Hermann's first NHC-Pd complexes employed in the Heck reaction.

1.8.2. Hydrogenation.

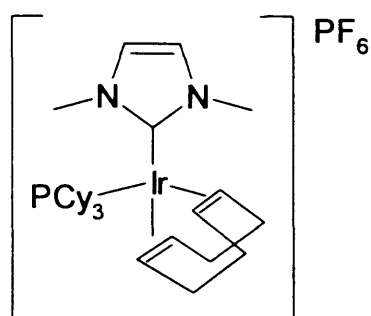
In his pioneering work, Nolan used a monodentate NHC-Ir complex **1.16** for the hydrogenation of cyclohexene and 1-methylcyclohexene (Figure 1-13). Catalyst **1.16** and Crabtree's catalyst **1.17** were found to have comparable activity at room temperature.^[169] However, catalyst **1.16** was found to be more robust and efficient at higher temperatures, probably due to the stability of the metal-carbene bond. In another investigation, Buriak discovered that combining NHC with phosphine ligands led to efficient systems for the hydrogenation of simple olefins.^[170] Comparing complex **1.18** with its analogue **1.19** (Figure 1-13) in the hydrogenation of 1-methylcyclohexene and 2,3-dimethyl-2-butene showed the superiority of catalyst **1.18**.



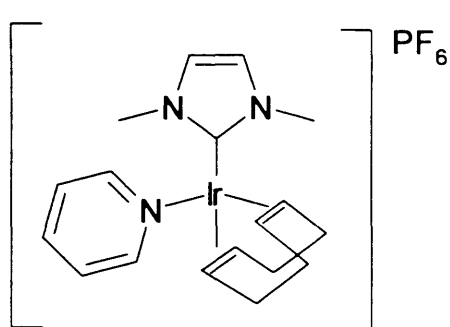
1.16



1.17



1.18



1.19

Figure 1-13: NHC and phosphine as ligands in Ir complexes.

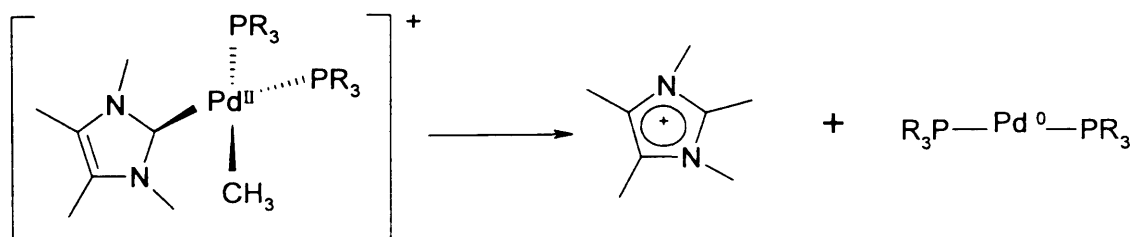
1.8.3. Transfer hydrogenation.

Conventional methods for the hydrogenation of unsaturated bonds have involved the use of molecular hydrogen which has drawbacks due to the dangers and difficult handling procedures involved with working at high pressure. Efforts have since been devoted to developing safer, more cost effective methods and transfer hydrogenation represents an ideal alternative. Transfer hydrogenation hydrogenates a double bond by abstracting hydrogen from a proton donor source such as *iso*-propanol with the reaction being

carried out in the presence of a catalyst and base. It is generally agreed that this research area was spearheaded by Noyori *et al.* in 1995.^[171] They discovered that chiral Ru(II) complexes were capable of asymmetric transfer hydrogenation at reflux temperature and had sufficient catalytic activity for aryl ketones at ambient temperatures. Rhodium and iridium are known to be effective catalysts for transfer hydrogenation of unsaturated substrates via hydrogen donors.^[172] Significantly, transfer hydrogenation of carbonyl compounds in ⁱPrOH is the most widely used reaction to test the catalytic properties due to its simplicity.^[156]

1.8.4. Catalyst decomposition.

In a study by McGuinness *et al.*, the carbene catalyst decomposed during the catalytic reaction, thus giving unsatisfactory results (Scheme 1-12). Further investigation indicated that decomposition was the result of reductive elimination of a *cis*-located carbene and acyl or alkyl ligand.^[173, 174]



Scheme 1-12: Decomposition pathways in carbon monoxide ethylene copolymerisation.

It is believed that the reaction is assisted by the twist of the plane of the carbene with respect to the square planar Pd(II) centre by approximately 60° , allowing the formally empty p orbital on the carbene centre to be directed toward the acyl/alkyl group adjacent to it on the metal centre. Since the acyl/carbene intermediates are necessary intermediates in a CO/ethylene copolymerisation catalytic cycle, the discovery of the decomposition route was quite disturbing and there have been no reports of successful monodentate carbene complex catalysis of this reaction since then.

The 6- and 7-membered ring sizes have been relatively unexplored and their chemistry is virtually unknown, mainly due to the difficulties in synthesising these larger ring compounds.^[33, 34, 36, 149, 175-177] The large ring NHCs are very basic and show unique structural characteristics, for example the NCN angle in the expanded ring is very large, causing the *N*-substituent to twist closer to the metal centre. It is timely to investigate the impact of very basic and sterically demanding expanded ring NHCs in catalytic chemistry.

1.9. Aims and Thesis Overview.

Carbene based ligand systems with functionalised groups have proved very effective as ligands for catalysis and there has been considerable work on these types of system.

The task of this thesis was to explore the synthesis, metal coordination and catalytic application of saturated expanded (6- and 7-membered) NHCs with *N*-functionalised group substituents.

Chapter Two describes the preparation and characterisation of a range of 6- and 7-membered carbenes, with Py, *o*-MeOPh, *o*-MeSPh, DiPP and Mes *N*-substituents. Donor-functionalised, including weak-donor functionalised, NHCs play an important role in organometallic chemistry and catalysis. Tridentate and bidentate ligands can provide considerable benefits due to the extra stability they impart to the catalytic reaction of intermediates. A new method for the synthesis of saturated (symmetrical and unsymmetrical) salts is presented, involving the use of potassium carbonate as a mild base for the deprotonation of the corresponding formamidines, which is reacted with di-electrophiles under aerobic condition. Additionally, expanded carbenes (6- and 7-membered) were found to be more basic than the 5-membered analogues. Ligands of this nature were largely unknown and this opens up an opportunity to develop a whole range of new systems with a cross section of properties.

Chapter Three deals with the synthesis and characterisation of a range of rhodium and iridium complexes. Expansion of the ring provides carbenes with NCN angles close to the sp^2 angle (120°) which consequently forces the *N*-substituents to bend towards the metal center. Some complexes were found to be biscarbenes and the nature of the functional group was found to influence the type of complex formed.

Chapter Four presents the results from the catalytic performance of Rh(I) and Ir(I) complexes in the transfer hydrogenation of ketones. They were also tested as catalysts in an olefin hydrogenation reaction with molecular hydrogen. The greater donor abilities and wide NCN angle of these expanded carbenes make them interesting candidates for the study of their

catalytic application. These complexes show enhanced activity and stability in comparison with non-functionalised NHC analogues. The results show that all the complexes were very active, giving a conversion of up to 100% in a short time with as little as 0.01-0.0001 mmol of the catalysts and 1 mmol of the substrate. The catalysts show excellent activity even after adding 3 mmol from the substrate.

1.10. References.

- [1] E. Buchner and T. Curtis, *Ber. Dtsch Chem. Ges.*, **1885**, 2377.
- [2] W. A. Herrmann and C. Köcher, *Angew. Chem. Int. Ed. Eng.*, **1997**, 36, 2162.
- [3] D. Bourissou, O. Guerret, F. P. Gabbai and G. Bertrand, *Chem. Rev.*, **2000**, 100, 39.
- [4] G. Schuster, *Adv. Phys. Org. Chem.*, **1986**, 22, 311.
- [5] K. K. Irikura, W. A. Goddard and J. L. Beauchamp, *J. Am. Chem. Soc.*, **1992**, 114, 48.
- [6] B. C. Gilbert, D. Griller and A. S. Nazran, *J. Org. Chem.*, **1985**, 50, 4738.
- [7] R. Gleiter and R. Hoffmann, *J. Am. Chem. Soc.*, **1968**, 90, 1475.
- [8] R. Hoffmann, G. D. Zeiss and G. W. Van Dine, *J. Am. Chem. Soc.*, **1968**, 90, 1485.
- [9] N. C. Baird and K. F. Taylor, *J. Am. Chem. Soc.*, **1978**, 100, 1333.
- [10] U. Kernbach, M. Ramm, P. Luger and W. P. Fehlhammer, *Angew. Chem. Int. Ed. Eng.*, **1996**, 35, 310.
- [11] H. W. Wanzlick and E. Schikora, *Angew. Chem.*, **1960**, 72, 494.
- [12] H. W. Wanzlick, *Angew. Chem. Int. Ed. Eng.*, **1962**, 1, 75.
- [13] H. W. Wanzlick and E. Schikora, *Chem. Ber.*, **1961**, 94, 2389.
- [14] H. W. Wanzlick, B. Lachmann and E. Schikora, *Chem. Ber.*, **1965**, 98, 3170.
- [15] H. J. Schönherr and H. W. Wanzlick, *Chem. Ber.*, **1970**, 103, 1037.

- [16] H. W. Wanzlick and H. J. Schönherr, *Angew. Chem. Int. Ed. Eng.*, **1968**, *7*, 141.
- [17] H. J. Schönherr and H. W. Wanzlick, *Liebigs Ann. Chem.*, **1970**, *731*, 176.
- [18] H. W. Wanzlick and H. J. Schönherr, *Liebigs Ann. Chem.*, **1970**, *731*, 176.
- [19] A. J. Arduengo, R. L. Harlow and M. Kline, *J. Am. Chem. Soc.*, **1991**, *113*, 361.
- [20] M. K. Denk, A. Thadani, K. Hatano and A. J. Lough, *Angew. Chem. Int. Ed. Eg.*, **1997**, *36*, 2607.
- ✧ [21] A. J. Arduengo, J. R. Goerlich and W. J. Marshall, *J. Am. Chem. Soc.*, **1995**, *117*, 11027.
- [22] A. J. Arduengo, H. V. R. Dias, R. L. Harlow and M. Kline, *J. Am. Chem. Soc.*, **1992**, *114*, 5530.
- [23] R. W. Alder, P. R. Allen, M. Murray and A. G. Orpen, *Angew. Chem. Int. Ed. Eng.*, **1996**, *35*, 1121.
- [24] D. Martin ,A. Baceiredo, H. Gornitzka, W. W. Schoeller and G. Bertrand, *Angew. Chem. Int. Ed. Eng.*, **2005**, *44*, 1700.
- [25] V. Lavallo, Y. Canac, C. Präsang, B. Donnadieu and G. Bertrand, *Angew. Chem. Int. Ed. Eng.*, **2005**, *44*, 5705.
- [26] R. W. Alder and M. E. Blake, *Chem. Commun.*, **1997**, 1513.
- [27] A. J. Arduengo, F. Davidson, H. V. R. Dias, J. R. Goerlich, D. Khasnis, W. J. Marshall and T. K. Prakasha, *J. Am. Chem. Soc.*, **1997**, *119*, 12742.
- [28] M. L. Cole, C. Jones and P. C. Junk , *New J. Chem.*, **2002**, *262*, 1296.
- [29] N. Kuhn and T. Kratz, *Synthesis*, **1993**, 561.
- [30] A. J. Arduengo, H. Bock, H. Chen, M. Denk, D. A. Dixon, J. C. Green, W. A. Herrmann, N. L. Jones, M. Wagner and R. West, *J. Am. Chem. Soc.*, **1994**, *116*, 6641.
- [31] D. Enders, K. Breuer, G. Raabe, J. Runsink, J. H. Teles, J. P. Melder, K. Ebel and S. Brode, *Angew. Chem. Int. Ed. Eng.*, **1995**, *34*, 1021.
- [32] E. Despagnet-Ayoub and R. H. Grubbs, *J. Am. Chem. Soc.*, **2004**, *126*, 10198.

- [33] P. Bezinet, G. P. A. Yap and D. S. Richeson, *J. Am. Chem. Soc.*, **2003**, *125*, 13314.
- [34] M. Mayr, K. Wurst, K. H. Ongania and M. R. Buchmeiser, *Chem. Eur. J.*, **2004**, *10*, 1256-1266.
- [35] R. W. Alder, M. E. Blake, C. Bortolotti, S. Bufali, C. P. Butts, E. Linehan, J. M. Oliva, A. G. Orpen and M. J. Quayle, *Chem. Commun.*, **1999**, 241.
- [36] C. C. Scarborough, M. J. W. Grady, I. A. Guzei, B. A. Gandhi, E. E. Bunel and S. S. Stahl, *Angew. Chem. Int. Ed. Eng.*, **2005**, *44*, 5269.
- [37] W. A. Herrmann, C. Köcher, L. J. Gooßen and G. R. J. Artus, *Chem. Eur. J.*, **1996**, *2*, 1627.
- [38] W. A. Herrmann, C. P. Reisinger and M. Spiegler, *J. Organomet. Chem.*, **1998**, *557*, 93.
- [39] C. Heinemann and W. Thiel, *Chem. phys. lett.*, **1994**, *217*, 11.
- [40] M. C. Perry, X. Cui and K. Burgess, *Tetrahedron: Asymmetry*, **2002**, *13*, 1969.
- [41] Arduengo, III, A. J. Goerlich, J. R. Mashall and W. J. Liebigs. *Ann.*, **1997**, 365.
- [42] J. Ruiz, G. Garcia, M. E. G. Mosquera, B. F. Perandones, M. P. Gonzalo and M. Vivanco, *J. Am. Chem. Soc.*, **2005**, *127*, 8584.
- [43] M. Tamm and F. E. Hahn, *Coord. Chem. Rev.*, **1999**, *182*, 175.
- [44] C. C. Scarborough, B. V. Popp, I. A. Guzei and S. S. Stahl, *J. Organomet. Chem.*, **2005**, *690*, 5414.
- [45] A. J. Arduengo, *Acc. Chem. Res.*, **1999**, *32*, 913.
- [46] T. Weskamp, V. P. W. Bohm and W. A. Herrmann, *J. Organomet. Chem.*, **2000**, *600*, 12.
- [47] A. Tulloch, A. Danopoulos, R. Tooze, S. Cafferkey, S. Kleinhenz and M. Hursthouse, *Chem. Commun.*, **2000**, *14*, 1247.
- [48] J. A. Loch, M. Albrecht, E. Peris, J. Mata, J. W. Faller and R. H. Crabtree, *Organometallics*, **2002**, *21*, 700.
- [49] A. Danopoulos, S. Winston, T. Gelbrich, M. B. Hursthouse and R. P. Tooze, *Chem. Commun.*, **2002**, 482.
- [50] A. A. Danopoulos, S. Winston and W. B. Motherwell, *Chem. Commun.*, **2002**, 1376.

- [51] J. H. Teles, J. P. Melder, K. Ebel, R. Schneider, E. Gehrler, W. Harder, S. Brode, D. Enders, K. Breuer and G. Raabe, *Helv. Chim. Acta.*, **1996**, *79*, 61.
- [52] H. W. Wanzlick and H. J. Kleiner, *Angew. Chem.*, **1961**, *73*, 493.
- [53] J. A. Chamizo, J. Morgado and S. Bernès, *Transition Met. Chem.*, **2000**, *25*, 161-165.
- [54] M. Scholl, S. Ding, C. W. Lee and R. H. Grubbs, *Org. Lett.*, **1999**, *1*, 953.
- [55] D. J. Cardin, B. Cetinkaya and M. F. Lappert, *Chem. Rev.*, **1972**, *72*, 545.
- [56] E. O. Fischer and A. Maasböl, *Angew. Chem. Int. Ed. Eng.*, **1964**, *3*, 580.
- ✓ [57] G. O. Spessard and G. L. Miessler, in *Organometallic Chemistry*, Prentice-Hall, New Jersey, 1996, 302.
- ✓ [58] C. Boehme and G. Frenking, *Organometallics*, **1998**, *17*, 5801.
- ✓ [59] S. F. Vyboishchikov and G. Frenking, *Chem. Eur. J.*, **1998**, *4*, 1428.
- ✓ [60] R. H. Crabtree, *The Organometallic Chemistry of the Transition Metals*, John Wiley & Sons, Inc., **1988**.
- [61] W. A. Herrmann, O. Runte and G. Artus, *J. Organomet. Chem.*, **1995**, 501.
- [62] A. J. Arduengo, M. Tamm, J. C. Calabrese, F. Davidson and W. J. Marshall, *Chem. Lett.*, **1999**, *28*, 1021.
- [63] J. C. Green, R. G. Scurr, P. L. Arnold and F. G. N. Cloke, *Chem. Commun.*, **1997**, 1963.
- [64] K. Öfele, W. A. Herrmann, D. Mihalios, M. Elison, E. Herdtweck, W. Scherer and J. Mink, *J. of Organomet. Chem.*, **1993**, *459*, 177.
- [65] J. Huang, H. J. Schanz, E. D. Stevens and S. P. Nolan, *Organometallics*, **1999**, *18*, 2370.
- [66] A. J. Arduengo, M. Tamm, S. J. McLain, J. C. Calabrese, F. Davidson and W. J. Marshall, *J. Am. Chem. Soc.*, **1994**, *116*, 7927.
- [67] J. C. Green and B. J. Herbert, *Dalton Trans.*, **2005**, 1214.
- [68] A. J. Arduengo, S. F. Gamper, J. C. Calabrese and F. Davidson, *J. Am. Chem. Soc.*, **1994**, *116*, 4391.

- [69] A. J. Arduengo, H. V. R. Dias, J. C. Calabrese and F. Davidson, *Inorg. Chem.*, **1993**, 32, 1541.
- [70] A. J. Arduengo, H. V. R. Dias, F. Davidson and R. L. Harlow, *J. Organomet. Chem.*, **1993**, 462, 19.
- [71] A. J. Arduengo, H. V. R. Dias, J. C. Calabrese and F. Davidson, *J. Am. Chem. Soc.*, **1992**, 114, 9724.
- [72] N. Kuhn, G. Henkel, T. Kratz, J. Kreutzberg, R. Boese and A. H. Maulitz, *Chem. Ber.*, **1993**, 126, 2041.
- [73] N. Kuhn, T. Kratz, D. Bläser and R. Boese, *Chem. Ber.*, **1995**, 128, 245.
- [74] W. A. Herrmann, K. Öfele, M. Elison, F. E. Kuhn and P. W. Roesky, *J. Organomet. Chem.*, **1994**, 480, 7.
- [75] W. A. Herrmann, M. Elison, J. Fischer, C. Köcher and G. R. J. Artus, *Chem. Eur. J.*, **1996**, 2, 772.
- [76] K. Öfele, W. A. Herrmann, D. Mihalios, M. Elison, E. Herdtweck, T. Priermeier and P. Kiprof, *J. Organomet. Chem.*, **1995**, 498, 1.
- [77] A. J. Arduengo, H. V. R. Dias, J. C. Calabrese and F. Davidson, *Organometallics*, **1993**, 12, 3405.
- [78] H. Schumann, M. Glanz, J. Winterfeld, H. Hemling, N. Kuhn and T. Kratz, *Chem. Ber.*, **1994**, 127, 2369.
- [79] H. Schumann, M. Glanz, J. Winterfeld, H. Hemling, N. Kuhn and T. Kratz, *Angew. Chem. Int. J. Ed. Eng.*, **1994**, 33, 1733.
- [80] K. Öfele, *J. Organomet. Chem.*, **1968**, 12, 42.
- [81] W. A. Herrmann, M. Elison, J. Fischer, C. Köcher and G. Artus, *Angew. Chem. Int. J. Ed. Eng.*, **1995**, 34, 2371.
- [82] W. A. Herrmann, J. Fischer, K. Öfele and G. R. J. Artus, *J. Organomet. Chem.*, **1997**, 530, 259.
- [83] H. W. Wanzlick and H. J. Schönherr, *Angew. Chem Int. Ed. Eng.*, **1968**, 80, 154.
- [84] W. A. Herrmann, G. Gerstberger and M. Spiegler, *Organometallics*, **1997**, 16, 2209.
- [85] W. A. Herrmann, J. Schwarz, M. G. Gardiner and M. Spiegler, *J. Organomet. Chem.*, **1999**, 575, 80.

- [86] W. A. Herrmann, J. Schwarz and M. G. Gardiner, *Organometallics*, **1999**, *18*, 4082.
- [87] C. Kocher and W. A. Herrmann, *J. Organomet. Chem.*, **1997**, *532*, 261.
- [88] B. Bildstein, M. Malaun, H. Kopacka, K. Wurst, M. Mitterbock, K. H. Ongania, G. Opromolla and P. Zanello, *Organometallics*, **1999**, *18*, 4325.
- [89] H. M. J. Wang and I. J. B. Lin, *Organometallics*, **1998**, *17*, 972.
- [90] K. Öfele and M. Herberhold, *Angew. Chem. Int. Ed. Eng.*, **1970**, *9*, 739.
- [91] K. Öfele, *Angew. Chem. Int. Ed. Eng.*, **1969**, *81*, 936.
- [92] W. A. Herrmann, L. J. Gooßen and M. Spiegler, *J. Organomet. Chem.*, **1997**, *547*, 357.
- [93] B. Bildstein, M. Malaun, H. Kopacka, K. H. Ongania and K. Wurst, *J. Organomet. Chem.*, **1999**, *572*, 177.
- [94] F. E. Hahn and M. Foth, *J. Organomet. Chem.*, **1999**, *585*, 241.
- [95] G. Bertrad, E. Diez-Barra, J. Fernandez-Baeza, H. Gornitzka, A. Moreno, A. Otero, R. I. Rodriguez-Curiel and J. Tejeda, *Eur. J. Inorg. Chem.*, **1999**, 1965.
- [96] K. Öfele, E. Roos and M. Herberhold, *Z. Naturforsch. B.*, **1976**, *31*, 1070.
- [97] K. Öfele and C. G. Kreiter, *Chem. Ber.*, **1972**, *105*, 529.
- [98] D. Enders, H. Gielen, G. Raabe, J. Runsink and J. H. Teles, *Chem. Ber.*, **1996**, *129*, 1483.
- [99] W. P. Fehlhammer, T. Bliss, U. Kernbach and I. Brudgam, *J. Organomet. Chem.*, **1995**, *490*, 149.
- [100] W. A. Herrmann, L. J. Goossen, C. Köcher and G. R. J. Artus, *Angew. Chem. Int. Ed. Eng.*, **1996**, *35*, 2805.
- [101] N. Kuhn, T. Kratz, R. Boese and D. Bläser, *J. Organomet. Chem.*, **1994**, *470*, 8.
- [102] T. Weskamp, W. C. Schattenmann, M. Spiegler and W. A. Herrmann, *Angew. Chem. Int. Ed. Eng.*, **1998**, *37*, 2490.
- [103] V. P. W. Böhm, C. W. K. Gstöttmayr, T. Weskamp and W. A. Herrmann, *J. Organomet. Chem.*, **2000**, *595*, 186 ,

- [104] R. E. Douthwaite, D. Haussinger, M. L. H. Green, P. J. Silcock, P. T. Gomes, A. M. Martins and A. A. Danopolous, *Organometallics*, **1999**, *18*, 4584.
- [105] L. R. Titcomb, S. Caddick, F. G. N. Cloke, D. J. Wilson and D. McKerrecher, *Chem. Commun.*, **2001**, 1388.
- [106] D. S. McGuinness, K. J. Cavell, B. W. Skelton and A. H. White, *Organometallics*, **1999**, *18*, 1596.
- [107] P. J. Fraser, W. R. Roper and F. G. A. Stone, *J. Chem. Soc., Dalton Trans.*, **1974**, 102.
- [108] P. J. Fraser, W. R. Roper and F. G. A. Stone, *J. Chem. Soc., Dalton Trans.*, **1974**, 760.
- [109] D. S. McGuinness, K. J. Cavell, B. F. Yates, B. W. Skelton and A. H. White, *J. Am. Chem. Soc.*, **2001**, *123*, 8317.
- [110] A. Furstner, G. Seidel, D. Kremzow and C. W. Lehmann, *Organometallics*, **2003**, *22* 907.
- [111] D. Kremzow, G. Seidel, C. W. Lehmann and A. Fürstner, *Chem. Eur. J.*, **2005**, *11*, 1833.
- [112] N. D. Clement, K. J. Cavell, C. Jones and C. J. Elsevier, *Angew. Chem. Int. Ed. Eng.*, **2004**, *43*, 1277.
- [113] S. Gründemann, M. Albrecht, A. Kovacevic, J. W. Faller and R. H. Crabtree, *J. Chem. Soc., Dalton Trans.*, **2002**, 2163.
- [114] D. S. McGuinness, K. J. Cavell and B. F. Yates, *Chem. Commun.*, **2001**, *4*, 355.
- [115] M. S. Viciu, G. A. Grasa and S. P. Nolan, *Organometallics*, **2001**, *20*, 3607.
- [116] K. J. Cavell and D. S. McGuinness, *Coord. Chem. Rev.*, **2004**, *248*, 671.
- [117] S. J. Roseblade, A. Ros, D. Monge, M. Alcarazo, E. Alvaraez, J. M. Lassaletta and R. Fernandez, *Organometallics*, **2007**, *26*, 2570.
- [118] D. C. Graham, K. J. Cavell and B. F. Yates, *Dalton Trans*, **2007**, 4650.
- [119] S. T. Liu, T. Y. Hsieh, G. H. Lee and S. M. Peng, *Organometallics*, **1998**, *17*, 993.

- [120] R. Z. Ku, J. C. Huang, J. Y. Cho, F. M. Kiang, K. R. Reddy, Y. C. Chen, K. J. Lee, J. H. Lee, G. H. Lee, S. M. Peng and S. T. Liu, *Organometallics*, **1999**, *18*, 2145.
- [121] X. Wang, S. Liu and G. X. Jin, *Organometallics*, **2004**, *23*, 6002.
- [122] D. S. McGuinness and K. J. Cavell, *Organometallics*, **2000**, *19*, 741.
- [123] A. M. Magill, D. S. McGuinness, K. J. Cavell, G. J. P. Britovsek, V. C. Gibson, A. J. P. White, D. J. Williams, A. H. White and B. W. Skelton, *J. Organomet. Chem.*, **2001**, *617*, 546.
- [124] R. S. Simons, P. Custer, C. A. Tessier and W. J. Youngs, *Organometallics*, **2003**, *22*, 1979.
- [125] D. J. Nielsen, A. M. Magill, B. F. Yates, K. J. Cavell, B. W. Skelton and A. H. White, *Chem. Commun.*, **2002**, 2500.
- [126] A. Tulloch, A. Danopoulos, G. J. Tizzard, S. J. Coles, M. B. Hursthouse, R. S. Hay-Motherwell and W. B. Motherwell, *Chem. Commun.*, **2001**, 1270.
- [127] D. J. Nielsen, K. J. Cavell, B. W. Skelton and A. H. White, *inorg. chim. acta.*, **2002**, *327*, 116.
- [128] H. M. J. Wang, C. Y. L. Chen and I. J. B. Lin, *Organometallics*, **1999**, *18*, 1216 .
- [129] S. Grundemann, A. Kovavevic, M. Albrecht, J. W. Faller and R. H. Crabtree, *Chem. Commun.*, **2001**, 2274.
- [130] H. Lebel, M. K. Janes, A. B. Charette and S. P. Nolan, *J. Am. Chem. Soc.*, **2004**, *126*, 5046.
- [131] M. Alcarazo, S. J. Roseblade, A. R. Cowley, R. Fernandez, J. M. Brown and J. M. Lassaletta, *J. Am. Chem. Soc.*, **2005**, *127*, 3290.
- [132] C. C. Scarborough, B. V. Popp, I. A. Guzei and S. S. Stahl, *J. Organomet. Chem.*, **2005**, *690*, 6143.
- [133] L. R. Yang, M. Mayr, K. Wurst and M. R. Buchmeiser, *Chem. Eur. J.*, **2004**, *10*, 5761.
- [134] J. Yun, E. R. Marinez and R. H. Grubbs, *Organometallics*, **2004**, *23*, 4127.
- [135] B. Bantu, D. R. Wang, K. Wurst and M. R. Buchmeiser, *Tetrahedron*, **2005**, *61*, 12145.

- [136] M. Bortenschlager, M. Mary, O. Nuyken and M. R. Buchmeiser, *J. Mol. Catal. A: Chem.*, **2005**, 233, 67.
- [137] N. Imlinger, K. Wurst and M. R. Buchmeiser, *Monatsh. Chem.*, **2005**, 136, 47.
- [138] Y. Zhang, D. R. Wang, K. Wurst and M. R. Buchmeiser, *J. Organomet. Chem.*, **2005**, 690, 5728.
- [139] S. K. Schneider, W. A. Herrmann and E. Herdtweck, *J. Mol. Catal. A: Chem.*, **2006**, 245, 248.
- [140] G. C. Lloyd-Jones, R. W. Alder and G. J. Owen-Smith, *Chem. Eur. J.*, **2006**, 12, 3561.
- [141] D. M. Khramov, E. L. Rosen, V. M. Lynch and C. W. Bielawski, *Angew. Chem. Int. Ed.*, **2008**, 47, 2267.
- [142] V. Cesar, N. Lukan and G. Lavigne, *J. Am. Chem. Soc.*, **2008**, 130, 11286.
- [143] C. C. Scarborough, A. Bergant, G. T. Sazama, I. A. Guzei and S. S. Stahl, *Tetrahedron*, **2009**, 65, 5084.
- [144] M. Iglesias, D. J. Beetstra, B. Kariuki, K. J. Cavell, A. Dervisi and J. W. Faller, *Eur. J. Inorg. Chem.*, **2009**, 1913.
- [145] U. Siemeling, C. Farber and C. Bruhn, *Chem. Commun.*, **2009**, 98.
- [146] A. Binobaid, M. Iglesias, D. J. Beetstra, B. Kariuki, A. Dervisi, J. W. Faller and K. J. Cavell, *Dalton Trans.*, **2009**, 7099.
- [147] M. Iglesias, D. J. Beetstra, A. Sasch, P. N. Horton, M. B. Hursthouse, A. Dervisi and I. A. Fallis, *Organometallics*, **2007**, 26, 4800.
- [148] M. Iglesias, D. J. Beetstra, J. C. Knight, L. Ooi, A. Stach, S. J. Coles, L. Male, M. B. Hursthouse, K. J. Cavell, A. Dervisi and I. Fallis, *Organometallics*, **2008**, 27, 3279.
- [149] R. Jazzar, B. Liang, B. Donnadiu and G. Bertrand, *J. Organomet. Chem.*, **2006**, 691, 3201.
- [150] J. T. Richeson, *Principle of catalyst development*; Plenum Press: New York, **1989**.
- [151] J. Hagen, *Industrial catalysis: a practical approach*; Wiley- VCH: Weinheim, **1999**.

[152] B. Cornils and W. A. Herrmann, *Eds. Applied homogeneous catalysis with organometallic compounds: A comprehensive textbook in 10 volumes*; VCH: Weinheim, **1996**.

[153] J. Schwarz, V. P. W. Böhm, M. G. Gardiner, M. Grosche, W. A. Herrmann, W. Hieber and G. Raudaschl-Sieber, *Chem. Eur. J.*, **2000**, *6*, 1773.

[154] M. C. Perry, X. Cui, M. T. Powell, D. R. Hou, J. H. Reibenspies and K. Burgess, *J. Am. Chem. Soc.*, **2003**, *125*, 113.

[155] V. Cesar, S. Bellemin-Laponnaz and L. H. Gade, *Chem. Eur. J.*, **2005**, *11*, 2862.

[156] M. Albrecht, J. R. Mięcznikowski, A. Samuel, J. W. Faller and R. H. Crabtree, *Organometallics*, **2002**, *21*, 3596.

[157] H. Seo, B. Y. Kim, J. H. Lee, H. J. Park, S. U. Son and Y. K. Chung, *Organometallics*, **2003**, *22*, 4783.

[158] A. Zapf and M. Beller, *Chem. Commun.*, **2005**, 431.

[159] A. C. Hillier, G. A. Grasa, M. S. Viciu, H. M. Lee, C. Yang and S. P. Nolan, *J. Organomet. Chem.*, **2002**, *653*, 69.

[160] N. Miyaura and A. Suzuki, *Chem. Rev.*, **1995**, *95*, 2457.

[161] A. Zapf, R. Jackstell, F. Rataboul, T. Riermeier, A. Monsees, C. Fuhrmann, N. Shaikh, U. Dingerdissen and M. Beller, *Chem. Commun.*, **2004**, *1*, 38.

[162] J. K. Stille, *Chem. Int. Ed. Engl.*, **1986**, *25*, 508.

[163] A. Sekia and N. Ishikawa, *J. Organometallic Chem.*, **1976**, *118*, 349.

[164] E. Erdik, *Tetrahedron*, **1992**, *48*, 77.

[165] D. Clyne, J. Jin, E. Genest, J. Gallucci and T. Rajanbabu, *Org. Lett.*, **2000**, *2*, 1125.

[166] A. Fursten, G. Seidel, D. Kremzow and C. W. Lehmann, *Organometallics*, **2003**, *22*, 907.

[167] N. Clement, K. J. Cavell, C. Jones and C. Elsevier, *Angew. Chem. Int. Ed. Engl.*, **2004**, *43*, 1277.

[168] W. A. Herrmann, M. Elison, J. Fischer, C. Kocher and G. R. Artus, *J. Angew. Chem. Int. Ed. Engl.*, **1995**, *34*, 2371.

- [169] L. D. Vazquez-Serrano, B. T. Owens and J. M. Buriak, *Chem. Commun.*, **2002**, 2518.
- [170] A. Pfaltz, J. Blum, R. Hilgraf, E. Hormann, F. McIntyre, M. Schöleber, S. P. Smidt, B. Wustenberg and N. Zimmermann, *Adv. Synth. Catal.*, **2003**, 345, 33.
- [171] S. Hashiguchi, A. Fujii, J. Takehara, T. Ikariya and R. Noyori, *J. Am. Chem. Soc.*, **1995**, 117, 7562.
- [172] A. T. Normand and K. J. Cavell, *Eur. J. Inorg. Chem.*, **2008**, 2781.
- [173] D. S. McGuinness and K. J. Cavell, *Organometallics*, **2000**, 19, 4918.
- [174] D. S. McGuinness, N. Saendig, B. F. Yates and K. J. Cavell, *J. Am. Chem. Soc.*, **2001**, 123, 4029.
- [175] C. C. Scarborough, B. V. Popp, I. A. Guzei and S. S. Stahl, *Organomet. Chem.*, **2005**, 690, 6143.
- [176] R. Jazzar, J. Bourg, R. D. Dewhurst, B. Donnadieu and G. Bertrand, *J. Org. Chem.*, **2007**, 72, 3492.
- [177] I. Ozdemir, N. Gurbuz, Y. Gok and B. Cetinkaya, *Heteroatom Chemistry*, **2008**, 19, 82.

Chapter Two

Synthesis of New Salt Precursors to Novel Expanded-Ring *N*- Functionalised Heterocyclic Carbenes

This synthetic methodology is often low-yielding when applied to the synthesis of expanded carbenes, which has limited the availability of the very basic, and unexplored 6- and 7-membered ring carbenes (Figure 2-1).^[1, 10]

In 2005, Stahl and co-workers reported the first example of a 7-membered amidinium salt **2.2**, which was synthesised in 65% yield (Figure 2-1).^[7]

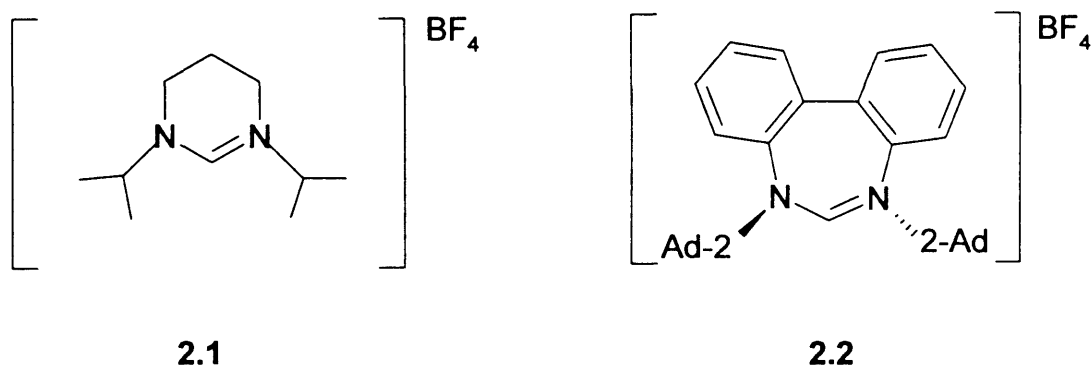
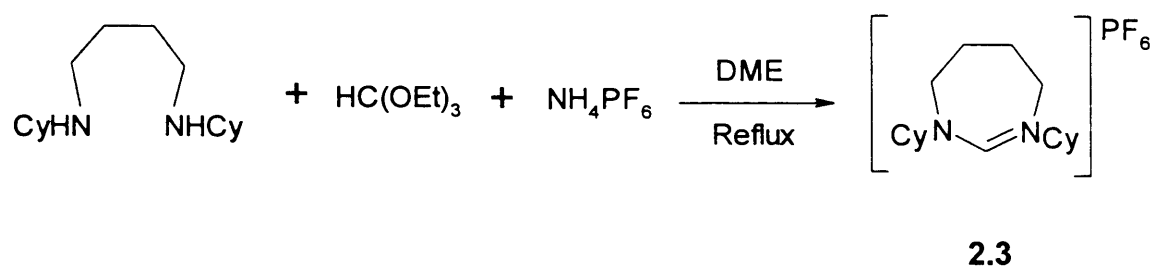


Figure 2-1: The first examples of expanded carbenes.

The synthesis of the amidinium salt **2.3** represented the first example of a completely saturated, unsubstituted, 7-membered carbene precursor.^[7, 10, 16]

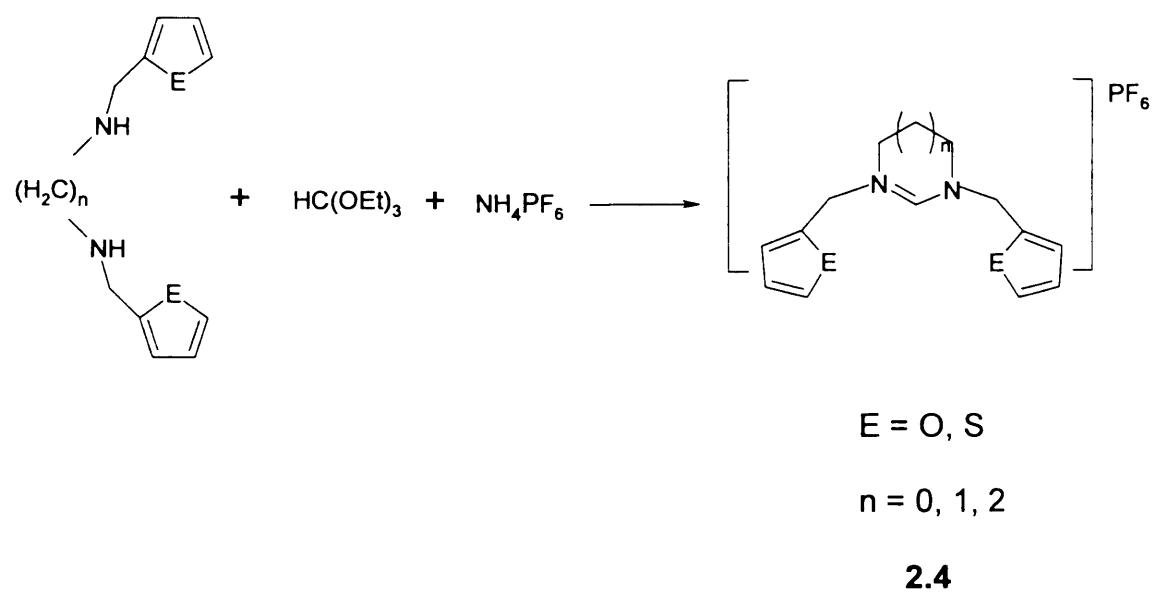
This salt was synthesised using the classic methodology of adding a formyl unit to the corresponding diamine.^[7] This method led to a low yield (10-20%).

Two equivalents of triethylorthoformate were reacted with the corresponding cyclohexyldiamine (Scheme 2-2).^[10, 16]



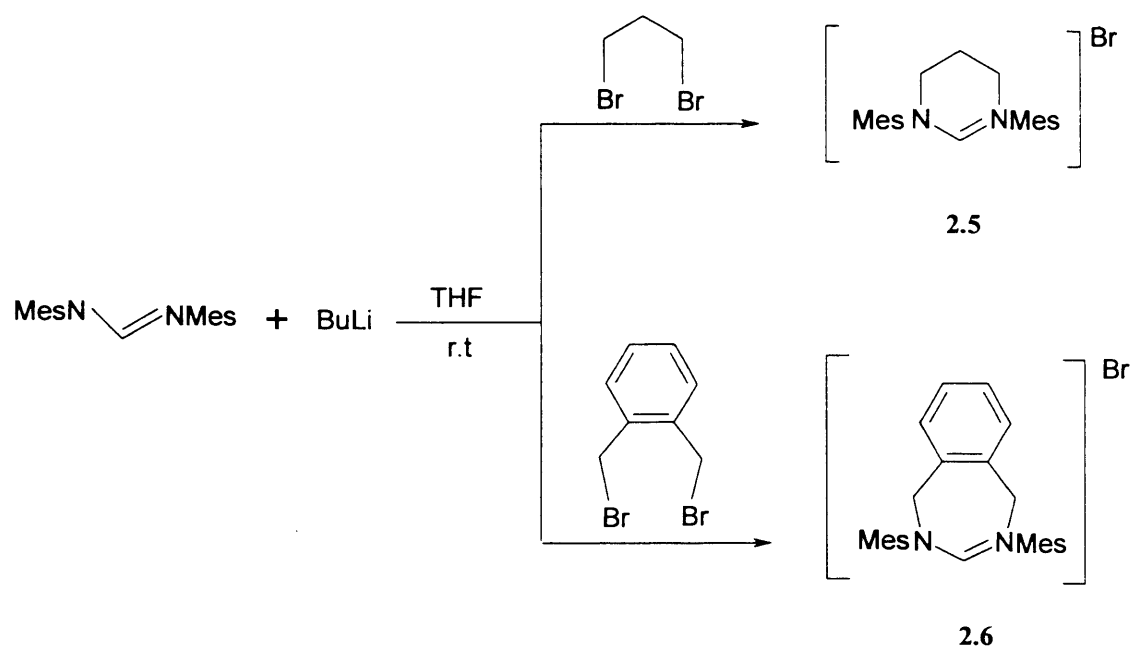
Scheme 2-2: Synthesis of amidinium salt **2.3**.

In recent years NHCs have attracted the attention of several research groups. Various NHC ligands have been synthesised within a short period of time. The symmetrical *N*-functionalised expanded NHC ligands **2.4** were prepared by Özdemir *et al.* Their synthesis was achieved by the reaction of diamines with triethylorthoformate and ammonium hexafluorophosphate (Scheme 2-3).^[17] All reactions for the preparation of these di-substituted NHC salts were carried out under argon using a standard Schlenk-type flask.



Scheme 2-3: Synthesis of 1,3-dialkylazolinium salts.

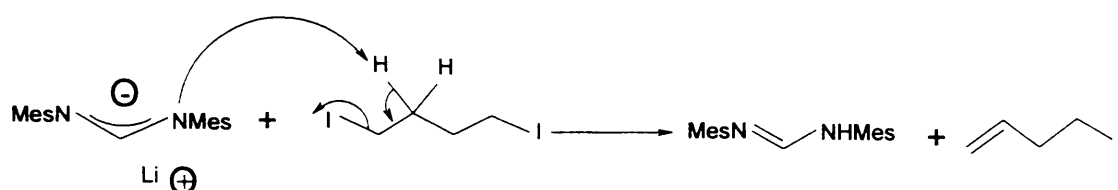
Recently, Bertrand *et al.* published the new method of ring-closure, in which an amidine fragment is first prepared then the ring closed with a dibromohydrocarbyl unit (Scheme 2-4).^[5]



Scheme 2-4: New method of ring- closure.

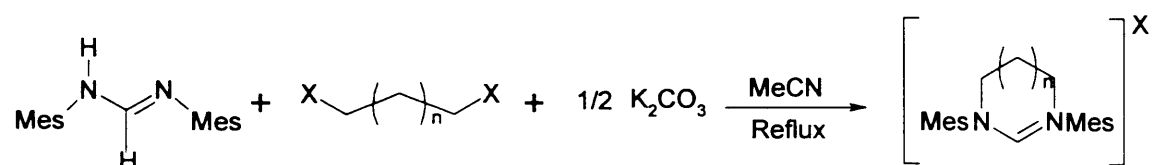
This new method proved to be very efficient for the synthesis of a range of azolium salts which included 6- and 7-membered ring salts (2.5 and 2.6 respectively) in better yield.^[4, 18]

The new method, reported by Bertrand,^[5] is limited by the nature of the di-electrophiles. For example, when applied to the synthesis of azolium salt by the ring-closure of 1,4-diiodobutane with a lithium salt of a formamidine, it unfortunately led to a low yield, probably due to HI-elimination (Scheme 2-5). Moreover, the use of BuLi requires the utilisation of Schlenk-tube techniques, which limits the scale of the reaction.



Scheme 2-5: Proposed decomposition pathway of the ring-closure method reported by Bertrand *et al.*

An improvement on Bertrand's method involved the use of highly polar solvent (MeCN) and a weaker base, such as potassium carbonate, in order to obtain a less basic nucleophile. For example, when half an equivalent of potassium carbonate was refluxed with dihalidealkane and formamidine in acetonitrile, it afforded a ring-closed product in an excellent yield (Scheme 2-6).^[10]



	Yield
2.7 (n = 0, X = Br)	76%
2.8 (n = 1, X = Br)	82%
2.9 (n = 2, X = I)	89%

Scheme 2-6: Synthesis of 5-, 6- and 7-membered saturated NHC salt in excellent yield.

The saturated expanded NHCs are more basic than their 5-membered equivalents.^[11] The main factor determining the basicity of the carbene is a greater NCN angle.^[19] Therefore, it is very important to synthesise a wider variety of new types of symmetrical and asymmetrical ligands using an expanded-ring system to provide control over basicity and the NCN angles.

2.2. Results and Discussion.

2.2.1. Preparation of Amidine Fragment.

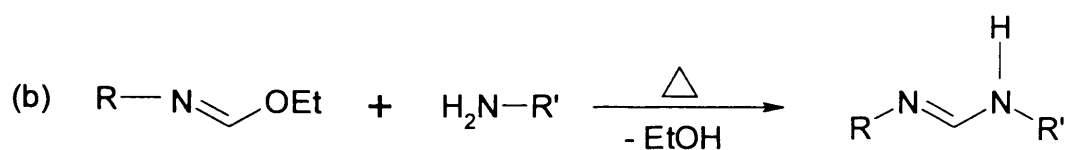
NHCs were classically prepared by closing the ring through the introduction of the CH⁺ fragment to the di-amines,^[3, 4, 20-30] which are often poorly reproducible when applied to the synthesis of expanded carbenes.^[8, 10, 12, 13] In the new method of ring-closure, a formamidine (amidine fragment) is first prepared and then the ring is closed.

2.2.1.1. Synthesis of New Asymmetrical Formamidines.

The synthesis of asymmetrical formamidines in excellent yield and facile separation was achieved in two steps.^[31-35] For example, in the first step, *o*-anisidine was reacted with two drops of acid and an excess of ethylorthoformate to form *o*-anisidylformimidate **2.11** (Scheme 2-7a). The asymmetrical formamidines were obtained by the reaction of formimidate with the corresponding aniline derivative, as shown in Scheme 2-7b.

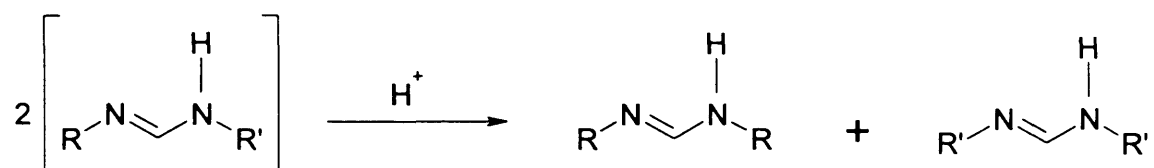
**Yield**

3

2.10 (R = Py)^[36] 60%**2.11** (R = *o*-MeOPh) 61%**2.12** (R = *o*-MeSPh) 64%**Yield****2.13** (R = Py, R' = Mes) 93%**2.14** (R = Py, R' = DIPP) 90%**2.15** (R = Py, R' = *o*-MeOPh) 91%**2.16** (R = *o*-MeOPh, R' = Mes) 92%**2.17** (R = *o*-MeOPh, R' = DIPP) 91%**2.18** (R = *o*-MeSPh, R' = Mes) 86%**2.19** (R = *o*-MeSPh, R' = DIPP) 72%**Scheme 2-7:** Synthesis of asymmetrical formamidines.

The use of catalytic amounts of hydrochloric acid and an excess of ethylorthoformate in the first step are essential for the success of the reaction. However, the second step of the reaction must be carried out in an acid-free environment because any traces of acid would cause the asymmetrical

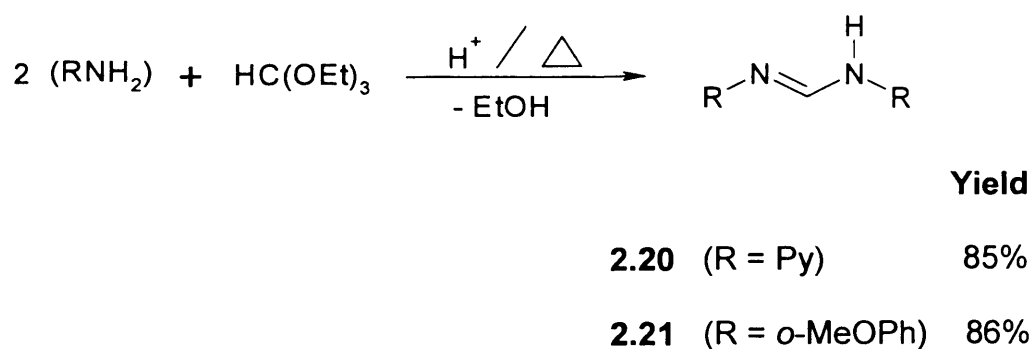
formamidines to undergo disproportionation to the corresponding symmetrical formamidines, as shown in Scheme 2-8.



Scheme 2-8: The impact of the presence of acid in the preparation of asymmetrical formamidines.

2.2.1.2. Synthesis of New Symmetrical Formamidines.

For the preparation of symmetrical formamidines a previously reported method has been used,^[37-39] but after employing some modification in order to improve productivity (Scheme 2-9).



Scheme 2-9: Reaction for symmetrical amidines.

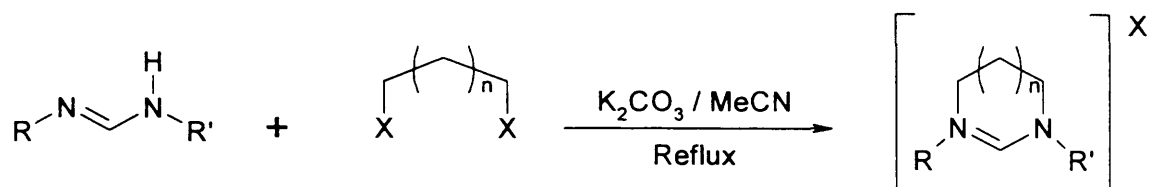
A mixture of amine, triethylorthoformate and a catalytic amount of acid are heated as depicted in Scheme 2-9. At approximately 110 °C, the ethanol began to distil. When 95% of the theoretical amount of ethanol had been collected, the mixture was allowed to cool slowly. Crystals were formed by recrystallisation from toluene and yields via this method were excellent.

2.2.2. Method of Ring-Closure.

2.2.2.1. Synthesis of Halide Salts.

Here we report a modified synthetic approach, which involves the addition of the formamidine to a compound featuring two “di-electrophile” leaving groups, and the use of a mild base, in this case potassium carbonate, in order to obtain a less basic nucleophile and prepare a wide range of NHC ligands in high yield.

This new synthetic approach has proved to be an effective method for the synthesis of 6- and 7-membered salts. For example, 1,3-dibromopropane or 1,4-diiodobutane and the formamidine derivative were refluxed with half an equivalent of potassium carbonate (heating is necessary to induce the ring-closure and cleanly obtain cyclic salts, presumably due to steric hindrance)^[5] to afford 6-membered-HBr or 7-membered-HI salts, respectively, in excellent yield. In order to prove the versatility of this method, we synthesised a wide range of salts using a variety of di-electrophiles and different types of formamidines (Scheme 2-10). All these salts were stable in air and moisture.



	Yield
2.22.HBr ($n = 1$, $R = \text{Py}$, $R' = \text{Mes}$)	80%
2.23.HBr ($n = 1$, $R = o\text{-MeOPh}$, $R' = \text{Mes}$)	82%
2.24.HBr ($n = 1$, $R = o\text{-MeOPh}$, $R' = \text{DIPP}$)	87%
2.25.HBr ($n = 1$, $R = R' = o\text{-MeOPh}$)	93%
2.26.HBr ($n = 1$, $R = o\text{-MeSPh}$, $R' = \text{Mes}$)	76%
2.27.HBr ($n = 1$, $R = o\text{-MeSPh}$, $R' = \text{DIPP}$)	72%
2.28.HI ($n = 2$, $R = \text{Py}$, $R' = \text{Mes}$)	76%
2.29.HI ($n = 2$, $R = o\text{-MeOPh}$, $R' = \text{Mes}$)	86%
2.30.HI ($n = 2$, $R = o\text{-MeOPh}$, $R' = \text{DIPP}$)	84%
2.31.HI ($n = 2$, $R = R' = o\text{-MeOPh}$)	88%

Scheme 2-10: Synthesis of 6- and 7-membered saturated NHC ligands.

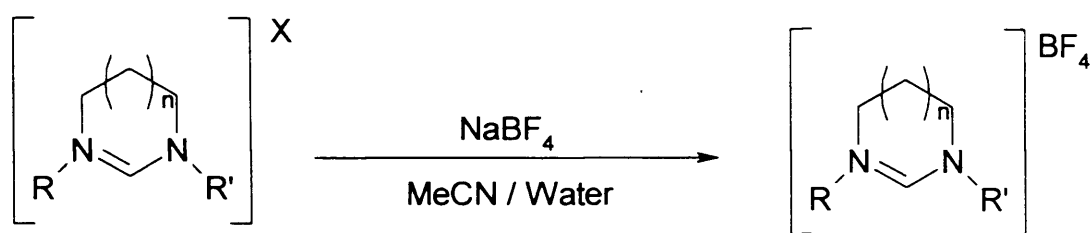
The solvent and excess dihalide were removed under vacuum and the resulting mixture was dissolved in dichloromethane, before filtering to remove the potassium salts. Slow addition of diethylether to the dichloromethane solution resulted in a high yield of pure product. Crystals suitable for X-ray analysis were obtained by the diffusion of diethylether into a dichloromethane solution of the NHC salt. The synthesis of these salts was confirmed by ^1H ,

^{13}C NMR, mass spectroscopy, micro-analysis and X-ray crystallographic determination.

The reaction in Scheme 2-10 proceeded rapidly for the larger ring sizes and lesser sterically congested amidines (for example 1,4-diiodobutane with **2.16** amidine needed 24 hours to close the ring), while decreasing the ring size or increasing steric congestion results in a longer reaction time (for example 1,3-dibromopropane with **2.17** amidine needed two weeks to close the ring). The 5-membered NHCs were not isolated when 1,2-dibromoethane was added to the corresponding amidine. Indeed, steric hindrance prevented the ring-closure reaction.

2.2.2.2. Formation of Tetrafluoroborate Salts – Counter-Anion Exchange.

All the halide salts were converted to tetrafluoroborate salts by mixing a solution of the halide salt in acetonitrile with a solution of an excess of sodium tetrafluoroborate in water (Scheme 2-11). The mixture was stirred for 10 minutes at room temperature. Evaporation of the solvent under vacuum resulted in the precipitation of solids in the remaining water. The product was dissolved in dichloromethane and the residual water was removed using a separating funnel. Slow addition of diethylether to the dichloromethane solution resulted in the crystallisation of the product in high yield.



- | | |
|--|------------------------------|
| 2.22. HBr (n = 1, R = Py, R' = Mes) | 2.22. HBF₄ |
| 2.23. HBr (n = 1, R = <i>o</i> -MeOPh, R' = Mes) | 2.23. HBF₄ |
| 2.24. HBr (n = 1, R = <i>o</i> -MeOPh, R' = DIPP) | 2.24. HBF₄ |
| 2.25. HBr (n = 1, R = R' = <i>o</i> -MeOPh) | 2.25. HBF₄ |
| 2.26. HBr (n = 1, R = <i>o</i> -MeSPh, R' = Mes) | 2.26. HBF₄ |
| 2.27. HBr (n = 1, R = <i>o</i> -MeSPh, R' = DIPP) | 2.27. HBF₄ |
| 2.28. HI (n = 2, R = Py, R' = Mes) | 2.28. HBF₄ |
| 2.29. HI (n = 2, R = <i>o</i> -MeOPh, R' = Mes) | 2.29. HBF₄ |
| 2.30. HI (n = 2, R = <i>o</i> -MeOPh, R' = DIPP) | 2.30. HBF₄ |
| 2.31. HI (n = 2, R = R' = <i>o</i> -MeOPh) | 2.31. HBF₄ |

Scheme 2-11: Counter-anion exchange.

It was possible to obtain the tetrafluoroborate salts in a one pot synthesis from the corresponding formamidines. A suspension of the formamidine with an (1-2) equivalent of the dihalide and a half-equivalent of potassium carbonate was refluxed in acetonitrile until the ring-closure was complete (as noted from the disappearance of the XCH_2 protons and appearance of the NCH_2 protons in the ^1H NMR). At the end of the reaction, 1.5 equivalent of sodium tetrafluoroborate in water solution was added to the reaction mixture.

After the mixture was stirred for 10 minutes, the solvent was removed under vacuum, the product dissolved in dichloromethane, separated from the remaining water and dried with magnesium sulphate. Slow addition of diethyl ether to the dichloromethane solution produced salts in virtually quantitative yields.

2.2.3. Solution NMR Studies.

During the preparation of the salt the reaction was followed with ^1H NMR and the reaction was complete with disappearance of the XCH_2 protons and appearance of NCH_2 protons (Figures 2-1 and 2-2).

The exchange of the counter-anion resulted in small shifts in the ^1H NMR and ^{13}C NMR. In the ^1H NMR spectra of the BF_4 salt (CDCl_3 solvent), the $\text{N-C}_{\text{NHC}}\text{H-N}$ proton was observed to move up-field while this type of change was only observed to a small extent in ^{13}C NMR (Table 2-1).

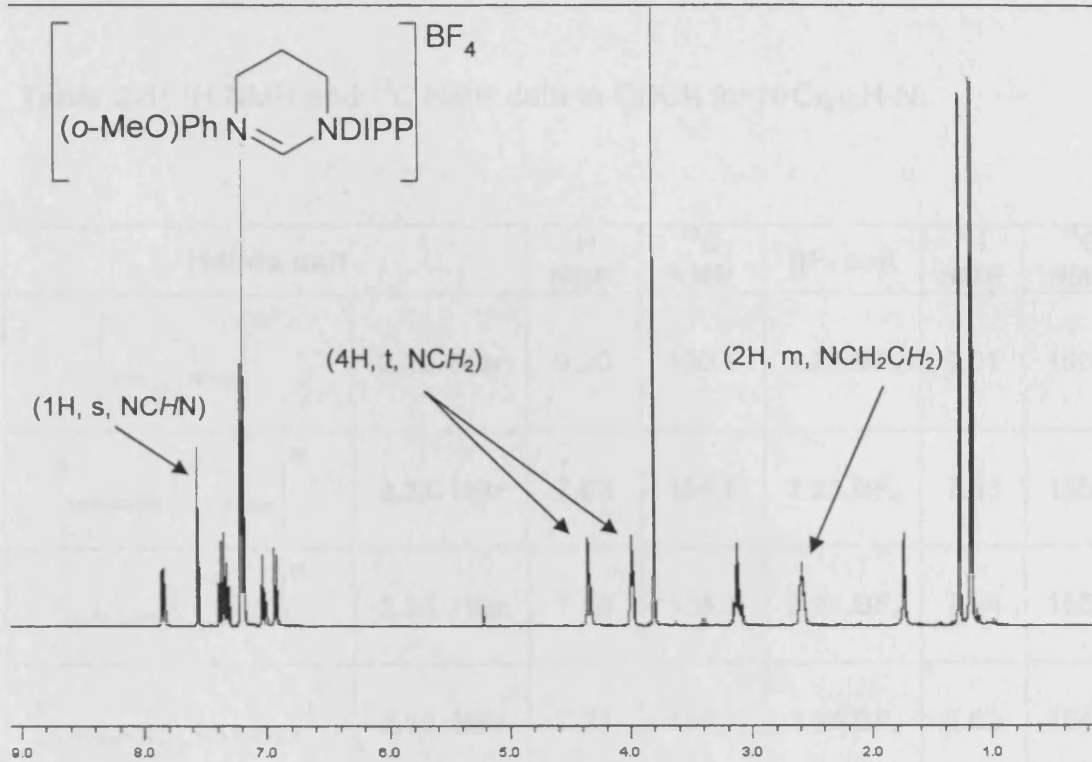


Figure 2-1: ^1H NMR (CDCl₃) for the 6-membered salt (2.24).

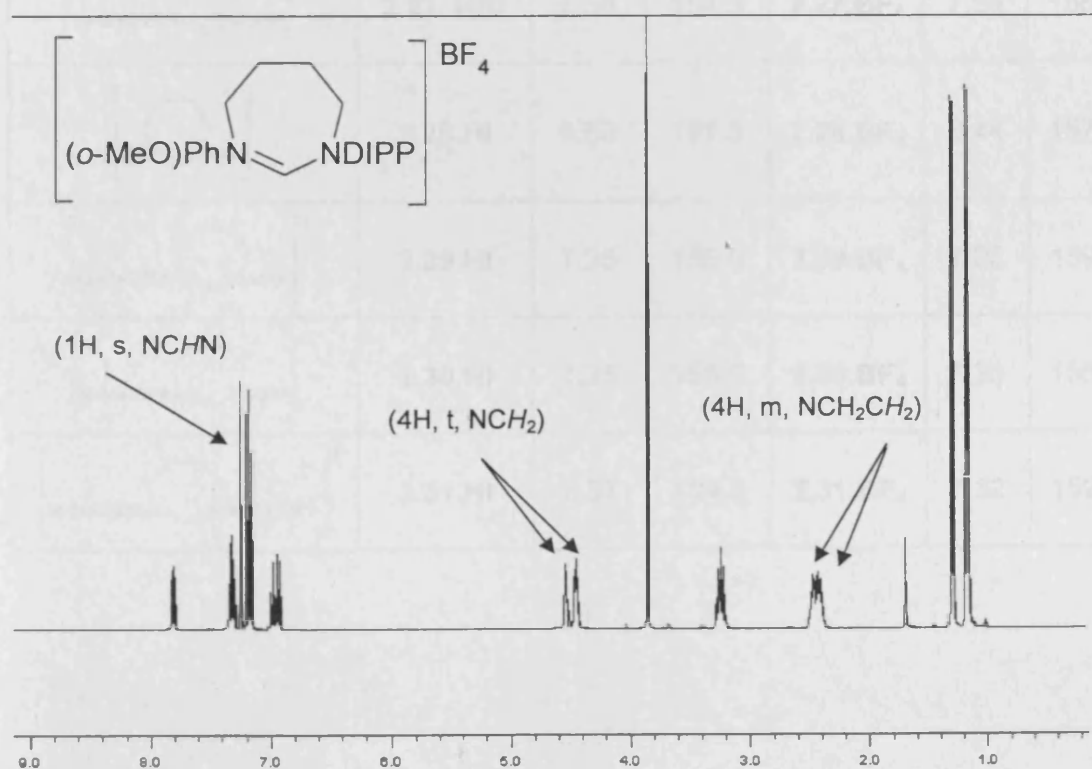
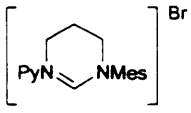
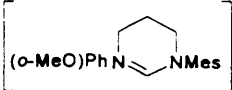
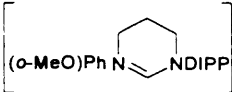
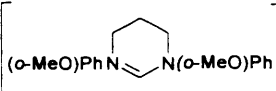
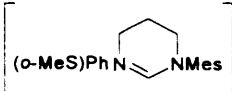
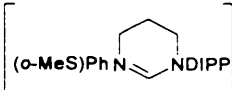
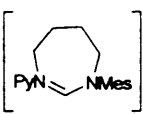
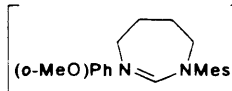
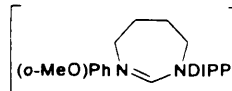
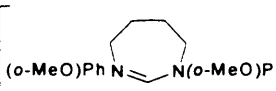


Figure 2-2: ^1H NMR (CDCl₃) for the 7-membered salt (2.30).

Chapter Two
 Synthesis of New Salt Precursors to Novel Expanded-Ring *N*-Functionalised
 Heterocyclic Carbenes

Table 2-1: ^1H NMR and ^{13}C NMR data in CDCl_3 for $\text{N-C}_{\text{NHCH-N}}$.

Halide salt	^1H NMR	^{13}C NMR	BF_4 salt	^1H NMR	^{13}C NMR	
	2.22.HBr	9.20	150.1	2.22.BF₄	9.01	150.3
	2.23.HBr	7.63	154.8	2.23.BF₄	7.53	155.1
	2.24.HBr	7.56	154.3	2.24.BF₄	7.54	158.7
	2.25.HBr	7.71	154.7	2.25.BF₄	7.62	154.6
	2.26.HBr	7.55	154.3	2.26.BF₄	7.44	154.1
	2.27.HBr	7.56	154.3	2.27.BF₄	7.54	158.7
	2.28.HI	8.53	157.5	2.28.BF₄	8.44	157.7
	2.29.HI	7.25	159.0	2.29.BF₄	7.22	159.2
	2.30.HI	7.25	158.0	2.30.BF₄	7.23	158.7
	2.31.HI	7.37	159.0	2.31.BF₄	7.32	159.2

In the ^1H NMR of the BF_4 salt, in CDCl_3 solvent, the $\text{N-C}_{\text{NCH}}\text{H-N}$ shifted up-field with increasing ring size, indicating reduced acidity for this hydrogen and increased basicity of the conjugate base of the free carbene.^[5, 10, 16, 17] A similar trend was not evident in the ^{13}C NMR for the amidinium carbon (the 7-membered rings are shifted down-field in comparison with the 6-membered rings).

2.2.4. X-Ray Analysis.

Single-crystal X-ray diffraction data were collected for the 6- and 7-membered salts and their ORTEP plots are shown in Figures 2-3 and 2-4 respectively.

Important bond lengths (\AA) and bond angles ($^\circ$) for the 6- and 7-membered salts are tabulated in Tables 2-2, 2-3, 2-4 and 2-5.

Chapter Two

Synthesis of New Salt Precursors to Novel Expanded-Ring *N*-Functionalised Heterocyclic Carbenes

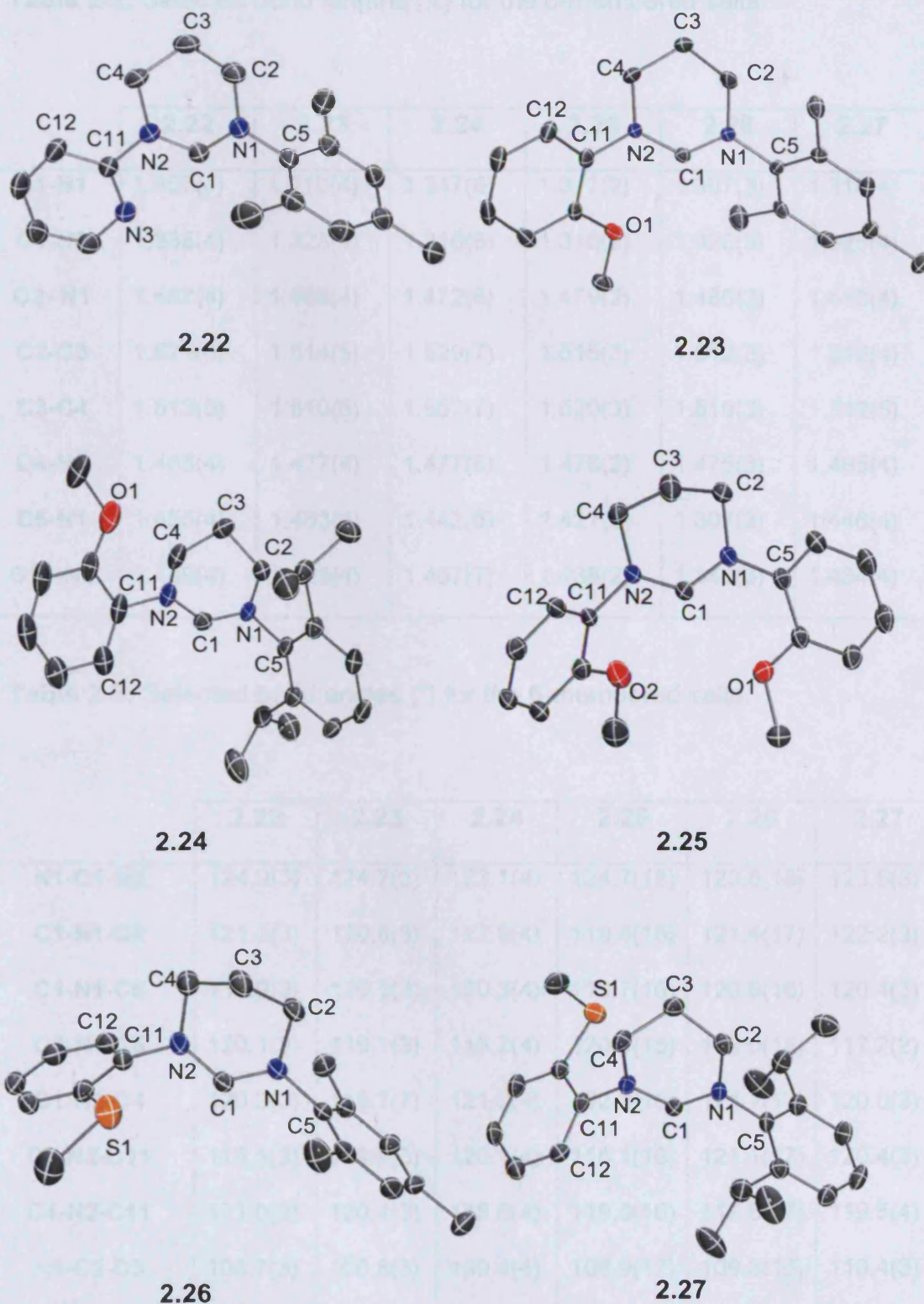


Figure 2-3: ORTEP ellipsoid plot at 30% probability of the 6-membered salts.

Hydrogen atoms and counter anions are omitted for clarity.

Table 2-2: Selected bond lengths (Å) for the 6-membered salts.

	2.22	2.23	2.24	2.25	2.26	2.27
C1-N1	1.307(4)	1.310(4)	1.347(6)	1.317(2)	1.307(3)	1.310(4)
C1-N2	1.338(4)	1.323(4)	1.316(6)	1.310(2)	1.320(3)	1.325(4)
C2-N1	1.482(4)	1.485(4)	1.472(6)	1.479(2)	1.480(3)	1.480(4)
C2-C3	1.521(6)	1.514(5)	1.529(7)	1.515(3)	1.512(3)	1.512(4)
C3-C4	1.513(5)	1.510(5)	1.557(7)	1.520(3)	1.510(3)	1.512(5)
C4-N2	1.485(4)	1.477(4)	1.477(6)	1.476(2)	1.475(3)	1.485(4)
C5-N1	1.455(4)	1.453(4)	1.442(6)	1.427(2)	1.307(3)	1/446(4)
C11-N2	1.439(4)	1.425(4)	1.457(7)	1.438(2)	1.441(3)	1.434(4)

Table 2-3: Selected bond angles (°) for the 6-membered salts.

	2.22	2.23	2.24	2.25	2.26	2.27
N1-C1-N2	124.9(3)	124.7(3)	123.1(4)	124.7(18)	123.8(18)	123.5(3)
C1-N1-C2	121.3(3)	120.6(3)	122.9(4)	119.8(16)	121.4(17)	122.2(3)
C1-N1-C5	117.9(3)	120.1(3)	120.3(4)	119.7(16)	120.6(16)	120.4(3)
C2-N1-C5	120.1(3)	119.1(3)	116.7(4)	120.3(15)	118.0(15)	117.2(2)
C1-N2-C4	120.3(3)	119.7(7)	121.0(4)	122.2(16)	121.1(17)	120.0(3)
C1-N2-C11	118.5(3)	119.9(3)	120.1(4)	118.1(16)	121.1(17)	120.4(3)
C4-N2-C11	121.0(3)	120.4(3)	118.6(4)	119.6(16)	117.8(17)	119.5(4)
N1-C2-C3	108.7(3)	108.8(3)	109.4(4)	108.9(17)	109.3(16)	110.4(3)
N2-C4-C3	109.8(3)	109.1(3)	108.6(4)	108.8(17)	109.6(19)	109.3(3)
C2-C3-C4	111.7(3)	109.1(3)	110.0(4)	110.9(18)	110.2(19)	110.1(3)

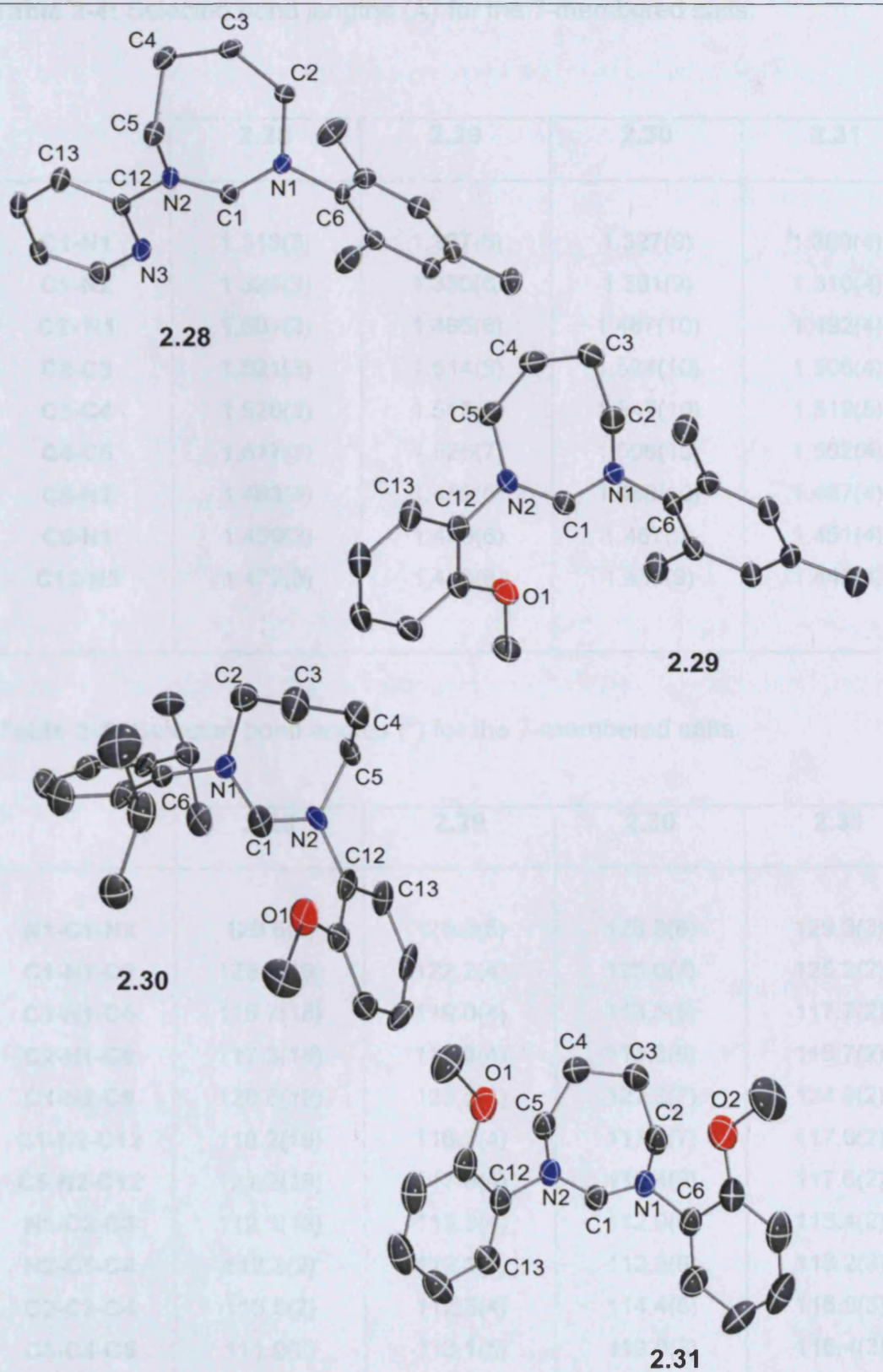


Figure 2-4: ORTEP ellipsoid plot at 30% probability of the 7-membered salts.

Hydrogen atoms and counter-anions are omitted for clarity.

Table 2-4: Selected bond lengths (Å) for the 7-membered salts.

	2.28	2.29	2.30	2.31
C1-N1	1.313(3)	1.307(6)	1.327(9)	1.309(4)
C1-N2	1.325(3)	1.330(6)	1.301(9)	1.310(4)
C2-N1	1.501(3)	1.485(6)	1.487(10)	1.492(4)
C2-C3	1.521(3)	1.514(8)	1.524(10)	1.506(4)
C3-C4	1.528(3)	1.515(8)	1.547(10)	1.519(5)
C4-C5	1.517(3)	1.526(7)	1.506(10)	1.502(4)
C5-N2	1.483(3)	1.489(6)	1.488(10)	1.487(4)
C6-N1	1.459(3)	1.459(6)	1.467(9)	1.451(4)
C12-N2	1.477(3)	1.446(6)	1.438(9)	1.445(4)

Table 2-5: Selected bond angles (°) for the 7-membered salts.

	2.28	2.29	2.30	2.31
N1-C1-N2	126.6(2)	126.2(5)	126.8(8)	129.3(3)
C1-N1-C2	125.1(19)	122.2(4)	125.0(7)	125.2(2)
C1-N1-C6	116.7(18)	119.0(4)	118.5(8)	117.7(2)
C2-N1-C6	117.3(18)	117.3(4)	116.3(6)	116.7(2)
C1-N2-C5	120.6(19)	125.3(4)	122.6(7)	124.9(2)
C1-N2-C12	118.2(19)	116.7(4)	117.8(7)	117.0(2)
C5-N2-C12	121.2(19)	117.9(4)	119.4(6)	117.6(2)
N1-C2-C3	112.1(18)	113.3(4)	112.9(6)	113.4(2)
N2-C5-C4	112.3(2)	112.1(4)	112.3(6)	113.2(3)
C2-C3-C4	113.5(2)	112.3(4)	114.4(6)	116.9(3)
C3-C4-C5	111.0(2)	113.1(5)	112.0(8)	116.4(3)

When the saturated 6- and 7-membered salts were compared with similar 5-membered salts, a widening of the NCN angle (126° - 129° for the 7-membered salts, and 123° - 124° for the 6-membered salts) was observed as the size of the ring increased but there was no significant difference in bond lengths (Tables 2-2 and 2-4), and they are consistent with the values reported in the literature.^[5, 10, 16, 17] There is a significant increase noted in the NCN angle between the expanded carbenes and that generally reported (115°) for the 5-membered imidazolium salts (Tables 2-3 and 2-5).^[40-43]

The C1-N1-C2 and C1-N2-C5 carbon ring angles in the 7-membered salts range from 121° to 125° . This fact, together with the large N-C1-N angle forced the carbene ring of the salt to adopt a chair type conformation with C3 and C4 above or below the N-C-N plane.^[10, 16]

The torsional angle (β) defined by the angle between C2-N1....N2-C5, in the 7-membered salt, or C2-N1....N2-C4, in the 6-membered salt, functions as a mechanism to release the steric tension resulting from the expansion of the ring. For example the twisting of the ring in the 7-membered salt (**2.30**) results in a torsional angle of 28.26° , whereas in the analogous 6-membered salt (**2.24**) the torsional angle deviated from planarity by only 5.27° .

The expansion of the ring from 6- to 7-membered does not lead to a significant augmentation of the NCN angle. In this case, the additional strain arising from the expansion of the ring results in an increase of the torsion angle (β) and a tetrahedral deviation of the ring carbon atoms (Tables 2-6 and 2-7).

Table 2-6: The torsion angle (β) ($^\circ$) in the 6-membered salts.

Salt	2.22	2.23	2.24	2.25	2.26	2.27
C2N1....N2C4 (β) ($^\circ$)	1.67	0.45	5.27	3.88	0.17	5.92

Table 2-7: The torsion angle (β) ($^\circ$) in the 7-membered salts.

Salt	2.28	2.29	2.30	2.31
C2N1....N2C5 (β) ($^\circ$)	29.06	26.36	28.26	0.99

The dihedral angle between the functional group (Py, *o*-MeOPh and *o*-MeSPh) and the carbene ring is shown in Tables 2-8 and 2-9.

The dihedral angle between the (C4-N2-C11-C12) in the **2.24** salt is approximately 114.30° while the dihedral angle between the (C5-N2-C12-C13) of the **2.30** salt is 51.82° .

Table 2-8: The dihedral angles ($^{\circ}$) between the (C4-N2-C11-C12) in the 6-membered salts.

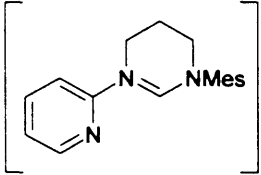
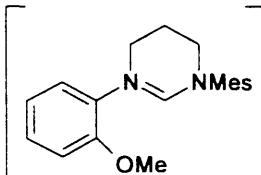
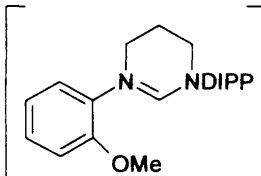
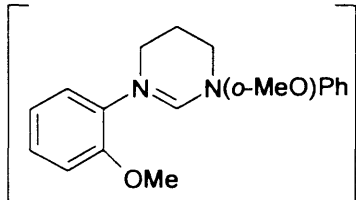
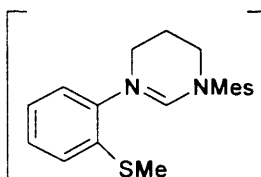
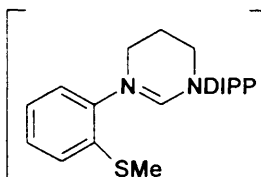
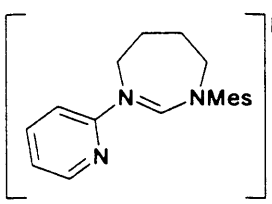
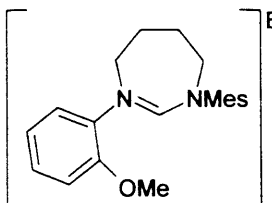
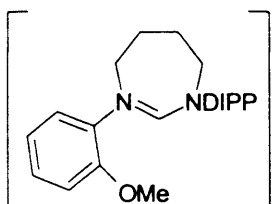
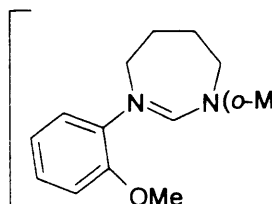
Salt	Dihedral angle ($^{\circ}$)
	1.91
	53.80
	114.30
	75.71
	86.20
	105.95

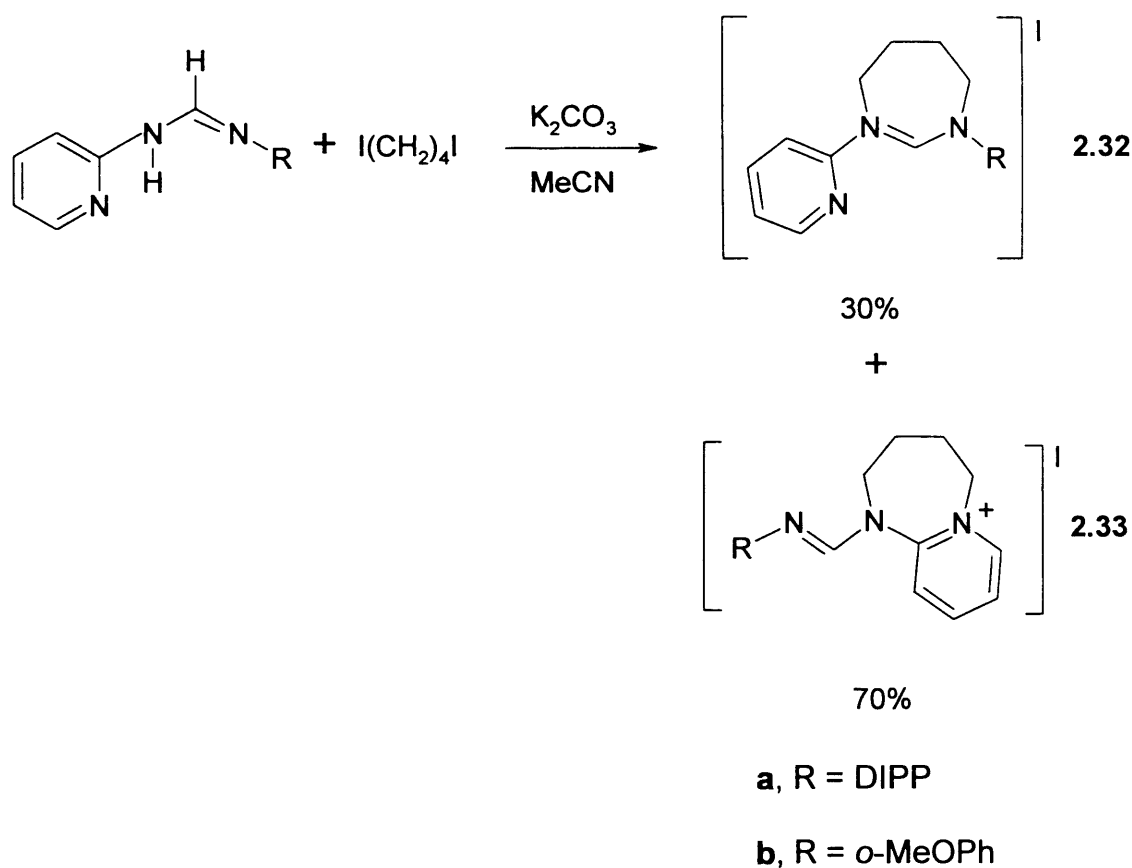
Table 2-9: The dihedral angles ($^{\circ}$) between the (C5-N2-C12-C13) in the 7-membered salts.

Salt	Dihedral angle ($^{\circ}$)
 <p style="text-align: center;">2.28</p>	14.14
 <p style="text-align: center;">2.29</p>	54.44
 <p style="text-align: center;">2.30</p>	51.82
 <p style="text-align: center;">2.31</p>	103.33

2.2.5. Synthesis of Compounds with Alternative Ring-Closure.

It is noteworthy that, despite the versatility of the new method for ring-closure, some attempts were unsuccessful because of the nature of the *N*-

substituent. During the synthesis of salts containing a pyridine substituent, **2.32**, an alternative ring-closure, via the N of the pyridine ring, was observed, giving rise to a novel ionic-fused ring product **2.33** (Scheme 2-12).



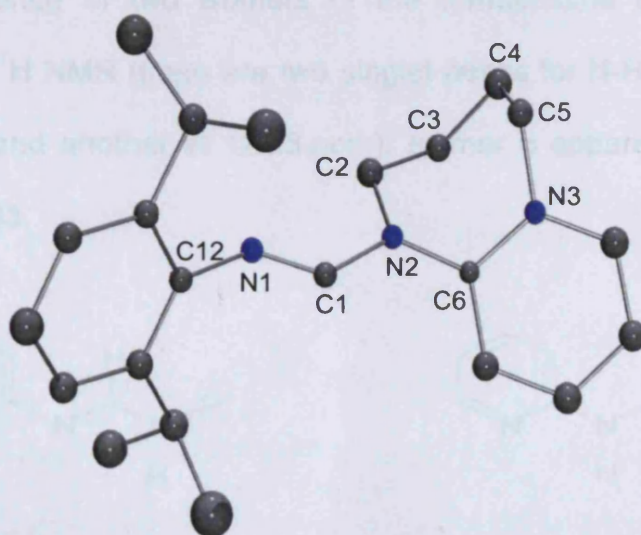
Scheme 2-12: Synthesis of a novel ionic-fused ring product.

The most notable changes in the ^1H NMR spectra of isomer **2.32** and **2.33** are the *NCHN* and the *o*-pyridine proton resonances. The pyridine proton adjacent to the nitrogen shows a large down-field shift from 8.25 ppm in **2.32** compared to 9.68 ppm in **2.33** (Table 2.10).

Table 2-10: ^1H NMR data in CDCl_3 for compounds **2.32a** and **2.33a**.

	^1H NMR			
	NCHN (s, 1H)	<i>o</i> -pyridine proton	NCH ₂ (t, 2H)	NCH ₂ CH ₂ (m, 2H)
2.32a	8.59	8.25	4.93 , 4.44	2.51 , 2.42
2.33a	7.69	9.68	4.98 , 4.14	2.34 , 2.01

Separation of **2.32** and **2.33** was achieved using toluene. Compound **2.33a** was obtained as yellow crystals which were characterised by single crystal X-ray analysis (Figure 2-5). Selected bond lengths and bond angles for compound **2.33a** are shown in Table 2-11.

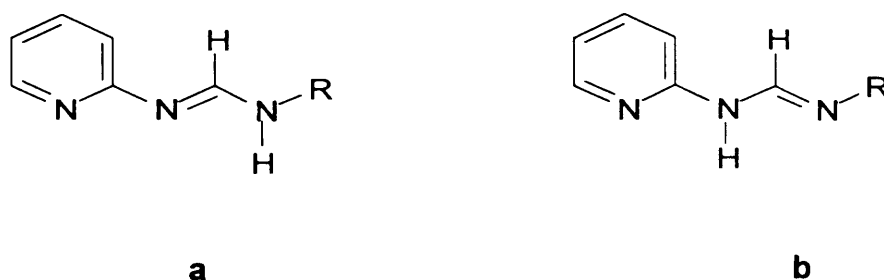
**Figure 2-5:** ORTEP ellipsoid plot at 30% probability of the compound **2.33a**.

Hydrogen atoms and the counter- anion are omitted for clarity.

Table 2-11: Selected bond lengths (Å) and bond angles (°) for **2.33a**.

Lengths (Å)		Angles(°)	
C1-N1	1.266(12)	N1-C1-N2	119.5(8)
C1-N2	1.399(11)	C1-N2-C6	119.4(7)
C2-N1	1.500(12)	N2-C6-N3	118.5(7)
C12-N1	1.419(11)	C6-N3-C5	119.7(8)
C6-N2	1.368(12)	N3-C5-C4	112.1(8)
C6-N3	1.378(11)	C5-C4-C3	110.6(8)
C5-N3	1.475(11)	C4-C3-C2	113.0(8)
C5-C4	1.531(14)	C2-N2-C6	124.3(7)
C4-C3	1.540(14)	C1-N1-C12	120.0(8)
C3-C2	1.005(10)		

The formation of the two compounds, **2.32** and **2.33**, would appear to result from the presence of two isomers of the formamidine (Figure 2-6), as indicated from ^1H NMR (there are two singlet peaks for N-H, R = DIPP, one at 10.11 ppm and another at 12.23.ppm). Isomer **b** apparently favours the formation of **2.33**.

**Figure 2-6:** The two isomers of the formamidine.

2.3. Experimental.

General remarks.

The solvents (dichloromethane, acetonitrile and diethylether) were used as purchased. All reagents (1,3-dibromopropane, 1,4-diiodobutane, 2-aminopyridine, *o*-anisidine, 2-(methylmercapto)aniline, 2,4,6-trimethylaniline, 2,6-diisopropylaniline, triethylorthoformate and sodium tetrafluoroborate) were used as received. ^1H and ^{13}C $\{^1\text{H}\}$ NMR spectra were obtained on Bruker Avance AMX 400, 500 or Jeol Eclipse 300 spectrometers. The chemical shifts are given as dimensionless δ values and are frequency-referenced relative to TMS. Coupling constants J are given in hertz (Hz) as positive values regardless of their real individual signs. High-resolution mass spectra were obtained in electrospray (ES) mode, unless otherwise reported, on a Waters Q-TOF micromass spectrometer.

General protocol for the synthesis of the halide salts.

A mixture of 1 mmol of amidine, 0.5 mmol of K_2CO_3 and 1-2 mmol of dihalide in 25 ml of acetonitrile was heated under reflux. At the end of the reaction, the volatiles were removed under vacuum and the residue freed of residual solvent by stirring with 3 portions of 5 ml of dichloromethane which were subsequently pumped off. The residue is dissolved in 5 ml of

dichloromethane and filtered through filter paper. Ether was slowly added to the resulting dichloromethane solution until the product started crystallising.

General protocol for the synthesis of the tetrafluoroborate salts.

A mixture of 1 mmol of salt in 10 ml of acetonitrile and 1.5 mmol of NaBF₄ in 10 ml of distilled water. The mixture was evaporated until a yellow solid product precipitated in the aqueous layer. The filtered product was dissolved in dichloromethane. By using a separating funnel the yellow organic layer was isolated and dried with magnesium sulphate. Ether was slowly added to the resulting dichloromethane solution until the product started crystallising.

Ethylanisidylformimidate (2.11).

COc1ccc(N=C(OCC)O)cc1 *o*-Anisidine (24.6g, 0.20 mol), triethylorthoformate (50ml, excess) and two drops of 2M HCl were

charged in to a 200 ml flask. The flask was heated slowly using a heating mantle. At approximately (110 °C), ethanol began to distil. When 95% (22ml) of the theoretical amount of ethanol had been collected, the flask was allowed to cool slowly. The excess of triethylorthoformate was removed by vacuum distillation at (60-80 °C) using a pump (10 mmHg). Upon further heating, the final product, a pale yellow liquid distilled at (100-120 °C). The yield was 22g, 61%.

¹H NMR (CDCl₃, 400 MHz, 298 K): δ 7.63 (1H, s, NCH), 7.02 (1H, d, *o*-CH), 6.96 (1H, t, *m*-CH), 6.80 (1H, t, *p*-CH), 6.73 (2H, d, *m*-CH), 4.27 (2H, q,

OCH₂CH₃), 3.72 (3H, s, OCH₃) 1.29 (3H, t, OCH₂CH₃). ¹³C NMR (CDCl₃, 100 MHz, 298 K): δ 156.2 (s, NCN), 152.3 (s, Ar-C), 151.7 (s, Ar-C), 125.3 (s, Ar-CH), 122.6 (s, Ar-CH), 121.5 (s, Ar-CH), 111.7 (s, Ar-CH), 62.6 (s, OCH₂CH₃), 55.9 (s, OCH₃), 14.7 (s, OCH₂CH₃).

Ethyl (2-methylthiophenyl) formimidate (2.12).

2-(methylmercapto)aniline (27.8 g, 0.20 mol),
triethylorthoformate (50 ml, excess) and two

drops of 2M HCl were charged in to a 200 ml flask. The flask was heated slowly using a heating mantle. At approximately (110 °C), ethanol began to distil. When 95% (22 ml) of the theoretical amount of ethanol had been collected, the flask was allowed to cool slowly. The excess of triethylorthoformate was removed by vacuum distillation at (60-80 °C) using a pump (10 mmHg). Upon further heating, the final product, a pale yellow liquid, distilled at (120-150 °C). The yield was 21g, 64%.

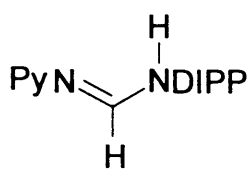
¹H NMR (CDCl₃, 400 MHz, 298 K): δ 7.53 (1H, s, NCH), 7.00 (1H, d, *o*-CH), 6.95 (1H, t, *m*-CH), 6.92 (1H, t, *p*-CH), 6.64 (2H, d, *m*-CH), 4.27 (2H, q, OCH₂CH₃), 2.28 (3H, s, SCH₃), 1.31 (3H, t, OCH₂CH₃). ¹³C NMR (CDCl₃, 100 MHz, 298 K): δ 155.4 (1C, s, NCHN), 145.5 (1C, s, Ar-C), 133.3 (1C, s, Ar-C), 125.4 (s, Ar-CH), 125.2 (s, Ar-CH), 124.7 (s, Ar-CH), 119.6 (s, Ar-CH), 63.1 (s, OCH₂CH₃), 14.9 (s, SCH₃), 14.7 (s, OCH₂CH₃).

N-(2-pyridyl) -N` - (2, 4, 6-trimethylphenyl) formamidine (2.13).

A 50 ml acid-free flask was charged with ethylpyridylformimidate (4.50 g, 30.0 mmol) and 2,4,6-trimethylaniline (4.05 g, 30.0 mmol). The mixture

solidified after stirring for 1 hour at 50 °C. The residue was recrystallised from toluene affording white crystals. Yield: 6.7 g (93%).

¹H NMR (CDCl₃, 400 MHz, 298 K): δ 8.94 (1H, s, *NH*), 8.43 (1H, s, *NCHN*), 8.15 (1H, d, *m-CH_{Py}*), 7.52 (1H, t, *p-CH_{Py}*), 7.31 (1H, d, *o-CH_{Py}*), 6.88 (1H, t, *m-CH_{Py}*), 6.83 (2H, s, *m-CH_{Mes}*), 2.26 (3H, s, *p-CH_{3 Mes}*), 2.12 (6H, s, *o-CH_{3 Mes}*). ¹³C NMR (CDCl₃, 100 MHz, 298 K): δ 154.4 (s, *NCN*), 150.4 (s, *Ar-C_{Py}*), 148.1 (s, *Ar-CH_{Py}*), 138.0 (s, *Ar-C_{Mes}*), 129.3 (s, *Ar-C_{Mes}*), 128.8 (s, *Ar-C_{Mes}*), 121.9 (s, *Ar-CH_{Mes}*), 117.4 (s, *Ar-CH_{Py}*), 111.5 (s, *Ar-CH_{Py}*), 20.8 (s, *p-CH₃*), 18.6 (s, *o-CH₃*).

N-(2-pyridyl) -N` - (2, 6-diisopropylphenyl) formamidine (2.14).

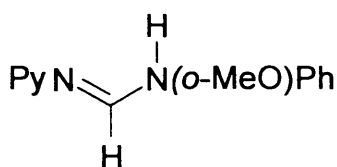
A 50 ml acid-free flask was charged with ethylpyridylformimidate (4.50 g, 30.0 mmol) and 2,6-diisopropylaniline (5.32 g, 30.0 mmol). The mixture

solidified after stirring for 1 hour at 50 °C. The residue was recrystallised from toluene affording white crystals. Yield: 7.6 g (90%).

¹H NMR (CDCl₃, 400 MHz, 298 K): δ 10.07 (1H, s, *NH*), 8.41 (1H, s, *NCHN*), 8.13 (1H, d, *o-CH_{Py}*), 7.35 (1H, t, *p-CH_{Py}*), 7.15 (1H, t, *p-CH_{DIPP}*), 7.11 (1H, d, *m-CH_{Py}*), 6.86 (1H, t, *m-CH_{Py}*), 6.58 (2H, d, *m-CH_{DIPP}*), 3.16 (2H, sept.,

$\text{CH}(\text{CH}_3)_2$ DIPP), 1.24 (6H, d, $\text{CH}(\text{CH}_3)_2$ DIPP), 1.21 (6H, d, $\text{CH}(\text{CH}_3)_2$ DIPP). ^{13}C NMR (CDCl_3 , 100 MHz, 298 K): δ 153.7 (s, NCN), 148.9 (s, Ar- C_{Py}), 140.7 (s, Ar- CH_{Py}), 139.1 (s, Ar- C_{DIPP}), 124.2 (s, Ar- C_{DIPP}), 123.5 (s, Ar- CH_{DIPP}), 122.3 (s, Ar- CH_{Py}), 118.6 (s, Ar- CH_{DIPP}), 111.1 (s, Ar- CH_{Py}), 109.2 (s, Ar- CH_{Py}), 28.9 (s, $\text{CH}(\text{CH}_3)_2$), 24.2 (s, $\text{CH}(\text{CH}_3)_2$), 23.9 (s, $\text{CH}(\text{CH}_3)_2$).

N-(2-pyridyl)-N'-(2-anisidyl) formamidine (2.15).

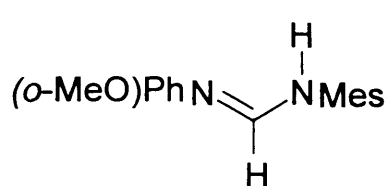


A 50 ml acid-free flask was charged with ethylpyridylformimidate (4.50 g, 30.0 mmol) and *o*-anisidine (3.69 g, 30.0 mmol). The mixture

solidified after stirring for 1 hour at 50 °C. The residue was recrystallised from toluene affording white crystals. Yield: 6.2 g (91%).

^1H NMR (CDCl_3 , 400 MHz, 298 K): δ 9.02 (1H, s, NH), 8.43 (1H, d, *o*- CH_{Py}) 8.26 (1H, d, *o*- $\text{CH}_{\text{o-MeOPh}}$), 7.61 (1H, s, NCHN), 7.52 (1H, t, *p*- CH_{Py}), 7.17 (1H, t, *m*- $\text{CH}_{\text{o-MeOPh}}$), 7.14 (1H, d, *m*- CH_{Py}), 6.93 (1H, t, *m*- CH_{Py}), 6.91 (1H, t, *p*- $\text{CH}_{\text{o-MeOPh}}$), 6.83 (1H, d, *m*- $\text{CH}_{\text{o-MeOPh}}$), 3.77 (3H, s, $\text{OCH}_{3\text{o-MeOPh}}$). ^{13}C NMR (CDCl_3 , 100 MHz, 298 K): δ 149.7 (s, NCN), 148.7 (s, Ar- C_{Py}), 147.2 (s, Ar- $\text{C}_{\text{o-MeOPh}}$), 146.5 (s, Ar- CH_{Py}), 138.4 (s, Ar- $\text{C}_{\text{o-MeOPh}}$), 129.5 (s, Ar- $\text{CH}_{\text{o-MeOPh}}$), 124.2 (s, Ar- $\text{CH}_{\text{o-MeOPh}}$), 122.5 (s, Ar- CH_{Py}), 121.5 (s, Ar- $\text{CH}_{\text{o-MeOPh}}$), 118.9 (s, Ar- CH_{Py}), 116.9 (s, Ar- $\text{CH}_{\text{o-MeOPh}}$), 114.6 (s, Ar- $\text{CH}_{\text{o-MeOPh}}$), 56.0 (s, OCH_3).

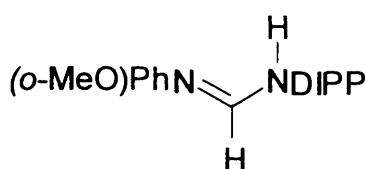
***N*-(2-anisidyl)-*N'*-(2, 4, 6-trimethylphenyl) formamidine (2.16).**



A 50 ml acid-free flask was charged with ethylanisidylformimidate (5.37 g, 30.0 mmol) and 2,4,6-Trimethylaniline (4.05 g, 30.0 mmol). The mixture solidified after stirring for 3 hours at 50 °C. The residue was recrystallised from toluene affording white crystals. Yield: 7.4 g (92%).

¹H NMR (CDCl₃, 400 MHz, 298 K): δ 7.71 (1H, d, *o*-CH_{o-MeOPh}), 7.62 (1H, s, NCHN), 7.37 (1H, s, NH), 6.95 (1H, t, *m*-CH_{o-MeOPh}), 6.86 (1H, t, *p*-CH_{o-MeOPh}), 6.75 (1H, d, *m*-CH_{o-MeOPh}), 6.52 (2H, s, *m*-CH_{Mes}), 3.19 (3H, s, OCH₃ *o*-MeOPh), 2.12 (3H, s, *p*-CH₃ Mes), 2.04 (6H, s, *o*-CH₃ Mes). ¹³C NMR (CDCl₃, 100 MHz, 298 K): δ 148.4 (s, NCN), 142.8 (s, Ar-C_{o-MeOPh}), 130.0 (s, Ar-C_{Mes}), 129.3 (s, Ar-C_{Mes}), 129.1 (s, Ar-C_{Mes}), 128.5 (s, Ar-C_{o-MeOPh}), 123.1 (s, Ar-CH_{o-MeOPh}), 122.4 (s, Ar-CH_{Mes}), 121.4 (s, Ar-CH_{o-MeOPh}), 114.5 (s, Ar-CH_{o-MeOPh}), 111.2 (s, Ar-CH_{o-MeOPh}), 56.1 (s, OCH₃), 21.1 (s, *p*-CH₃), 19.1 (s, *o*-CH₃).

***N*-(2-anisidyl)-*N'*-(2, 6-diisopropylphenyl) formamidine (2.17).**

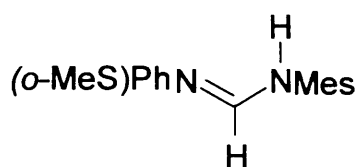


A 50 ml acid-free flask was charged with ethylanisidylformimidate (5.37 g, 30.0 mmol) and 2,6-diisopropylaniline (5.32 g, 30.0 mmol).

The mixture solidified after stirring for 3 hours at 50 °C. The residue was recrystallised from toluene affording white crystals. Yield: 8.5 g (91%).

^1H NMR (CDCl_3 , 400 MHz, 298 K): δ 7.84 (1H, d, *o*- $\text{CH}_{\text{O-MeOPh}}$), 7.77 (1H, s, NCHN), 7.44 (1H, s, NH), 7.29 (1H, t, *m*- $\text{CH}_{\text{O-MeOPh}}$), 7.10 (1H, t, *P*- CH_{DIPP}), 6.94 (2H, d, *m*- CH_{DIPP}), 6.87 (1H, t, *p*- $\text{CH}_{\text{O-MeOPh}}$), 6.75 (1H, d, *m*- $\text{CH}_{\text{O-MeOPh}}$), 3.86 (3H, s, $\text{OCH}_3_{\text{O-MeOPh}}$), 3.14 (2H, sept., $\text{CH}(\text{CH}_3)_2_{\text{DIPP}}$), 1.25 (12H, d, $\text{CH}(\text{CH}_3)_2_{\text{DIPP}}$). ^{13}C NMR (CDCl_3 , 100 MHz, 298 K): δ 148.2 (s, NCN), 147.2 (s, Ar- $\text{C}_{\text{O-MeOPh}}$), 143.2 (s, Ar- C_{DIPP}), 140.6 (s, Ar- C_{DIPP}), 139.2 (s, Ar- $\text{C}_{\text{O-MeOPh}}$), 124.2 (s, Ar- $\text{CH}_{\text{O-MeOPh}}$), 123.8 (s, Ar- CH_{DIPP}), 123.3 (s, Ar- CH_{DIPP}), 121.6 (s, Ar- $\text{CH}_{\text{O-MeOPh}}$), 114.7 (s, Ar- $\text{CH}_{\text{O-MeOPh}}$), 111.2 (s, Ar- $\text{CH}_{\text{O-MeOPh}}$), 56.1 (s, OCH_3), 28.2 (s, $\text{CH}(\text{CH}_3)_2$), 24.1 (s, $\text{CH}(\text{CH}_3)_2$), 23.9 (s, $\text{CH}(\text{CH}_3)_2$).

N-(2-methylthiophenyl)-N'-(2, 4, 6-trimethylphenyl) formamidine (2.18).



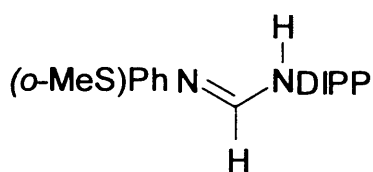
A 50 ml acid-free flask was charged with ethyl(2-methylthiophenyl)formimidate (5.85 g, 30.0 mmol) and 2,4,6-Trimethylaniline (4.05 g, 30.0

mmol). The mixture solidified after stirring for 3 hours at 50 °C. The residue was recrystallised from toluene affording white crystals. Yield: 7.3 g (86%).

^1H NMR (CDCl_3 , 400 MHz, 298 K): δ 7.82 (1H, s, NH), 7.68 (1H, d, *o*- $\text{CH}_{\text{O-MeSPh}}$), 7.58 (1H, s, NCHN), 7.25 (1H, t, *m*- $\text{CH}_{\text{O-MeSPh}}$), 7.07 (1H, t, *p*- $\text{CH}_{\text{O-MeSPh}}$), 6.92 (1H, d, *m*- $\text{CH}_{\text{O-MeSPh}}$), 6.83 (2H, s, *m*- CH_{Mes}), 2.33 (3H, s, $\text{SCH}_3_{\text{O-MeSPh}}$), 2.18 (3H, s, *p*- CH_3_{Mes}), 2.04 (6H, s, *o*- CH_3_{Mes}). ^{13}C NMR (CDCl_3 , 100 MHz, 298 K): δ 149.6 (s, NCN), 133.8 (s, Ar- $\text{C}_{\text{O-Mesph}}$), 131.0 (s, Ar- C_{Mes}), 128.9 (s, Ar- C_{Mes}), 128.2 (s, Ar- C_{Mes}), 127.7 (s, Ar- $\text{C}_{\text{O-MeSPh}}$), 125.3 (s, Ar- $\text{CH}_{\text{O-MeSPh}}$), 123.1 (s, Ar- CH_{Mes}), 119.3 (s, Ar- $\text{CH}_{\text{O-MeSPh}}$), 116.6 (s, Ar- $\text{CH}_{\text{O-MeSPh}}$).

MeSPh), 114.6 (s, Ar-CH_o-MeSPh), 18.6 (s, *p*-CH₃), 17.3 (s, *o*-CH₃), 14.2 (s, SCH₃).

N-(2-methylthiophenyl)-N'-(2,6-diisopropylphenyl) formamidine (2.19).

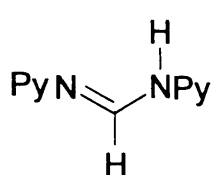


A 50 ml acid-free flask was charged with ethyl(2-methylthiophenyl)formimidate (5.85 g, 30.0 mmol) and 2,6-diisopropylaniline (5.32

g, 30.0 mmol). The mixture solidified after stirring for 3 hours at 50 °C. The residue was recrystallised from toluene affording white crystals. Yield: 7.1 g (72%).

¹H NMR (CDCl₃, 400 MHz, 298 K): δ 8.10 (1H, s, NH), 7.93 (1H, d, *o*-CH_o-Mesph), 7.71 (1H, s, NCHN), 7.16 (1H, t, *m*-CH_o-MeSPh), 7.12 (1H, t, *P*-CH_{DIPP}), 7.05 (2H, d, *m*-CH_{DIPP}), 6.92 (1H, t, *p*-CH_o-MeSPh), 6.83 (1H, d, *m*-CH_o-MeSPh), 3.13 (2H, sept., CH(CH₃)₂ DIPP), 2.34 (3H, s, SCH₃ *o*-MeSPh), 1.12 (12H, d, CH(CH₃)₂ DIPP). ¹³C NMR (CDCl₃, 100 MHz, 298 K): δ 155.5 (s, NCN), 142.6 (s, Ar-C_o-MeSPh), 133.8 (s, Ar-C_{DIPP}), 132.8 (s, Ar-C_{DIPP}), 129.4 (s, Ar-C_o-MeSPh), 125.5 (s, Ar-CH_o-MeSPh), 124.7 (s, Ar-CH_{DIPP}), 123.9 (s, Ar-CH_{DIPP}), 119.6 (s, Ar-CH_o-MeSPh), 118.9 (s, Ar-CH_o-MeSPh), 114.2 (s, Ar-CH_o-MeSPh), 28.4 (s, CH(CH₃)₂ DIPP) 24.1 (s, CH(CH₃)₂), 18.5 (s, CH(CH₃)₂), 14.9 (s, SCH₃).

N-N'-di(2-pyridyl) formamidine (2.20).

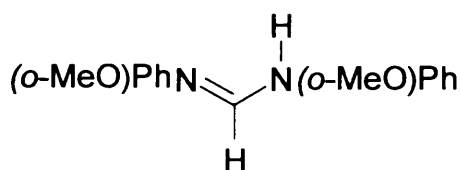


2-Aminopyridine (9.40 g, 0.10 mol), triethylorthoformate (16.65 ml, 0.10 mol) and two drops of 2M HCl were charged in to a 200 ml flask. The mixture was heated

using a heating mantle at 110 °C for 24 hours. The resulting mixture was allowed to cool slowly, white solid were obtained by recrystallisation from toluene. The yield was 8g, 82%.

¹H NMR (CDCl₃, 400 MHz, 298 K): δ 9.50 (1H, s, NH), 8.52 (2H, d, *o*-CH) 8.32 (1H, s, NCHN), 7.61 (2H, t, *p*-CH), 7.23 (2H, d, *m*-CH), 6.95 (1H, t, *m*-CH). ¹³C NMR (CDCl₃, 100 MHz, 298 K): δ 150.6 (s, NCN), 147.5 (s, Ar-C), 145.0 (s, Ar-CH), 121.7 (s, Ar-CH), 117.6(s, Ar-CH), 109.7 (s, Ar-CH).

N-N'-di(2-anisidyl) formamidine (2.21).



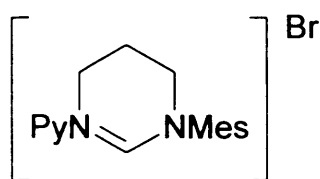
o-Anisidine (12.32 g, 0.10 mol), triethylorthoformate (16.65 ml, 0.10 mol) and two drops of 2M HCl were charged in

to a 200 ml flask. The mixture was heated using a heating mantle at 110 °C for 24 hours. The resulting mixture was allowed to cool slowly, white solid were obtained by recrystallisation from toluene. The yield was 11g, 86%.

¹H NMR (CDCl₃, 400 MHz, 298 K): δ 8.16 (1H, s, NCHN), 7.73 (1H, s, NH), 7.04 (2H, d, *o*-CH), 6.95 (2H, t, *m*-CH), 6.85 (2H, t, *p*-CH), 6.85 (2H, d, *m*-CH), 3.78 (6H, s, OCH₃). ¹³C NMR (CDCl₃, 100 MHz, 298 K): δ 150.4 (s,

NCN), 147.7 (s, Ar-C), 135.2 (s, Ar-C), 123.8 (s, Ar-CH), 121.5 (s, Ar-CH),
117.6 (s, Ar-CH), 111.4 (s, Ar-CH), 56.1 (s, OCH₃).

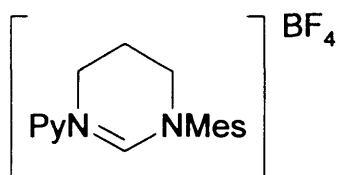
**1-(2-pyridyl)-3-(2, 4, 6-trimethylphenyl)-3, 4, 5, 6-tetrahydro-3H-[1, 3]
pyrimidinium bromide (2.22).**



The reaction was performed on a 10 mmol scale
of formamidine (2.39 g), 0.7 g of K₂CO₃ (5.0
mmol) and 2.03 ml of 1,3-dibromopropan (20.0
mmol) in 250 ml acetonitrile. The solution was

heated under reflux for 5 days to yield 2.90 g (80%) of yellow, crystalline
material.

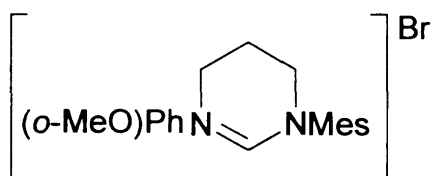
¹H NMR (CDCl₃, 400 MHz, 298 K): δ 9.20 (1H, s, NCHN), 8.297 (1H, d, ³J_{HH}
= 6.3, *o*-CH_{Py}), 7.92 (1H, t, ³J_{HH} = 6.4, *p*-CH_{Py}), 7.56 (1H, d, ³J_{HH} = 6.3, *m*-
CH_{Py}), 7.26 (1H, t, ³J_{HH} = 6.4, *m*-CH_{Py}), 6.95 (2H, s, *m*-CH_{Mes}), 4.41 (2H, t,
³J_{HH} = 5.2, NCH₂), 4.05 (2H, t, ³J_{HH} = 5.2, NCH₂), 2.55 (2H, m, NCH₂CH₂),
2.29 (6H, s, *o*-CH₃ Mes), 2.27 (3H, s, *p*-CH₃ Mes). ¹³C NMR (CDCl₃, 100 MHz,
298 K): δ 150.1 (s, NCN), 149.6 (s, Ar-C_{Py}), 149.3 (s, Ar-CH_{Py}), 140.3 (s, Ar-
C_{Mes}), 136.1 (s, Ar-C_{Mes}), 133.3 (s, Ar-C_{Mes}), 129.4 (s, Ar-CH_{Mes}), 122.3 (s,
Ar-CH_{Py}), 111.8 (s, Ar-CH_{Py}), 47.2 (s, NCH₂), 42.6 (s, NCH₂), 20.7 (s,
NCH₂CH₂), 19.1 (s, *p*-CH₃), 17.5 (s, *o*-CH₃). Anal. Found (Calcd) for:
C₁₈H₂₂N₃Br C, 58.83 (58.88); H, 5.98 (5.99); N, 11.39 (11.45). HRMS (ES):
m/z 280.1813 ([M-Br]⁺ C₁₈H₂₂N₃ requires 280.1814).

1-(2-pyridyl)-3-(2, 4, 6-trimethylphenyl)-3, 4, 5, 6-tetrahydro-3H-[1, 3]**pyrimidinium tetrafluoroborate.**

A solution of pyrimidinium salt 2.10 g (6.0 mmol) in 30 ml acetonitrile was mixed with a solution of sodium tetrafluoroborate 0.99 g (9.0 mmol) in 30

ml distilled water. Pale yellow crystals were formed (1.90 g, 86%).

^1H NMR (CDCl_3 , 400 MHz, 298 K): δ 9.01 (1H, s, NCHN), 8.25 (1H, d, $^3J_{\text{HH}} = 6.3$, *o*-CH_{Py}), 7.87 (1H, t, $^3J_{\text{HH}} = 6.7$, *p*-CH_{Py}), 7.48 (1H, d, $^3J_{\text{HH}} = 6.3$, *m*-CH_{Py}), 7.24 (1H, t, $^3J_{\text{HH}} = 6.7$, *m*-CH_{Py}), 6.93 (2H, s, *m*-CH_{Mes}), 4.24 (2H, t, $^3J_{\text{HH}} = 5.5$, NCH₂), 3.82 (2H, t, $^3J_{\text{HH}} = 5.5$, NCH₂), 2.55 (2H, m, NCH₂CH₂), 2.29 (6H, s, *o*-CH₃ Mes), 2.27 (3H, s, *p*-CH₃ Mes). ^{13}C NMR (CDCl_3 , 100 MHz, 298 K): δ 150.3 (s, NCN), 149.4 (s, Ar-C_{Py}), 147.1 (s, Ar-CH_{Py}), 139.4 (s, Ar-C_{Mes}), 136.1 (s, Ar-C_{Mes}), 133.3 (s, Ar-C_{Mes}), 129.2 (s, Ar-CH_{Mes}), 122.3 (s, Ar-CH_{Py}), 111.8 (s, Ar-CH_{Py}), 46.2 (s, NCH₂), 41.6 (s, NCH₂), 19.9 (s, NCH₂CH₂), 18.1 (s, *p*-CH₃), 16.6 (s, *o*-CH₃).

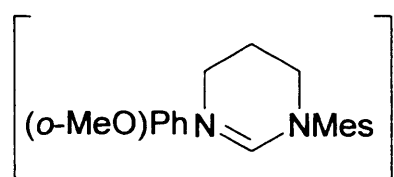
1-(2-anisidyl)-3-(2, 4, 6-trimethylphenyl)-3, 4, 5, 6-tetrahydro-3H-[1, 3]**pyrimidinium bromide (2.23).**

The reaction was performed on a 10 mmol scale of formamidine (2.68 g), 0.7 g of K_2CO_3 (5.0 mmol) and 2.03 ml of 1,3-

dibromopropan (20.0 mmol) in 250 ml acetonitrile. The solution was heated under reflux for 48 hours to yield 3.22 g (82%) of white, crystalline material.

^1H NMR (CDCl_3 , 400 MHz, 298 K): δ 7.77 (1H, d, $^3J_{\text{HH}} = 6.7$, $o\text{-CH}_{o\text{-MeOPh}}$), 7.63 (1H, s, NCHN), 7.34 (1H, t, $^3J_{\text{HH}} = 6.8$, $m\text{-CH}_{o\text{-MeOPh}}$), 7.02 (1H, t, $^3J_{\text{HH}} = 6.8$, $p\text{-CH}_{o\text{-MeOPh}}$), 6.94 (1H, d, $^3J_{\text{HH}} = 6.7$, $m\text{-CH}_{o\text{-MeOPh}}$), 6.89 (2H, s, $m\text{-CH}_{\text{Mes}}$), 4.26 (2H, t, $^3J_{\text{HH}} = 5.7$, NCH₂), 3.97 (2H, t, $^3J_{\text{HH}} = 5.7$, NCH₂), 3.82 (3H, s, OCH₃ $o\text{-MeOPh}$), 2.56 (2H, m, NCH₂CH₂), 2.33 (6H, s, $o\text{-CH}_3$ Mes), 2.24 (3H, s, $p\text{-CH}_3$ Mes). ^{13}C NMR (CDCl_3 , 100 MHz, 298 K): δ 154.8 (s, NCN), 153.0 (s, Ar-C $_{o\text{-MeOPh}}$), 140.7 (s, Ar-C $_{\text{Mes}}$), 137.0 (s, Ar-C $_{\text{Mes}}$), 135.0 (s, Ar-C $_{\text{Mes}}$), 131.4 (s, Ar-C $_{o\text{-MeOPh}}$), 130.4 (s, Ar-CH $_{o\text{-MeOPh}}$), 129.7 (s, Ar-CH $_{\text{Mes}}$), 127.8 (s, Ar-CH $_{o\text{-MeOPh}}$), 122.2 (s, Ar-CH $_{o\text{-MeOPh}}$), 112.5 (s, Ar-CH $_{o\text{-MeOPh}}$), 56.6 (s, OCH₃ $o\text{-MeOPh}$), 48.1 (s, NCH₂), 47.1 (s, NCH₂), 21.4 (s, NCH₂CH₂), 20.1 (s, $p\text{-CH}_3$ Mes), 18.4 (s, $o\text{-CH}_3$ Mes). Anal. Found (Calcd) for C₂₀H₂₅N₂OBr: C, 62.15 (61.71); H, 6.55 (6.43); N, 7.59 (7.20). HRMS (ES): m/z 309.1954 ([M-Br]⁺ C₂₀H₂₅N₂O requires 309.1967).

1-(2-anisidyl)-3-(2, 4, 6-trimethylphenyl)-3, 4, 5, 6-tetrahydro-3H-[1, 3]pyrimidinium tetrafluoroborate.



BF_4 A solution of pyrimidinium salt 2.32 g (6.0 mmol) in 30 ml acetonitrile was mixed with a solution of sodium

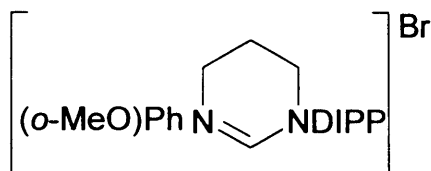
tetrafluoroborate 0.99 g (9.0 mmol) in 30 ml distilled water. White crystals were formed (2.10 g, 88%).

^1H NMR (CDCl_3 , 400 MHz, 298 K): δ 7.59 (1H, d, $^3J_{\text{HH}} = 6.7$, $o\text{-CH}_{o\text{-MeOPh}}$), 7.53 (1H, s, NCHN), 7.32 (1H, t, $^3J_{\text{HH}} = 6.8$, $m\text{-CH}_{o\text{-MeOPh}}$), 7.00 (1H, t, $^3J_{\text{HH}} = 6.8$, $p\text{-CH}_{o\text{-MeOPh}}$), 6.94 (1H, d, $^3J_{\text{HH}} = 6.7$, $m\text{-CH}_{o\text{-MeOPh}}$), 6.88 (2H, s, $m\text{-CH}_{\text{Mes}}$), 4.26 (2H, t, $^3J_{\text{HH}} = 5.7$, NCH₂), 3.97 (2H, t, $^3J_{\text{HH}} = 5.7$, NCH₂), 3.82 (3H, s, OCH₃ $o\text{-MeOPh}$), 2.56 (2H, m, NCH₂CH₂), 2.33 (6H, s, $o\text{-CH}_3$ Mes), 2.24 (3H, s, $p\text{-CH}_3$ Mes).

CH_{Mes}), 3.96 (2H, t, $^3J_{HH} = 5.7$, NCH_2), 3.83 (3H, s, OCH_3 *o*-MeOPh), 3.76 (2H, t, $^3J_{HH} = 5.7$, NCH_2), 2.47 (2H, m, NCH_2CH_2), 2.27 (6H, s, *o*- CH_3 Mes), 2.20 (3H, s, *p*- CH_3 Mes).

^{13}C NMR ($CDCl_3$, 100 MHz, 298 K): δ 155.1 (s, NCN), 153.2 (s, Ar- $C_{o-MeOPh}$), 140.7 (s, Ar- C_{Mes}), 137.1 (s, Ar- C_{Mes}), 135.1 (s, Ar- C_{Mes}), 131.5 (s, Ar- $C_{o-MeOPh}$), 130.4 (s, Ar- $CH_{o-MeOPh}$), 129.8 (s, Ar- CH_{Mes}), 127.6 (s, Ar- $CH_{o-MeOPh}$), 122.3 (s, Ar- $CH_{o-MeOPh}$), 112.5 (s, Ar- $CH_{o-MeOPh}$), 56.5 (s, OCH_3 *o*-MeOPh), 47.5 (s, NCH_2), 46.7 (s, NCH_2), 21.4 (s, NCH_2CH_2), 19.8 (s, *p*- CH_3 Mes), 17.8 (s, *o*- CH_3 Mes).

1-(2-anisidyl)-3-(2, 6-diisopropylphenyl)-3, 4, 5, 6-tetrahydro-3H-[1, 3] pyrimidinium bromide (2.24).



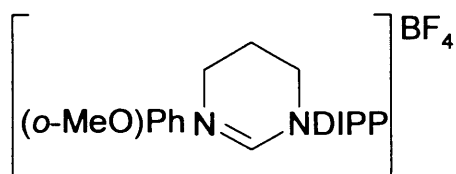
The reaction was performed on a 10 mmol scale of formamidine (3.10 g), 0.7 g of K_2CO_3 (5mmol) and 2.03 ml of 1,3-

dibromopropan (20. mmol) in 250 ml acetonitrile. The solution was heated under reflux for 2 weeks to yield 3.75 g (87%) of white, crystalline material.

1H NMR ($CDCl_3$, 400 MHz, 298 K): δ 7.88 (1H, d, $^3J_{HH} = 6.7$, *o*- $CH_{o-MeOPh}$), 7.56 (1H, s, $NCHN$), 7.37 (1H, t, $^3J_{HH} = 6.8$, *m*- $CH_{o-MeOPh}$), 7.34 (1H, t, $^3J_{HH} = 7.8$, $-CH_{DIPP}$), 7.20 (2H, d, $^3J_{HH} = 7.8$, *m*- CH_{DIPP}), 7.04 (1H, t, $^3J_{HH} = 6.8$, *p*- $CH_{o-MeOPh}$), 6.94 (1H, d, $^3J_{HH} = 6.7$, *m*- $CH_{o-MeOPh}$), 4.38 (2H, t, $^3J_{HH} = 5.5$, NCH_2), 4.02 (2H, t, $^3J_{HH} = 5.5$, NCH_2), 3.83 (3H, s, OCH_3 *o*-MeOPh), 3.14 (2H, sept., $^3J_{HH} = 6.8$, $CH(CH_3)_2$ $DIPP$), 2.59 (2H, m, NCH_2CH_2), 1.27 (6H, d, $^3J_{HH} = 6.8$, $CH(CH_3)_2$ $DIPP$), 1.17 (6H, d, $^3J_{HH} = 6.8$, $CH(CH_3)_2$ $DIPP$). ^{13}C NMR ($CDCl_3$,

100 MHz, 298 K): δ 154.3 (s, NCN), 152.9 (s, Ar-C_o-MeOPh), 149.3 (s, Ar-C_{DIPP}), 136.7 (s, Ar-C_{DIPP}), 131.6 (s, Ar-C_o-MeOPh), 131.5 (s, Ar-CH_o-MeOPh), 129.7 (s, Ar-CH_{DIPP}), 128.1 (s, Ar-CH_{DIPP}), 125.5 (s, Ar-CH_o-MeOPh), 122.4 (s, Ar-CH_o-MeOPh), 112.5 (s, Ar-CH_o-MeOPh), 56.6 (s, OCH₃), 48.9 (s, NCH₂), 48.4 (s, NCH₂), 28.9 (s, CH(CH₃)₂), 25.1 (s, NCH₂CH₂), 24.8 (s, CH(CH₃)₂), 20.0 (s, CH(CH₃)₂). Anal. Found (Calcd) for: C₂₃H₃₁N₂OBr C, 63.92 (64.05); H, 7.33 (7.19); N, 6.36 (6.50). HRMS (ES): *m/z* 351.2437 ([M-Br]⁺ C₂₃H₃₁N₂O requires 351.2436).

1-(2-anisidyl)-3-(2, 6-diisopropylphenyl)-3, 4, 5, 6-tetrahydro-3H-[1, 3] pyrimidinium tetrafluoroborate.

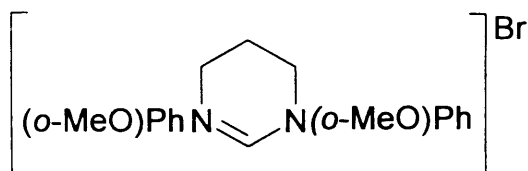


A solution of pyrimidinium salt 2.58 g (6.0 mmol) in 30 ml acetonitrile was mixed with a solution of sodium tetrafluoroborate 0.99 g (9.0 mmol) in 30 ml distilled water. White crystals were formed (2.33 g, 89%).

¹H NMR (CDCl₃, 400 MHz, 298 K): δ 7.59 (1H, d, ³J_{HH} = 6.7, *o*-CH_o-MeOPh), 7.54 (1H, s, NCHN), 7.38 (1H, t, ³J_{HH} = 6.8, *m*-CH_o-MeOPh), 7.35 (1H, t, ³J_{HH} = 7.8, *p*-CH_{DIPP}), 7.18 (2H, d, ³J_{HH} = 7.8, *m*-CH_{DIPP}), 7.03 (1H, t, ³J_{HH} = 6.8, *p*-CH_o-MeOPh), 6.96 (1H, d, ³J_{HH} = 6.7, *m*-CH_o-MeOPh), 4.03 (2H, t, ³J_{HH} = 5.5, NCH₂), 3.85 (3H, s, OCH₃ *o*-MeOPh), 3.81 (2H, t, ³J_{HH} = 5.5, NCH₂), 3.03 (2H, sept., ³J_{HH} = 6.8, CH(CH₃)₂ DIPP), 2.55 (2H, m, NCH₂CH₂), 1.28 (6H, d, ³J_{HH} = 6.8, CH(CH₃)₂ DIPP), 1.21 (6H, d, ³J_{HH} = 6.8, CH(CH₃)₂ DIPP). ¹³C NMR (CDCl₃, 100 MHz, 298 K): δ 158.7 (s, NCN), 153.5 (s, Ar-C_o-MeOPh), 145.4 (s, Ar-

C_{DIPP} , 139.5 (s, Ar- C_{DIPP}), 132.2 (s, Ar- $C_{\text{o-MeOPh}}$), 131.9 (s, Ar- $\text{CH}_{\text{o-MeOPh}}$), 131.2 (s, Ar- CH_{DIPP}), 128.1 (s, Ar- CH_{DIPP}), 125.6 (s, Ar- $\text{CH}_{\text{o-MeOPh}}$), 122.4 (s, Ar- $\text{CH}_{\text{o-MeOPh}}$), 112.7 (s, Ar- $\text{CH}_{\text{o-MeOPh}}$), 56.7 (s, OCH_3), 56.2 (s, NCH_2), 55.9 (s, NCH_2), 29.0 (s, $\text{CH}(\text{CH}_3)_2$), 25.3 (s, NCH_2CH_2), 25.0 (s, $\text{CH}(\text{CH}_3)_2$), 24.5 (s, $\text{CH}(\text{CH}_3)_2$).

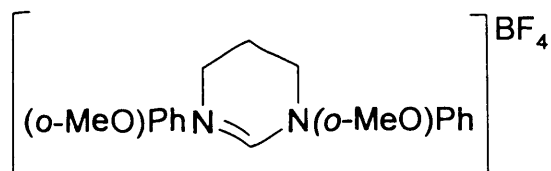
1, 3-di(2-anisidyl)-3, 4, 5, 6-tetrahydro-3H-[1, 3]pyrimidinium bromide (2.25).



The reaction was performed on a 10 mmol scale of formamidine (2.56 g), 0.7 g of K_2CO_3 (5.0 mmol)

and 2.03 ml of 1,3-dibromopropan (20.0 mmol) in 250 ml acetonitrile. The solution was heated under reflux for 1 week to yield 3.50 g (93%) of pale yellow, crystalline material.

^1H NMR (CDCl_3 , 400 MHz, 298 K): δ 7.88 (2H, d, $^3J_{\text{HH}} = 6.7$, $\text{o-CH}_{\text{o-MeOPh}}$), 7.71 (1H, s, NCHN), 7.32 (2H, t, $^3J_{\text{HH}} = 6.8$, $\text{m-CH}_{\text{o-MeOPh}}$), 6.97 (2H, t, $^3J_{\text{HH}} = 6.8$, $\text{p-CH}_{\text{o-MeOPh}}$), 6.94 (2H, d, $^3J_{\text{HH}} = 6.7$, $\text{m-CH}_{\text{o-MeOPh}}$), 4.05 (4H, t, $^3J_{\text{HH}} = 5.4$, NCH_2), 3.85 (6H, s, OCH_3 o-MeOPh), 2.48 (2H, m, NCH_2CH_2). ^{13}C NMR (CDCl_3 , 100 MHz, 298 K): δ 154.7 (s, NCN), 153.6 (s, Ar- $C_{\text{o-MeOPh}}$), 131.4 (s, Ar- $C_{\text{o-MeOPh}}$), 130.1 (s, Ar- $\text{CH}_{\text{o-MeOPh}}$), 128.5 (s, Ar- $\text{CH}_{\text{o-MeOPh}}$), 122.1 (s, Ar- $\text{CH}_{\text{o-MeOPh}}$), 112.3 (s, Ar- $\text{CH}_{\text{o-MeOPh}}$), 56.5 (s, OCH_3), 47.7 (s, NCH_2), 20.0 (s, NCH_2CH_2). Anal. Found (Calcd) for: $\text{C}_{18}\text{H}_{21}\text{N}_2\text{O}_2\text{Br}$ C, 56.08 (56.28); H, 5.46 (5.47); N, 7.26 (7.29). HRMS (ES): m/z 297.1607 ($[\text{M}-\text{Br}]^+$ $\text{C}_{18}\text{H}_{21}\text{N}_2\text{O}_2$ requires 297.1603).

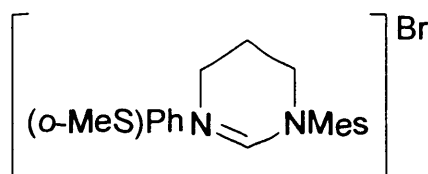
1, 3-di(2-anisidyl)-3, 4, 5, 6-tetrahydro-3H-[1, 3]pyrimidinium**tetrafluoroborate.**

A solution of pyrimidinium salt
2.26 g (6.0 mmol) in 30 ml
acetonitrile was mixed with a

solution of sodium tetrafluoroborate 0.99 g (9.0 mmol) in 30 ml distilled water.

White crystals were formed (2.12 g, 92%).

^1H NMR (CDCl_3 , 400 MHz, 298 K): δ 7.62 (1H, s, NCHN), 7.58 (2H, d, $^3J_{\text{HH}} = 6.7$, $o\text{-CH}_{o\text{-MeOPh}}$), 7.33 (2H, t, $^3J_{\text{HH}} = 6.8$, $m\text{-CH}_{o\text{-MeOPh}}$), 6.99 (2H, t, $^3J_{\text{HH}} = 6.8$, $p\text{-CH}_{o\text{-MeOPh}}$), 6.94 (2H, d, $^3J_{\text{HH}} = 6.7$, $m\text{-CH}_{o\text{-MeOPh}}$), 3.89 (4H, t, $^3J_{\text{HH}} = 5.4$, NCH₂), 3.88 (6H, s, OCH₃ $o\text{-MeOPh}$), 2.43 (2H, m, NCH₂CH₂). ^{13}C NMR (CDCl_3 , 100 MHz, 298 K): δ 154.6 (s, NCN), 153.7 (s, Ar-C $_{o\text{-MeOPh}}$), 131.2 (s, Ar-C $_{o\text{-MeOPh}}$), 130.1 (s, Ar-CH $_{o\text{-MeOPh}}$), 127.9 (s, Ar-CH $_{o\text{-MeOPh}}$), 122.1 (s, Ar-CH $_{o\text{-MeOPh}}$), 112.4 (s, Ar-CH $_{o\text{-MeOPh}}$), 56.5 (s, OCH₃ $o\text{-MeOPh}$), 47.2 (s, NCH₂), 19.8 (s, NCH₂CH₂).

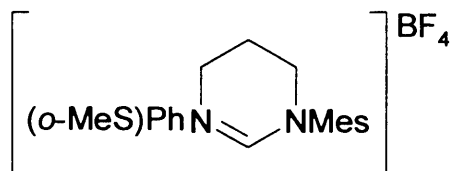
1-(2-methylthiophenyl)-3-(2, 4, 6-trimethylphenyl)-3, 4, 5, 6-tetrahydro-3H-[1,3] pyrimidinium bromide (2.26).

The reaction was performed on a 10
mmol scale of formamidine (2.84 g), 0.7 g
of K₂CO₃ (5.0 mmol) and 2.03 ml of 1,3-

dibromopropan (20.0 mmol) in 250 ml acetonitrile. The solution was heated
under reflux for 2 weeks to yield 3.10 g (76%) of white, crystalline material.

^1H NMR (CDCl_3 , 400 MHz, 298 K): δ 8.06 (1H, d, $^3J_{\text{HH}} = 6.7$, $o\text{-CH}_{o\text{-MeSPH}}$), 7.55 (1H, s, NCHN), 7.41 (1H, t, $^3J_{\text{HH}} = 6.2$, $m\text{-CH}_{o\text{-MeSPH}}$), 7.21 (1H, t, $^3J_{\text{HH}} = 6.2$, $p\text{-CH}_{o\text{-MeSPH}}$), 7.18 (1H, d, $^3J_{\text{HH}} = 6.7$, $m\text{-CH}_{o\text{-MeSPH}}$), 6.88 (2H, s, $m\text{-CH}_{\text{Mes}}$), 4.29 (2H, t, $^3J_{\text{HH}} = 5.2$, NCH₂), 4.05 (2H, t, $^3J_{\text{HH}} = 5.2$, NCH₂), 2.61 (2H, m, NCH₂CH₂), 2.49 (3H, s, SCH₃ $o\text{-MeSPH}$), 2.37 (6H, s, $o\text{-CH}_{3\text{Mes}}$), 2.23 (3H, s, $p\text{-CH}_{3\text{Mes}}$). ^{13}C NMR (CDCl_3 , 100 MHz, 298 K): δ 154.3 (s, NCN), 140.3 (s, Ar-C $_{o\text{-MeSPH}}$), 137.7 (s, Ar-C $_{\text{Mes}}$), 136.7 (s, Ar-C $_{\text{Mes}}$), 135.6 (s, Ar-C $_{\text{Mes}}$), 134.7 (s, Ar-C $_{o\text{-MeSPH}}$), 131.1 (s, Ar-CH $_{o\text{-MeSPH}}$), 129.9 (s, Ar-CH $_{\text{Mes}}$), 128.9 (s, Ar-CH $_{o\text{-MeSPH}}$), 126.5 (s, Ar-CH $_{o\text{-MeSPH}}$), 125.8 (s, Ar-CH $_{o\text{-MeSPH}}$), 47.4 (s, NCH₂), 46.8 (s, NCH₂), 20.9 (s, NCH₂CH₂), 19.7 (s, $p\text{-CH}_{3\text{Mes}}$), 18.4 (s, $o\text{-CH}_{3\text{Mes}}$), 14.9 (s, SCH₃ $o\text{-MeSPH}$). Anal. Found (Calcd) for: C₂₀H₂₅N₂OBr C, 58.09 (58.27); H, 6.07 (6.07); N, 6.99 (6.80). HRMS (ES): m/z 325.1748 ([M-Br]⁺ C₂₀H₂₅N₂O requires 325.1738).

1-(2-methylthiophenyl)-3-(2, 4, 6-trimethylphenyl)-3, 4, 5, 6-tetrahydro-3H-[1, 3] pyrimidinium tetrafluoroborate.



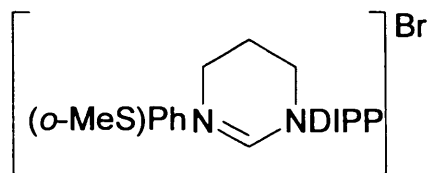
A solution of pyrimidinium salt 2.42 g (6.0 mmol) in 30 ml acetonitrile was mixed with a solution of sodium tetrafluoroborate 0.99 g (9.0 mmol) in 30

ml distilled water. White crystals were formed (2.15 g, 87%).

^1H NMR (CDCl_3 , 400 MHz, 298 K): δ 7.68 (1H, d, $^3J_{\text{HH}} = 6.5$, $o\text{-CH}_{o\text{-MeSPH}}$), 7.44 (1H, s, NCHN), 7.38 (1H, t, $^3J_{\text{HH}} = 6.4$, $m\text{-CH}_{o\text{-MeSPH}}$), 7.21 (1H, t, $^3J_{\text{HH}} = 6.4$, $p\text{-CH}_{o\text{-MeSPH}}$), 7.18 (1H, d, $^3J_{\text{HH}} = 6.5$, $m\text{-CH}_{o\text{-MeSPH}}$), 6.86 (2H, s, $m\text{-CH}_{\text{Mes}}$), 4.29 (2H, t, $^3J_{\text{HH}} = 5.2$, NCH₂), 4.05 (2H, t, $^3J_{\text{HH}} = 5.2$, NCH₂), 2.61 (2H, m, NCH₂CH₂), 2.49 (3H, s, SCH₃ $o\text{-MeSPH}$), 2.37 (6H, s, $o\text{-CH}_{3\text{Mes}}$), 2.23 (3H, s, $p\text{-CH}_{3\text{Mes}}$).

CH_{Mes}), 3.94 (2H, t, $^3J_{HH} = 5.4$, NCH_2), 3.81 (2H, t, $^3J_{HH} = 5.4$, NCH_2), 2.52 (2H, m, NCH_2CH_2), 2.46 (3H, s, SCH_3 o -MeSPh) 2.30 (6H, s, o - CH_3 Mes), 2.21 (3H, s, p - CH_3 Mes). ^{13}C NMR ($CDCl_3$, 100 MHz, 298 K): δ 154.1 (s, NCN), 140.4 (s, Ar- C_{o -MeSPh), 137.8 (s, Ar- C_{Mes}), 136.7 (s, Ar- C_{Mes}), 135.7 (s, Ar- C_{Mes}), 134.8 (s, Ar- C_{o -MeSPh), 131.1 (s, Ar- CH_{o -MeSPh), 130.1 (s, Ar- CH_{Mes}), 128.3 (s, Ar- CH_{o -MeSPh), 126.7 (s, Ar- CH_{o -MeSPh), 125.9 (s, Ar- CH_{o -MeSPh), 46.8 (s, NCH_2), 46.4 (s, NCH_2), 20.9 (s, NCH_2CH_2), 19.4 (s, p - CH_3 Mes), 17.7 (s, o - CH_3 Mes) 14.9 (s, SCH_{o -MeSPh).

1-(2-methylthiophenyl)-3-(2, 6-diisopropylphenyl)-3, 4, 5, 6-tetrahydro-3H-[1, 3] pyrimidinium bromide (2.27).



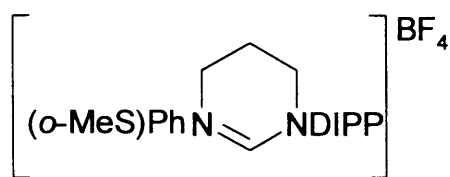
The reaction was performed on a 10 mmol scale of formamidine (3.26 g), 0.7 g of K_2CO_3 (5mmol) and 2.03 ml of 1,3-

dibromopropan (20. mmol) in 250 ml acetonitrile. The solution was heated under reflux for 3 weeks to yield 3.25 g (72%) of white, crystalline material.

1H NMR ($CDCl_3$, 400 MHz, 298 K): δ 7.88 (1H, d, $^3J_{HH} = 6.7$, o - CH_{o -MeSPh), 7.56 (1H, s, NCHN), 7.37 (1H, t, $^3J_{HH} = 6.8$, m - CH_{o -MeSPh), 7.34 (1H, t, $^3J_{HH} = 7.8$, p - CH_{DIPP}), 7.20 (2H, d, $^3J_{HH} = 7.8$, m - CH_{DIPP}), 7.04 (1H, t, $^3J_{HH} = 6.8$, p - CH_{o -MeSPh), 6.94 (1H, d, $^3J_{HH} = 6.7$, m - CH_{o -MeSPh), 4.38 (2H, t, $^3J_{HH} = 5.5$, NCH_2), 4.02 (2H, t, $^3J_{HH} = 5.5$, NCH_2), 3.83 (3H, s, SCH_3 o -MeSPh), 3.14 (2H, sept., $^3J_{HH} = 6.8$, $CH(CH_3)_2$ DIPP), 2.59 (2H, m, NCH_2CH_2), 1.27 (6H, d, $^3J_{HH} = 6.8$, $CH(CH_3)_2$ DIPP), 1.17 (6H, d, $^3J_{HH} = 6.8$, $CH(CH_3)_2$ DIPP). ^{13}C NMR ($CDCl_3$, 100 MHz, 298 K): δ 154.3 (s, NCN), 152.9 (s, Ar- C_{o -MeSPh), 149.3 (s, Ar-

C_{DIPP} , 136.7 (s, Ar- C_{DIPP}), 131.6 (s, Ar- $C_{\text{o-MeSPh}}$), 131.5 (s, Ar- $\text{CH}_{\text{o-MeSPh}}$), 129.7 (s, Ar- CH_{DIPP}), 128.1 (s, Ar- CH_{DIPP}), 125.5 (s, Ar- $\text{CH}_{\text{o-MeSPh}}$), 122.4 (s, Ar- $\text{CH}_{\text{o-MeSPh}}$), 112.5 (s, Ar- $\text{CH}_{\text{o-MeSPh}}$), 56.6 (s, OCH_3), 48.9 (s, NCH_2), 48.4 (s, NCH_2), 28.9 (s, $\text{CH}(\text{CH}_3)_2$), 25.1 (s, NCH_2CH_2), 24.8 (s, $\text{CH}(\text{CH}_3)_2$), 20.0 (s, $\text{CH}(\text{CH}_3)_2$). Anal. Found (Calcd) for: $\text{C}_{23}\text{H}_{31}\text{N}_2\text{OBr}$ C, 60.62 (60.81); H, 6.81 (6.83); N, 6.15 (6.17). HRMS (ES): m/z 367.2216 ($[\text{M}-\text{Br}]^+$ $\text{C}_{23}\text{H}_{31}\text{N}_2\text{O}$ requires 367.2208).

1-(2-methylthiophenyl)-3-(2, 6-diisopropylphenyl)-3, 4, 5, 6-tetrahydro-3H-[1, 3] pyrimidinium tetrafluoroborate.



A solution of pyrimidinium salt 2.68 g (6.0 mmol) in 30 ml acetonitrile was mixed with a solution of sodium tetrafluoroborate 0.99 g (9.0 mmol) in 30 ml distilled water. White crystals were formed (2.30 g, 84%).

^1H NMR (CDCl_3 , 400 MHz, 298 K): δ 7.59 (1H, d, $^3J_{\text{HH}} = 6.7$, $\text{o-CH}_{\text{o-MeSPh}}$), 7.54 (1H, s, NCHN), 7.38 (1H, t, $^3J_{\text{HH}} = 6.8$, $\text{m-CH}_{\text{o-MeSPh}}$), 7.35 (1H, t, $^3J_{\text{HH}} = 7.8$, $\text{p-CH}_{\text{DIPP}}$), 7.18 (2H, d, $^3J_{\text{HH}} = 7.8$, $\text{m-CH}_{\text{DIPP}}$), 7.03 (1H, t, $^3J_{\text{HH}} = 6.8$, $\text{p-CH}_{\text{o-MeSPh}}$), 6.96 (1H, d, $^3J_{\text{HH}} = 6.7$, $\text{m-CH}_{\text{o-MeSPh}}$), 4.03 (2H, t, $^3J_{\text{HH}} = 5.5$, NCH_2), 3.85 (3H, s, $\text{SCH}_3_{\text{o-MeSPh}}$), 3.81 (2H, t, $^3J_{\text{HH}} = 5.5$, NCH_2), 3.03 (2H, sept., $^3J_{\text{HH}} = 6.8$, $\text{CH}(\text{CH}_3)_2_{\text{DIPP}}$), 2.55 (2H, m, NCH_2CH_2), 1.28 (6H, d, $^3J_{\text{HH}} = 6.8$, $\text{CH}(\text{CH}_3)_2_{\text{DIPP}}$), 1.21 (6H, d, $^3J_{\text{HH}} = 6.8$, $\text{CH}(\text{CH}_3)_2_{\text{DIPP}}$). ^{13}C NMR (CDCl_3 , 100 MHz, 298 K): δ 158.7 (s, NCN), 153.5 (s, Ar- $C_{\text{o-MeSPh}}$), 145.4 (s, Ar- C_{DIPP}), 139.5 (s, Ar- C_{DIPP}), 132.2 (s, Ar- $C_{\text{o-MeSPh}}$), 131.9 (s, Ar- $\text{CH}_{\text{o-MeSPh}}$),

131.2 (s, Ar-CH_{DIPP}), 128.1 (s, Ar-CH_{DIPP}), 125.6 (s, Ar-CH_{o-MeSPh}), 122.4 (s, Ar-CH_{o-MeSPh}), 112.7 (s, Ar-CH_{o-MeSPh}), 56.7 (s, OCH₃), 56.2 (s, NCH₂), 55.9 (s, NCH₂), 29.0 (s, CH(CH₃)₂), 25.3 (s, NCH₂CH₂), 25.0 (s, CH(CH₃)₂), 24.5 (s, CH(CH₃)₂).

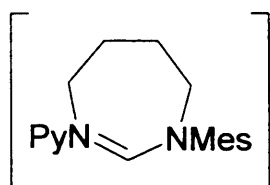
1-(2-pyridyl)-3-(2, 4, 6-trimethylphenyl)-4, 5, 6, 7-tetrahydro-3H-[1, 3] diazepinium Iodide (2.28).



The reaction was performed on a 10 mmol scale of formamidine (2.39 g), 0.70 g of K₂CO₃ (5 mmol) and 1.31 ml of 1,4-diiodobutane (10mmol) in 250 ml of acetonitrile. The solution was heated under reflux

for 24 hours to yield 3.20 g (76%) of pale yellow, crystalline material.

¹H NMR (CDCl₃, 400 MHz, 298 K): δ 8.53 (1H, s, NCHN), 8.29 (1H, d, ³J_{HH} = 6.3, *o*-CH_{Py}), 7.92 (1H, t, ³J_{HH} = 6.7, *p*-CH_{Py}), 7.74 (1H, d, ³J_{HH} = 6.3, *m*-CH_{Py}), 7.28 (1H, t, ³J_{HH} = 6.7, *m*-CH_{Py}), 6.93 (2H, s, *m*-CH_{Mes}), 4.82 (2H, t, ³J_{HH} = 5.8, NCH₂), 4.41 (2H, t, ³J_{HH} = 5.8, NCH₂), 2.45 (4H, m, NCH₂CH₂), 2.37 (6H, s, *o*-CH₃ Mes), 2.26 (3H, s, *p*-CH₃ Mes). ¹³C NMR (CDCl₃, 100 MHz, 298 K): δ 157.5 (s, NCN), 152.9 (s, Ar-C_{Py}), 148.7 (s, Ar-CH_{Py}), 140.7 (s, Ar-C_{Mes}), 140.2 (s, Ar-C_{Mes}), 134.1 (s, Ar-C_{Mes}), 130.7 (s, Ar-CH_{Mes}), 123.9 (s, Ar-CH_{Py}), 115.7 (s, Ar-CH_{Py}), 55.5 (s, NCH₂), 51.7 (s, NCH₂), 25.3 (s, NCH₂CH₂), 24.9 (s, NCH₂CH₂), 21.4 (s, *p*-CH₃), 19.1 (s, *o*-CH₃). Anal. Found (Calcd) for: C₁₉H₂₄N₃I C, 54.02 (54.17); H, 5.70 (5.70); N, 9.87 (9.98). HRMS (ES): *m/z* 294.1958 ([M-I]⁺ C₁₉H₂₄N₃ requires 294.1970).

1-(2-pyridyl)-3-(2, 4, 6-trimethylphenyl)-4, 5, 6, 7-tetrahydro-3H-[1, 3]**diazepinium tetrafluoroborate.**BF₄

A solution of diazepinium salt 2.53 g (6.0 mmol) in 30 ml acetonitrile was mixed with a solution of sodium tetrafluoroborate 0.99 g (9.0 mmol) in 30

ml distilled water. Yellow crystals were formed (1.90 g, 83%).

¹H NMR (CDCl₃, 400 MHz, 298 K): δ 8.44 (1H, s, NCHN), 8.27 (1H, d, ³J_{HH} = 6.8, *o*-CH_{Py}), 7.86 (1H, t, ³J_{HH} = 6.2, *p*-CH_{Py}), 7.65 (1H, d, ³J_{HH} = 6.8, *m*-CH_{Py}), 7.24 (1H, t, ³J_{HH} = 6.2, *m*-CH_{Py}), 6.94 (2H, s, *m*-CH_{Mes}), 4.73 (2H, t, ³J_{HH} = 5.4, NCH₂), 4.26 (2H, t, ³J_{HH} = 5.4, NCH₂), 2.42 (4H, m, NCH₂CH₂), 2.35 (6H, s, *o*-CH₃ Mes), 2.25 (3H, s, *p*-CH₃ Mes). ¹³C NMR (CDCl₃, 100 MHz, 298 K): δ 157.7 (s, NCN), 148.7 (s, Ar-C_{Py}), 140.8 (s, Ar-CH_{Py}), 140.7 (s, Ar-C_{Mes}), 140.2 (s, Ar-C_{Mes}), 134.1 (s, Ar-C_{Mes}), 130.7 (s, Ar-CH_{Mes}), 123.9 (s, Ar-CH_{Py}), 115.5 (s, Ar-CH_{Py}), 55.1 (s, NCH₂), 50.8 (s, NCH₂), 25.3 (s, NCH₂CH₂), 24.8 (s, NCH₂CH₂), 21.4 (s, *p*-CH₃), 18.6 (s, *o*-CH₃).

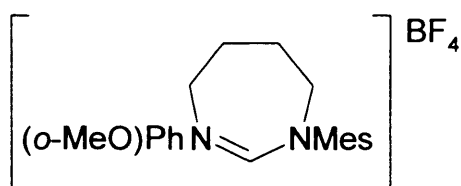
1-(2-anisidyl)-3-(2, 4, 6-trimethylphenyl)-4, 5, 6, 7-tetrahydro-3H-[1, 3]**diazepinium iodide (2.29).**

The reaction was performed on a 10 mmol scale of formamidine (2.68 g), 0.70 g of K₂CO₃ (5 mmol) and 1.31 ml of 1,4-

diiodobutane (10mmol) in 250 ml of acetonitrile. The solution was heated under reflux for 24 hours to yield 3.88 g (86%) of pale yellow, crystalline material.

^1H NMR (CDCl_3 , 400 MHz, 298 K): δ 7.76 (1H, d, $^3J_{\text{HH}} = 6.3$, $o\text{-CH}_{o\text{-MeOPh}}$), 7.33 (1H, t, $^3J_{\text{HH}} = 6.2$, $m\text{-CH}_{o\text{-MeOPh}}$), 7.25 (1H, s, NCHN), 6.98 (1H, t, $^3J_{\text{HH}} = 6.2$, $p\text{-CH}_{o\text{-MeOPh}}$), 6.94 (1H, d, $^3J_{\text{HH}} = 6.3$, $m\text{-CH}_{o\text{-MeOPh}}$), 6.87 (2H, s, $m\text{-CH}_{\text{Mes}}$), 4.52 (2H, t, $^3J_{\text{HH}} = 5.8$, NCH₂), 4.49 (2H, t, $^3J_{\text{HH}} = 5.8$, NCH₂), 3.88 (3H, s, OCH₃ $_{o\text{-MeOPh}}$), 2.44 (4H, m, NCH₂CH₂), 2.39 (6H, s, $o\text{-CH}_3$ $_{\text{Mes}}$), 2.23 (3H, s, $p\text{-CH}_3$ $_{\text{Mes}}$). ^{13}C NMR (CDCl_3 , 100 MHz, 298 K): δ 159.0 (s, NCN), 153.2 (s, Ar-C $_{o\text{-MeOPh}}$), 140.5 (s, Ar-C $_{\text{Mes}}$), 139.7 (s, Ar-C $_{\text{Mes}}$), 134.4 (s, Ar-C $_{\text{Mes}}$), 131.9 (s, Ar-C $_{o\text{-MeOPh}}$), 131.6 (s, Ar-CH $_{o\text{-MeOPh}}$), 130.5 (s, Ar-CH $_{\text{Mes}}$), 128.0 (s, Ar-CH $_{o\text{-MeOPh}}$), 122.1 (s, Ar-CH $_{o\text{-MeOPh}}$), 112.7 (s, Ar-CH $_{o\text{-MeOPh}}$), 56.8 (s, OCH₃), 56.1 (s, NCH₂), 55.0 (s, NCH₂), 25.6 (s, NCH₂CH₂), 25.3 (s, NCH₂CH₂), 21.3 (s, $p\text{-CH}_3$), 18.9 (s, $o\text{-CH}_3$). Anal. Found (Calcd) for C₂₁H₂₇N₂O: C, 55.95 (56.01); H, 6.05 (6.00); N, 6.16 (6.22). HRMS (ES): m/z 323.2110 ([M-I]⁺ C₂₁H₂₇N₂O requires 323.2123).

1-(2-anisidyl)-3-(2, 4, 6-trimethylphenyl)-4, 5, 6, 7-tetrahydro-3H-[1, 3] diazepinium tetrafluoroborete.

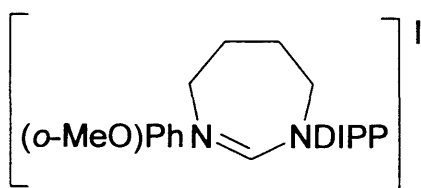


A solution of diazepinium salt 2.70 g (6.0 mmol) in 30 ml acetonitrile was mixed with a solution of sodium tetrafluoroborate 0.99 g (9.0 mmol) in

30 ml distilled water. Yellow crystals were formed (2.15 g, 90%).

^1H NMR (CDCl_3 , 400 MHz, 298 K): δ 7.63 (1H, d, $^3J_{\text{HH}} = 6.7$, *o*- $\text{CH}_{\text{o-MeOPh}}$), 7.31 (1H, t, $^3J_{\text{HH}} = 6.8$, *m*- $\text{CH}_{\text{o-MeOPh}}$), 7.22 (1H, s, NCHN), 6.97 (1H, t, $^3J_{\text{HH}} = 6.8$, *p*- $\text{CH}_{\text{o-MeOPh}}$), 6.93 (1H, d, $^3J_{\text{HH}} = 6.7$, *m*- $\text{CH}_{\text{o-MeOPh}}$), 6.85 (2H, s, *m*- CH_{Mes}), 4.40 (2H, t, $^3J_{\text{HH}} = 5.4$, NCH₂), 4.38 (2H, t, $^3J_{\text{HH}} = 5.4$, NCH₂), 3.88 (3H, s, OCH₃ *o-MeOPh*), 2.40 (4H, m, NCH₂CH₂), 2.34 (6H, s, *o*-CH₃ *Mes*), 2.20 (3H, s, *p*-CH₃ *Mes*). ^{13}C NMR (CDCl_3 , 100 MHz, 298 K): δ 159.2 (s, NCN), 153.3 (s, *Ar*-C_{o-MeOPh}), 140.5 (s, *Ar*-C_{Mes}), 139.7 (s, *Ar*-C_{Mes}), 134.4 (s, *Ar*-C_{Mes}), 132.0 (s, *Ar*-C_{o-MeOPh}), 131.6 (s, *Ar*-CH_{o-MeOPh}), 130.5 (s, *Ar*-CH_{Mes}), 127.9 (s, *Ar*-CH_{o-MeOPh}), 122.2 (s, *Ar*-CH_{o-MeOPh}), 112.7 (s, *Ar*-CH_{o-MeOPh}), 56.7 (s, OCH₃), 55.7 (s, NCH₂), 54.7 (s, NCH₂), 25.6 (s, NCH₂CH₂), 25.3 (s, NCH₂CH₂), 21.3 (s, *p*-CH₃), 18.5 (s, *o*-CH₃).

1-(2-anisidyl)-3-(2, 6-diisopropylphenyl)-4, 5, 6, 7-tetrahydro-3H-[1, 3] diazepinium iodide (2.30).



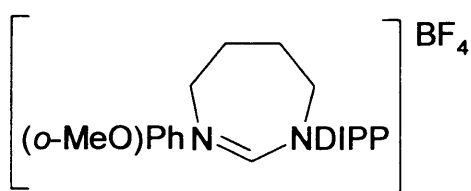
The reaction was performed on a 10 mmol scale of formamidine (3.10 g), 0.70 g of K_2CO_3 (5mmol) and 1.31 ml of 1,4-diiodobutane (10mmol) in 250 ml of

acetonitrile. The solution was heated under reflux for 48 hours to yield 4.11 g (84%) of white, crystalline material.

^1H NMR (CDCl_3 , 400 MHz, 298 K): δ 7.82 (1H, d, $^3J_{\text{HH}} = 6.7$, *o*- $\text{CH}_{\text{o-MeOPh}}$), 7.35 (1H, t, $^3J_{\text{HH}} = 6.8$, *m*- $\text{CH}_{\text{o-MeOPh}}$), 7.31 (1H, t, $^3J_{\text{HH}} = 7.8$, *p*- CH_{DIPP}), 7.25 (1H, s, NCHN), 7.17 (2H, d, $^3J_{\text{HH}} = 7.8$, *m*- CH_{DIPP}), 7.00 (1H, t, $^3J_{\text{HH}} = 6.8$, *p*- $\text{CH}_{\text{o-MeOPh}}$), 6.95 (1H, d, $^3J_{\text{HH}} = 6.7$, *m*- $\text{CH}_{\text{o-MeOPh}}$), 4.53 (2H, t, $^3J_{\text{HH}} = 5.5$,

NCH_2), 4.46 (2H, t, $^3J_{\text{HH}} = 5.5$, NCH_2), 3.87 (3H, s, OCH_3 *o*-MeOPh), 2.25 (2H, sept., $^3J_{\text{HH}} = 6.8$, $\text{CH}(\text{CH}_3)_2$ DIPP), 2.44 (4H, m, NCH_2CH_2), 1.30 (6H, d, $^3J_{\text{HH}} = 6.8$, $\text{CH}(\text{CH}_3)_2$ DIPP), 1.18 (6H, d, $^3J_{\text{HH}} = 6.8$, $\text{CH}(\text{CH}_3)_2$ DIPP). ^{13}C NMR (CDCl_3 , 100 MHz, 298 K): δ 158.0 (s, NCN), 153.4 (s, Ar-C_{*o*}-MeOPh), 145.3 (s, Ar-C_{DIPP}), 139.5 (s, Ar-C_{DIPP}), 132.2 (s, Ar-C_{*o*}-MeOPh), 131.8 (s, Ar-CH_{*o*}-MeOPh), 131.2 (s, Ar-CH_{DIPP}), 128.3 (s, Ar-CH_{DIPP}), 125.7 (s, Ar-CH_{*o*}-MeOPh), 122.3 (s, Ar-CH_{*o*}-MeOPh), 112.7 (s, Ar-CH_{*o*}-MeOPh), 56.8 (s, OCH_3), 56.5 (s, NCH_2), 56.4 (s, NCH_2), 29.1 (s, $\text{CH}(\text{CH}_3)_2$), 25.7 (s, NCH_2CH_2), 25.3 (s, NCH_2CH_2), 25.2 (s, $\text{CH}(\text{CH}_3)_2$), 24.5 (s, $\text{CH}(\text{CH}_3)_2$). Anal. Found (Calcd) for: $\text{C}_{24}\text{H}_{33}\text{N}_2\text{O}$ C, 58.53 (58.55); H, 7.19 (6.71); N, 5.55 (5.69). HRMS (ES): m/z 365.2586 ($[\text{M}-\text{I}]^+$ $\text{C}_{24}\text{H}_{33}\text{N}_2\text{O}$ requires 309.1967).

1-(2-anisidyl)-3-(2, 6-diisopropylphenyl)-4, 5, 6, 7-tetrahydro-3H-[1, 3] diazepinium tetrafluoroborete.



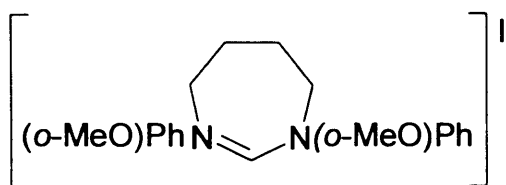
A solution of diazepinium salt 2.95 g (6mmol) in 30 ml acetonitrile was mixed with a solution of sodium

tetrafluoroborate 0.99 g (9mmol) in 30 ml distilled water. Yellow crystals were formed (2.34 g, 86%).

^1H NMR (CDCl_3 , 400 MHz, 298 K): δ 7.63 (1H, d, $^3J_{\text{HH}} = 6.7$, *o*-CH_{*o*}-MeOPh), 7.34 (1H, t, $^3J_{\text{HH}} = 6.8$, *m*-CH_{*o*}-MeOPh), 7.30 (1H, t, $^3J_{\text{HH}} = 7.8$, *p*-CH_{DIPP}), 7.23 (1H, s, NCHN), 7.17 (2H, d, $^3J_{\text{HH}} = 7.8$, *m*-CH_{DIPP}), 6.97 (1H, t, $^3J_{\text{HH}} = 6.8$, *p*-CH_{*o*}-MeOPh), 6.94 (1H, d, $^3J_{\text{HH}} = 6.7$, *m*-CH_{*o*}-MeOPh), 4.33 (2H, t, $^3J_{\text{HH}} = 5.5$, NCH_2), 4.23 (2H, t, $^3J_{\text{HH}} = 5.5$, NCH_2), 3.87 (3H, s, OCH_3 *o*-MeOPh), 3.18 (2H,

sept., $^3J_{\text{HH}} = 6.8$, $\text{CH}(\text{CH}_3)_2$ DIPP), 2.42 (4H, m, NCH_2CH_2), 1.30 (6H, d, $^3J_{\text{HH}} = 6.8$, $\text{CH}(\text{CH}_3)_2$ DIPP), 1.19 (6H, d, $^3J_{\text{HH}} = 6.8$, $\text{CH}(\text{CH}_3)_2$ DIPP). ^{13}C NMR (CDCl_3 , 100 MHz, 298 K): δ 158.7 (s, NCN), 153.5 (s, Ar-C_o-MeOPh), 145.4 (s, Ar-C_{DIPP}), 139.6 (s, Ar-C_{DIPP}), 132.2 (s, Ar-C_o-MeOPh), 131.9 (s, Ar-CH_o-MeOPh), 131.2 (s, Ar-CH_{DIPP}), 128.1 (s, Ar-CH_{DIPP}), 125.7 (s, Ar-CH_o-MeOPh), 122.4 (s, Ar-CH_o-MeOPh), 112.7 (s, Ar-CH_o-MeOPh), 56.7 (s, OCH₃), 56.2 (s, NCH₂), 55.9 (s, NCH₂), 29.0 (s, $\text{CH}(\text{CH}_3)_2$), 25.6 (s, NCH_2CH_2), 25.3 (s, NCH_2CH_2), 25.1 (s, $\text{CH}(\text{CH}_3)_2$), 24.5 (s, $\text{CH}(\text{CH}_3)_2$).

1, 3-di(2-anisidyl)-4, 5, 6, 7-tetrahydro-3H-[1, 3] diazepinium iodide (2.31).



The reaction was performed on a 10 mmol scale of formamidine (2.56 g), 0.70 g of K_2CO_3 (5 mmol) and 1.31 ml of 1,4-diiodobutane (10mmol) in

250 ml of acetonitrile. The solution was heated under reflux for 5 days to yield 3.85 g (88%) of white, crystalline material.

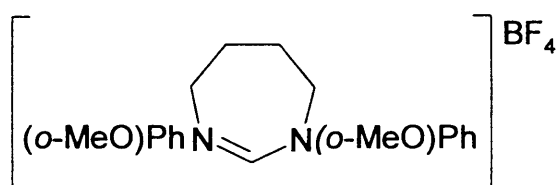
^1H NMR (CDCl_3 , 400 MHz, 298 K): δ 7.92 (2H, d, $^3J_{\text{HH}} = 6.3$, *o*-CH_o-MeOPh), 7.37 (1H, s, NCHN), 7.31 (2H, t, $^3J_{\text{HH}} = 6.8$, *m*-CH_o-MeOPh), 6.96 (2H, t, $^3J_{\text{HH}} = 6.8$, *p*-CH_o-MeOPh), 6.93 (2H, d, $^3J_{\text{HH}} = 6.3$, *m*-CH_o-MeOPh), 4.41 (4H, t, $^3J_{\text{HH}} = 5.8$, NCH₂), 3.88 (6H, s, OCH₃ *o*-MeOPh), 2.43 (4H, m, NCH₂CH₂). ^{13}C NMR (CDCl_3 , 100 MHz, 298 K): δ 159.0 (s, NCN), 153.6 (s, Ar-C_o-MeOPh), 132.4 (s, Ar-C_o-MeOPh), 131.5 (s, Ar-CH_o-MeOPh), 128.5 (s, Ar-CH_o-MeOPh), 122.0 (s, Ar-CH_o-MeOPh), 112.5 (s, Ar-CH_o-MeOPh), 56.7 (s, OCH₃), 55.5 (s, NCH₂), 25.4 (s, NCH₂CH₂). Anal. Found (Calcd) for: $\text{C}_{19}\text{H}_{23}\text{N}_2\text{O}_2\text{I}$ C, 51.80 (52.07); H, 5.25



(5.25); N, 6.30 (6.39). HRMS (ES): m/z 311.1745 ($[M-I]^+$ $C_{19}H_{23}N_2O_2$ requires 311.1760).

1, 3-di-(2-anisidyl)-4, 5, 6, 7-tetrahydro-3H-[1, 3] diazepinium

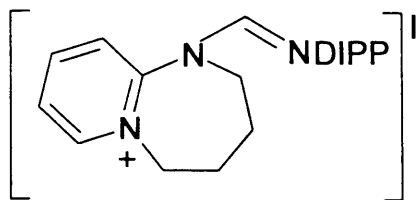
tetrafluoroborete.



A solution of diazepinium salt 2.63 g (6.0 mmol) in 30 ml acetonitrile was mixed with a solution of sodium

tetrafluoroborate 0.99 g (9.0 mmol) in 30 ml distilled water. White crystals were formed (2.20 g, 92%).

1H NMR ($CDCl_3$, 400 MHz, 298 K): δ 7.62 (2H, d, $^3J_{HH} = 6.3$, $o-CH_{o-MeOPh}$), 7.32 (1H, s, NCHN), 7.31 (2H, t, $^3J_{HH} = 6.8$, $m-CH_{o-MeOPh}$), 6.97 (2H, t, $^3J_{HH} = 6.8$, $p-CH_{o-MeOPh}$), 6.95 (2H, d, $^3J_{HH} = 6.3$, $m-CH_{o-MeOPh}$), 4.27 (4H, t, $^3J_{HH} = 5.8$, NCH₂), 3.88 (6H, s, OCH₃ $o-MeOPh$), 2.37 (4H, m, NCH₂CH₂). ^{13}C NMR ($CDCl_3$, 100 MHz, 298 K): δ 159.2 (s, NCN), 153.6 (s, Ar-C $_{o-MeOPh}$), 132.3 (s, Ar-C $_{o-MeOPh}$), 131.5 (s, Ar-CH $_{o-MeOPh}$), 128.1 (s, Ar-CH $_{o-MeOPh}$), 121.9 (s, Ar-CH $_{o-MeOPh}$), 112.6 (s, Ar-CH $_{o-MeOPh}$), 56.6 (s, OCH₃), 54.9 (s, NCH₂), 25.2 (s, NCH₂CH₂).

Preparation of compound 2.33a.

The reaction was performed on a 10 mmol scale of formamidine (2.81 g), 0.70 g of K_2CO_3 (5 mmol) and 1.31 ml of 1,4-diodobutane (10mmol) in 250 ml of

acetonitrile. The solution was heated under reflux. At the end of the reaction, the volatiles were removed in vacuo and the residue freed of residual solvent by stirring with 3 portions of 5 ml of dichloromethane, which were subsequently pumped off. The yellow oil of the mixture product was washed with toluene until a pale yellow solid precipitated. The solid was dissolved in 2 ml of dichloromethane. Ether was slowly added to the resulting dichloromethane solution until the product started crystallising. The yield was 0.88 g (26%).

1H NMR ($CDCl_3$, 400 MHz, 298 K): δ 9.68 (1H, d, α - CH_{Py}), 8.41 (1H, t, p - CH_{Py}), 7.90 (1H, t, p - CH_{DIPP}), 7.69 (1H, s, NCHN), 7.48 (1H, d, m - CH_{Py}), 7.08 (1H, t, m - CH_{Py}), 7.04 (2H, d, m - CH_{DIPP}), 4.98 (2H, t, $^3J_{HH} = 5.8$, NCH_2), 4.14 (2H, t, $^3J_{HH} = 5.8$, NCH_2), 2.92 (2H, sept., $CH(CH_3)_2$ DIPP), 2.34 (2H, m, NCH_2CH_2), 2.34 (2H, m, NCH_2CH_2), 1.16 (12H, d, $CH(CH_3)_2$ DIPP). ^{13}C NMR ($CDCl_3$, 100 MHz, 298 K): δ 151.5 (s, NCN), 146.7 (s, Ar- C_{Py}), 146.1 (s, Ar- CH_{Py}), 145.8 (s, Ar- C_{DIPP}), 143.4 (s, Ar- C_{DIPP}), 137.5 (s, Ar- CH_{DIPP}), 123.9 (s, Ar- CH_{Py}), 123.4 (s, Ar- CH_{DIPP}), 122.7 (s, Ar- CH_{Py}), 122.1 (s, Ar- CH_{Py}), 59.3 (s, NCH_2), 46.4 (s, NCH_2), 27.1 (s, $CH(CH_3)_2$), 24.6 (s, NCH_2CH_2), 23.1 (s, NCH_2CH_2), 22.7 (s, $CH(CH_3)_2$), 22.5 (s, $CH(CH_3)_2$).

2.4. References.

- [1] R. W. Alder, M. E. Blake, C. Bortolotti, S. Bufali, C. P. Butts, E. Linehan, J. M. Oliva, A. G. Orpen and M. J. Quayle, *Chem. Commun.*, **1999**, 241.
- [2] P. Bazinet, G. P. A. Yap and D. S. Richeson, *J. Am. Chem. Soc.*, **2003**, *125*, 13314.
- [3] M. Mayr, K. Wurst, K.-H. Ongania and M. R. Buchmeiser, *Chem. Eur. J.*, **2004**, *10*, 1256.
- [4] W. A. Herrmann, S. K. Schneider, K. Öfele, M. Sakamoto and E. Herdtweck, *J. Organomet. Chem.*, **2004**, *689*, 2441.
- [5] R. Jazzar, H. Liang, B. Donnadieu and G. Bertrand, *J. Organomet. Chem.*, **2006**, *691*, 3201.
- [6] P. Bazinet, T.-G. Ong, J. S. O'Brien, N. Lavoie, E. Bell, G. P. A. Yap, I. Korobkov and D. S. Richeson, *Organometallics*, **2007**, *26*, 2885.
- [7] C. C. Scarborough, M. J. W. Grady, I. A. Guzei, B. A. Gandhi, E. E. Bunel and S. S. Stahl, *Angew. Chem. Int. Ed. Eng.*, **2005**, *44*, 5269.
- [8] C. C. Scarborough, B. V. Popp, I. A. Guzei and S. S. Stahl, *J. Organomet. Chem.*, **2005**, *690*, 6143.
- [9] M. M. Rogers, J. E. Wendlandt, I. A. Guzei and S. S. Stahl, *Org. Lett.*, **2006**, *8*, 2257.
- [10] M. Iglesias, D. J. Beetstra, A. Stasch, P. N. Horton, M. B. Hursthouse, S. J. Coles, K. J. Cavell, A. Dervisi and I. A. Fallis, *Organometallics*, **2007**, *26*, 4800.

- [11] E. Teuma, C. Lyon-Saunier, H. Gornitzka, G. Mignani, A. Baceiredo and G. Bertrand, *J. Organomet. Chem.*, **2005**, *690*, 5541.
- [12] S. Saba, A. Brescia and M. K. Kaloustian, *Tetrahedron Lett.*, **1991**, *32*, 5031.
- [13] A. H. Wolfgang, *Angew. Chem. Int. Ed. Eng*, **2002**, *41*, 1290.
- [14] J. Y. Cheng and Y. H. Chu, *Tetrahedron Lett.*, **2006**, *47*, 1575.
- [15] I. J. B. Lin and C. S. Vasam, *J. Organomet. Chem.*, **2005**, *690*, 3498.
- [16] M. Iglesias, D. J. Beetstra, J. C. Knight, L. Ooi, A. Stach, S. J. Coles, L. Male, M. B. Hursthouse, K. J. Cavell, A. Dervisi and I. Fallis, *Organometallics*, **2008**, *27*, 3279.
- [17] I. Özdemir, N. Gurbuz, Y. Gok and B. Cetinkaya, *Heteroatom Chem.*, **2008**, *19*, 82.
- [18] K. M. kuhn and R. H. Grubbs, *Org. Lett.*, **2008**, *10*, 2075.
- [19] A. M. Magill, K. J. Cavell and B. F. Yates, *J. Am. Chem. Soc.*, **2004**, *126*, 8717.
- [20] K. Vehlow, S. Gessler and S. Blechert, *Angew. Chem. Int. Ed. Eng.*, **2007**, *46*, 8082.
- [21] M. Kuriyame, R. Shimazawa and R. Shirai, *Tetrahedron*, **2007**, *63*, 9393.
- [22] N. Styliades, A. A. Danopoulos, D. Pugn, F. Hancock and A. Zanotti-Gevole, *Organometallics*, **2007**, *26*, 5627.
- [23] S. Balof, S. J. Ppool, N. J. Berger, E. J. Valente, A. M. Shiller and H. Schanz, *Dalton Trans.*, **2008**, 5791.
- [24] J. E. Thomson, C. D. Cambloeil, C. Concellon, N. Duguet, K. Rix, A. Slawin and A. D. Smith, *J. Org. Chem.*, **2008**, *73*, 2784.

- [25] X. Luar, R. Mariz, M. Gatti, C. Costabile, A. Poater, L. Cavallo, A. Linden and R. Dortaz, *J. Am. Chem. Soc.*, **2008**, *130*, 6848.
- [26] S. Leuthauser, V. Schmidts, C. M. Thiele and H. Plenio, *Chem. Eur. J.*, **2008**, *14*, 5465.
- [27] A. Paczal, A. C. Bnyei and A. Kotschy, *J. Org. Chem.*, **2006**, *71*, 5969.
- [28] I. Özdemir, S. Demir, S. Yasar and B. Cetinkaya, *Appl. Organometal. Chem.* **2005**, *19*, 55.
- [29] I. Özdemir, S. Yasar, S. Demir and B. Cetinkaya, *Heteroatom Chem.*, **2005**, *16*, 557.
- [30] S. Yasar, I. Özdemir, B. Cetinkaya, J. Renaud and C. Bruneau, *Eur. J. Org. Chem.*, **2008**, 2142.
- [31] L. Strekowski, R. L. Wydra, M. T. Cegla, A. Czarny and S. Patteron, *J. Org. Chem.*, **1989**, *54*, 6120.
- [32] R. M. Roberts, *J. Am. Chem. Soc.*, **1949**, *71*, 3848.
- [33] R. M. Roberts, R. H. Dewolfe and J. H. Ross, *J. Am. Chem. Soc.*, **1951**, *73*, 2277.
- [34] R. M. Roberts, *J. Am. Chem. Soc.*, **1950**, *72*, 3603.
- [35] E. B. Knott and R. A. Jeffreys, *J. Org. Chem.*, **1949**, *14*, 879.
- [36] F. A. Cotton, P. Lei, C. A. Murillo and L.-S. Wang, *Inorg. Chim. Acta.*, **2003**, *349*, 165.
- [37] R. M. Roberts, *J. Org. Chem.*, **1949**, *14*, 277.
- [38] F. A. Cotton, S. C. Haefner, J. H. Matonic, W. Xiaoping and C. A. Murillo, *Polyhedron*, **1997**, *16*, 541.
- [39] K. E. Krahulic, G. D. Enright, M. Parvez and R. Roesler, *J. Am. Chem. Soc.*, **2005**, *127*, 4142-4143.

[40] R. Alcántara, L. Canoira, P. Guilherme-Joao and J. P. Pérez-Mendo, *Appl. Cata.*, **2001**, *218*, 269.

[41] A. J. Arduengo, J. R. Goerlich and W. J. Marshall, *J. Am. Chem. Soc.*, **1995**, *117*, 11027.

[42] A. Danopoulos, S. Winston, T. Gelbrich, M. Hursthouse and R. Tooze, *Chem. Comm.*, **2002**, 482.

[43] D. Nielsen, K. J. Cavell, B. Skelton and A. White, *Inorg. Chem. Acta.*, **2002**, *327*, 116.

Chapter Three

Synthesis of Complexes with Expanded NHCs as Functionalised Ligands

Chapter Three

Synthesis of Complexes with Expanded NHCs as Functionalised Ligands

3.1. Introduction.

Prior to 1991, when the first stable, free carbenes were isolated by Arduengo *et al.*,^[1] metal complexes of NHCs were reported by Öfele **3.1**^[2] and Wanzlick **3.2**,^[3] prepared directly from imidazolium salts. A wide range of transition metal-NHC complexes including **3.3** and **3.4** were prepared by Lappert in 1970 from electron- rich olefins (Figure 3-1).^[4]

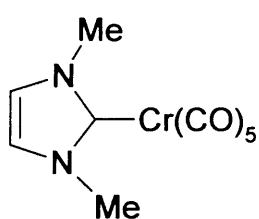
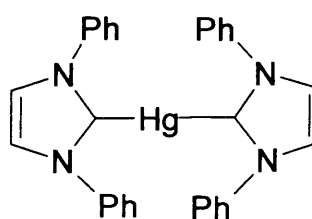
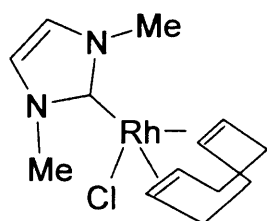
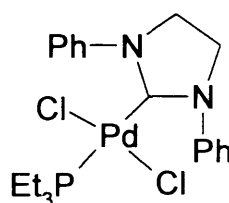
**3.1****3.2****3.3****3.4**

Figure 3-1: Early metal complexes of NHCs.

Encouraged by the early applications utilising Rh(I) and Ir(I) complexes of simple monodentate NHC ligands, there was a natural progression to expand the catalytic application of Rh- and Ir-NHC complex systems through some modification of the NHC ligands.^[5-10] This included the incorporation of functional groups leading to easily recoverable catalysts (soluble in water and methanol) and catalysts containing flexible, sterically bulky ligands (chiral, bidentate and pincer)^[11] with a combination of strongly-bound NHC moiety and weakly-bound nucleophilic, functional groups. This would furnish the ligands with hemilabile donor groups as these can increase catalytic activities by stabilising the low-valent centres formed during catalysis. These functional groups can be incorporated at one or both nitrogens of the NHC-ring to give access to bi- or tridentate NHC ligands. Rh(I) and Ir(I) complexes of functionalised NHC ligands are limited. They have been reported with pyridyls (3.5, 3.6, 3.7, 3.8),^[8] amines (3.9, 3.10),^[7] esters, ethers and amides (3.11, 3.12, 3.13)^[6] (Figure 3-2).

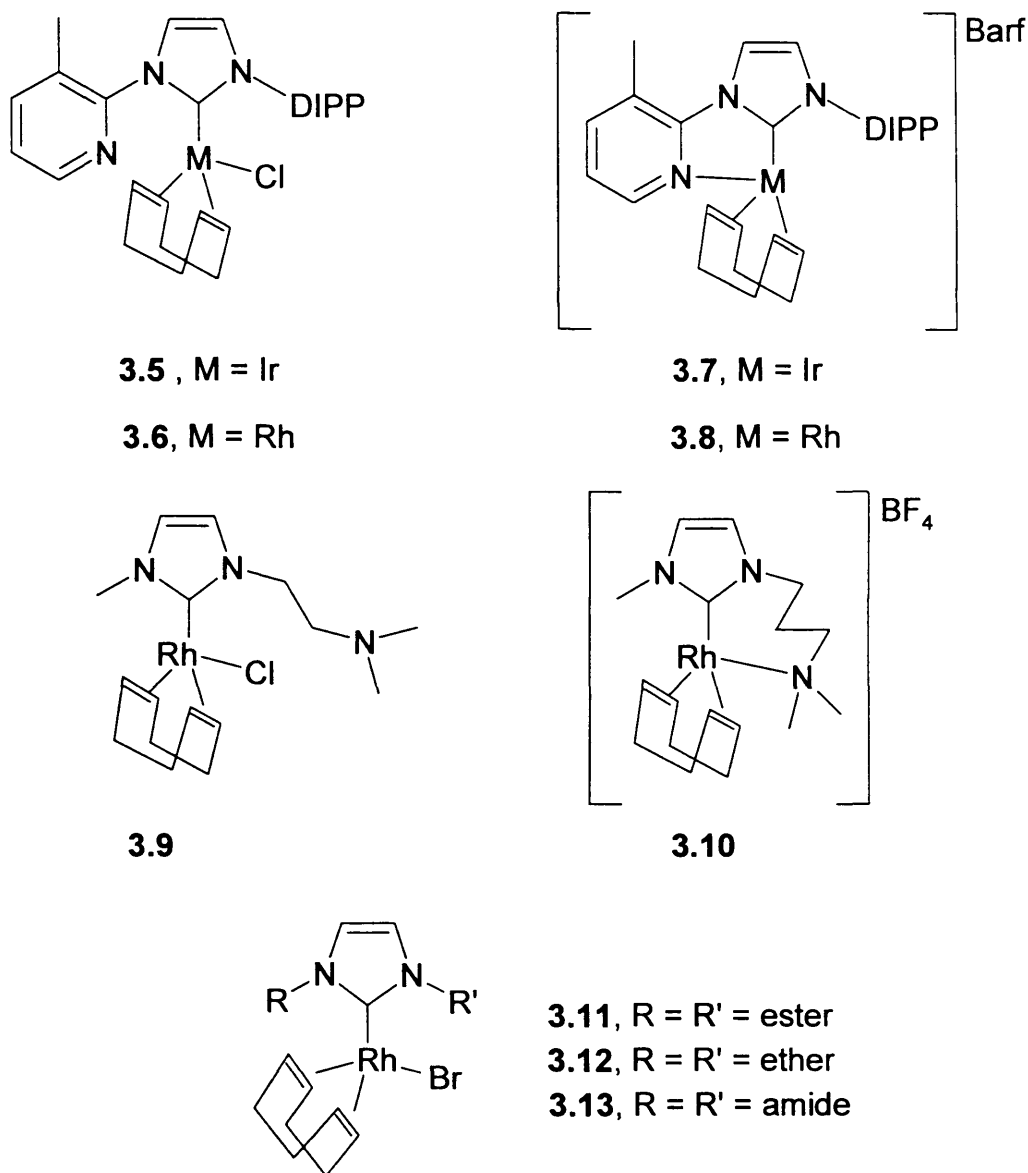
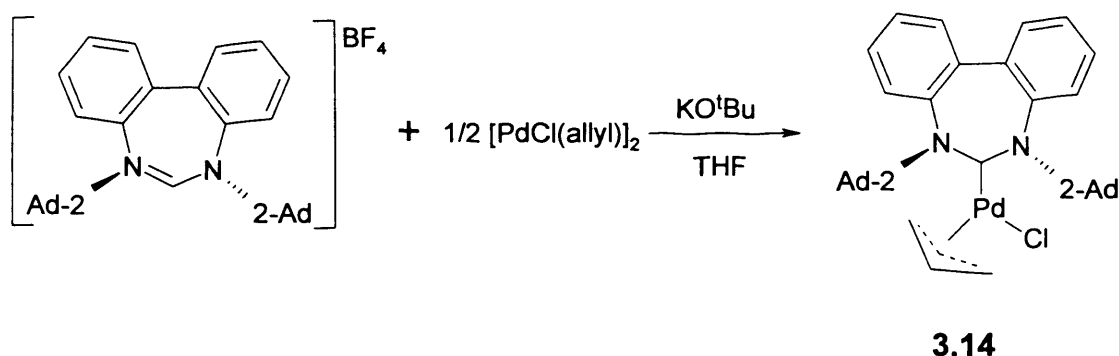


Figure 3-2: Example of Rh(I) and Ir(I) complexes of functionalised NHC ligands.

Crabtree *et al.* has reported the effect of linker length and counterions on the formation of the chelated Ir(I) NHC complexes. These complexes have demonstrated that long linker length and coordinated counterions disfavour the formation of chelated complexes, while short linker length and non-coordinating counterions favour chelated complexes.^[12]

A number of complexes of 6-membered NHCs have been reported. The crystal structure analysis of corresponding expanded ring NHC-complexes shows the opening of the NCN angle and the decrease of the $C_{\text{NHC}}\text{-N-C}_{\text{subs}}$ angle as main features, which increase the steric hindrance around the metal core.^[13-18]

The structure; electronic and steric properties; as well as the coordination chemistry and catalytic performance of the 7-membered carbene complexes have been relatively unexplored compared with their saturated and unsaturated 5-membered analogues. The first 7-membered carbene complex was prepared in 2005 by Stahl and co-workers. It was synthesised by *in situ* deprotonation of the BF_4 salt with KO^tBu in the presence of a metal precursor as shown in Scheme 3-1.^[19, 20]



Scheme 3-1: Synthesis of the first 7-membered carbene complex.

When compared with 5- or 6-membered carbenes, torsional twist is the most distinctive feature of the 7-membered carbene complexes. Stahl defines this as a dihedral angle between the two aryl rings of the biphenyl backbone and the torsional angle (β) between the $(C_{\text{ring}}\text{-N}\dots\text{N-C}_{\text{ring}})$ of the carbene ring,

which dictate the spatial disposition of the substituents into the coordination sphere. The repositioning of the substituents (by a modification of the dihedral angle and β) is permitted by the flexibility of the ligand. This depends on the steric requirements of the ligands present in the metal coordination sphere.

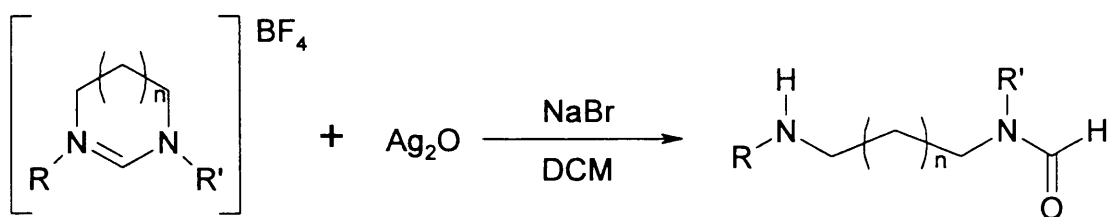
This chapter presents the synthesis and characterisation of Rhodium- and Iridium-expanded ring carbene complexes. All the Rh and Ir NHC-complexes obtained are found to be air and moisture stable. In order to study the effects of the expansion of the ring on the square planar complexes, the crystal structure data of these complexes are presented and compared to the 5-membered carbene complexes.

3.2. Results and Discussion.

3.2.1. Attempted Synthesis of Silver (I) Carbene Complexes.

Since the isolation of the first Ag(I) carbene complexes employing a silver base, their use as carbene transfer agents have become a convenient and sometimes essential route for the synthesis of other metal carbene complexes, such as Rh and Ir.^[6, 9, 10, 20, 21] Wang and Lin^[22] have demonstrated that Ag(I) complexes of NHCs could be synthesised directly from imidazolium salts with silver(I)oxide as a source of basic silver and that this has now become the most widely used method for the synthesis of Ag(I) carbene complexes.^[23] According to the literature review, the best way to

obtain the expanded NHC silver complexes in good yield is through the reaction of amidinium tetrafluoroborate salts with Ag_2O in the presence of NaBr .^[24, 25] Our attempts to prepare $\text{Ag}(\text{I})$ complexes of expanded, functionalised NHC carbenes by using a variety of methods leads to hydrolysis of the carbene (Scheme 3-2).



$$n = 1, 2$$

$$R = \text{Py}, o\text{-MeOPh}, o\text{-MeSPh}$$

$$R' = \text{Mes}, \text{DIPP}$$

Scheme 3-2: An attempt to prepare rigid, expanded, functionalised $\text{Ag}(\text{I})$ NHC carbene complexes.

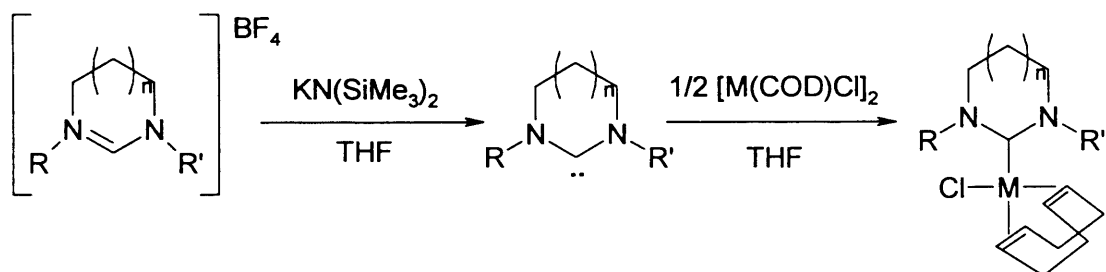
It is not clear if this result is a consequence of the instability of the silver carbene complexes under ambient conditions or of some changes in the concerted mechanism of deprotonation and subsequent coordination.^[24, 25]

3.2.2. Rhodium (I) and Iridium (I) COD Complexes.

$\text{Rh}(\text{I})$ and $\text{Ir}(\text{I})$ complexes of expanded ring NHCs were synthesised. There is an extensive literature on complexes of imidazolylidenes with these metals.^[16,26-29] $[\text{Rh}(\text{NHC})(\text{COD})\text{Cl}]$ and $[\text{Ir}(\text{NHC})(\text{COD})\text{Cl}]$ complexes with different ring-size carbenes and the same substituents on the nitrogens were

synthesised, which would allow the comparison of our complexes with a wide variety of carbenes.^[30, 31]

The use of the free carbene route, achieved by deprotonation of the NHC carbene salts with a strong base was successful, but due to the relative instability of the free carbenes, Rh(I) and Ir(I) complexes were best synthesised by an *in situ* reaction of the corresponding NHC-BF₄ salt in THF with KN(SiMe₃)₂, followed by the addition of 0.5 equiv. of [M(COD)Cl]₂, M = Rh or Ir, at ambient temperature. This was to give the desired rhodium complexes (**3.15**, **3.16**, **3.17**, **3.18**, **3.19** and **3.20**) and iridium complexes (**3.21**, **3.22**, **3.23** and **3.24**) as yellow air stable solids in good yields after work-up, as shown in Scheme 3-3.



M = Rh

M = Ir

n = 1, R = *o*-MeOPh, R' = Mes, **3.15** / n = 1, R = *o*-MeOPh, R' = Mes, **3.21**

R = *o*-MeOPh, R' = DIPP, **3.16** / R = *o*-MeOPh, R' = DIPP, **3.22**

R = R' = *o*-MeOPh, **3.17**

n = 2, R = *o*-MeOPh, R' = Mes, **3.18** / n = 2, R = *o*-MeOPh, R' = Mes, **3.23**

R = *o*-MeOPh, R' = DIPP, **3.19** / R = *o*-MeOPh, R' = DIPP, **3.24**

R = R' = *o*-MeOPh, **3.20**

Scheme 3-3: Preparation of Rh(I) and Ir(I) COD complexes with functionalised expanded NHC ligands.

3.2.2.1. Solution NMR Studies of Rh(I) and Ir(I) COD

Complexes.

The characteristic NMR chemical shifts for Rh(I) and Ir(I) COD complexes are shown in Table 3-1. The most characteristic chemical shift in the ^1H NMR spectrum is that for the $o\text{-CH}_{o\text{-MeOPh}}$ on the ring of the *N*-functionalised substituents, which changes, for example, from 7.63 ppm in the carbene salt to 8.35 ppm in the Rh(I) complex **3.18** $[\text{Rh}(7\text{-}o\text{-MeOPh-Mes})(\text{COD})\text{Cl}]$ and to 8.05 ppm in the Ir(I) complex **3.23** $[\text{Ir}(7\text{-}o\text{-MeOPh-Mes})(\text{COD})\text{Cl}]$. This change in the ^1H NMR is attributed to close proximity to the electron rich metal centres.

In ^{13}C NMR spectrum the most notable chemical shift is that of the carbene carbon (Table 3-1), which for example changes from a singlet at 159.2 ppm in the carbene salt to a doublet at 221.7 ppm ($^1J_{\text{RhC}} = 46.3$) and a singlet at 215.8 ppm for complex **3.18** $[\text{Rh}(7\text{-}o\text{-MeOPh-Mes})(\text{COD})\text{Cl}]$ and complex **3.23** $[\text{Ir}(7\text{-}o\text{-MeOPh-Mes})(\text{COD})\text{Cl}]$, respectively.

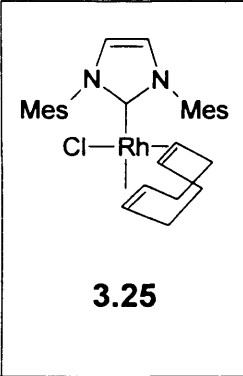
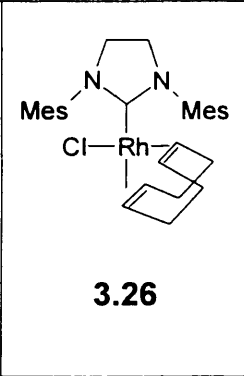
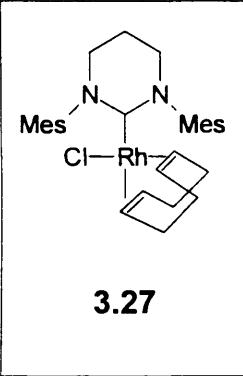
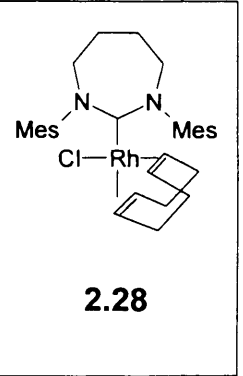
Table 3-1: Characteristic NMR for the carbene salt and their Rh(I) and Ir(I) complexes in CDCl₃ solution.

		<i>o</i> -CH _o -MeOPh (δ_{H}) ppm	OCH ₃ (δ_{H}) ppm	C _N CN (δ_{C}) ppm
6- <i>o</i> -MeOPh-Mes	2.23	7.59	3.83	155.1
Rh(6- <i>o</i> -MeOPh-Mes)(COD)Cl]	3.15	8.39	3.80	210.0
Ir(6- <i>o</i> -MeOPh-Mes)(COD)Cl]	3.21	8.09	3.79	205.5
6- <i>o</i> -MeOPh-DIPP	2.24	7.59	3.85	158.7
Rh(6- <i>o</i> -MeOPh-DIPP)(COD)Cl]	3.16	8.36	3.80	211.5
Ir(6- <i>o</i> -MeOPh-DIPP)(COD)Cl]	3.22	8.04	3.76	207.5
6- <i>o</i> -MeOPh	2.25	7.62	3.88	154.6
Rh(6- <i>o</i> -MeOPh)(COD)Cl]	3.17	8.45	3.81	208.6
7- <i>o</i> -MeOPh-Mes	2.29	7.63	3.88	159.6
Rh(7- <i>o</i> -MeOPh-Mes)(COD)Cl]	3.18	8.35	3.81	224.0
Ir(7- <i>o</i> -MeOPh-Mes)(COD)Cl]	3.23	8.05	3.79	215.8
7- <i>o</i> -MeOPh-DIPP	2.30	7.63	3.87	158.7
Rh(7- <i>o</i> -MeOPh-DIPP)(COD)Cl]	3.19	8.41	3.84	224.0
Ir(6- <i>o</i> -MeOPh-DIPP)(COD)Cl]	3.24	8.08	3.78	218.1
7- <i>o</i> -MeOPh	2.31	7.62	3.88	159.2
Rh(7- <i>o</i> -MeOPh)(COD)Cl]	3.20	8.43	3.85	215.6

The values of the carbene carbon chemical shift for 7-membered NHC Rh(I) and Ir(I) complexes are substantially downfield from the ones reported for 5-membered carbene complexes.^[18, 30, 32] Table 3-2 shows carbene

carbon values for closely related 5-, 6- and 7-membered carbene Rh(I) complexes.^[25, 33]

Table 3-2: ¹³C NMR chemical shift values for NCN for previously reported Rh(I) carbene complexes.

				
	3.25	3.26	3.27	2.28
$C_{NCN} (\delta_C)$ ppm	184.8	211.6	211.5	224.0

3.2.2.2. Solid State Structures of Rh(I) and Ir(I) COD Complexes.

Crystals suitable for X-ray diffraction for all Rh(I) and Ir(I) COD complexes were obtained by layering a dichloromethane solution of the corresponding complex with hexane at ambient temperature. The crystal structures for complexes **3.15**, **3.18**, **3.21** and **3.23** (ones with Mes substituent) are shown in Figure 3-3 and selected bond length and angles can be found in Table 3-3. Elemental analysis and mass spectra gave satisfactory results consistent with the formulation of the complexes.

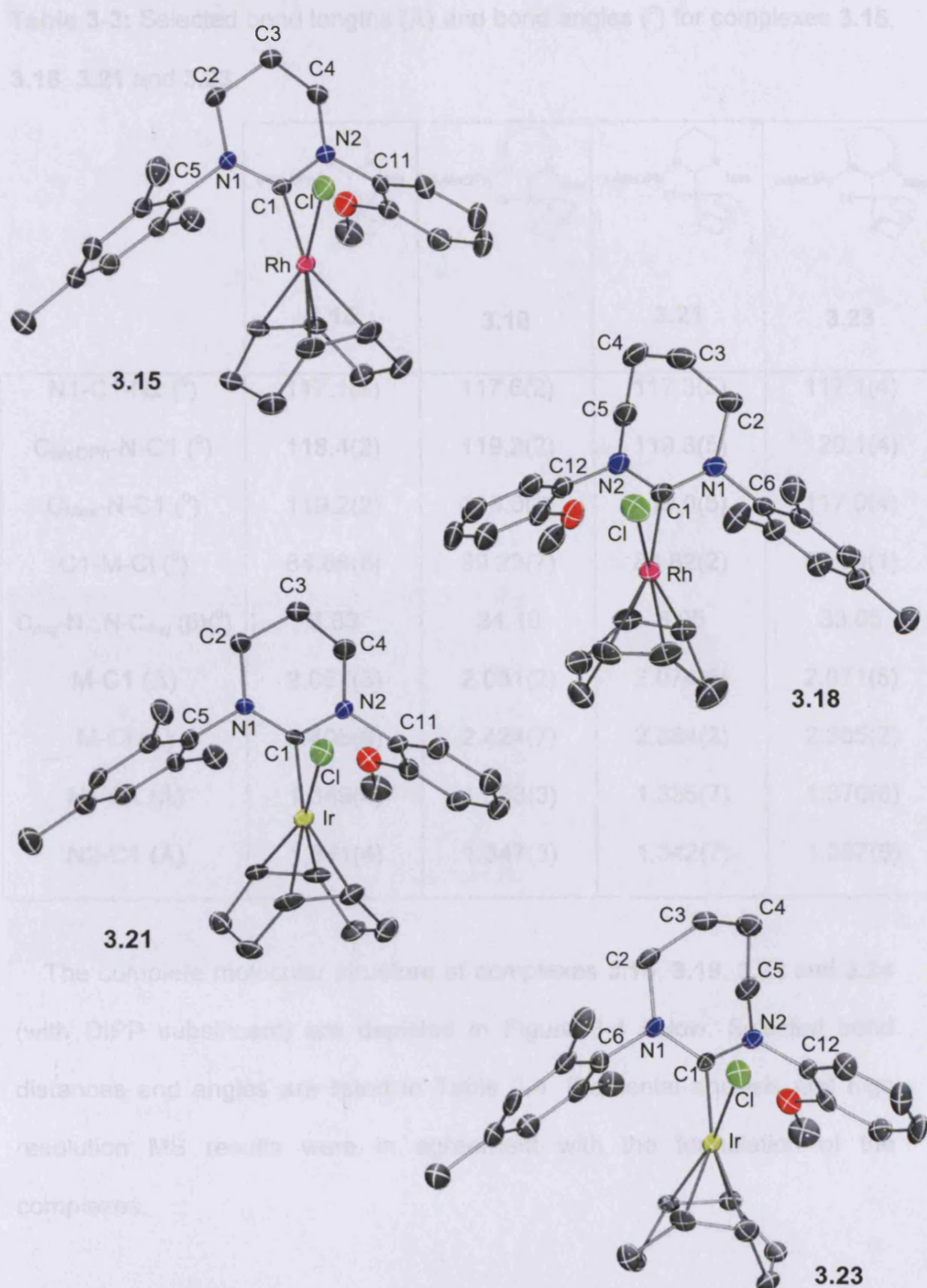
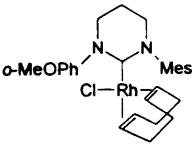
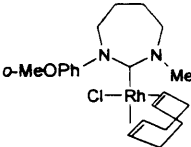
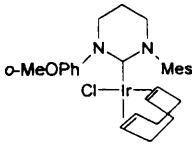
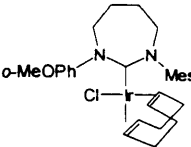


Figure 3-3: ORTEP ellipsoid plot at 30% probability of complexes 3.15, 3.18, 3.21, and 3.23. Hydrogen atoms have been omitted for clarity.

Table 3-3: Selected bond lengths (Å) and bond angles (°) for complexes **3.15**, **3.18**, **3.21** and **3.23**.

				
	3.15	3.18	3.21	3.23
N1-C1-N2 (°)	117.1(2)	117.6(2)	117.3(5)	117.1(4)
C _{MeOPh} -N-C1 (°)	118.4(2)	119.2(2)	119.3(5)	120.1(4)
C _{Mes} -N-C1 (°)	119.2(2)	118.0(2)	119.0(5)	117.0(4)
C1-M-Cl (°)	84.88(8)	89.23(7)	84.82(2)	88.09(1)
C _{ring} -N...N-C _{ring} (β)(°)	6.83	34.19	8.05	33.05
M-C1 (Å)	2.057(3)	2.051(2)	2.074(5)	2.071(5)
M-Cl (Å)	2.405(8)	2.424(7)	2.384(2)	2.385(2)
N1-C1 (Å)	1.349(4)	1.363(3)	1.335(7)	1.370(6)
N2-C1 (Å)	1.341(4)	1.347(3)	1.342(7)	1.357(6)

The complete molecular structure of complexes **3.16**, **3.19**, **3.22** and **3.24** (with DIPP substituent) are depicted in Figure 3-4 below. Selected bond distances and angles are listed in Table 3-4. Elemental analysis and high resolution MS results were in agreement with the formulation of the complexes.

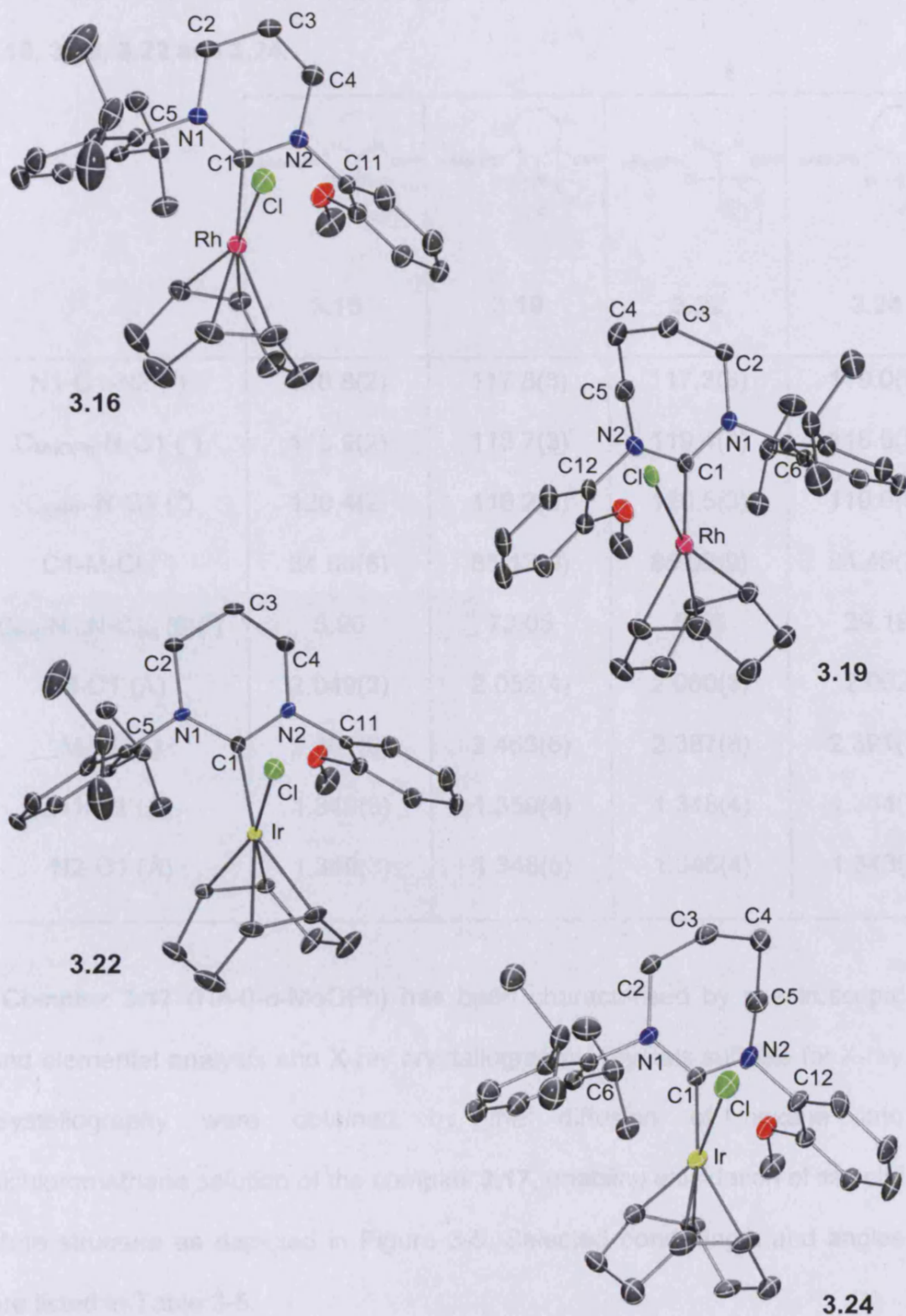
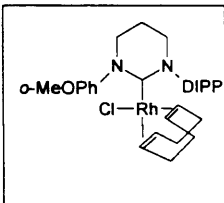
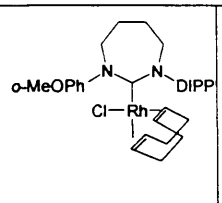
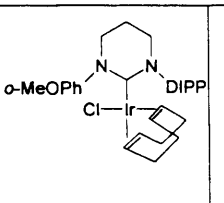
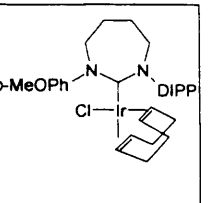


Figure 3-4: ORTEP ellipsoid plot at 30% probability of complexes 3.16, 3.19, 3.22, and 3.24. Hydrogen atoms have been omitted for clarity.

Table 3-4: Selected bond lengths (Å) and bond angles (°) for complexes **3.16**, **3.19**, **3.22** and **3.24**.

				
	3.16	3.19	3.22	3.24
N1-C1-N2 (°)	116.8(2)	117.8(3)	117.3(3)	119.0(5)
C _{MeOPh} -N-C1 (°)	118.9(2)	118.7(3)	119.4(3)	118.6(5)
C _{DIPP} -N-C1 (°)	120.4(2)	118.2(3)	120.5(3)	119.6(5)
C1-M-Cl (°)	84.60(6)	85.12(9)	85.02(9)	84.49(2)
C _{ring} -N...N-C _{ring} (β)(°)	5.96	73.05	6.56	29.19
M-C1 (Å)	2.049(2)	2.052(4)	2.060(3)	2.062
M-Cl (Å)	2.401(6)	2.463(8)	2.387(8)	2.391(2)
N1-C1 (Å)	1.349(3)	1.359(4)	1.348(4)	1.364(7)
N2-C1 (Å)	1.349(3)	1.348(5)	1.346(4)	1.343(8)

Complex **3.17** (Rh-6-*o*-MeOPh) has been characterised by spectroscopic and elemental analysis and X-ray crystallography. Crystals suitable for X-ray crystallography were obtained by the diffusion of hexane into dichloromethane solution of the complex **3.17**, enabling elucidation of its solid state structure as depicted in Figure 3-5. Selected bond length and angles are listed in Table 3-5.

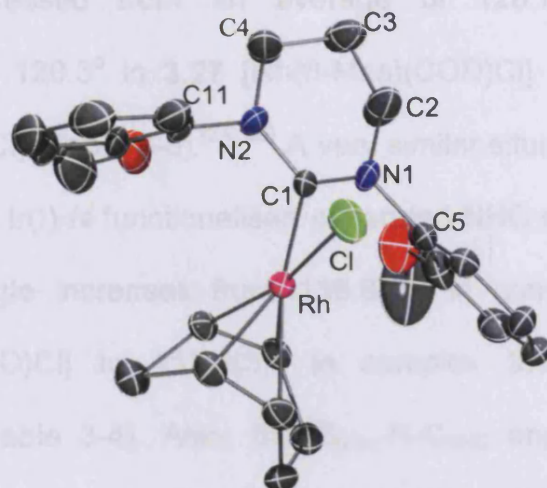


Figure 3-5: ORTEP ellipsoid plot at 30% probability of complex **3.17**.

Hydrogen atoms have been omitted for clarity

Table 3-5: Selected bond length (Å) and bond angle (°) for complex **3.17**.

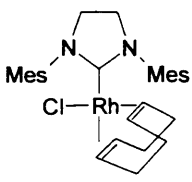
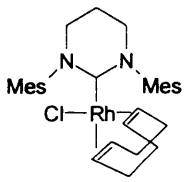
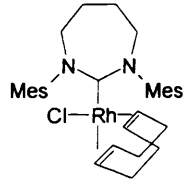
N1-C1-N2 (°)	116.5(4)	Rh-C1 (Å)	2.030(4)
C _{MeOPh} -N1-C1 (°)	120.2(3)	Rh-Cl (Å)	2.419(1)
C _{MeOPh} -N2-C1 (°)	119.6(3)	N1-C1 (Å)	1.333(5)
C1-Rh-Cl (°)	90.85(1)	N2-C1 (Å)	1.357(5)
C _{ring} -N...N-C _{ring} (β)(°)	2.13		

Crystals suitable for X-ray crystallography were not obtained for the complex **3.20** (Rh-7-*o*-MeOPh), but high resolution MS and elemental analysis gave results consistent with the proposed formulation.

A significant increase in NCN angle is observed between 5-membered ring **3.26** [Rh(5-Mes)(COD)Cl] (106.8(3)°) and the expanded ring carbenes **3.27** [Rh(6-Mes)(COD)Cl], and **3.28** [Rh(7-Mes)(COD)Cl] (117.5(4)° and 118.0°, respectively). This leads to a dramatic change in the C_{Mes}-N-C_{NHC} angles that

are again compressed from an average of 126.7° in **3.26** [Rh(5-Mes)(COD)Cl] to 120.3° in **3.27** [Rh(6-Mes)(COD)Cl] and 118.1° in **3.28** [Rh(7-Mes)(COD)Cl] (Table 3-6).^[24, 25] A very similar situation is observed for the new Rh(I) and Ir(I) *N*-functionalised expanded NHC complexes, in which the N-C_{NHC}-N angle increases from $116.8(2)^\circ$ in complex **3.16** [Rh(6-*o*-MeOPh-DIPP)(COD)Cl] to $117.8(3)^\circ$ in complex **3.19** [Rh(7-*o*-MeOPh-DIPP)(COD)Cl] (Table 3-4). Also, the C_{Mes}-N-C_{NHC} angle decreases from $120.4(2)^\circ$ in **3.16** [Rh(6-*o*-MeOPh-DIPP)(COD)Cl] to $118.2(3)^\circ$ in **3.19** [Rh(7-*o*-MeOPh-DIPP)(COD)Cl] (Table 3-4). As a result of this, the functionalised substituents on the nitrogens come closer to the metal centre in the expanded carbenes, virtually blocking the two faces of the metal coordination sphere.

Table 3-6: Comparison of selected bond length (Å) and angles ($^\circ$) for some reported Rh(I) COD complexes.

			
	3.26	3.27	3.28
N-C _{NHC} -N ($^\circ$)	106.8(3)	117.5(4)	118.0
C _{Mes} -N-C _{NHC} ($^\circ$)	127.4/126.0	120.6/119.9	119.0/117.2
C _{ring} -N...N-C _{ring} (β) ($^\circ$)	7.4	4.9	29.5
N-C _{NHC} (Å)	1.354/1.354	1.365/1.466	1.360/1.352
Rh-C _{NHC} (Å)	2.068(3)	2.075(10)	2.085

From Tables 3-3, 3-4 and 3-5, the main structural feature of the complexes is their distorted square planer geometry with Cl-M-C_{NHC} angles within the range of 84.60(6) – 90.85(1)°.

As previously described for 6- and 7-membered carbene ligands in Chapter 2, the extra torsion originating from the expansion of the ring does not only result in an increase of the NCN angle, but also in an enlargement of the torsion angle C_{ring}-N...N-C_{ring} (β), which is shown in Tables 3-3, 3-4 and 3-5. For example, the torsion angle (β) increases from 6.83° in complex **3.15** [Rh(6-*o*-MeOPh-Mes)(COD)Cl] to 34.19° in complex **3.18** [Rh(7-*o*-MeOPh-Mes)(COD)Cl].

For all the complexes, a pyramidal distortion of nitrogen atoms is observed. The The orthogonal distance between the nitrogen atom and the C_{ring}-C_{NHC}-C_{sub} plane is shown in Table 3-7.

Table 3-7: The distance (Å) between the nitrogen atoms and [C_{ring}-C_{NHC}-C_{sub}] plane in the Rh(I) and Ir(I) complexes.

	3.15	3.16	3.17	3.18	3.19
N1-[C _{ring} -C _{NHC} -C _{ring}] (Å)	0.087	0.065	0.023	0.022	0.022
N2-[C _{ring} -C _{NHC} -C _{ring}] (Å)	0.074	0.045	0.010	0.079	0.079
	3.21	3.22	3.23	3.24	
N1-[C _{ring} -C _{NHC} -C _{ring}] (Å)	0.084	0.071	0.007	0.024	
N2-[C _{ring} -C _{NHC} -C _{ring}] (Å)	0.062	0.059	0.041	0.083	

In the expanded carbene, the carbene carbon is not in the N-M-N plane, but there is a pyramidal distortion of the carbene carbon. The orthogonal distance between the carbene carbon and the N-M-N plane is shown in Table 3-8.

Table 3-8: The distance (Å) between the carbene carbon and [N-M-N], (M=Rh or Ir), plane in the Rh(I) and Ir(I) complexes.

	3.15	3.16	3.17	3.18	3.19
$C_{\text{NHC}}\text{-[N-Rh-N]} (\text{Å})$	0.109	0.106	0.001	0.059	0.115
	3.21	3.22	3.23	3.24	
$C_{\text{NHC}}\text{-[N-Ir-N]} (\text{Å})$	0.092	0.100	0.042	0.101	

In these expanded carbene Rh(I) and Ir(I) complexes, the carbene ligand adopts an almost perpendicular arrangement with respect to the coordination plane. The tilt angle (θ), defined by the coordination and N1-C_{NHC}-N2 plane, is shown in Table 3-9 for rhodium and iridium complexes, respectively.

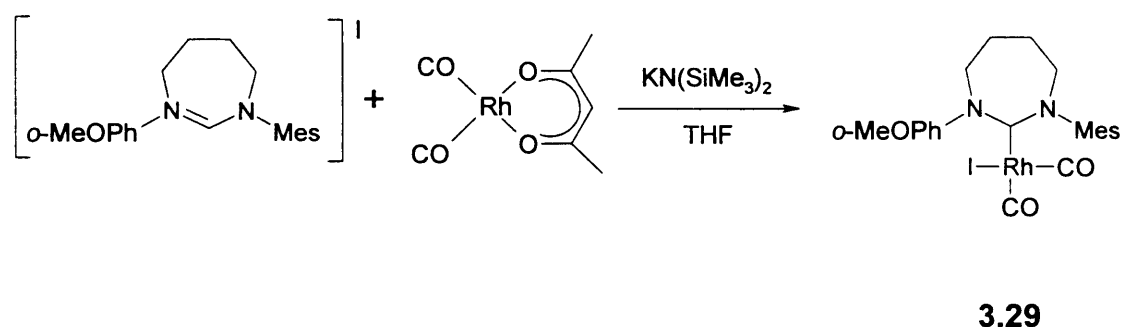
Table 3-9: The tilt angle (θ) ($^\circ$), defined by the coordination and N1-C_{NHC}-N2 plane, in the Rh(I) and Ir(I) complexes .

	3.15	3.16	3.17	3.18	3.19
(θ) ($^\circ$)	83.34	80.73	85.27	82.38	83.45
	3.21	3.22	3.23	3.24	
(θ) ($^\circ$)	84.09	80.84	82.74	82.97	

3.2.3. Rh(I) Biscarbonyl Complex *Cis*-[Rh(7-*o*-MeOPh-Mes)(CO)₂I] .

One of the fundamental chemical properties of NHCs is their strong electron-donor ability. In general saturated carbenes donate a greater electron density than their unsaturated analogues. The infrared carbonyl-stretching frequencies of the Rh(I) carbonyl complex, *cis*-[Rh(L)(CO)₂X], are well documented as being a good measure of the donor ability of ligands.^[34] To assess the electron-donating ability of our carbenes, we prepared the air-stable rhodium carbonyl complex with a 7-membered carbene ligand, *cis*-[Rh(7-*o*-MeOPh-Mes)(CO)₂I], **3.29**. It was obtained in good yield after

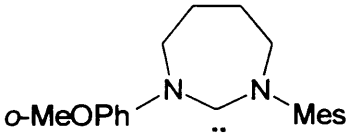
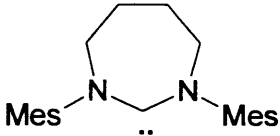
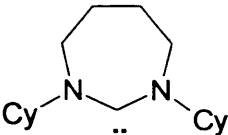
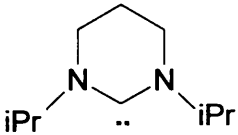
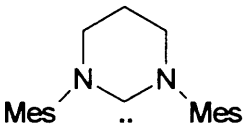
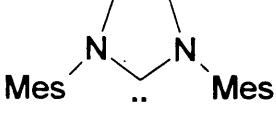
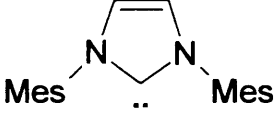
treatment of a THF solution of the corresponding NHC iodide salt with (acetyl acetone) di-carbonyl rhodium(I) and $\text{KN}(\text{SiMe}_3)_2$ for four hours (Scheme 3-4).



Scheme 3-4: Synthesis of Rh carbonyl complex, *cis*-[Rh(7-*o*-MeOPh-Mes)(CO)₂I], **3.29**.

The ^1H NMR spectrum shows a noteworthy downfield shift of *o*- $\text{CH}_{\text{o-MeOPh}}$ proton when compared to the COD complex **3.18** (from 8.35 ppm in [Rh(7-*o*-MeOPh-Mes)(COD)Cl] **3.18** to 7.62 ppm in *cis*-[Rh(7-*o*-MeOPh-Mes)(CO)₂I] **3.29**), attributed to the stronger donor ability of the carbonyl ligand in comparison with COD. The ^{13}C NMR signal for Rh- C_{NHC} appears at 214.2 ppm ($^1J_{\text{RhC}} = 40.8$) as a doublet due to the Rh coupling. The *cis*-geometry for complex **3.29** is supported by the appearance of two ^{13}C NMR signals for the CO carbons and through IR spectroscopy. The carbonyl-stretching frequencies of complex **3.29**, *cis*-[Rh(7-*o*-MeOPh-Mes)(CO)₂I], are listed and compared to analogous complexes in Table 3-10.

Table 3-10: IR $\nu(\text{CO})$ for $[\text{Rh}(\text{L})(\text{CO})_2\text{X}]$ complexes in DCM.

L	X	$\nu(\text{CO})(\text{cm}^{-1})$	$\nu_{\text{av}}(\text{CO})(\text{cm}^{-1})$	Ref.
	I	2059 , 1967	2013	This work
	Cl	2081 , 1996	2039	[24, 25]
	Cl	2071 , 1990	2031	[24, 25]
	Cl	2063 , 1982	2023	[26-28]
	Cl	2062 , 1979	2019	[26-28]
	Cl	2081, 1996	2039	[18]
	Cl	2076, 2006	2041	[18]

The values of $\nu(\text{CO})$ can be used to gauge the donor ability of the ligand. The average carbonyl-stretching frequency for rhodium complex **3.29** is 2013 cm^{-1} which suggests that the donor ability of carbene ligand (7-*o*-MeOPh-Mes) is higher than the symmetrical saturated and unsaturated 5-, 6- and 7-membered NHC ligands ($\nu_{\text{av}}(\text{CO}) = 2019 - 2041\text{ cm}^{-1}$) (Table 3-10).^[34]

Crystal data for the rhodium complex **3.29** were collected and an ORTEP representation is shown in Figure 3-6. Selected bond lengths and angles are summarised in Table 3-11.

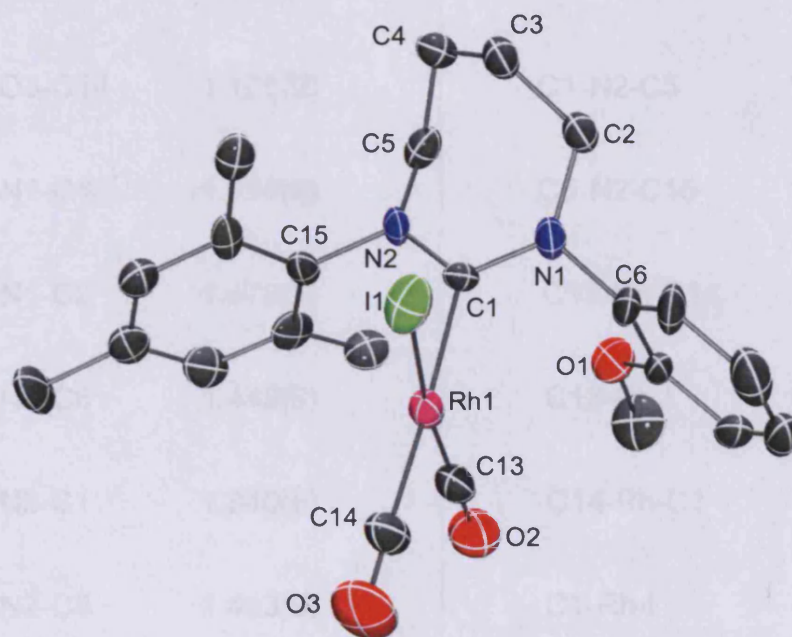


Figure 3-6: ORTEP ellipsoid plot at 30% probability of complexes **3.29**. Hydrogen atoms have been omitted for clarity.

Table 3-11: Selected bond lengths (Å) and bond angles (°) for complex **3.29**.

Lengths (Å)		Angles (°)	
Rh-C1	2.096(7)	N1-C1-N2	119.6(6)
Rh-I	2.655(9)	C1-N1-C6	115.8(6)
Rh-C13	1.869(1)	C2-N1-C6	114.5(5)
Rh-C14	1.898(9)	C1-N1-C2	129.8(5)
O2-C13	1.106(1)	C1-N2-C15	118.1(6)
O3-C14	1.125(9)	C1-N2-C5	123.2(6)
N1-C1	1.350(9)	C5-N2-C15	116.2(6)
N1-C2	1.478(1)	C13-Rh-C14	90.6(4)
N1-C6	1.449(8)	C13-Rh-I	93.6(3)
N2-C1	1.340(8)	C14-Rh-C1	86.8(3)
N2-C5	1.493(9)	C1-Rh-I	89.7(2)
N2-C15	1.453(1)		

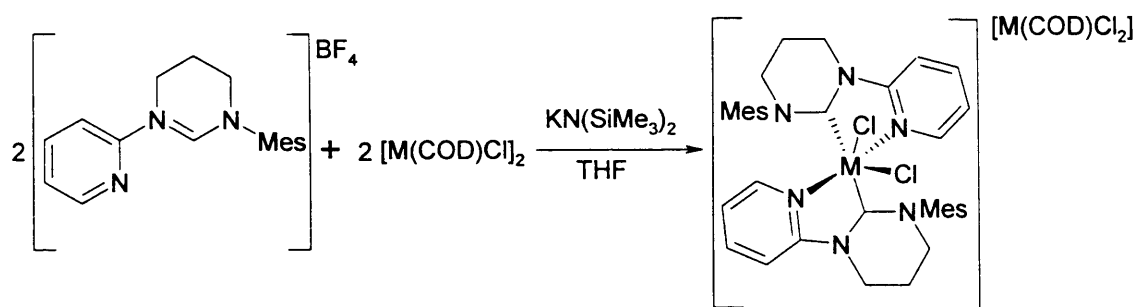
The coordination is square planar at the Rh(I) center. The two Rh-CO bond lengths are similar at 1.869(1) and 1.898(9) Å, despite having different *trans*-

substituents. The C-O bond *trans* to the carbene is longer than the one *trans* to the iodide by 0.019 Å, in line with the higher *trans* influence of the carbene ligand. A similar trend can also be observed in the crystal structures of other *cis*-[M(NHC)(CO)₂Cl] (M = Rh, Ir).^[24, 25, 35]

A longer Rh-C_{NHC} bond is observed upon substitution of the COD by two carbonyl ligands, from 2.051(2) to 2.096(7) Å, respectively. The tilt θ angle, defined by the coordination and N1-C_{NHC}-N2 plane, shows a small deviation from a right angle at 86.78°.

3.2.4. The Reaction of 6-Py-Mes Salt with [M(COD)Cl₂] (M = Rh or Ir) Unexpected Formation of M(III) Complexes.

The reaction of the pyridyl-functionalised salt (6-Py-Mes), with KN(SiMe₂)₃ and [M(COD)Cl]₂, (M = Rh or Ir), leads to the formation of unexpected M(III) / M(I) bis carbene complex **3.30**, [Rh(6-Py-Mes)₂Cl₂][Rh(COD)Cl₂], and complex **3.31**, [Ir(6-Py-Mes)₂Cl₂][Ir(COD)Cl₂], (Scheme 3-5). From the Scheme it is clear that M(I) in the compound [M(COD)Cl]₂ lost two electrons to become M(III) in the unexpected complex [M(6-Py-Mes)₂Cl₂]⁺ (M = Rh or Ir), while at the same time, the chloride in the compound [M(COD)Cl]₂ used the two electrons to form the anionic Rh(I) compound [MCl₂(COD)]⁻.



3.30, M = Rh

3.31, M = Ir

Scheme 3-5: Synthesis of pyridyl carbene complexes **3.30** and **3.31**.

The Rh(III) and Ir(III) complexes have been characterised by ^1H NMR, ^{13}C NMR, mass spectroscopy and elemental analysis. The ^{13}C NMR data for the coordinating carbene carbons appears as a doublet at 188.8 ppm for complex **3.30** and singlet at 184.3 ppm for complex **3.31**, suggesting the formation of the M-C bond (M = Rh or Ir). These are in the usual range for the other Rh(III)- or Ir(III)- NHC complexes.^[36, 37] The ^1H NMR spectrum shows that the carbene ligands are symmetrically related. For example, two sharp singlets (s, 6H) for the (*o*-CH₃)_{Mes} at 2.27 and 2.19 ppm and one singlet (s,6H) for (*p*-CH₃)_{Mes} at 2.01 ppm in complex **3.30** and at 2.36, 2.28 ppm and 2.05 ppm in complex **3.31**. The ^1H NMR signals for *o*-CH_{py} (hydrogen atom next to the pyridyl nitrogen) is shifted downfield (Table 3-12), indicating that the pyridyl nitrogen is coordinating to the metal.

Table 3-12: ^1H NMR and ^{13}C NMR data for carbene salts and their Rh(III) and Ir(III) complexes.

	^1H NMR (δ H) ppm			^{13}C NMR (δ C) ppm
	<i>o</i> -CH _{Py}	<i>o</i> -CH ₃ Mes	<i>p</i> -CH ₃ Mes	C _{NCN}
Salt (6-Py-Mes)	8.25	2.29	2.27	150.3
Rh(III)-NHC Complex 3.30	8.80	2.31-2.22	2.01	188.8
Ir(III)-NHC Complex 3.31	8.88	2.36-2.28	2.05	184.3

Crystals suitable for X-ray crystallography were obtained for the Rh(III)-NHC complex **3.30** by diffusion of hexane into DCM solution of the complex at ambient temperature. The detailed solid state coordination sphere around the rhodium centre of complex **3.30** was confirmed by X-ray crystal structure analysis. The complete molecular structure of complex **3.30** is depicted in Figure 3-7 below. Selected bond lengths and angles are listed in Table 3-13.

Table 3-13: Selected bond lengths (Å) and angles (°) for complex **3.30**.

Lengths (Å)		Angles (°)			
C9-Rh1	2.031(9)	N3-C9-N2	117.8(8)	N4-Rh1-Cl2	94.0(3)
C27-Rh1	1.950(1)	N6-C27-N5	114.5(1)	C9-N2-C5	119.9(8)
N1-Rh1	2.031(8)	C27-Rh1-C9	96.4(4)	C9-N3-C10	125.3(8)
N4-Rh1	2.036(9)	C9-Rh1-N1	80.4(4)	C27-N5-C23	117.6(1)
Cl1-Rh1	2.412(3)	C27-Rh1-N4	80.5(5)	C27-N6-C28	124.1(1)
Cl2-Rh1	2.418(2)	C9-Rh1-N4	102.6(4)	Cl1-Rh-Cl2	91.92(9)
C9-N3	1.288(1)	C27-Rh1-N1	102.8(4)		
C9-N2	1.380(1)	C9-Rh1-Cl1	86.3(3)		
C27-N6	1.363(1)	C27-Rh1-Cl2	85.8(3)		
C27-N5	1.401(1)	N1-Rh1-Cl1	82.6(2)		

The distances between Rh(III) and the carbene carbon (2.031(9), 1.950(1) Å) are normal for Rh-C (σ -bond) and imply a symmetric ligand coordination mode. The Rh(III)-C_{NHC} distances are shorter than the distances between

Rh(III) and the chloride (2.412(3), 2.418(2) Å), owing to the strong electron-donating ability of NHCs.

The heavy steric demands imposed by 7-membered carbenes upon coordination prevent NHCs with bulkier substituents from coordinating to the metal. For example, no reaction was observed between the carbene salt (7-Py-Mes) and $[\text{Rh}(\text{COD})\text{Cl}]_2$. Instead, the hydrolysis products of the free carbene and the metal particulate were recovered. Figure 3-8 shows the steric interaction in complex **3.30** between the aromatic substituents on the carbene with chloride ligands, which presumably leaves no room for more encumbered N-substituents or the use of a 7-membered carbene as a ligand.

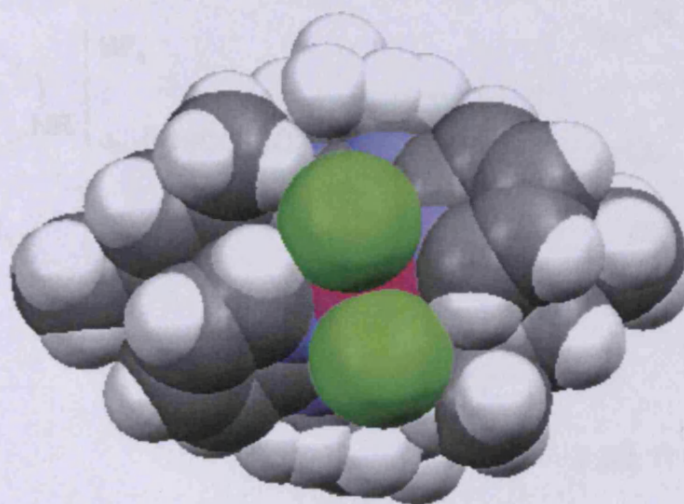
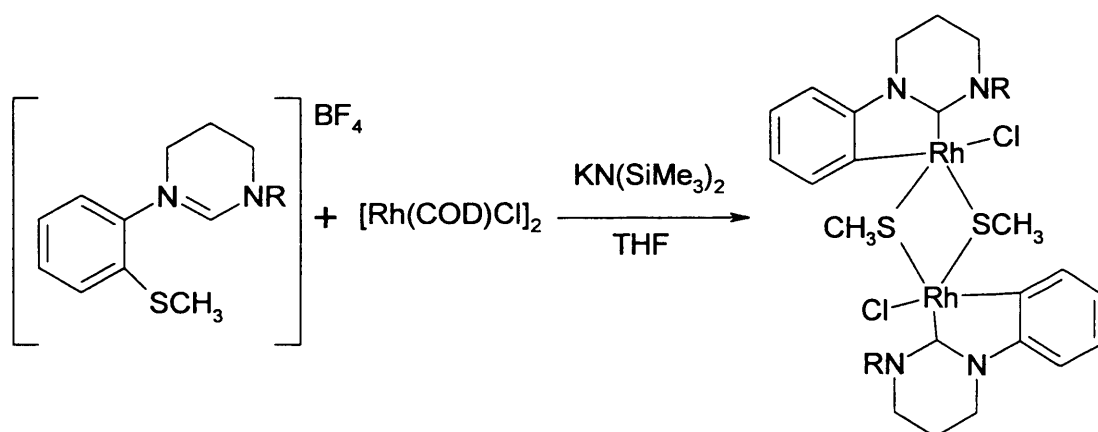


Figure 3-8: Mercury spacefill depiction of complex **3.30**, $[\text{Rh}(\text{III})-(6\text{-Py-Mes})_2\text{Cl}_2]^+$.

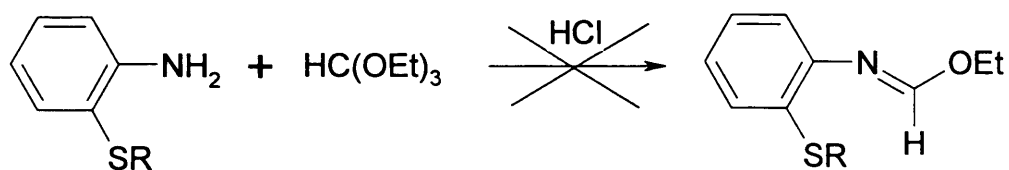
3.2.5. Reaction of 6-MeSPh-Mes and 6-MeSPh-DIPP Salts with [Rh(COD)Cl]₂ Unexpected Ar-SMe Cleavage and Synthesis of a Novel Rh(III)NHC Complex.

The reaction of a *N*-functionalised (*o*-MeSPh) NHC salt with KN(SiMe₃)₂ and [Rh(COD)Cl]₂ in THF leads to formation of a novel dimeric Rh(III) bis-carbene complex which is shown in Scheme 3-6. The reaction involves the unexpected cleavage oxidative addition of the aryl-sulphur bond to give metalated Rh and a bridging thio-methyl moiety. This is a unique reaction which does not correspond to anything similar in the literature.



Scheme 3-6: Synthesis of novel Rh(III) bis-carbene complexes **3.32** and **3.33** by a unique Ar-SMe cleavage.

Attempts were made to prepare similar complexes, in order to gain some understanding of the reaction mechanism but unfortunately failed from the first step (Scheme 3-7).



R = ethyl

R = isopropyl

Scheme 3-7: An attempt to prepare ethyl (2-ethylthiophenyl) formimide and ethyl (2-isopropylthiophenyl) formimide.

The detailed mechanism of this reaction (Scheme 3-6) is unclear. However, in broad terms, it is thought that the NHC carbon first coordinates to the Rh(I) to generate an extremely electron rich metal centre, which then undergoes rapid *intra*-molecular oxidative addition of the MeS-phenyl moiety to form the *o*-metallated thio-bridged Rh(III) dimer. It would appear that these expanded-ring NHCs are extremely powerful electron donors, which promote oxidation of the metal center, as seen in this case and also with the pyridine functionalised NHC (Section 3.2.4).

Characterisation of these complexes was carried out by ^1H NMR, ^{13}C NMR and mass spectroscopy. The ^{13}C NMR signals for the carbene carbon appeared as a doublet at 202.3 ppm for complex **3.32** and a doublet at 202.7 ppm for complex **3.33**, indicating the formation of a Rh-C_{NHC} bond. The signals are within the range of Rh-C_{NHC} observed for other Rh complexes. The ^1H NMR signals of *m*-CH_{Ar} are shifted downfield and the hydrogen atoms in the SCH₃ group appeared as a sharp singlet at 1.69 ppm and 1.52 ppm for complex **3.32** and **3.33**, respectively. The large shift compared to the salt indicating that these groups have coordinated to the metal (Table 3-14).

Table 3-14: ^1H NMR and ^{13}C NMR data for carbene salt and their Rh(I) complexes.

	^1H NMR (δ H) ppm		^{13}C NMR (δ C) ppm
	<i>m</i> -CH _{Ar}	SCH ₃	
Salt (6-MeSPh-Mes)	7.38	2.46	154.1
Salt (6-MeSPh-DIPP)	7.38	3.85	158.8
Complex 3.32	7.56	1.69	202.3
Complex 3.33	7.53	1.52	202.7

Crystals suitable for X-ray crystallography of complex **3.33** were obtained by the diffusion of hexane into the saturated THF solution of the complex. The crystal structure of complex **3.33** and selected bond distances and angles are presented in Figure 3-9 and Table 3-15 respectively.

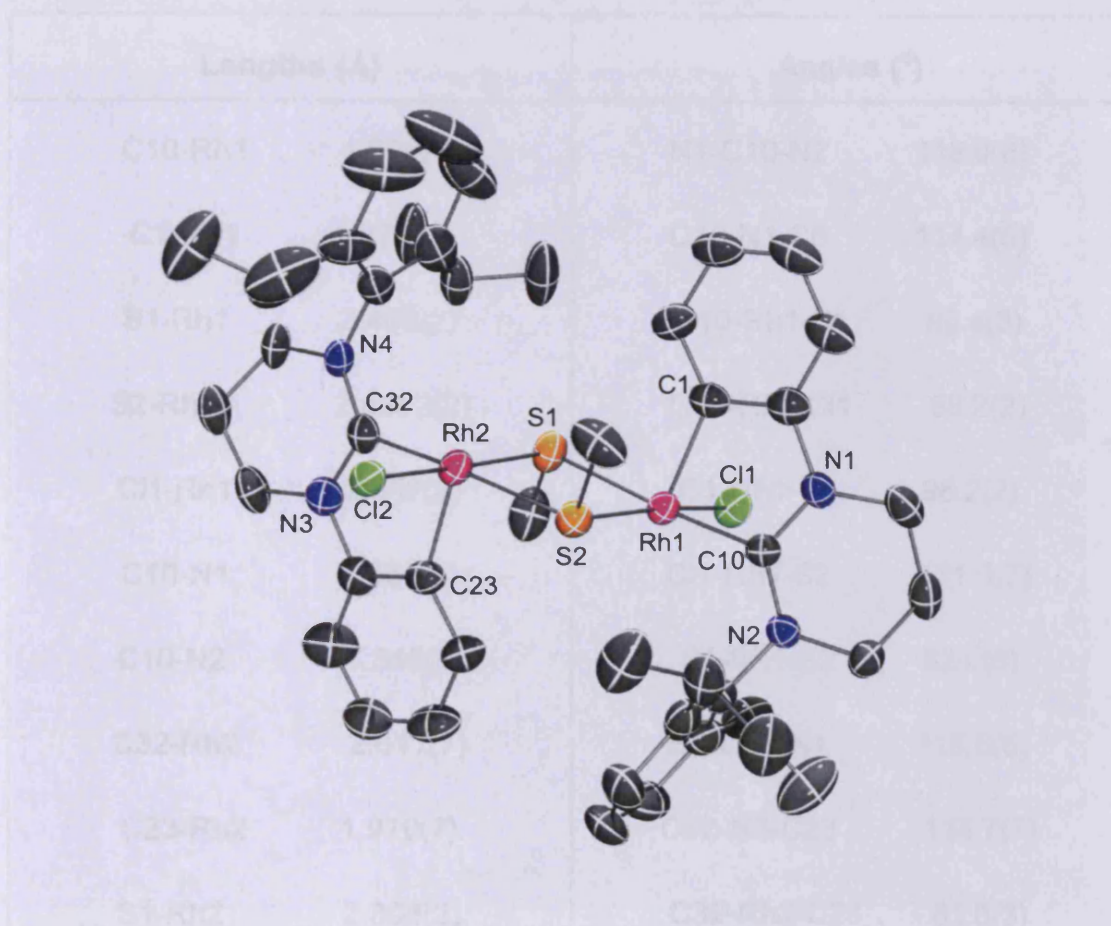


Figure 3-9: ORTEP ellipsoid plot at 30% probability of complexes **3.33**. Hydrogen atoms have been omitted for clarity.

The structural arrangement of complex **3.33** shows that the molecular geometry around the rhodium ion is trigonal bipyramidal with two coordination sites occupied by bidentate carbene, one coordination site

occupied by chloride (the two chloride atoms are in trans arrangement overall), and the other two coordination sites occupied by two SCH₃ groups.

Table 3-15: Selected bond lengths (Å) and angles (°) for complex **3.33**.

Lengths (Å)		Angles (°)	
C10-Rh1	1.996(7)	N1-C10-N2	118.0(6)
C1-Rh1	1.971(7)	C10-N1-C6	114.4(6)
S1-Rh1	2.406(2)	C10-Rh1-C1	80.4(3)
S2-Rh1	2.4302(2)	C10-Rh1-Cl1	88.2(2)
Cl1-Rh1	2.362(2)	C1-Rh1-S1	96.2(2)
C10-N1	1.334(8)	Cl1-Rh1-S2	171.0(7)
C10-N2	1.345(8)	S1-Rh1-S2	82.6(6)
C32-Rh2	2.011(7)	N3-C32-N4	116.8(6)
C23-Rh2	1.970(7)	C32-N3-C23	114.7(7)
S1-Rh2	2.308(2)	C32-Rh2-C23	81.0(3)
S2-Rh2	2.417(2)	C32-Rh2-Cl2	92.6(2)
Cl2-Rh2	2.370(2)	C23-Rh2-S2	95.3(2)
C32-N3	1.358(9)	Cl2-Rh2-S1	171.1(7)
C32-N4	1.339(9)	S1-Rh2-S2	82.2(4)

The Rh-C_{NHC} bond lengths (1.996(7), 2.011(7) Å) are normal for Rh-C_{NHC} (σ -bond) complexes and imply a symmetric ligand coordination mode. The two Rh-C_{NHC} are the same, within experimental error, and also very similar to the C_{Ph}(sp²)-Rh bond lengths. The C_{NHC}-Rh-C_{Ph} bite-angles (C10-Rh1-C1) and (C32-Rh2-C23) are 80.4(3)^o and 81.0(3)^o. The tilt θ angle, defined by the coordination and the N1-C_{NHC}-N2 plane, are 79.38^o and 86.85^o.

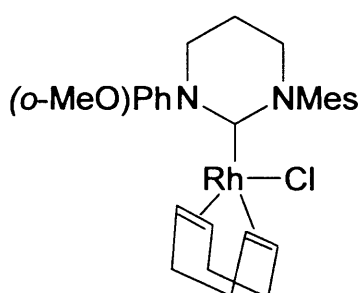
3.3. Experimental.

General Remarks.

All manipulations were performed using standard Schlenk techniques under an argon atmosphere, except where otherwise noted. Solvents were freshly distilled from sodium/benzophenone (THF, hexane) or from calcium hydride (CH₂Cl₂). Deuterated solvents for NMR measurements were distilled from the appropriate drying agents under N₂ immediately prior to use, following standard literature methods. Air-sensitive compounds were stored and weighed in a glovebox. ¹H and ¹³C {¹H} NMR spectra were obtained on Bruker Avance AMX 400, 500 or Jeol Eclipse 300 spectrometers. The chemical shifts are given as dimensionless δ values and are frequency-referenced relative to TMS. Coupling constants J are given in hertz (Hz) as positive values regardless of their real individual signs. The multiplicity of the signals is indicated as: s, d, t or m for singlet, doublet, triplet, multiplet, mass

spectra and high-resolution mass spectra were obtained in electrospray (ES) mode unless otherwise reported, on a Waters Q-TOF micromass spectrometer. Infrared spectra were recorded using a JASCO FT/IR-600 *plus* spectrometer and analysed in solution (dichloromethane).

[Rh(6-*o*-MeOPh-Mes)(COD)Cl] (3.15).



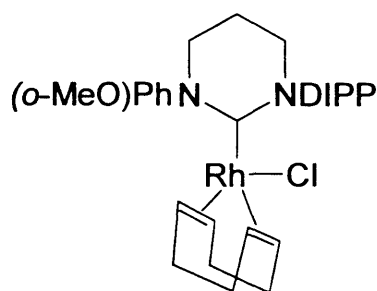
$\text{KN}(\text{SiMe}_3)_2$ (82 mg, 0.41 mmol) and (6-*o*-MeOPh-Mes) BF_4 salt (162 mg, 0.41 mmol) were placed in a Schlenk-tube followed by the addition of THF (15 ml). The solution was stirred

for 30 minutes and subsequently filtered in to another Schlenk-tube containing a 10 ml THF solution of $[\text{Rh}(\text{COD})\text{Cl}]_2$ (0.20 mmol). An immediate colour change was observed from light to dark yellow. After the reaction was stirred at room temperature for 2 hours, the volatiles were removed in vacuo. The yellow solid obtained was washed with hexane (2 x 10 ml) and dried. Crystals suitable for X-ray diffraction were obtained by layering a dichloromethane solution of the compound with hexane. The yield was 62% (0.141 g).

^1H NMR (CDCl_3 , 500 MHz, 298 K): δ 8.39 (1H, d, *o*- $\text{CH}_{\text{o-MeOPh}}$), 7.29 (1H, t, *m*- $\text{CH}_{\text{o-MeOPh}}$), 7.07 (1H, t, *p*- $\text{CH}_{\text{o-MeOPh}}$), 6.97 (1H, s, *m*- CH_{Mes}), 6.91 (1H, d, *m*- $\text{CH}_{\text{o-MeOPh}}$), 6.82 (1H, s, *m*- CH_{Mes}), 4.29 (1H, m, CH_{COD}), 4.23 (1H, m, CH_{COD}), 3.80 (3H, s, OCH_3), 3.55 (2H, t, NCH_2), 3.24 (2H, t, NCH_2), 2.93 (1H, m, CH_{COD}), 2.79 (1H, m, CH_{COD}), 2.59 (3H, s, *o*- CH_3), 2.25 (3H, s, *o*- CH_3), 2.21 (2H, m, NCH_2CH_2), 2.05 (3H, s, *p*- CH_3), 1.57 (2H, m, CH_{COD}),

1.38 (2H, m, CH_{COD}), 1.25 (2H, m, CH_{COD}), 1.13 (2H, m, CH_{COD}). ^{13}C NMR (CDCl_3 , 100 MHz, 298 K): δ 210.0 (d, $^1J_{\text{RhC}} = 46.9$, C_{NHC}), 154.2 (s, Ar- $\text{C}_{\text{O-MeOPh}}$), 140.8 (s, Ar- C_{Mes}), 136.4 (s, Ar- C_{Mes}), 136.2 (s, Ar- C_{Mes}), 135.1 (s, Ar- C_{Mes}), 134.5 (s, Ar- $\text{C}_{\text{O-MeOPh}}$), 133.0 (s, Ar- $\text{CH}_{\text{O-MeOPh}}$), 128.9 (s, Ar- CH_{Mes}), 127.4 (s, Ar- CH_{Mes}), 127.0 (s, Ar- $\text{CH}_{\text{O-MeOPh}}$), 119.8 (s, Ar- $\text{CH}_{\text{O-MeOPh}}$), 109.4 (s, Ar- $\text{CH}_{\text{O-MeOPh}}$), 93.3 (d, C_{COD}), 66.3 (d, C_{COD}), 54.2 (s, OCH_3), 47.2 (s, NCH_2), 46.4 (s, NCH_2), 31.5 (s, CH_2_{COD}), 30.4 (s, CH_2_{COD}), 27.4 (s, CH_2_{COD}), 25.9 (s, CH_2_{COD}), 20.4 (s, NCH_2CH_2), 19.9 (s, CH_3), 18.8 (s, CH_3), 16.9 (s, CH_3). Anal. Found (Calcd) for $\text{C}_{28}\text{H}_{36}\text{N}_2\text{ORhCl}$: C, 60.58 (60.61); H, 6.69 (6.49); N, 4.90 (5.05). HRMS (ES): m/z 519.1868 ($[\text{M}-\text{Cl}]^+$ $\text{C}_{28}\text{H}_{36}\text{N}_2\text{ORh}$ requires 519.1883).

[Rh(6-*o*-MeOPh-DIPP)(COD)Cl] (3.16).



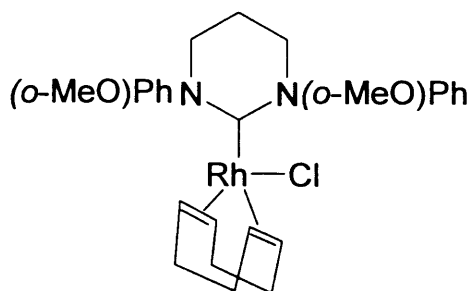
$\text{KN}(\text{SiMe}_3)_2$ (82 mg, 0.41 mmol) and (6-*o*-MeOPh-DIPP) BF_4 salt (178 mg, 0.41 mmol) were placed in a Schlenk-tube followed by the addition of THF (15 ml). The solution was

stirred for 30 minutes and subsequently filtered into another Schlenk-tube containing a 10 ml THF solution of $[\text{Rh}(\text{COD})\text{Cl}]_2$ (0.20 mmol). An immediate colour change was observed from light to dark yellow. After the reaction was stirred at room temperature for 2 hours, the volatiles were removed in vacuo. The yellow solid obtained was washed with hexane (2 x 10 ml) and dried. Crystals suitable for X-ray diffraction were obtained by layering a

dichloromethane solution of the compound with hexane. The yield was 62% (0.152 g).

^1H NMR (CDCl_3 , 500 MHz, 298 K): δ 8.36 (1H, d, *o*- $\text{CH}_{\text{o-MeOPh}}$), 7.34 (1H, t, *m*- $\text{CH}_{\text{o-MeOPh}}$), 7.31 (1H, t, *p*- CH_{DIPP}), 7.28 (1H, d, *m*- CH_{DIPP}), 7.10 (1H, d, *m*- CH_{DIPP}), 7.05 (1H, t, *p*- $\text{CH}_{\text{o-MeOPh}}$), 6.91 (1H, d, *m*- $\text{CH}_{\text{o-MeOPh}}$), 4.39 (1H, m, CH_{COD}), 4.24 (1H, m, CH_{COD}), 4.04 (2H, t, NCH_2), 3.80 (3H, s, OCH_3), 3.54 (2H, t, NCH_2), 3.00 (1H, m, CH_{COD}), 2.91 (1H, m, CH_{COD}), 2.49 (1H, m, $\text{CH}(\text{CH}_3)_2$), 2.37 (1H, m, $\text{CH}(\text{CH}_3)_2$), 2.08 (2H, m, NCH_2CH_2), 1.64 (2H, m, CH_{COD}), 1.75 (3H, d, $\text{CH}(\text{CH}_3)_2$), 1.52 (3H, d, $\text{CH}(\text{CH}_3)_2$), 1.31 (2H, m, CH_{COD}), 1.25 (2H, m, CH_{COD}), 1.18 (3H, d, $\text{CH}(\text{CH}_3)_2$), 1.14 (3H, d, $\text{CH}(\text{CH}_3)_2$), 1.04 (2H, m, CH_{COD}). ^{13}C NMR (CDCl_3 , 100 MHz, 298 K): δ 211.5 (d, $^1J_{\text{RhC}} = 46.5$, C_{NHC}), 154.6 (s, $\text{Ar-C}_{\text{o-MeOPh}}$), 147.4 (s, $\text{Ar-C}_{\text{DIPP}}$), 145.7 (s, $\text{Ar-C}_{\text{DIPP}}$), 140.6 (s, $\text{Ar-C}_{\text{DIPP}}$), 134.9 (s, $\text{Ar-C}_{\text{o-MeOPh}}$), 133.4 (s, $\text{Ar-CH}_{\text{o-MeOPh}}$), 127.5 (s, $\text{Ar-CH}_{\text{DIPP}}$), 127.4 (1C, s, $\text{Ar-CH}_{\text{DIPP}}$), 124.3 (1C, s, $\text{Ar-CH}_{\text{DIPP}}$), 122.0 (1C, s, $\text{Ar-CH}_{\text{o-MeOPh}}$), 119.8 (1C, s, $\text{Ar-CH}_{\text{o-MeOPh}}$), 109.3 (1C, s, $\text{Ar-CH}_{\text{o-MeOPh}}$), 93.7 (d, C_{COD}), 67.8 (d, C_{COD}), 54.2 (s, OCH_3), 48.7 (s, NCH_2), 47.9 (s, NCH_2), 31.5 (s, $\text{CH}(\text{CH}_3)_2$), 30.6 (s, $\text{CH}(\text{CH}_3)_2$), 28.8 (s, NCH_2CH_2), 27.5 (s, CH_2_{COD}), 27.1 (s, CH_2_{COD}), 26.6 (s, CH_2_{COD}), 26.5 (s, CH_2_{COD}), 25.4 (s, CH_3), 24.0 (s, CH_3), 22.5 (s, CH_3), 21.0 (s, CH_3). Anal. Found (Calcd) for $\text{C}_{31}\text{H}_{42}\text{N}_2\text{ORhCl}$: C, 61.98 (62.37); H, 7.23 (7.04); N, 4.41 (4.69). HRMS (ES): m/z 561.2330 ($[\text{M-Cl}]^+$ $\text{C}_{31}\text{H}_{42}\text{N}_2\text{ORh}$ requires 561.2352).

[Rh(6-*o*-MeOPh)(COD)Cl] (3.17).

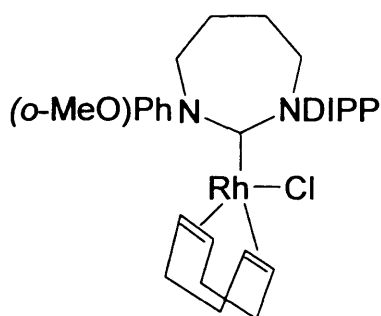


KN(SiMe₃)₂ (82 mg, 0.41 mmol) and (6-*o*-MeOPh)BF₄ salt (157 mg, 0.41 mmol) were placed in a Schlenk-tube followed by the addition of THF (15 ml). The solution was stirred for 30 minutes and subsequently filtered into another Schlenk-tube containing a 10 ml THF solution of [Rh(COD)Cl]₂ (0.20 mmol). An immediate colour change was observed from light to dark yellow. After the reaction was stirred at room temperature for 2 hours, the volatiles were removed in vacuo. The yellow solid obtained was washed with hexane (2 x 10 ml) and dried. Crystals suitable for X-ray diffraction were obtained by layering a dichloromethane solution of the compound with hexane. The yield was 64% (0.142 g).

¹H NMR (CDCl₃, 500 MHz, 298 K): δ 8.45 (2H, d, *o*-CH_o-MeOPh), 7.28 (2H, t, *m*-CH_o-MeOPh), 7.07 (2H, t, *p*-CH_o-MeOPh), 6.88 (2H, d, *m*-CH_o-MeOPh), 4.27 (2H, m, CH_{COD}), 3.81 (6H, s, OCH₃), 3.57 (2H, t, NCH₂), 3.31 (2H, t, NCH₂), 2.18 (2H, m, CH_{COD}), 2.12 (2H, m, NCH₂CH₂), 1.66 (4H, m, CH_{COD}), 1.25 (4H, m, CH_{COD}). ¹³C NMR (CDCl₃, 100 MHz, 298 K): δ 208.6 (d, ¹J_{RhC} = 46.7, C_{NHC}), 153.3 (s, Ar-C_o-MeOPh), 134.5 (s, Ar-C_o-MeOPh), 132.9 (s, Ar-CH_o-MeOPh), 127.9 (s, Ar-CH_o-MeOPh), 119.9 (s, Ar-CH_o-MeOPh), 109.5 (s, Ar-CH_o-MeOPh), 93.9 (d, C_{COD}), 65.3 (d, C_{COD}), 54.5 (s, OCH₃), 46.9 (s, NCH₂), 30.9 (s, CH₂ COD), 26.8 (s, CH₂ COD), 20.2 (NCH₂CH₂). Anal. Found (Calcd) for C₂₆H₃₂N₂O₂RhCl: C, 57.90 (57.52); H, 5.77 (5.89); N, 5.09 (5.16). HRMS (ES): *m/z* 507.1538 ([M-Cl]⁺ C₂₆H₃₂N₂O₂Rh requires 507.1519).

Ar-CH_o-MeOPh), 109.4 (s, Ar-CH_o-MeOPh), 93.7 (d, C_{COD}), 67.1 (d, C_{COD}), 55.0 (s, OCH₃), 53.9 (s, NCH₂), 53.2 (s, NCH₂), 31.4 (s, CH₂ COD), 30.6 (s, CH₂ COD), 27.3 (s, CH₂ COD), 25.8 (s, CH₂ COD), 23.0 (s, NCH₂CH₂), 22.7 (s, NCH₂CH₂), 19.9 (s, CH₃), 19.2 (s, CH₃), 17.3 (s, CH₃). Anal. Found (Calcd) for C₂₉H₃₈N₂ORhCl: C, 60.77 (61.22); H, 6.71 (6.68); N, 4.79 (4.93). HRMS (ES): *m/z* 533.2033 ([M-Cl]⁺ C₂₉H₃₈N₂ORh requires 533.2039).

[Rh(7-*o*-MeOPh-DIPP)(COD)Cl] (3.19).



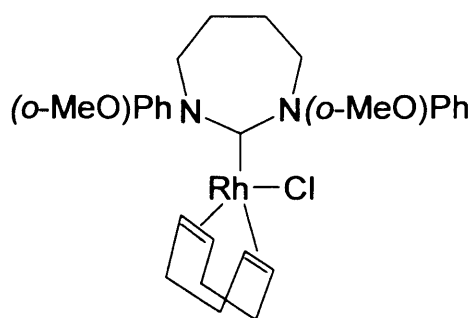
KN(SiMe₃)₂ (82 mg, 0.41 mmol) and (7-*o*-MeOPh-DIPP)BF₄ salt (185 mg, 0.41 mmol) were placed in to a Schlenk-tube followed by the addition of THF (15 ml). The solution was stirred for 30 minutes and subsequently filtered

into another Schlenk-tube containing a 10 ml THF solution of [Rh(COD)Cl]₂ (0.20 mmol). An immediate colour change was observed from light to dark yellow. After the reaction was stirred at room temperature for 2 hours, the volatiles were removed in vacuo. The yellow solid obtained was washed with hexane (2 x 10 ml) and dried. Crystals suitable for X-ray diffraction were obtained by layering a dichloromethane solution of the compound with hexane. The yield was 60% (0.150 g).

¹H NMR (CDCl₃, 500 MHz, 298 K): δ 8.41 (1H, d, *o*-CH_o-MeOPh), 7.35 (1H, t, *m*-CH_o-MeOPh), 7.31 (1H, t, *p*-CH_{DIPP}), 7.26 (1H, d, *m*-CH_{DIPP}) 7.09 (1H, d, *m*-CH_{DIPP}), 7.04 (1H, t, *p*-CH_o-MeOPh), 6.94 (1H, d, *m*-CH_o-MeOPh), 4.48 (1H, m, CH_{COD}), 4.41 (1H, m, CH_{COD}), 4.07 (2H, t, NCH₂), 3.93 (2H, t, NCH₂), 3.84

(3H, s, OCH₃), 3.35 (1H, m, CH_{COD}), 3.22 (1H, m, CH_{COD}), 2.75 (1H, m, CH(CH₃)₂), 2.41 (1H, m, CH(CH₃)₂), 2.16 (2H, m, NCH₂CH₂), 2.04 (2H, m, NCH₂CH₂), 1.72 (2H, m, CH_{COD}), 1.66 (3H, d, CH(CH₃)₂), 1.56 (3H, d, CH(CH₃)₂), 1.42 (2H, m, CH_{COD}), 1.36 (2H, m, CH_{COD}), 1.23 (3H, d, CH(CH₃)₂), 1.15 (3H, d, CH(CH₃)₂), 1.08 (2H, m, CH_{COD}). ¹³C NMR (CDCl₃, 100 MHz, 298 K): δ 224.0 (d, ¹J_{RhC} = 46.4, C_{NHC}), 153.1 (s, Ar-C_o-MeOPh), 147.6 (s, Ar-C_{DIPP}), 146.8 (s, Ar-C_{DIPP}), 141.7 (s, Ar-C_{DIPP}), 135.2 (s, Ar-C_o-MeOPh), 134.0 (s, Ar-CH_o-MeOPh), 127.4 (s, Ar-CH_{DIPP}), 127.2 (s, Ar-CH_{DIPP}), 125.0 (s, Ar-CH_{DIPP}), 121.6 (s, Ar-CH_o-MeOPh), 119.1 (s, Ar-CH_o-MeOPh), 109.5 (s, Ar-CH_o-MeOPh), 95.1 (d, C_{COD}), 68.8 (d, C_{COD}), 55.5 (s, OCH₃), 54.2 (s, NCH₂), 53.4 (s, NCH₂), 32.8 (s, CH(CH₃)₂), 29.8 (s, CH(CH₃)₂), 28.9 (s, NCH₂CH₂), 27.3 (s, NCH₂CH₂), 27.1 (s, CH₂ COD), 26.0 (s, CH₂ COD), 25.6 (s, CH₂ COD), 25.0 (s, CH₂ COD), 24.9 (s, CH₃), 23.6 (s, CH₃), 22.8 (s, CH₃), 21.2 (s, CH₃). Anal. Found (Calcd) for C₃₂H₄₄N₂ORhCl: C, 62.16 (62.91); H, 7.63 (7.21); N, 4.97 (4.59). HRMS (ES): *m/z* 575.2501 ([M-Cl]⁺ C₃₂H₄₄N₂ORh requires 575.2509).

[Rh(7-*o*-MeOPh)(COD)Cl] (3.20).

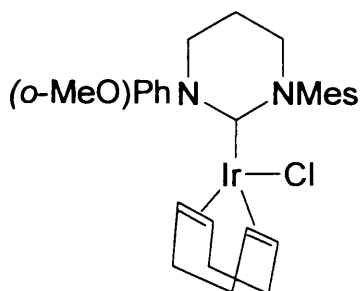


KN(SiMe₃)₂ (82 mg, 0.41 mmol) and (7-*o*-MeOPh)BF₄ salt (163 mg, 0.41 mmol) were placed in a Schlenk-tube followed by the addition of THF (15 ml). The solution was stirred for 30 minutes and subsequently filtered into another Schlenk-tube containing a 10 ml THF

solution of $[\text{Rh}(\text{COD})\text{Cl}]_2$ (0.20 mmol). An immediate colour change was observed from light to dark yellow. After the reaction was stirred at room temperature for 2 hours, the volatiles were removed in vacuo. The yellow solid obtained was washed with hexane (2 x 10 ml) and dried. Crystals suitable for X-ray diffraction were obtained by layering a dichloromethane solution of the compound with hexane. The yield was 50% (0.114 g).

^1H NMR (CDCl_3 , 500 MHz, 298 K): δ 8.43 (2H, d, $o\text{-CH}_{o\text{-MeOPh}}$), 7.27 (2H, t, $m\text{-CH}_{o\text{-MeOPh}}$), 7.05 (2H, t, $p\text{-CH}_{o\text{-MeOPh}}$), 6.67 (2H, d, $m\text{-CH}_{o\text{-MeOPh}}$), 4.29 (2H, m, CH_{COD}), 3.85 (6H, s, OCH_3), 3.71 (2H, t, NCH_2), 3.58 (2H, t, NCH_2), 3.05 (2H, m, CH_{COD}), 2.41 (2H, m, NCH_2CH_2), 2.17 (2H, m, NCH_2CH_2), 1.59 (4H, m, CH_{COD}), 1.21 (4H, m, CH_{COD}). ^{13}C NMR (CDCl_3 , 100 MHz, 298 K): δ 215.6 (d, $^1J_{\text{RhC}} = 46.3$, C_{NHC}), 154.5 (s, $\text{Ar-C}_{o\text{-MeOPh}}$), 135.3 (s, $\text{Ar-C}_{o\text{-MeOPh}}$), 133.1 (s, $\text{Ar-CH}_{o\text{-MeOPh}}$), 127.9 (s, $\text{Ar-CH}_{o\text{-MeOPh}}$), 119.9 (s, $\text{Ar-CH}_{o\text{-MeOPh}}$), 110.9 (s, $\text{Ar-CH}_{o\text{-MeOPh}}$), 94.5 (d, C_{COD}), 66.9 (d, C_{COD}), 54.9 (s, OCH_3), 43.8 (s, NCH_2), 30.6 (s, CH_2_{COD}), 26. (s, CH_2_{COD}), 21.6 (s, NCH_2CH_2). Anal. Found (Calcd) for $\text{C}_{27}\text{H}_{34}\text{N}_2\text{O}_2\text{RhCl}$: C, 58.35 (58.23); H, 6.03 (6.11); N, 4.95 (5.03). HRMS (ES): m/z 521.1535 ($[\text{M}-\text{Cl}]^+$ $\text{C}_{27}\text{H}_{34}\text{N}_2\text{O}_2\text{Rh}$ requires 521.1527).

$[\text{Ir}(\text{6-}o\text{-MeOPh-Mes})(\text{COD})\text{Cl}]$ (3.21).

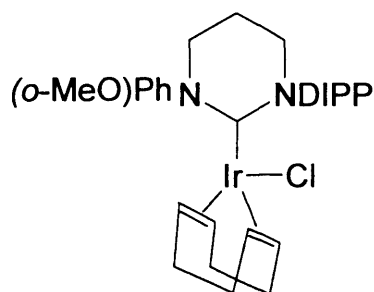


$\text{KN}(\text{SiMe}_3)_2$ (59 mg, 0.30 mmol) and (6- o -MeOPh-Mes) BF_4 salt (118 mg, 0.30 mmol) were placed in a Schlenk-tube followed by the addition of THF (15 ml). The solution was stirred

for 30 minutes and subsequently filtered into another Schlenk-tube containing a 10 ml THF solution of $[\text{Ir}(\text{COD})\text{Cl}]_2$ (0.15 mmol). An immediate colour change was observed from light to dark orange. After the reaction was stirred at room temperature for 3 hours, the volatiles were removed in vacuo. The yellow solid obtained was washed with hexane (2 x 10 ml) and dried. Crystals suitable for X-ray diffraction were obtained by layering a dichloromethane solution of the compound with hexane. The yield was 64% (0.123 g).

^1H NMR (CDCl_3 , 500 MHz, 298 K): δ 8.09 (1H, d, $o\text{-CH}_{o\text{-MeOPh}}$), 7.25 (1H, t, $m\text{-CH}_{o\text{-MeOPh}}$), 6.96 (1H, t, $p\text{-CH}_{o\text{-MeOPh}}$), 6.89 (1H, s, $m\text{-CH}_{\text{Mes}}$), 6.85 (1H, d, $m\text{-CH}_{o\text{-MeOPh}}$), 6.81 (1H, s, $m\text{-CH}_{\text{Mes}}$), 3.85 (1H, m, CH_{COD}), 3.79 (3H, s, OCH_3), 3.68 (1H, m, CH_{COD}), 3.63 (2H, t, NCH_2), 3.29 (2H, t, NCH_2), 2.66 (1H, m, CH_{COD}), 2.54 (1H, m, CH_{COD}), 2.45 (3H, s, $o\text{-CH}_3$), 2.22 (3H, s, $o\text{-CH}_3$), 2.12 (3H, s, $p\text{-CH}_3$), 1.78 (2H, m, NCH_2CH_2), 1.38 (2H, m, CH_{COD}), 1.21 (2H, m, CH_{COD}), 1.19 (2H, m, CH_{COD}), 1.07 (2H, m, CH_{COD}). ^{13}C NMR (CDCl_3 , 100 MHz, 298 K): δ 205.5 (s, NClrN), 154.9 (s, $\text{Ar-C}_{o\text{-MeOPh}}$), 141.3 (s, Ar-C_{Mes}), 137.2 (s, Ar-C_{Mes}), 137.1 (s, Ar-C_{Mes}), 135.5 (s, Ar-C_{Mes}), 135.2 (s, $\text{Ar-C}_{o\text{-MeOPh}}$), 134.7 (s, $\text{Ar-CH}_{o\text{-MeOPh}}$), 129.6 (s, $\text{Ar-CH}_{\text{Mes}}$), 128.3 (s, $\text{Ar-CH}_{\text{Mes}}$), 127.9 (s, $\text{Ar-CH}_{o\text{-MeOPh}}$), 120.4 (s, $\text{Ar-CH}_{o\text{-MeOPh}}$), 110.4 (s, $\text{Ar-CH}_{o\text{-MeOPh}}$), 79.6 (d, C_{COD}), 67.9 (d, C_{COD}), 55.2 (s, OCH_3), 50.9 (s, NCH_2), 48.8 (s, NCH_2), 33.6 (s, CH_2COD), 32.2 (s, CH_2COD), 29.1 (s, CH_2COD), 25.6 (s, CH_2COD), 21.5 (s, NCH_2CH_2), 20.9 (s, CH_3), 19.6 (s, CH_3), 18.1 (s, CH_3). Anal. Found (Calcd) for $\text{C}_{28}\text{H}_{36}\text{N}_2\text{OIrCl}$: C, 52.45 (52.20); H, 5.50 (5.59); N, 4.04 (4.35). HRMS (ES): m/z 607.2433 ($[\text{M-Cl}]^+$ $\text{C}_{28}\text{H}_{36}\text{N}_2\text{OIr}$ requires 607.2434).

[Ir(6-*o*-MeOPh-DIPP)(COD)Cl] (3.22).



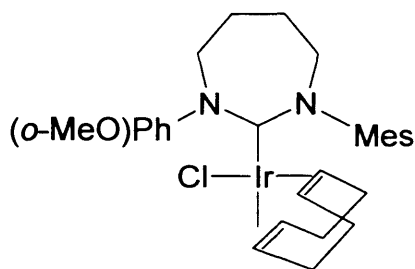
KN(SiMe₃)₂ (59 mg, 0.30 mmol) and (6-*o*-MeOPh-DIPP)BF₄ salt (131 mg, 0.30 mmol) were placed in a Schlenk-tube followed by the addition of THE (15 ml). The solution was

stirred for 30 minutes and subsequently filtered into another Schlenk-tube containing a 10ml THF solution of [Ir(COD)Cl]₂ (0.15 mmol). An immediate colour change was observed from light to dark orange. After the reaction was stirred at room temperature for 3 hours, the volatiles were removed in vacuo. The yellow solid obtained was washed with hexane (2 x 10 ml) and dried. Crystals suitable for X-ray diffraction were obtained by layering a dichloromethane solution of the compound with hexane. The yield was 63% (0.129 g).

¹H NMR (CDCl₃, 500 MHz, 298 K): δ 8.04 (1H, d, *o*-CH_{*o*-MeOPh}), 7.28 (1H, t, *m*-CH_{*o*-MeOPh}), 7.25 (1H, t, *p*-CH_{DIPP}), 7.21 (1H, d, *m*-CH_{DIPP}), 7.05 (1H, d, *m*-CH_{DIPP}), 6.97 (1H, t, *p*-CH_{*o*-MeOPh}), 6.86 (1H, d, *m*-CH_{*o*-MeOPh}), 4.11 (1H, m, CH_{COD}), 3.87 (1H, m, CH_{COD}), 3.82 (2H, t, NCH₂), 3.76 (3H, s, OCH₃), 3.59 (2H, t, NCH₂), 3.36 (1H, m, CH_{COD}), 3.32 (1H, m, CH_{COD}), 3.09 (1H, m, CH(CH₃)₂), 2.62 (1H, m, CH(CH₃)₂), 2.25 (2H, m, NCH₂CH₂), 1.62 (2H, m, CH_{COD}), 1.44 (3H, d, CH(CH₃)₂), 1.42 (3H, d, CH(CH₃)₂), 1.25 (2H, m, CH_{COD}), 1.03 (2H, m, CH_{COD}), 1.17 (3H, d, CH(CH₃)₂), 1.10 (3H, d, CH(CH₃)₂), 1.04 (2H, m, CH_{COD}). ¹³C NMR (CDCl₃, 100 MHz, 298 K): δ 207.5 (s, NClrN), 155.3 (s, Ar-C_{*o*-MeOPh}), 148.4 (s, Ar-C_{DIPP}), 146.6 (s, Ar-C_{DIPP}), 141.1 (s, Ar-C_{DIPP}), 135.4 (s, Ar-C_{*o*-MeOPh}), 134.9 (s, Ar-CH_{*o*-MeOPh}), 128.6 (s, Ar-CH_{DIPP}),

128.5 (s, Ar-CH_{DIPP}), 125.1 (s, Ar-CH_{DIPP}), 122.8 (s, Ar-CH_{o-MeOPh}), 120.8 (s, Ar-CH_{o-MeOPh}), 110.2 (s, Ar-CH_{o-MeOPh}), 80.4 (d, C_{COD}), 77.9 (d, C_{COD}), 55.2 (s, OCH₃), 53.4 (s, NCH₂), 50.4 (s, NCH₂), 33.3 (s, CH(CH₃)₂), 32.6 (s, CH(CH₃)₂), 28.3 (s, NCH₂CH₂), 28.1 (s, CH₂ COD), 28.0 (s, CH₂ COD), 27.7 (s, CH₂ COD), 27.3 (s, CH₂ COD), 26.4 (s, CH₃), 24.6 (s, CH₃), 23.3 (s, CH₃), 21.7 (s, CH₃). Anal. Found (Calcd) for C₃₁H₄₂N₂OIrCl: C, 54.70 (54.32); H, 6.04 (6.12); N, 3.79 (4.07). HRMS (ES): *m/z* 649.3903 ([M-Cl]⁺ C₃₁H₄₂N₂OIr requires 649.2931).

[Ir(7-*o*-MeOPh-Mes)(COD)Cl] (3.23).



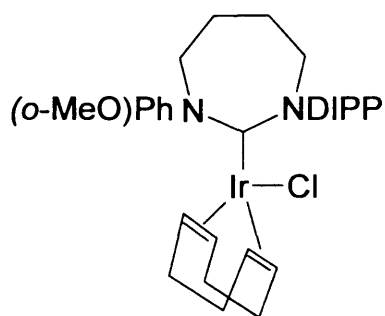
KN(SiMe₃)₂ (59 mg, 0.30 mmol) and (7-*o*-MeOPh-Mes)BF₄ salt (122 mg, 0.30 mmol) were placed in to a Schlenk-tube followed by the addition of THF (15 ml). The solution was

stirred for 30 minutes and subsequently filtered into another Schlenk-tube containing a 10 ml THF solution of [Ir(COD)Cl]₂ (0.15 mmol). An immediate colour change was observed from light to dark orange. After the reaction was stirred at room temperature for 3 hours, the volatiles were removed in vacuo. The yellow solid obtained was washed with hexane (2 x 10 ml) and dried. Crystals suitable for X-ray diffraction were obtained by layering a dichloromethane solution of the compound with hexane. The yield was 62% (0.122 g).

¹H NMR (CDCl₃, 500 MHz, 298 K): δ 8.05 (1H, d, *o*-CH_{o-MeOPh}), 7.25 (1H, t, *m*-CH_{o-MeOPh}), 6.98 (1H, t, *p*-CH_{o-MeOPh}), 6.92 (1H, s, *m*-CH_{Mes}), 6.88 (1H, d,

m-CH_o-MeOPh), 6.79 (1H, s, *m*-CH_{Mes}), 4.54 (1H, m, CH_{COD}), 4.39 (1H, m, CH_{COD}), 3.79 (3H, s, OCH₃), 3.66 (2H, t, NCH₂), 3.31 (2H, t, NCH₂), 2.82 (1H, m, CH_{COD}), 2.76 (1H, m, CH_{COD}), 2.56 (3H, s, *o*-CH₃), 2.43 (2H, m, NCH₂CH₂), 2.25 (3H, s, *o*-CH₃), 2.17 (3H, s, *p*-CH₃), 2.08 (2H, m, NCH₂CH₂) 1.67 (2H, m, CH_{COD}), 1.43 (2H, m, CH_{COD}), 1.24 (2H, m, CH_{COD}), 1.15 (2H, m, CH_{COD}). ¹³C NMR (CDCl₃, 100 MHz, 298 K): δ 215.8 (s, NClrN), 157.7 (s, Ar-C_o-MeOPh), 141.6 (s, Ar-C_{Mes}), 138.9 (s, Ar-C_{Mes}), 138.6 (s, Ar-C_{Mes}), 136.0 (s, Ar-C_{Mes}), 135.4 (s, Ar-C_o-MeOPh), 134.5 (s, Ar-CH_o-MeOPh), 129.9 (s, Ar-CH_{Mes}), 127.6 (s, Ar-CH_{Mes}), 127.2 (s, Ar-CH_o-MeOPh), 118.9 (s, Ar-CH_o-MeOPh), 109.4 (s, Ar-CH_o-MeOPh), 97.8 (d, C_{COD}), 66.9 (d, C_{COD}), 53.8 (s, OCH₃), 50.8 (s, NCH₂), 49.6 (s, NCH₂), 32.9 (s, CH₂ COD), 31.1 (s, CH₂ COD), 28.1 (s, CH₂ COD), 26.1 (s, CH₂ COD), 24.2 (s, NCH₂CH₂), 23.2 (s, NCH₂CH₂), 19.9 (s, CH₃), 19.1 (s, CH₃), 17.5 (s, CH₃). Anal. Found (Calcd) for C₂₉H₃₈N₂OIrCl: C, 52.99 (52.91); H, 5.62 (5.78); N, 4.20 (4.26). HRMS (ES): *m/z* 623.2611 ([M-Cl]⁺ C₂₉H₃₈N₂OIr requires 623.2614).

[Ir(7-*o*-MeOPh-DIPP)(COD)Cl] (3.24).

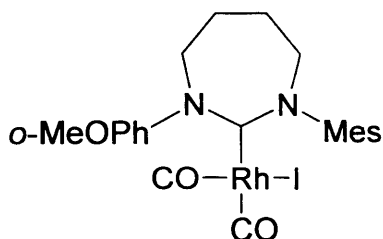


KN(SiMe₃)₂ (59 mg, 0.30 mmol) and (7-*o*-MeOPh-DIPP)BF₄ salt (135 mg, 0.30 mmol) were placed in a Schlenk-tube followed by the addition of THF (15 ml). The solution was stirred for 30 minutes and subsequently filtered

into another Schlenk-tube containing a 10 ml THF solution of [Ir(COD)Cl]₂ (0.15 mmol). An immediate colour change was observed from light to dark

orange. After the reaction was stirred at room temperature for 3 hours, the volatiles were removed in vacuo. The yellow solid obtained was washed with hexane (2 x 10 ml) and dried. Crystals suitable for X-ray diffraction were obtained by layering a dichloromethane solution of the compound with hexane. The yield was 57% (0.120 g).

^1H NMR (CDCl_3 , 500 MHz, 298 K): δ 8.08 (1H, d, $o\text{-CH}_{o\text{-MeOPh}}$), 7.30 (1H, t, $m\text{-CH}_{o\text{-MeOPh}}$), 7.27 (1H, t, $p\text{-CH}_{\text{DIPP}}$), 7.25 (1H, d, $m\text{-CH}_{\text{DIPP}}$) 7.04(1H, d, $m\text{-CH}_{\text{DIPP}}$), 6.96 (1H, t, $p\text{-CH}_{o\text{-MeOPh}}$), 6.87 (1H, d, $m\text{-CH}_{o\text{-MeOPh}}$), 4.47 (1H, m, CH_{COD}), 4.00 (1H, m, CH_{COD}), 3.95 (2H, t, NCH_2), 3.82 (2H, t, NCH_2), 3.78 (3H, s, OCH_3), 3.32 (1H, m, CH_{COD}), 3.21 (1H, m, CH_{COD}), 3.03 (1H, m, $\text{CH}(\text{CH}_3)_2$), 2.62 (1H, m, $\text{CH}(\text{CH}_3)_2$), 2.12 (2H, m, NCH_2CH_2), 2.00 (2H, m, NCH_2CH_2), 1.61 (2H, m, CH_{COD}), 1.47 (3H, d, $\text{CH}(\text{CH}_3)_2$), 1.32 (3H, d, $\text{CH}(\text{CH}_3)_2$), 1.29 (2H, m, CH_{COD}), 1.23 (2H, m, CH_{COD}), 1.18 (3H, d, $\text{CH}(\text{CH}_3)_2$), 1.12 (3H, d, $\text{CH}(\text{CH}_3)_2$), 1.02 (2H, m, CH_{COD}). ^{13}C NMR (CDCl_3 , 100 MHz, 298 K): δ 218.1 (s, NClrN), 153.8 (s, $\text{Ar-C}_{o\text{-MeOPh}}$), 148.7 (s, $\text{Ar-C}_{\text{DIPP}}$), 147.8 (s, $\text{Ar-C}_{\text{DIPP}}$), 142.1 (s, $\text{Ar-C}_{\text{DIPP}}$), 135.7 (s, $\text{Ar-C}_{o\text{-MeOPh}}$), 135.3 (s, $\text{Ar-CH}_{o\text{-MeOPh}}$), 128.2 (s, $\text{Ar-CH}_{\text{DIPP}}$), 128.1 (s, $\text{Ar-CH}_{\text{DIPP}}$), 125.8 (s, $\text{Ar-CH}_{\text{DIPP}}$), 122.4 (s, $\text{Ar-CH}_{o\text{-MeOPh}}$), 119.7 (s, $\text{Ar-CH}_{o\text{-MeOPh}}$), 110.5 (s, $\text{Ar-CH}_{o\text{-MeOPh}}$), 81.8 (d, C_{COD}), 67.9 (d, C_{COD}), 55.1 (s, OCH_3), 54.6 (s, NCH_2), 53.9 (s, NCH_2), 34.3 (s, $\text{CH}(\text{CH}_3)_2$), 31.9 (s, $\text{CH}(\text{CH}_3)_2$), 28.7 (s, NCH_2CH_2), 28.2 (s, NCH_2CH_2), 27.2 (s, CH_2COD), 26.1 (s, CH_2COD), 25.9 (s, CH_2COD), 25.6 (s, CH_2COD), 24.1(s, CH_3), 23.7 (s, CH_3), 23.2 (s, CH_3), 22.1 (s, CH_3). Anal. Found (Calcd) for $\text{C}_{32}\text{H}_{44}\text{N}_2\text{OIrCl}$: C, 54.80 (54.88); H, 6.31 (6.29); N, 4.34 (4.00). HRMS (ES): m/z 663.3082 ($[\text{M-Cl}]^+$ $\text{C}_{32}\text{H}_{44}\text{N}_2\text{OIr}$ requires 663.3060).

***Cis*-[Rh(7-*o*MeOPh-Mes)(CO)₂I] (3.29).**

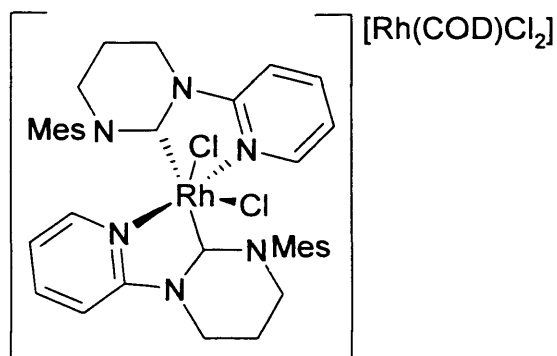
KN(SiMe₃)₂ (82 mg, 0.41 mmol), (7-*o*-MeOPh-Mes)I salt (184 mg, 0.41 mmol) and (acetylaceton)dicarbonylrhodium(I) (106 mg, 0.41 mmol) were placed in a Schlenk-tube

followed by the addition of THF (25 ml). The solution was stirred for 4 hours and subsequently filtered in to another Schlenk-tube then the volatiles were removed in vacuo. The yellow solid obtained was washed with diethylether (2 x 10 ml) and dried. Crystals suitable for X-ray diffraction were obtained by layering a dichloromethane solution of the compound with hexane. The yield was 59% (0.125 g).

¹H NMR (*p* CDCl₃, 500 MHz, 298 K): δ 7.62 (1H, d, *o*-CH_{*o*-MeOPh}), 7.26 (1H, t, *m*-CH_{*o*-MeOPh}), 7.19 (1H, t, *p*-CH_{*o*-MeOPh}), 6.90 (1H, s, *m*-CH_{Mes}), 6.85 (1H, d, *m*-CH_{*o*-MeOPh}), 6.81 (1H, s, *m*-CH_{Mes}), 3.84 (3H, s, OCH₃), 3.72 (2H, t, NCH₂), 3.58 (2H, t, NCH₂), 2.50 (3H, s, *o*-CH₃), 2.39 (2H, m, NCH₂CH₂), 2.26 (3H, s, *o*-CH₃), 2.20 (3H, s, *p*-CH₃), 2.09 (2H, m, NCH₂CH₂). ¹³C NMR (CDCl₃, 100 MHz, 298 K): δ 214.2 (d, ¹J_{RhC} = 40.8, C_{NHC}), 189.9 (d, ¹J_{RhC} = 52.5, CO), 186.9 (d, ¹J_{RhC} = 77.7, CO), 154.2 (s, Ar-C_{*o*-MeOPh}), 143.6 (s, Ar-C_{Mes}), 141.7 (s, Ar-C_{Mes}), 136.5 (s, Ar-C_{Mes}), 135.3 (s, Ar-C_{Mes}), 133.8 (s, Ar-C_{*o*-MeOPh}), 132.1 (s, Ar-CH_{*o*-MeOPh}), 129.2 (s, Ar-CH_{Mes}), 128.0 (s, Ar-CH_{Mes}), 126.9 (s, Ar-CH_{*o*-MeOPh}), 118.8 (s, Ar-CH_{*o*-MeOPh}), 109.7 (s, Ar-CH_{*o*-MeOPh}), 55.5 (1C, s, OCH₃), 54.9 (s, NCH₂), 54.8 (s, NCH₂), 26.6 (s, NCH₂CH₂), 23.5 (s, NCH₂CH₂), 21.0 (s, CH₃), 19.6 (s, CH₃), 18.5 (s, CH₃). IR (cm⁻¹): 1967, 2059

(CH₂Cl₂). HRMS (ES): *m/z* 481.1021 ([M-I]⁺ C₂₃H₂₆N₂O₃Rh requires 481.0998).

[Rh(6-Py-Mes)₂Cl₂] (3.30).



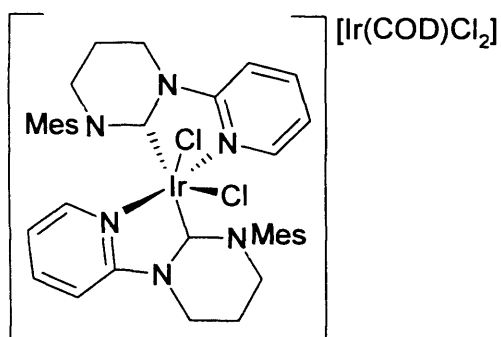
KN(SiMe₃)₂ (82 mg, 0.41 mmol) and (6-Py-Mes)BF₄ salt (150 mg, 0.41 mmol) were placed in a Schlenk-tube followed by the addition of THF (15 ml). The

solution was stirred for 30 minutes and subsequently filtered into another Schlenk-tube containing a 10 ml THF solution of [Rh(COD)Cl]₂ (0.20 mmol). An immediate colour change was observed from light to dark yellow. After the reaction was stirred at room temperature for 2 hours, the volatiles were removed in vacuo. The yellow solid obtained was washed with hexane (2 x 10 ml) and dried. Crystals suitable for X-ray diffraction were obtained by layering a dichloromethane solution of the compound with hexane. The yield was 58% (0.085 g).

¹H NMR (CDCl₃, 500 MHz, 298 K): δ 8.80 (1H, d, *o*-CH_{Py}), 7.62 (1H, t, *p*-CH_{Py}), 6.94 (1H, d, *m*-CH_{Py}), 6.73 (1H, t, *m*-CH_{Py}), 6.44 (1H, s, *m*-CH_{Mes}), 6.37 (1H, s, *m*-CH_{Mes}), 3.91 (2H, t, NCH₂), 3.60 (2H, t, NCH₂), 2.46 (2H, m, NCH₂CH₂), 2.31 (3H, s, *o*-CH₃ Mes), 2.22 (3H, s, *o*-CH₃ Mes), 2.01 (3H, s, *p*-CH₃ Mes). ¹³C NMR (CDCl₃, 100 MHz, 298 K): δ 188.8 (d, ¹J_{RhC} = 45.8, C_{NHC}), 156.8 (s, Ar-C_{Py}), 149.5 (s, Ar-C_{Py}), 139.0 (s, Ar-C_{Mes}), 138.3 (s, Ar-C_{Mes}), 137.8 (s, Ar-C_{Mes}), 131.3 (s, Ar-C_{Mes}), 129.7 (s, Ar-CH_{Mes}), 128.3 (s, Ar-

CH_{Mes}), 118.8 (s, Ar- CH_{Py}), 110.1 (s, Ar- CH_{Py}), 51.9 (s, NCH_2), 44.1 (s, NCH_2), 26.9 (s, NCH_2CH_2), 19.1 (s, *p*- CH_3), 18.3 (s, *o*- CH_3), 18.2 (s, *o*- CH_3).
 Anal. Found (Calcd) for $\text{C}_{45}\text{H}_{56}\text{N}_6\text{Cl}_6\text{Rh}_2$ C, 48.90 (49.20); H, 5.05 (5.10); N, 7.64 (7.66). HRMS (ES): m/z 731.1922 ($[\text{M}-\text{Cl}]^+$ $\text{C}_{36}\text{H}_{42}\text{N}_6\text{Cl}_2\text{Rh}$ requires 731.1903).

$[\text{Ir}(\text{6-Py-Mes})_2\text{Cl}_2]$ (3.31).



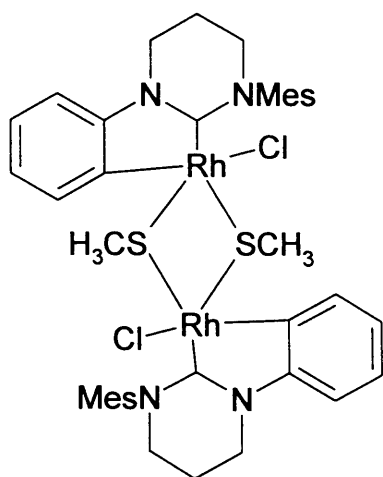
$[\text{Ir}(\text{COD})\text{Cl}_2]$ $\text{KN}(\text{SiMe}_3)_2$ (82 mg, 0.41 mmol) and (6-Py-Mes) BF_4 salt (150 mg, 0.41 mmol) were placed in a Schlenk-tube followed by the addition of THF (15 ml). The solution was stirred for

30 minutes and subsequently filtered into another Schlenk-tube containing a 10 ml THF solution of $[\text{Ir}(\text{COD})\text{Cl}_2]$ (0.20 mmol). An immediate colour change was observed from light to dark yellow. After the reaction was stirred at room temperature for 2 hours, the volatiles were removed in vacuo. The yellow solid obtained was washed with hexane (2 x 10 ml) and dried. Crystals suitable for X-ray diffraction were obtained by layering a dichloromethane solution of the compound with hexane. The yield was 52% (0.082 g).

^1H NMR (CDCl_3 , 500 MHz, 298 K): δ 8.88 (1H, d, *o*- CH_{Py}), 7.66 (1H, t, *p*- CH_{Py}), 6.93 (1H, d, *m*- CH_{Py}), 6.74 (1H, t, *m*- CH_{Py}), 6.56 (1H, s, *m*- CH_{Mes}), 6.41 (1H, s, *m*- CH_{Mes}), 4.01 (2H, t, NCH_2), 3.70 (2H, t, NCH_2), 2.55 (2H, m, NCH_2CH_2), 2.36 (3H, s, *o*- CH_3_{Mes}), 2.28 (3H, s, *o*- CH_3_{Mes}), 2.01 (3H, s, *p*- CH_3_{Mes}). ^{13}C NMR (CDCl_3 , 100 MHz, 298 K): δ 184.3 (s, NClrN), 146.0 (s,

Ar-C_{Py}), 142.6 (s, Ar-C_{Py}), 138.7 (s, Ar-C_{Mes}), 137.4 (s, Ar-C_{Mes}), 136.8 (s, Ar-C_{Mes}), 130.7 (s, Ar-C_{Mes}), 129.1 (s, Ar-CH_{Mes}), 128.1 (s, Ar-CH_{Mes}), 118.4 (s, Ar-CH_{Py}), 108.2 (s, Ar-CH_{Py}), 51.5 (s, NCH₂), 42.8 (s, NCH₂), 25.5 (s, NCH₂CH₂), 19.3 (s, *p*-CH₃), 18.3 (s, *o*-CH₃), 18.1 (s, *o*-CH₃). HRMS (ES): *m/z* 820.3121 ([M-Cl]⁺ C₃₆H₄₂N₆Cl₂Ir requires 820.3119).

[Rh(6-Ph-Mes)(SMe)Cl]₂ (3.32).



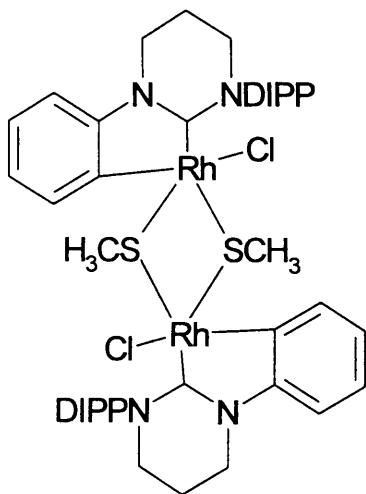
KN(SiMe₃)₂ (82 mg, 0.41 mmol) and (6-*o*-MeSPh-Mes)BF₄ salt (0.168 mg, 0.41 mmol) were placed in a Schlenk-tube followed by the addition of THF (15 ml). The solution was stirred for 30 minutes and subsequently filtered into another Schlenk-tube containing a 10 ml THF solution of [Rh(COD)Cl]₂ (0.20

mmol). An immediate colour change was observed from light to dark yellow. After the reaction was stirred at room temperature for 4 hours, the volatiles were removed in vacuo. The yellow solid obtained was washed with hexane (2 x 10 ml) and dried. Crystals suitable for X-ray diffraction were obtained by layering a dichloromethane solution of the compound with hexane. The yield was 60% (0.114 g).

¹H NMR (CD₂Cl₂, 500 MHz, 298 K): δ 7.56 (1H, t, *m*-CH_{Ph}), 7.45 (1H, d, *o*-CH_{Ph}), 7.34 (1H, d, *m*-CH_{Ph}), 6.91 (1H, t, *p*-CH_{Ph}), 6.84 (1H, s, *m*-CH_{Mes}), 6.80 (1H, s, *m*-CH_{Mes}), 3.83 (2H, t, NCH₂), 3.72 (2H, t, NCH₂), 2.38 (2H, m, NCH₂CH₂), 2.25 (3H, s, *o*-CH₃), 1.69 (3H, s, SCH₃), 1.67 (3H, s, *o*-CH₃),

1.61 (3H, s, *p*-CH₃), ¹³C NMR (CD₂Cl₂, 100 MHz, 298 K): δ 202.3 (d, ¹J_{RhC} = 46.8, C_{NHC}), 201.8 (d, ¹J_{RhC} = 48.2, Ar-C_{Ph}), 148.0 (s, Ar-C_{Mes}), 140.3 (s, Ar-C_{Mes}), 140.1 (s, Ar-C_{Mes}), 137.3 (s, Ar-C_{Mes}), 136.4 (s, Ar-C_{Ph}), 132.9 (s, Ar-CH_{Ph}), 123.4 (s, Ar-CH_{Mes}), 122.2 (s, Ar-CH_{Mes}), 121.9 (s, Ar-CH_{Ph}), 120.6 (s, Ar-CH_{Ph}), 108.3 (s, Ar-CH_{Ph}), 45.4 (s, NCH₂), 44.2 (s, NCH₂), 20.5 (s, NCH₂CH₂), 19.2 (s, *p*-CH₃), 18.3 (s, *o*-CH₃), 17.7 (s, *o*-CH₃), 9.6 (s, SCH₃). HRMS (ES): *m/z* 930.1425 ([M-Cl])⁺ C₄₀H₄₈N₄S₂Rh₂ClCH₃CN requires 930.1384).

[Rh(6-Ph-DIPP)(SMe)Cl]₂ (3.33).



KN(SiMe₃)₂ (82 mg, 0.41 mmol) and (6-*o*-MeSPh-DIPP)BF₄ salt (0.187 mg, 0.41 mmol) were placed in a Schlenk-tube followed by the addition of THF (15 ml). The solution was stirred for 30 minutes and subsequently filtered into another Schlenk-tube containing a 10 ml THF solution of [Rh(COD)Cl]₂ (0.20

mmol). An immediate colour change was observed from light to dark yellow. After the reaction was stirred at room temperature for 4 hours, the volatiles were removed in vacuo. The yellow solid obtained was washed with hexane (2 x 10 ml) and dried. Crystals suitable for X-ray diffraction were obtained by layering a dichloromethane solution of the compound with hexane. The yield was 55% (0.113 g).

^1H NMR (CD_2Cl_2 , 500 MHz, 298 K): δ 7.53 (1H, t, $m\text{-CH}_{\text{Ph}}$), 7.40 (1H, d, $o\text{-CH}_{\text{Ph}}$), 7.31 (1H, d, $m\text{-CH}_{\text{Ph}}$), 6.89 (1H, t, $p\text{-CH}_{\text{Ph}}$), 6.59 (1H, t, $p\text{-CH}_{\text{DIPP}}$), 6.56 (1H, d, $m\text{-CH}_{\text{DIPP}}$), 6.52 (1H, d, $m\text{-CH}_{\text{DIPP}}$), 3.77 (2H, t, NCH_2), 3.68 (2H, t, NCH_2), 3.01 (2H, m, $\text{CH}(\text{CH}_3)_{\text{DIPP}}$), 2.31 (2H, m, NCH_2CH_2), 1.52 (3H, s, SCH_3), 1.45 (3H, s, $\text{CH}(\text{CH}_3)_{\text{DIPP}}$), 1.28 (3H, s, $\text{CH}(\text{CH}_3)_{\text{DIPP}}$), 1.22 (3H, s, $\text{CH}(\text{CH}_3)_{\text{DIPP}}$), 1.08 (3H, s, $\text{CH}(\text{CH}_3)_{\text{DIPP}}$), ^{13}C NMR (CD_2Cl_2 , 100 MHz, 298 K): δ 202.7 (d, $^1J_{\text{RhC}} = 46.9$, C_{NHC}), 202.1 (d, $^1J_{\text{RhC}} = 48.8$, Ar-C_{Ph}), 148.0 (s, $\text{Ar-C}_{\text{DIPP}}$), 140.6 (s, $\text{Ar-C}_{\text{DIPP}}$), 137.3 (s, Ar-C_{Ph}), 135.4 (s, Ar-CH_{Ph}), 129.1 (s, $\text{Ar-CH}_{\text{DIPP}}$), 123.9 (s, $\text{Ar-CH}_{\text{DIPP}}$), 123.5 (s, $\text{Ar-CH}_{\text{DIPP}}$), 122.2 (s, Ar-CH_{Ph}), 121.9 (s, Ar-CH_{Ph}), 109.5 (s, Ar-CH_{Ph}), 50.4 (s, NCH_2), 40.9 (s, NCH_2), 28.3 (s, $\text{CH}(\text{CH}_3)_{\text{DIPP}}$), 26.6 (s, $\text{CH}(\text{CH}_3)_{\text{DIPP}}$), 25.9 (s, NCH_2CH_2), 23.2 (s, CH_3), 22.9 (s, CH_3), 21.1 (s, CH_3), 19.6 (s, CH_3), 9.6 (s, SCH_3). HRMS (ES): m/z 1014.3142 ($[\text{M-Cl}]^+$ $\text{C}_{46}\text{H}_{60}\text{N}_4\text{S}_2\text{Rh}_2\text{ClCH}_3\text{CN}$ requires 1014.3138).

3.4. References.

- [1] A. J. Arduengo, R. L. Harlow and M. Kline, *J. Am. Chem. Soc.*, **1991**, *113*, 361.
- [2] K. Öfele, *J. Organomet. Chem.*, **1968**, *12*, 42.
- [3] H. W. Wanzlick and H. J. Schönherr, *Angew. Chem. Int. Ed. Eng.*, **1968**, *7*, 141.
- [4] M. F. Lappert, *J. Organomet. Chem.*, **1975**, *100*, 139.
- [5] E. Mas-Marza, M. Sanau and E. Peris, *Inorg. Chem.*, **2005**, *44*, 9961.

- [6] W. A. Herrmann, L. J. Goen and M. Spiegler, *J. Organomet. Chem.*, **1997**, *547*, 357.
- [7] M. V. Jimenez, J. J. Perez-Torrente, M. I. Bartolome, V. Gierz, F. J. Lahoz and L. A. Oro, *Organometallics*, **2008**, *27*, 224.
- [8] N. Stylianides, A. A. Danopoulos and N. Tsoureas, *J. Organomet. Chem.*, **2005**, *690*, 5948.
- [9] K S. Coleman, H T. Chamberlayne, S Turberville, M. L. H. Green and A. R. Cowley, *Dalton Trans*, **2003**, 2917.
- [10] C. Y. Wang, C.-F. Fu, Y.-H. Liu, S.-M. Peng and S.-T. Liu, *Inorg. Chem.*, **2007**, *46*, 5779.
- [11] R. S. Bon, F. J. J. de Kanter, M. Lutz, A. L. Spek, M. C. Jahnke, F. E. Hahn, M. B. Groen and R. V. A. Orru, *Organometallics*, **2007**, *26*, 3639.
- [12] C. H. Leung, C. D. Incarvito and R. H. Crabtree, *Organometallics*, **2006**, *25*, 6099.
- [13] M. Bortenschlager, M. Mayr, O. Nuyken and M. R. Buchmeiser, *J. Molecul. Cata. Chem.*, **2005**, *233*, 67.
- [14] J. Yun, E. R. Marinez and R. H. Grubbs, *Organometallics*, **2004**, *23*, 4172.
- [15] D Kremzow, G Seidel, C W. Lehmann and A. Fürstner, *Chem. Eur. J.*, **2005**, *11*, 1833.
- [16] N Imlinger, M Mayr, D Wang, K Wurst and M. R. Buchmeiser, *Adv. Synth. Catal.*, **2004**, *346*, 1836.
- [17] D Wang, L Yang, U Decker, M Findeisen and M. R. Buchmeiser, *Macromolecul. Rap. Commun.*, **2005**, *26*, 1757.

- [18] M Mayr, K Wurst, K-H Ongania and M. R. Buchmeiser, *Chem. Eur. J.*, **2004**, *10*, 1256.
- [19] C. C. Scarborough, M. J. W. Grady, I. A. Guzei, B. A. Gandhi, E. E. Bunel and S. S. Stahl, *Angew. Chem. Int. Ed. Eng.*, **2005**, *44*, 5269.
- [20] C. C. Scarborough, B. V. Popp, I. A. Guzei and S. S. Stahl, *J. Organomet. Chem.*, **2005**, *690*, 6143.
- [21] R. S. Simons, P. Custer, C. A. Tessier and W. J. Youngs, *Organometallics*, **2003**, *22*, 1979.
- [22] S. Díez-González and S. P. Nolan, *Coordination Chem. Rev.*, **2007**, *251*, 874.
- [23] M. Scholl, T. M. Trnka, J. P. Morgan and R. H. Grubbs, *Tetrahedron Lett.*, **1999**, *40*, 2247.
- [24] M. Iglesias, D. J. Beetstra, A. Stasch, P. N. Horton, M. B. Hursthouse, S. J. Coles, K. J. Cavell, A. Dervisi and I. A. Fallis, *Organometallics*, **2007**, *26*, 4800.
- [25] M. Iglesias, D. J. Beetstra, J. C. Knight, L. Ooi, A. Stach, S. J. Coles, L. Male, M. B. Hursthouse, K. J. Cavell, A. Dervisi and I. Fallis, *Organometallics*, **2008**, *27*, 3279.
- [26] H. M. Lee, T. Jiang, E. D. Stevens and S. P. Nolan, *Organometallics*, **2001**, *20*, 1255.
- [27] A. R. Chianese, X. Li, M. C. Janzen, J. W. Faller and R. H. Crabtree, *Organometallics*, **2003**, *22*, 1663.
- [28] F. Hanasaka, K. Fujita and R. Yamaguchi, *Organometallics*, **2005**, *24*, 3422.

- [29] Y. Zhang, D. Wang, K. Wurst and M. R. Buchmeiser, *J. Organomet. Chem.*, **2005**, 690, 5728.
- [30] K. Denk, P. Sirsch and W. A. Herrmann, *J. Organomet. Chem.*, **2002**, 649, 219.
- [31] A. P. Blum, T. Ritter and R. H. Grubbs, *Organometallics*, **2007**, 26, 2122.
- [32] M. J. Doyle and M. F. Lappert, *J. Chem. Soc., Chem. Commun.*, **1974**, 679.
- [33] Y. Yanyu, O. P. Brian and R. J. Brian, *Organometallics*, **2006**, 25, 2359.
- [34] A. R. Chianese, A. Kovacevic, B. M. Zeglis, J. W. Faller and R. H. Crabtree, *Organometallics*, **2004**, 23, 2461.
- [35] H. Schumann, G. Gielusek, J. Pickardt and N. Bruncks, *J. Organomet. Chem.*, **1979**, 172, 359.
- [36] R. H. Albrecht, R. H. Crabtree, É. Mata and E. Peris, *Chem. Commun.*, **2002**, 32.
- [37] M. Albrecht, J. R. Miecznikowski, A. Samual, J. W. Faller and R. H. Crabtree, *Organometallics*, **2002**, 21, 3596.

Chapter Four

Investigation of Catalytic Transfer Hydrogenation and Hydrogenation Reaction Using Expanded Ring NHCs

Chapter Four

Investigation of Catalytic Transfer Hydrogenation and Hydrogenation Reaction Using Expanded Ring NHCs

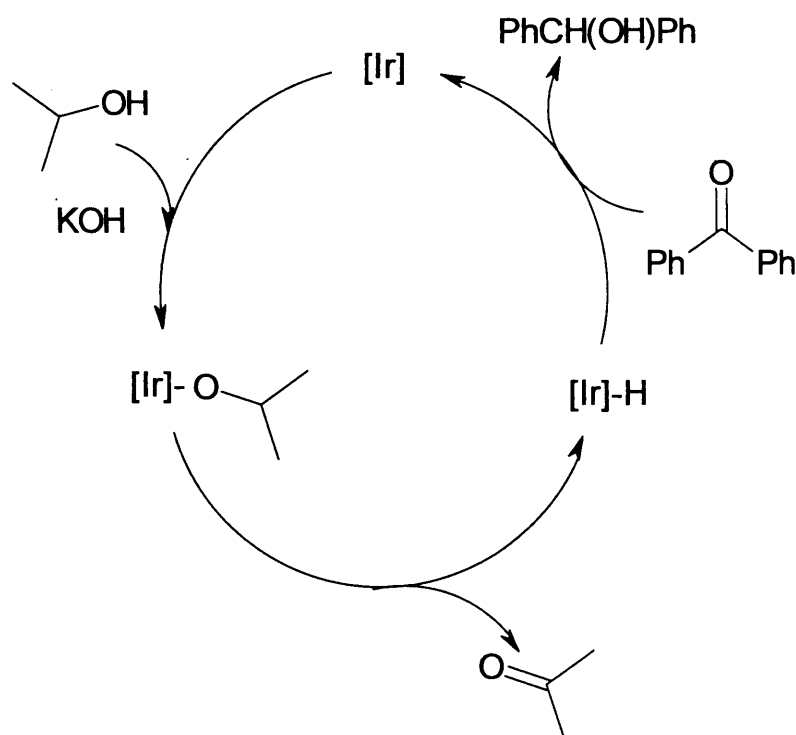
4.1. Introduction.

It is timely to investigate the impact of very basic and sterically demanding expanded ring NHCs in catalytic chemistry. The catalytic reactions chosen here are transfer hydrogenation and hydrogenation with H₂. The reduction of ketones or aldehydes is a successful approach to the synthesis of alcohols with respect to industrial applications. The most commonly used methods for the reduction of ketones are metal hydride reduction, catalytic hydrogenation and transfer hydrogenation.^[1] The latter represents a powerful strategy due to the wide number of alcohols accessible and mild reaction conditions which make this type of reaction economical.^[2-6]

Transfer hydrogenation is a variant of hydrogenation where the source of hydrogen is not molecular H₂, but a hydrogen donor in the presence of a catalyst (no need for hydrogen pressure) with potassium *tert*-butoxide or potassium hydroxide as a base used to assist deprotonation.

Transfer hydrogenation hydrogenates a double bond (C=C in olefins,^[7] N=O in nitro groups^[8] and C=O in carbonyls^[9]) by abstracting hydrogen from a proton donor source such as *iso*-propanol which is employed as a solvent (a large excess is needed in order to overcome the unfavourable equilibrium).^[10]

^{11]} The hydrogen transfer reduction of a carbonyl function, catalysed by transition metal complexes, is well documented and an accepted mechanism for catalytic transfer hydrogenation in the reduction of benzophenone, is given in Scheme 4-1 below.^[12]

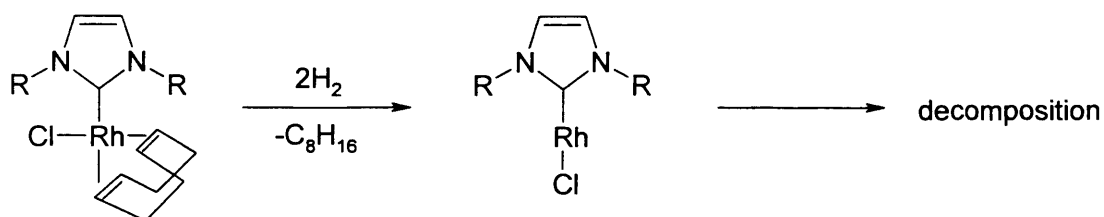


Scheme 4-1: Mechanism of transfer hydrogenation of benzophenone.

The attractiveness of this method lies in its inexpensive raw materials and simple experimental procedure which has been exploited at extensive levels of development in this area.^[9, 13, 14] It has been established that iridium

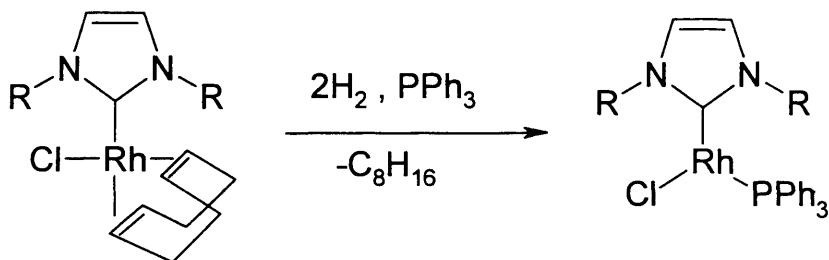
carbene complexes are more active than rhodium analogues in transfer hydrogenation.^[4, 9, 15-17]

Since the synthesis of Wilkinson's hydrogenation catalyst, $[\text{Rh}(\text{PPh}_3)_3\text{Cl}]$,^[18] a considerable number of rhodium and iridium complexes bearing bulky phosphines,^[15, 19-25] and more recently, *N*-heterocyclic carbenes, have been established as catalysts for alkene hydrogenation with molecular H_2 . Rhodium NHC complexes tested in the catalytic hydrogenation of alkenes have employed 5-membered ring monodentate NHCs as ligands and included complexes of type $[\text{Rh}(\text{NHC})(\text{CO})_2\text{X}]$ and $[\text{Rh}(\text{NHC})(\text{COD})\text{Cl}]$. The former complexes were found to be inactive because of unfavourable electronic effects: the strong donor ability of NHCs make the metal more electron-rich, resulting in the strengthening of the M-CO bond through back-bonding. The latter complexes are not effective for hydrogenation due to decomposition during the reaction. Herrmann *et al.* have proposed that, due to the presumably high stability of the $\text{C}_{\text{NHC}}\text{-M}$ bond, the olefinic chelating ligand (COD) is reduced to an alkane under reaction conditions, forming a linear Rh intermediate (Scheme 4-2). The resulting complex is unstable and decomposes to give rhodium particles.^[18, 22]



Scheme 4-2: Possible decomposition pathway of $[\text{Rh}(\text{NHC})(\text{COD})\text{Cl}]$ complexes.

Addition of PPh_3 to the reaction mixture stabilises the active species by forming three coordinate complexes (Scheme 4-3), thus preventing decomposition and improving activity.^[22, 26]



Scheme 4-3: Stabilisation of the active species.

The use of the NHC analogues of Crabtree's catalyst, $[\text{Ir}(\text{COD})(\text{PCy}_3)(\text{Py})]\text{PF}_6$,^[27] in which one or both donor ligands were replaced by NHCs, has also been investigated.^[7]

This chapter focuses on the catalytic performance of functionalised, expanded ring NHC complexes of rhodium and iridium (Figure 4-1) in catalytic transfer hydrogenation and hydrogenation reactions. Some comparisons are made between 5-, 6- and 7-membered ring systems. The large ring NHCs are shown to provide a unique catalytic performance, possibly due to enhanced catalyst stability.

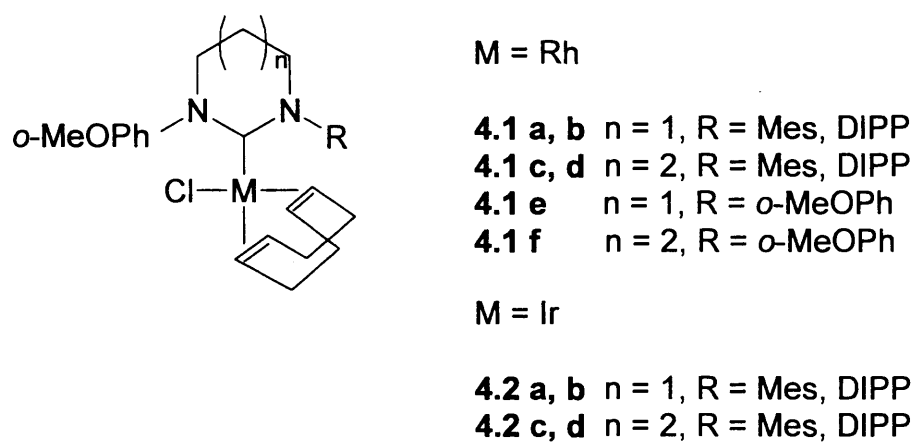
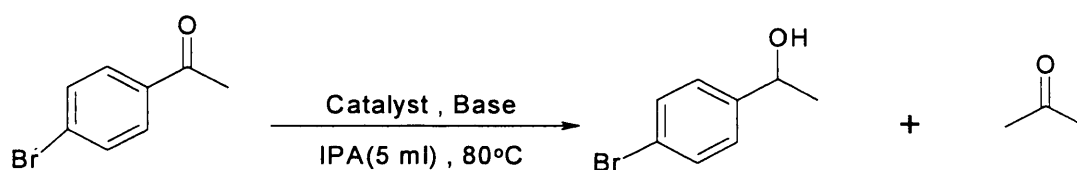


Figure 4-1: Carbene complexes which were used in catalytic transfer hydrogenation and hydrogenation reactions.

4.2. Results and Discussion.

4.2.1. Catalytic Transfer Hydrogenation of Ketones.

Catalytic transfer hydrogenation was examined using *iso*-propanol as a hydrogen source (Scheme 4-4). The carbene complexes, which were used in the catalytic hydrogenation are shown in Figure 4-1.



Scheme 4-4: Catalytic hydrogen transfer of 4-bromoacetophenone.

The activity of carbene complexes was tested at various catalyst concentrations. This allowed a direct comparison between Rh(I) and Ir(I) complexes of expanded carbenes and also the opportunity to study the effects of alkyl and aromatic carbene *N*-substituents. The results of the catalytic tests are presented in Table 4-1 and 4-2 (each reaction has been repeated several times to demonstrate reproducibility). The Ir(I) complexes catalyse the reduction of 4-bromoacetophenone at 80 °C via hydrogen transfer from *iso*-propanol with potassium *tert*-butoxide (Table 4-1) or potassium hydroxide (Table 4-2) as the base promoter. The Rh(I) complexes of saturated carbenes with aromatic *N*-substituents show no activity whatsoever towards transfer hydrogenation under the previously described conditions.^[28, 29]

As presented in the tables below, all of the Ir (I) catalysts showed excellent catalytic activity towards transfer hydrogenation with no significant change when the catalyst loading was reduced to 0.001 mmol. When 0.0001 mmol of the catalyst was used, the catalyst still showed good activity with a small drop in conversion. The function of the base in the transfer hydrogenation reaction is to abstract a proton from the solvent, *iso*-propanol, promoting the formation of acetone and converting the substrate to the corresponding alcohol. Table 4-1 shows that potassium *tert*-butoxide is a slightly more efficient promoting agent than potassium hydroxide. Kanger and co-workers have previously shown the importance of the type of base added and the levels required.^[30, 31]

Table 4-1: Reaction conditions: substrate 4-bromoacetophenone: 1.0 mmol; KO^tBu: 0.1 mmol; ⁱPrOH: 5ml; 80 °C; 24 h. Conversion calculated from ¹H NMR.

Catalyst	Concentration (mmol)	Conversion (%)	TON
4.2a	0.01	100	100
	0.001	99	990
	0.0001	71	7100
4.2b	0.01	100	100
	0.001	99	990
	0.0001	73	7300
4.2c	0.01	100	100
	0.001	99	990
	0.0001	96	9600
4.2d	0.01	100	100
	0.001	99	990
	0.0001	97	9700
4.1a	0.01	0	0
4.1b	0.01	0	0
4.1c	0.01	0	0
4.1d	0.01	0	0

Table 4-2: Reaction conditions: substrate 4-bromoacetophenone: 1.0 mmol; KOH: 0.1 mmol; ¹PrOH: 5ml; 80 °C; 24 h. Conversion calculated from ¹H NMR.

Catalyst	Concentration (mmol)	Conversion (%)	TON
4.2c	0.01	100	100
	0.001	99	990
	0.0001	95	9500
4.2d	0.01	100	100
	0.001	99	990
	0.0001	96	9600

4.2.1.1. Reaction Timescale.

As well as the risks to catalyst stability posed by higher temperatures, concerns have been raised regarding longer reaction times. Reactions were monitored *in situ* by removing small aliquots (0.1 ml) from the reaction mixture at 5 minute intervals. In order to evaluate the differences in catalytic performance carbene complexes **4.2c** and **4.2d** were tested using a catalyst loading of (0.01mmol) and a temperature of 80 °C. The yield for the transfer hydrogenation of 4-bromoacetophenone was monitored over a period of 3 hours by taking samples at regular intervals and measuring the product by GC. The results are presented in Figures 4-2 and 4-3 below. It is evident

from the diagrams that the curves do not follow a sigmoidal shape, and furthermore, there is no induction period apparent. This would suggest that metal nanoparticles are not forming and it is well-defined molecular species that is catalysing the reaction.

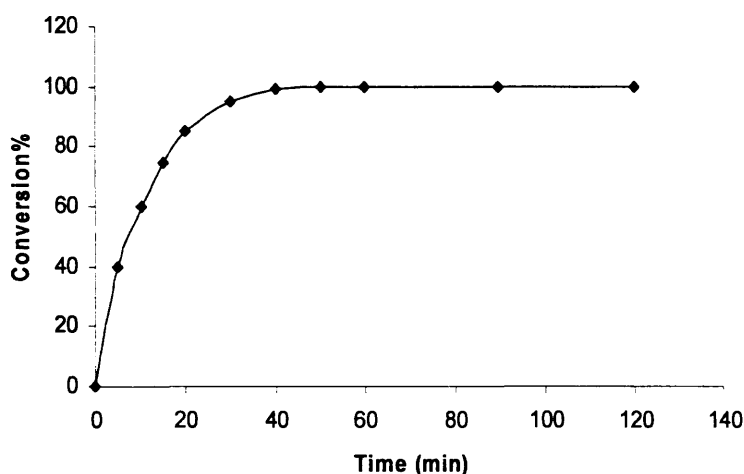


Figure 4-2: Time dependence of the transfer hydrogenation reaction with 1.0 mmol of 4-bromoacetophenone using 0.01 mmol of catalyst **4.2c**, 0.1 mmol KO^tBu: and ⁱPrOH: 5 ml at 80 °C. Conversion calculated from GC.

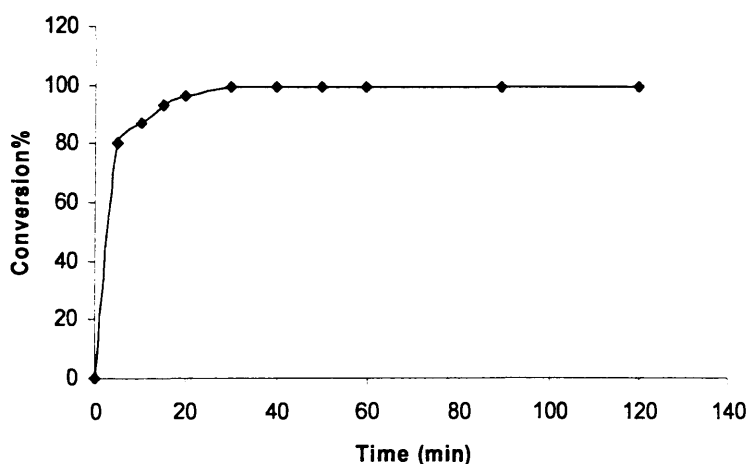
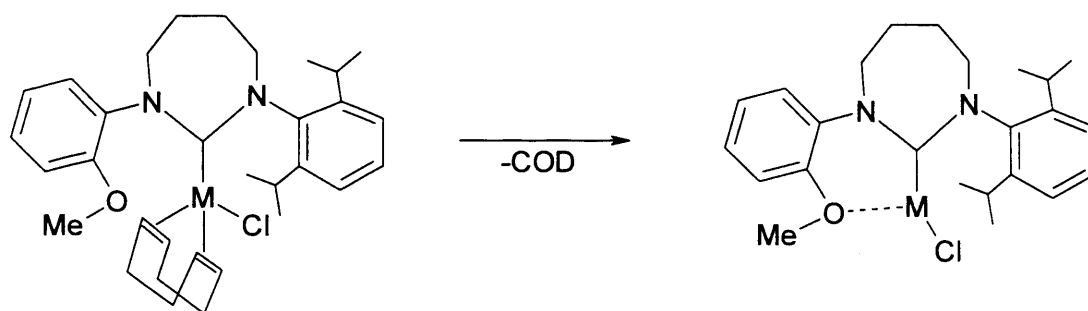


Figure 4-3: Time dependence of the transfer hydrogenation reaction with 1.0 mmol of 4-bromoacetophenone using 0.01 mmol of catalyst **4.2d**, 0.1 mmol KO^tBu: and ⁱPrOH: 5 ml at 80 °C. Conversion calculated from GC.

As shown in the diagrams, both catalysts **4.2c** and **4.2d** appear to be highly efficient in the transfer hydrogenation of 4-bromoacetophenone to 1-(4-bromobenzene) ethanol, each giving over 95% conversion in less than 30 minutes. However, **4.2d** (80% conversion in 5 minutes) gave rise to a more efficient catalyst than **4.2c**, which took 20 minutes for a similar conversion. The catalytic performance of these large ring NHC-Ir complexes appears to be significantly better than those reported by Crabtree,^[9] Hahn^[32] and Peris^[33] for the 5-membered ring systems. The consequential steric properties of the large ring NHCs resulting from their very large NCN angles, may have played an important role in the improved performance of these systems. It is evident that complex **4.2d** is significantly more sterically hindered than **4.2c**, because of the presence of the bulky DIPP moiety, which appears to lead to the catalyst generated from **4.2d** being more active. In addition, weak interaction between the *o*-methoxy-substituent and the metal centre may also help to stabilise the highly coordinatively unsaturated intermediate, which is believed to be generated during catalysis (Scheme 4-5).



Scheme 4-5: Formation of possible active catalytic intermediate.

4.2.1.2. Investigation of Catalyst Stability.

An extended catalytic experiment was conducted in order to establish the limits of the catalyst's efficiency and stability. Due to the encouraging results obtained for 4-bromoacetophenone, this substrate was chosen for this study. Catalyst **4.2d** was used and the conditions employed were identical to those used in previous screening procedures. The entire reaction was monitored *insitu* by removing aliquots (0.1 ml) from the reaction mixture at 5 minutes intervals. Following initiation of the reaction, after 20 minutes, and then after 40 minutes additional aliquots (1 mmol each time) of 4-bromoacetophenone were added to the reaction mixture. Figure 4-4 shows the continuing excellent activity of catalyst **4.2d** even after of two additional aliquots of substrate had been added. Catalyst activity was maintained with little diminution in catalyst performance. The small drop in performance observed may be a consequence of the change in reaction mixture caused by product build-up in solution. It is evident that the catalyst shows excellent stability, probably resulting from the coordination of the *o*-methoxy moiety during catalysis (Scheme 4-5), and also from the steric protection provided by the bulky DIPP group.

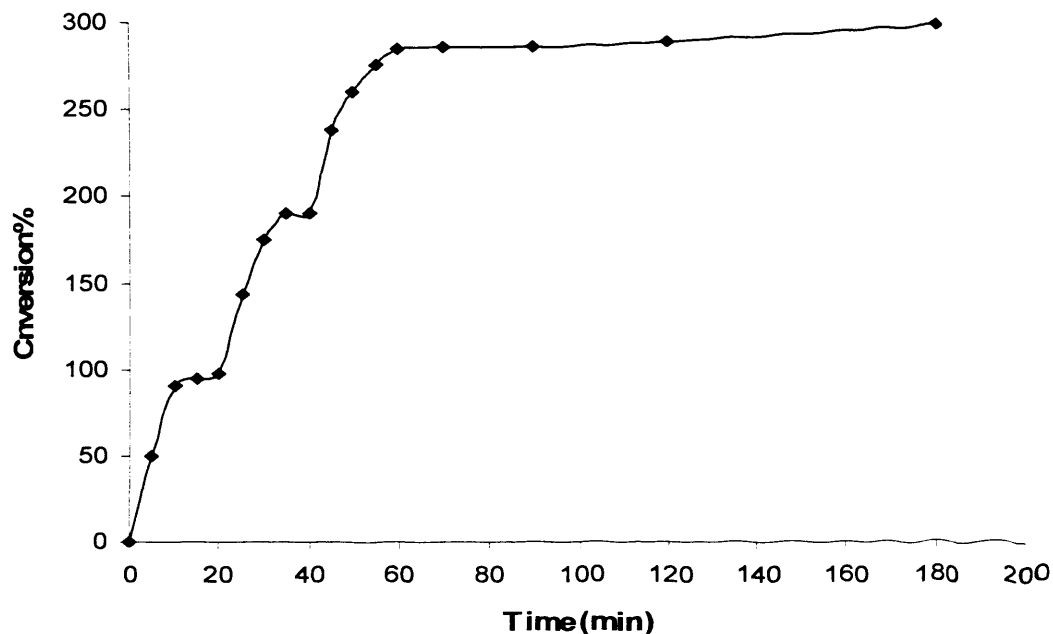


Figure 4-4: Influence of catalyst loading by using 3.0 mmol of 4-bromoacetophenone, 0.01 mmol of catalyst **4.2d**, 0.1 mmol KO^tBu : and $^i\text{PrOH}$: 5 ml at 80 °C. Conversion calculated by GC analysis.

4.2.1.3. Temperature Dependence.

In the transfer hydrogenation of 4-bromoacetophenone to 1-(4-bromobenzene) ethanol a chiral centre is generated (Scheme 4-4). Evidence in the literature suggests that enantioselectivity in transfer hydrogenation is improved at lower temperatures.^[34, 35] Consequently, although the catalysts investigated in this study are not chiral, studies were undertaken to investigate the temperature dependence of the reaction to reveal whether milder operating conditions might be feasible. Figure 4-5 summarises the findings.

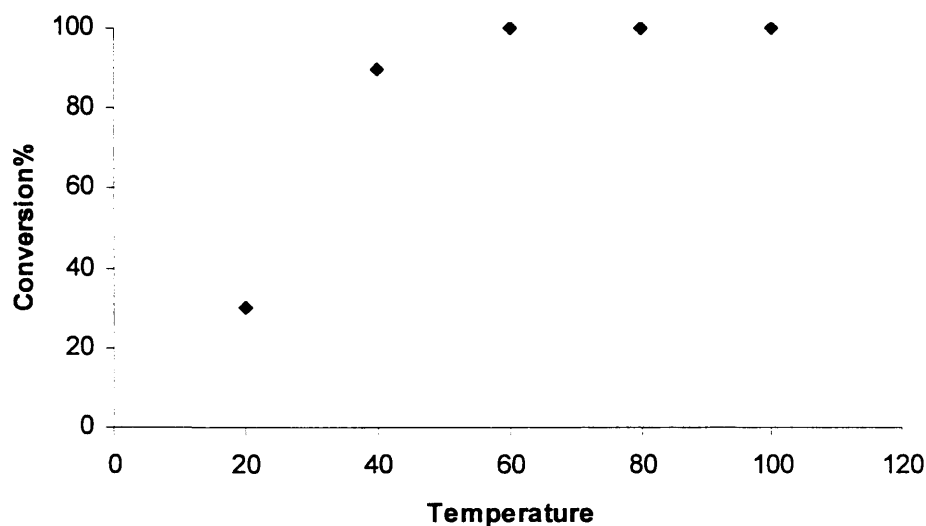


Figure 4-5: Transfer hydrogenation of 1.0 mmol of 4-bromoacetophenone at various temperatures using catalyst **4.2d**: 0.01 mmol, KO^tBu: 0.1 mmol and ⁱPrOH: 5 ml in 24 h. Conversion calculated from ¹H NMR.

Figure 4-5 indicates that whilst operating under iso-propanol reflux temperature (80 °C) brings about rapid reaction and quantitative yield, a temperature as low as 40 °C can be used and still give a yield above 90% in a 24 hours period. This could be a major advantage in some application, particularly if a chiral catalyst based on large ring structure was developed.

4.2.1.4. Catalytic Performance with Different Substrates.

Acetophenone and cyclohexanone were tested under identical conditions. The results are summarised in Table 4-3.

Table 4-3: Reaction conditions: substrate: 1.0 mmol; base: 0.1 mmol; ⁱPrOH: 5ml; 80 °C; 24 h. Conversion calculated from ¹H NMR.

Substrate	Catalyst	Concentration (mmol)	Base	Conversion (%)	TON		
Acetophenone	4.2c	0.01	KO ^t Bu	100	100		
		0.01	KOH	100	100		
		0.001	KO ^t Bu	99	990		
		0.001	KOH	98	980		
		0.0001	KO ^t Bu	83	8300		
		0.0001	KOH	80	8000		
	4.2d	0.01	KO ^t Bu	100	100		
		0.01	KOH	100	100		
		0.001	KO ^t Bu	99	990		
		0.001	KOH	98	980		
		0.0001	KO ^t Bu	86	8600		
		0.0001	KOH	81	8100		
		Cyclohexanone	4.2c	0.01	KO ^t Bu	100	100
				0.01	KOH	100	100
0.001	KO ^t Bu			99	990		
0.001	KOH			99	990		
0.0001	KO ^t Bu			98	9800		
0.0001	KOH			97	9700		
4.2d	0.01		KO ^t Bu	100	100		
	0.01		KOH	100	100		
	0.001		KO ^t Bu	99	990		
	0.001		KOH	99	990		
		0.0001	KO ^t Bu	99	9900		
		0.0001	KOH	98	9800		

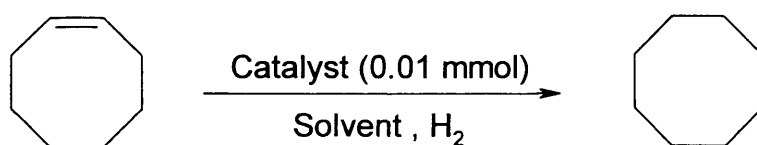
The result revealed some interesting details regarding the influence of the substrate on the catalytic activity. A comparison of 4-bromoacetophenone (Table 4-1 and 4-2) and acetophenone (Table 4-3) shows that the electron-withdrawing substituent appears to assist the hydrogenation process and delivers a quantitative yield, even with the use of a very low concentration of catalyst. Results achieved by Xiao *et al.* when testing their ligand, concur to some degree. Their catalyst exhibited a similar response to electronic effects, with substrates containing electron-withdrawing groups showing a greater propensity to react.^[36] This observation was also confirmed by Adolfsson *et al.*^[37]

4.2.2. Catalytic Hydrogenation with Molecular Hydrogen.

As mentioned in the introduction of this chapter where $[\text{Rh}(\text{NHC})(\text{COD})\text{Cl}]$ complexes are used as catalysts in the catalytic hydrogenation of alkenes, the active species involved is assumed to be a linear NHC-Rh-Cl. Due to the lack of stabilisation, this linear complex generally decomposes to rhodium particles. Therefore, a ligand capable of providing better steric protection of the metal centre, such as an expanded-ring carbene, would enhance the catalytic performance of this type of complex by avoiding the decomposition of the active species.

As previously mentioned, the effect of opening up the NCN angle in the expanded carbenes is to twist the *N*-substituents towards the metal centre, effectively blocking two faces of the metal coordination sphere.

Consequently, the use of expanded carbenes in catalytic hydrogenation should render active species more resistant to decomposition. Weak-donor, functionalised large ring ligands may be expected to add a further benefit by stabilising unsaturated intermediates through weak coordination to the metal centre. To test the effect of a weak donor group on catalytic performance, the *o*-methoxyphenyl-functionalised complexes (Figure 4-1) were investigated as pre-catalysts in the hydrogenation of cyclooctene (Scheme 4-6).



Scheme 4-6: Catalytic hydrogenation of cyclooctene.

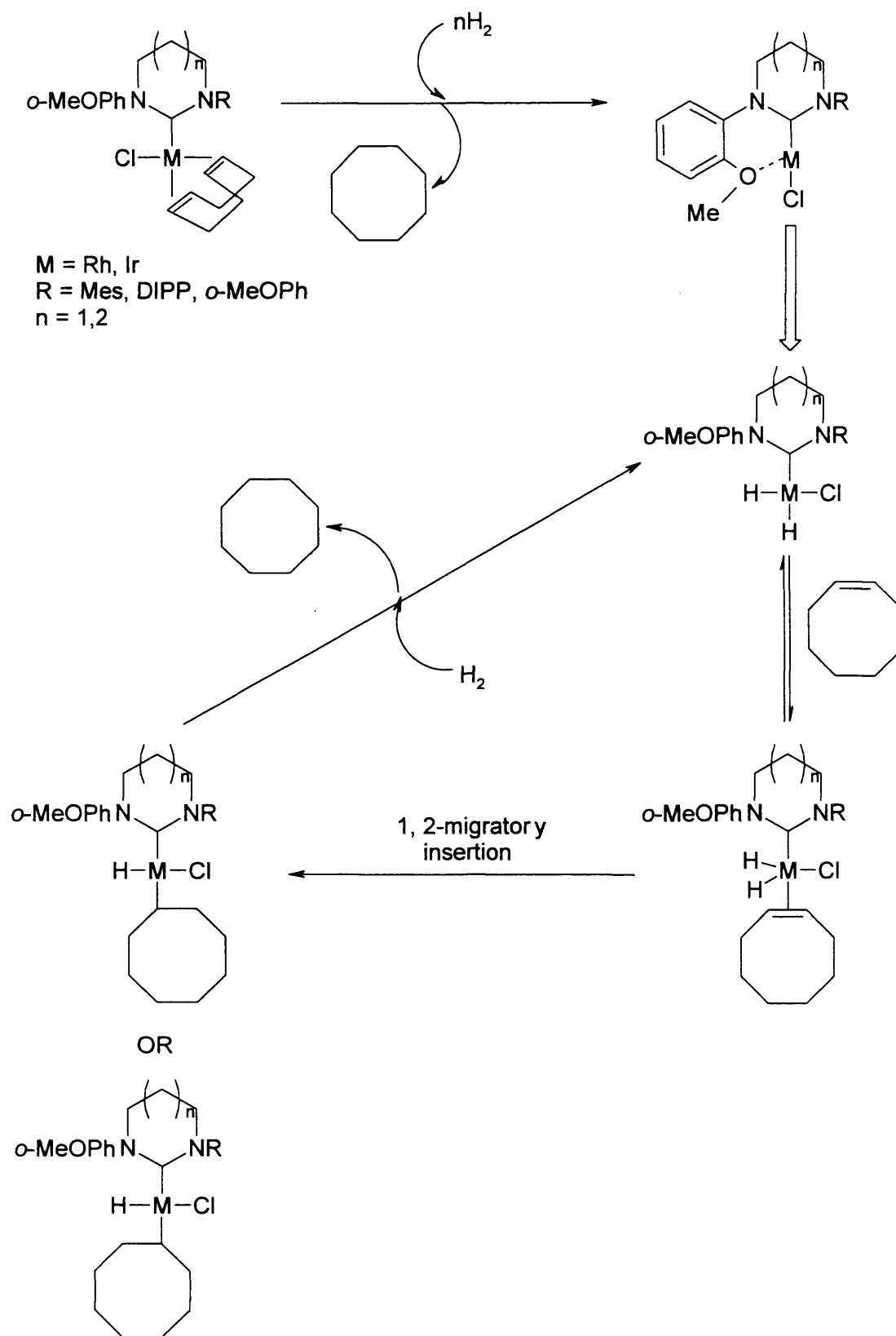
Table 4-4: Catalytic hydrogenation of cyclooctene. Reaction conditions: 1.0 mmol of alkene; 0.01 mmol catalyst; 5 ml of EtOH or 10 ml of DCE; 24 h; ambient temperature. Conversion calculated from GC.

Catalyst	P(H ₂) [atm]	Solvent	Conversion (%)
4.1 a-f	3.5	EtOH	>99
4.1 a-f	1	EtOH	>99
4.1 c	3.5	DCE	39
4.1 c	1	DCE	28
4.1 d	3.5	DCE	35
4.1d	1	DCE	26
4.1 f	3.5	DCE	36
4.1 f	1	DCE	26
4.2 a-d	3.5	EtOH	>99
4.2 a-d	1	EtOH	>99

From the results summarized in Table 4-4, it can be concluded that 6- and 7-membered *N*-functionalised carbenes show excellent activity, giving high yields of cyclooctane. Using ethanol as a solvent and at 0.01 mmol (1 mol%) catalyst loading, complete substrate conversion was observed, both at 1 and 3.5 atm of hydrogen pressure. Notably, no significant difference in activity was observed between the 6- and 7-membered carbene complexes under these conditions which are consistent with the fact that the difference in NCN angle for the two classes of NHC is small. The significantly enhanced catalytic performance using expanded ring carbenes as ligands, compared with the analogous 5-membered ring NHCs, indicates that the active species could be a linear structure of the type NHC-M-Cl (M = Rh, Ir), as previously proposed. Such a structure would be stabilised by the sterically demanding large ring carbenes, and in the case of the *o*-methoxyphenyl substituent, by weak chelation of the ligand. The reactive intermediate would then readily undergo oxidative addition with molecular hydrogen.^[22] A mechanism based on the work reported by Buriak *et al.*^[15, 38] on complexes of general formula [Ir(NHC)(COD)L]X is depicted in Scheme 4-7.

Chapter Four

Investigation of catalytic transfer hydrogenation and hydrogenation reaction using expanded ring NHCs



Scheme 4-7: Proposed mechanism for the hydrogenation of cyclooctene.

4.2.2.1. Reaction Timescale.

The reaction rate was monitored by taking samples of the reaction mixture every 20 minutes and determining the conversion by GC. Monitoring the reaction with catalyst **4.1d** (0.01 mmol), 50% mol conversion was observed after 60 minutes under 1 atm of hydrogen and in less than 30 minutes for 3.5 atm of H₂ pressure (Figure 4-6 and 4-7). Reaction was complete after five hours by using catalyst **4.1d** with 1 atm of H₂ pressure and after only two hours with 3.5 atm of H₂ pressure. In contrast to the non-functionalised NHC complexes,^[28, 29, 39] no catalyst decomposition was observed when using complexes **4.1a-f** and **4.2a-d**. The catalyst solution remained bright yellow throughout the reaction. Furthermore, the non-sigmoidal shape of the reaction curve and the lack of an induction period would also indicate a stable molecular catalyst.

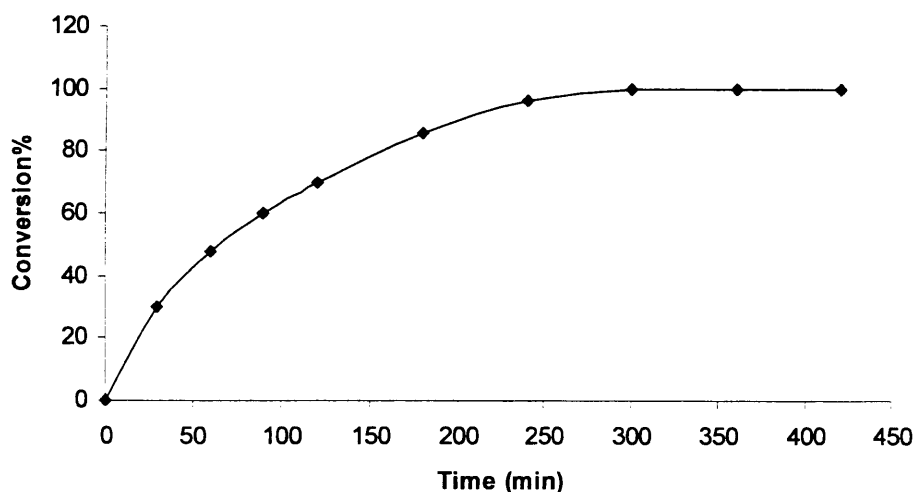


Figure 4-6: Time dependence of the hydrogenation of 1.0 mmol of cyclooctene using 0.01 mmol of catalyst **4.1d** with EtOH (5 ml) and H₂ (1 atm) at ambient temperature. Conversion calculated from GC.

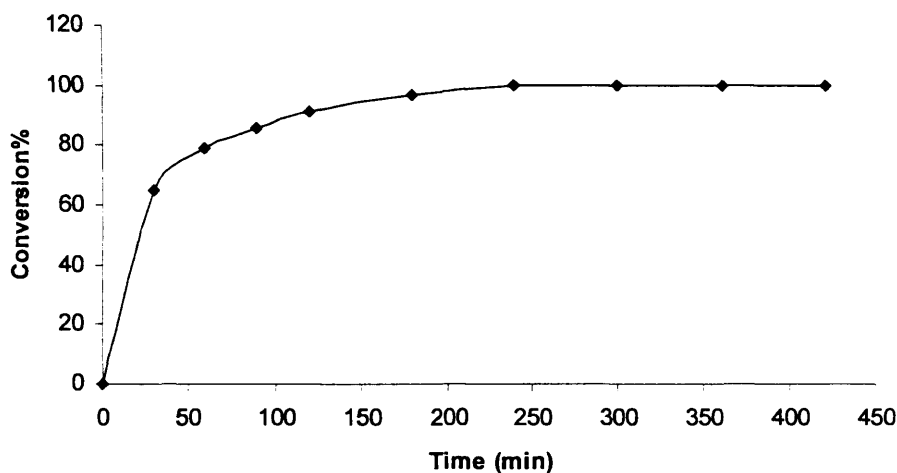


Figure 4-7: Time dependence of the hydrogenation of 1.0 mmol of cyclooctene using 0.01 mmol of catalyst **4.1d** with EtOH (5 ml) and H₂ (3.5 atm) at ambient temperature. Conversion calculated by GC system.

The iridium complexes **4.2a-d** were also tested in the hydrogenation of cyclooctene under the same conditions used for the rhodium system (Table 4-4). A 50% conversion using catalyst **4.2d** was observed at 160 minutes for 1 atm of H₂ (Figure 4-8) and at 70 minutes for 3.5 atm (Figure 4-9). Complete conversion using catalyst **4.2d** was observed in 6 hours for 3.5 atm (Figure 4-9). These results show that the Ir complexes generate a less active system than that of rhodium **4.1d**. This is in contrast with results reported in the literature, where iridium-NHC systems normally form more active catalysts than their rhodium analogues in the hydrogenation of non-functionalised olefins.^[15]

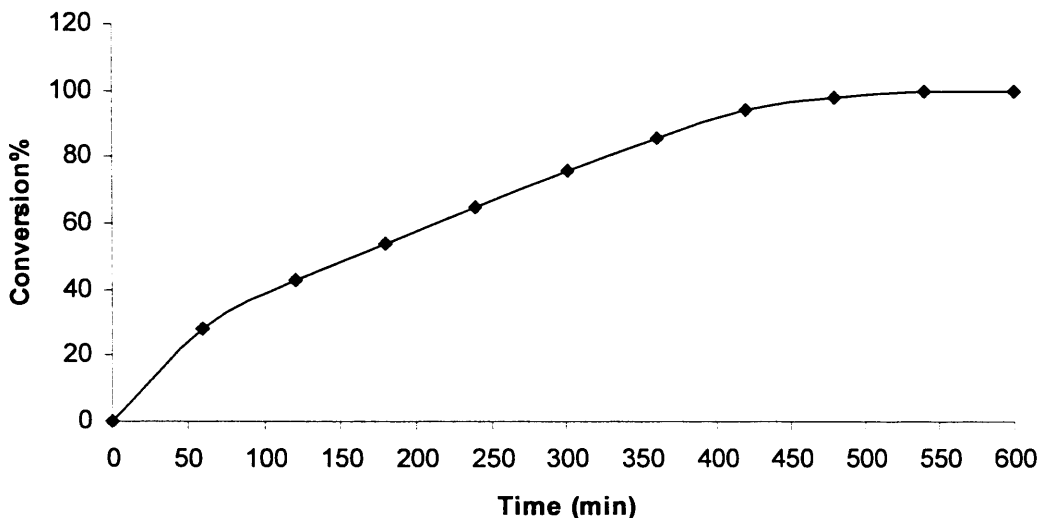


Figure 4-8: Time dependence of the hydrogenation of 1.0 mmol of cyclooctene using 0.01 mmol of catalyst **4.2d** with EtOH (5 ml) and H₂ (1 atm) at ambient temperature. Conversion calculated from GC.

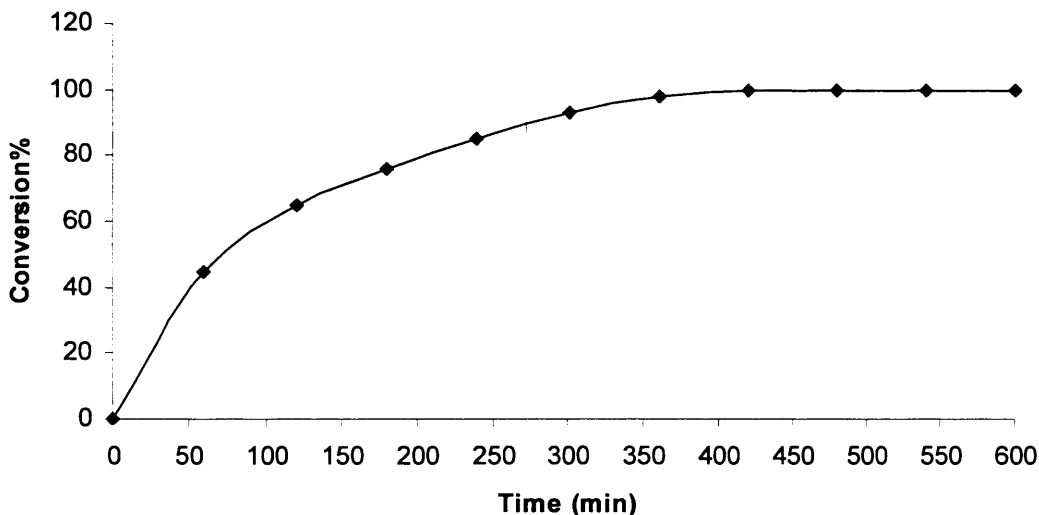


Figure 4-9: Time dependence of the hydrogenation of 1.0 mmol of cyclooctene using 0.01 mmol of catalyst **4.2d** with EtOH (5 ml) and H₂ (3.5 atm) at ambient temperature. Conversion calculated from GC.

4.2.2.2. Catalytic Hydrogenation of Alternative Substrate.

To extend the range of alkenes tested, 1-methylstyrene and 1-methylcyclohexene were also hydrogenated using the catalyst **4.1a-d** (Table 4-5). As was the case for 1-cyclooctene, efficient conversion was observed in ethanol for the less sterically hindered substrate 1-methylstyrene. In the case of the more sterically crowded substrate 1-methylcyclohexene, the most active catalyst, was formed with the 6-membered NHC complexes **4.1a,b**. Changing the solvent to dichloromethane again dramatically decreased the activity of these rhodium catalysts.

Table 4-5: Catalytic hydrogenation of alkenes. Reaction conditions: 1.0 mmol of alkene; 0.01 mmol catalyst; 5 ml of EtOH or 10 ml of DCM; $P(H_2) = 3.5$ atm, 24 h; ambient temperature. Conversion calculated from GC.

Substrate	Catalyst	Solvent	Conversion (%)
1-methylstyrene	4.1a-b	EtOH	>99
	4.1c	EtOH	97
	4.1d	EtOH	96
1-methyl-cyclohexene	4.1a	EtOH	89
	4.1b	EtOH	81
	4.1c	EtOH	53
	4.1d	EtOH	46
	4.1a	DCM	31
	4.1d	DCM	22
	4.1c	DCM	20
	4.1d	DCM	13

4.3. Experimental.

General Remarks.

All air-sensitive experiments were performed under a nitrogen atmosphere. Solvents were distilled from the appropriate drying agent under nitrogen atmosphere immediately prior to use following standard literature methods.

Typical Transfer Hydrogenation Protocol.

Ketone (1.0 mmol), base (0.1 mmol) and Ir complexes (0.01 mmol) were charged to a 50 ml Schlenk. The solids were degassed and *iso*-propanol (5ml) subsequently added under a nitrogen atmosphere. The resulting orange solution was refluxed (80 °C) for 24 hours. The solvents were then evaporated under vacuum and the % conversion determined by ¹H NMR.

General Protocol for Catalytic Hydrogenation.

The catalyst (0.01 mmol) and the substrate (1 mmol) were dissolved in 5 ml ethanol or 10 ml dichloroethane in an autoclave. The autoclave was put under vacuum and finally pressurised with hydrogen (1 or 3.5 atm). The solution was stirred at ambient temperature and at the end of the reaction the yield was calculated from GC.

Description of GC/MS Analysis.

Yields and substrate identities were determined by GC-MS analysis of reaction mixtures using an Agilent Technologies 6890N GC system with an Agilent Technologies 5973 inert MS detector with MSD. Column: Agilent 190915-433 capillary, 0.25 mm x 30 m x 0.25 μm . Capillary: 30 m x 250 μm x 0.25 μm nominal. Initial temperature at 50 $^{\circ}\text{C}$, held for 4 minutes; ramp 5 $^{\circ}\text{C}$ /minute; next 100 $^{\circ}\text{C}$; ramp 10 $^{\circ}\text{C}$ /minute next 240 $^{\circ}\text{C}$ and held for 15 minutes. The temperature of the injector and the detector were held at 240 $^{\circ}\text{C}$. The retention times for analyses are given in minutes.

4.4. References.

- [1] S. Enthaler, R. Jackstell, B. Hagemann, K. Junge, G. Erre and B. Matthias, *J. Organomet. Chem.*, **2006**, *691*, 4652.
- [2] S. Gladiali and E. Alberico, *Chem. Soc. Rev.*, **2006**, *35*, 226.
- [3] G. Zassionovich, G. Mestroni and S. Gladiali, *Chem. Rev.*, **1992**, *51*, 1051.
- [4] R. Noyori and S. Hashiguchi, *Acc. Chem. Res.* **1997**, *30*, 97.
- [5] H. U. Blaser, C. Malan, B. Pugin, F. Spindler and M. Studer, *Adv. Synth. Catal.*, **2003**, *345*, 103.
- [6] S. Gladiali, G. Mestroni, M. Beller and C. Bolm, *Transition Metals for Organic Synthesis, second ed.*, Wiley-VCH, Weinheim, **2004**, 145.

- [7] H. M. Lee, T. Jiang, E. D. Stevens and S. P. Nolan, *Organometallics*, **2001**, *20*, 1255.
- [8] C. Wang, C. Fu and S. Liu, *Inorg. Chem.*, **2007**.
- [9] M. Albrecht, J. R. Miecznikowski, A. Samuel, J. W. Faller and R. H. Crabtree, *Organometallics*, **2002**, *21*, 3596.
- [10] M. J. Palmer and M. Wills, *Tetrahedron: Asymmetry*, **1999**, *10*, 2045.
- [11] H. Adkins, R. M. Eloffson, A. G. Rossow and C. C. Robinson, *J. Am. Chem. Soc.*, **1949**, *71*, 3622.
- [12] C. Sauzzo and M. Lemaie, *Adv. Synth. Catal.*, **2002**, *344*, 915.
- [13] A. T. Normand and K. J. Cavell, *Eur. J. Inorg. Chem.*, **2008**, 2781.
- [14] S. Hashiguchi, A. Fujii, T. Takehara and R. Noyori, *J. Am. Chem. Soc.*, **1995**, *117*, 7562.
- [15] L. D. Vazquez-Serrano and B. T. Owens, *Inorg. Chim. Acta.*, **2006**, *359*, 2786.
- [16] D. E. linn and G. Halpern, *J. Am. Chem. Soc.*, **1987**, *109*, 2969.
- [17] G. Zassionovich, G. Mestroni and S. Gladiali, *Chem. Rev.*, **1992**, *92*, 1051.
- [18] J. A. Osborn, F. H. Jardine, J. F. Young and G. Wilkinson, *J. Chem. Soc.*, **1966**, 1711.
- [19] D. A. Evans and A. H. Hoveyda, *J. Am. Chem. Soc.*, **1992**, *114*, 6671.
- [20] G. Stork and D. E. Kahne, *J. Am. Chem. Soc.*, **1983**, *105*, 1072.
- [21] R. H. Crabtree and M. W. Davis, *Organometallics*, **1983**, *2*, 681.
- [22] W. A. Herrmann, G. D. Frey, E. Herdtweck and M. Steinbecka, *Adv. Synth. Catal.*, **2007**, *349*, 1677.

- [23] D. P. Allen, C. M. Crudden, L. A. Calhoun and R. Wang, *J. Organomet. Chem.*, **2004**, *689*, 3203.
- [24] D. P. Allen, C. M. Crudden, L. A. Calhoun, R. Wang and A. Decken, *J. Organomet. Chem.*, **2005**, *690*, 5736.
- [25] W. A. Herrmann, D. Baskakov, E. Herdtweck, S. D. Hoffmann, T. Bunlaksananusorn, F. Rampf and L. Rodefeld, *Organometallics*, **2006**, *25*, 2449.
- [26] A. Neveling, G. R. Julius, S. Cronje, C. Esterhuysen and H. G. Raubenheimer, *J. Chem. Soc. Dalton Trans.*, **2005**, 181.
- [27] R. H. Crabtree, *Acc. Chem. Res.*, **1979**, *12*, 331.
- [28] M. Iglesias, D. J. Beetstra, A. Stasch, P. N. Horton, M. B. Hursthouse, S. J. Coles, K. J. Cavell, A. Dervisi and I. A. Fallis, *Organometallics*, **2007**, *26*, 4800.
- [29] M. Iglesias, D. J. Beetstra, J. C. Knight, L. Ooi, A. Stach, S. J. Coles, L. Male, M. B. Hursthouse, K. J. Cavell, A. Dervisi and I. Fallis, *Organometallics*, **2008**, *27*, 3279.
- [30] N. Debono, M. Besson, C. Pinel and L. Djakovitch, *Tetrahedron Lett.*, **2004**, *45*, 2237
- [31] K. Kriis, T. Kanger and M. Lopp, *Tetrahedron Lett.*, **2004**, *15*, 2689.
- [32] H. Turkmen, T. Pape, E. Hahn and B. Cetinkaya, *Organometallics*, **2008**, *27*, 571.
- [33] E. Mas-Marza, M. Sanau and E. Peris, *Inorg. Chem.*, **2005**, *44*, 9961.
- [34] W. He, P. Liu, B. L. Zhang, X. L. Sun and S. Y. Zhang, *Appl. Organomet. Chem.*, **2006**, *20*, 328.

Chapter Four

Investigation of catalytic transfer hydrogenation and hydrogenation reaction using expanded ring NHCs

[35] Y. Jiang, Q. Jiang, G. Zhu and X. Zhang, *Tetrahedron Lett.*, **1997**, *38*, 6565.

[36] X. Li, W. Chen, W. Hems, F. King and J. Xiao, *Tetrahedron Lett.*, **2004**, *45*, 952.

[37] I. M. Pastor, P. Vastila and H. Adolfsson, *Chem. Eur. J.*, **2003**, *9*, 4037.

[38] L. D. Vazquez-Serrano, B. T. Owens and J. M. Buriak, *Chem. Commun.*, **2002**, 2518.

[39] A. Binobaid, M. Iglesias, D. Beetstra, B. Kariuki, A. Dervisi, I. Fallis and K. J. Cavell, *Dalton Trans.*, **2009**, 7099.

Publication from this Thesis

**Expanded ring and functionalised expanded ring *N*-heterocyclic
carbenes as ligands in catalysis.**

Abeer Binobaid, Manuel Iglesias, Dirk J. Beetstra, Benson Kariuki, Athanasia
Dervisi,* Ian A. Fallis* and Kingsley J. Cavell*

Dalton Trans., 2009, Issue 35, 7099 - 7112

Tables of Bond Distances and Angles

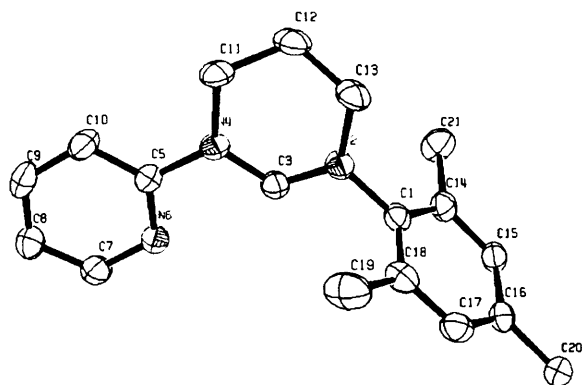


Table A.1: Crystal data and structure refinement for (6-Py-Mes).

Identification code	kjc0715	
Empirical formula	C ₁₈ H ₂₂ B F ₄ N ₃	
Formula weight	367.20	
Temperature	150(2) K	
Wavelength	0.71073 Å	
Crystal system	Monoclinic	
Space group	P2 ₁ /c	
Unit cell dimensions	a = 13.1180(2) Å	a = 90°.
	b = 17.8690(6) Å	β = 104.657(2)°.
	c = 8.0030(4) Å	γ = 90°.
Volume	1814.90(11) Å ³	
Z	4	
Density (calculated)	1.344 Mg/m ³	
Absorption coefficient	0.108 mm ⁻¹	
F(000)	768	
Crystal size	0.30 x 0.30 x 0.20 mm ³	
Theta range for data collection	2.94 to 27.48°.	
Index ranges	-17 ≤ h ≤ 15, -23 ≤ k ≤ 21, -	
	10 ≤ l ≤ 10	
Reflections collected	14070	
Independent reflections	4124 [R(int) = 0.1454]	
Completeness to theta = 27.48°	99.3 %	
Absorption correction	Empirical	
Max. and min. transmission	0.9786 and 0.9682	

Refinement method	Full-matrix least-squares on F ²
Data / restraints / parameters	4124 / 0 / 239
Goodness-of-fit on F ²	1.038
Final R indices [I > 2σ(I)]	R1 = 0.0732, wR2 = 0.1866
R indices (all data)	R1 = 0.1176, wR2 = 0.2152
Extinction coefficient	0.018(4)
Largest diff. peak and hole	0.465 and -0.348 e.Å ⁻³

Table A. 2: Bond lengths (Å) for (6-Py-Mes).

C1 . N2 . 1.455(4)	C14 . C15 . 1.392(5)
C1 . C14 . 1.392(5)	C14 . C21 . 1.506(5)
C1 . C18 . 1.385(5)	C15 . C16 . 1.389(5)
N2 . C3 . 1.307(4)	C15 . H151 . 0.925
N2 . C13 . 1.482(4)	C16 . C17 . 1.378(5)
C3 . N4 . 1.338(4)	C16 . C20 . 1.524(5)
C3 . H31 . 0.943	C17 . C18 . 1.386(5)
N4 . C5 . 1.439(4)	C17 . H171 . 0.915
N4 . C11 . 1.485(4)	C18 . C19 . 1.522(5)
C5 . N6 . 1.332(4)	C19 . H191 . 0.954
C5 . C10 . 1.387(5)	C19 . H192 . 0.935
N6 . C7 . 1.345(5)	C19 . H193 . 0.982
C7 . C8 . 1.379(5)	C20 . H201 . 0.982
C7 . H71 . 0.896	C20 . H202 . 0.944
C8 . C9 . 1.373(6)	C20 . H203 . 0.978
C8 . H81 . 0.958	C21 . H211 . 1.001
C9 . C10 . 1.383(5)	C21 . H212 . 0.929
C9 . H91 . 0.933	C21 . H213 . 0.943
C10 . H101 . 0.945	B22 . F190 . 1.506(16)
C11 . C12 . 1.513(5)	B22 . F191 . 1.25(2)
C11 . H111 . 1.020	B22 . F220 . 1.27(2)
C11 . H112 . 0.953	B22 . F221 . 1.45(2)
C12 . C13 . 1.521(6)	B22 . F250 . 1.345(15)
C12 . H121 . 0.947	B22 . F251 . 1.397(15)
C12 . H122 . 0.986	B22 . F260 . 1.39(2)
C13 . H131 . 0.979	B22 . F261 . 1.36(2)
C13 . H132 . 0.989	

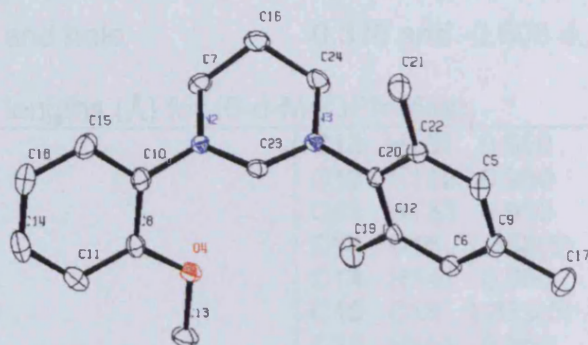
Table A.3: Bond angles (°) for (6-Py-Mes).

N2 . C1 . C14 . 118.8(3)	H211 . C21 . H213 . 106.5
N2 . C1 . C18 . 118.2(3)	H212 . C21 . H213 . 112.8
C14 . C1 . C18 . 123.0(3)	F190 . B22 . F191 . 10.4(17)
C1 . N2 . C3 . 117.9(3)	F190 . B22 . F220 . 111.9(15)
C1 . N2 . C13 . 120.1(3)	F191 . B22 . F220 . 118.1(16)
C3 . N2 . C13 . 121.3(3)	F190 . B22 . F221 . 105.1(13)
N2 . C3 . N4 . 124.9(3)	F191 . B22 . F221 . 110.4(14)
N2 . C3 . H31 . 117.6	F220 . B22 . F221 . 9(2)
N4 . C3 . H31 . 117.6	F190 . B22 . F250 . 121.9(14)
C3 . N4 . C5 . 118.5(3)	F191 . B22 . F250 . 111.5(14)
C3 . N4 . C11 . 120.3(3)	F220 . B22 . F250 . 109.5(15)

Appendix 2. Tables of Bond Distances and Angles

C5 . N4 . C11 . 121.0(3)	F221 . B22 . F250 . 110.5(13)
N4 . C5 . N6 . 114.7(3)	F190 . B22 . F251 . 108.4(12)
N4 . C5 . C10 . 120.7(3)	F191 . B22 . F251 . 98.1(14)
N6 . C5 . C10 . 124.5(3)	F220 . B22 . F251 . 108.9(13)
C5 . N6 . C7 . 116.7(3)	F221 . B22 . F251 . 107.1(11)
N6 . C7 . C8 . 123.5(4)	F250 . B22 . F251 . 17.5(18)
N6 . C7 . H71 . 118.6	F190 . B22 . F260 . 101.1(12)
C8 . C7 . H71 . 117.9	F191 . B22 . F260 . 107.5(14)
C7 . C8 . C9 . 117.9(4)	F220 . B22 . F260 . 97.8(15)
C7 . C8 . H81 . 122.3	F221 . B22 . F260 . 105.1(13)
C9 . C8 . H81 . 119.7	F250 . B22 . F260 . 111.7(13)
C8 . C9 . C10 . 120.6(3)	F190 . B22 . F261 . 109.2(11)
C8 . C9 . H91 . 118.6	F191 . B22 . F261 . 112.1(13)
C10 . C9 . H91 . 120.7	F220 . B22 . F261 . 111.9(14)
C5 . C10 . C9 . 116.7(3)	F221 . B22 . F261 . 120.4(12)
C5 . C10 . H101 . 122.2	F250 . B22 . F261 . 90.4(13)
C9 . C10 . H101 . 121.0	F251 . B22 . F260 . 128.1(12)
N4 . C11 . C12 . 109.8(3)	F251 . B22 . F261 . 106.2(11)
N4 . C11 . H111 . 106.1	F260 . B22 . F261 . 22.2(13)
C12 . C11 . H111 . 110.7	H131 . C13 . H132 . 108.4
N4 . C11 . H112 . 108.2	C1 . C14 . C15 . 117.4(3)
C12 . C11 . H112 . 113.6	C1 . C14 . C21 . 122.3(3)
H111 . C11 . H112 . 108.2	C15 . C14 . C21 . 120.3(3)
C11 . C12 . C13 . 111.7(3)	C14 . C15 . C16 . 121.0(3)
C11 . C12 . H121 . 109.1	C14 . C15 . H151 . 119.3
C13 . C12 . H121 . 109.8	C16 . C15 . H151 . 119.6
C11 . C12 . H122 . 107.2	C15 . C16 . C17 . 119.4(3)
C13 . C12 . H122 . 108.2	C15 . C16 . C20 . 120.6(3)
H121 . C12 . H122 . 110.8	C17 . C16 . C20 . 120.1(3)
C12 . C13 . N2 . 108.7(3)	C16 . C17 . C18 . 121.7(3)
C12 . C13 . H131 . 112.0	C16 . C17 . H171 . 120.1
N2 . C13 . H131 . 108.2	C18 . C17 . H171 . 118.2
C12 . C13 . H132 . 111.2	C17 . C18 . C1 . 117.5(3)
N2 . C13 . H132 . 108.2	C17 . C18 . C19 . 119.7(3)
H201 . C20 . H202 . 109.0	C1 . C18 . C19 . 122.8(3)
C16 . C20 . H203 . 109.7	C18 . C19 . H191 . 108.7
H201 . C20 . H203 . 105.2	C18 . C19 . H192 . 110.5
H202 . C20 . H203 . 111.0	H191 . C19 . H192 . 111.5
C14 . C21 . H211 . 109.9	C18 . C19 . H193 . 110.4
C14 . C21 . H212 . 110.0	H191 . C19 . H193 . 106.2
H211 . C21 . H212 . 107.3	H192 . C19 . H193 . 109.5
C14 . C21 . H213 . 110.2	C16 . C20 . H201 . 110.8
	C16 . C20 . H202 . 110.9

Appendix 2. Tables of Bond Distances and Angles


Table B.1: Crystal data and structure refinement for (6-o-MeOPh-Mes).

Identification code	kjc0737
Empirical formula	C ₂₀ H ₂₅ Br N ₂ O
Formula weight	389.33
Temperature	150(2) K
Wavelength	0.71073 Å
Crystal system	Monoclinic
Space group	P21/a
Unit cell dimensions	a = 8.11730(10) Å a = 90°. b = 16.0772(3) Å β = 99.7060(10)°. c = 14.2610(3) Å γ = 90°.
Volume	1834.47(6) Å ³
Z	4
Density (calculated)	1.410 Mg/m ³
Absorption coefficient	2.250 mm ⁻¹
F(000)	808
Crystal size	0.15 x 0.10 x 0.10 mm ³
Theta range for data collection	2.92 to 27.45°.
Index ranges	-10 ≤ h ≤ 10, -20 ≤ k ≤ 20, -
	18 ≤ l ≤ 18
Reflections collected	29436
Independent reflections	4195 [R(int) = 0.1035]
Completeness to theta = 27.45°	99.8 %
Absorption correction	Empirical
Max. and min. transmission	0.8063 and 0.7290
Refinement method	Full-matrix least-squares on F ²
Data / restraints / parameters	4195 / 0 / 221
Goodness-of-fit on F ²	1.045
Final R indices [I > 2σ(I)]	R1 = 0.0420, wR2 = 0.0927

R indices (all data) R1 = 0.0566, wR2 = 0.0995
 Largest diff. peak and hole 0.316 and -0.608 e.Å⁻³

Table B. 2: Bond lengths (Å) for (6-o-MeOPh-Mes).

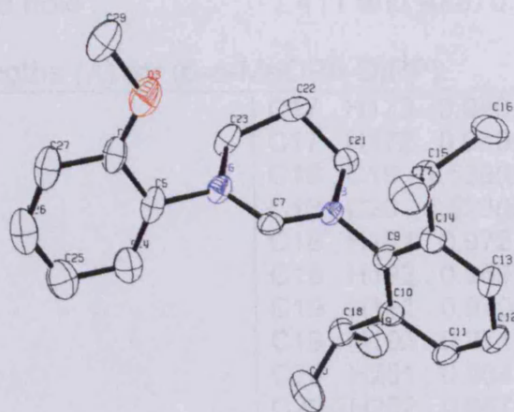
N2 . C7 . 1.477(4)	C13 . H131 . 0.950
N2 . C10 . 1.425(4)	C13 . H132 . 0.950
N2 . C23 . 1.323(4)	C13 . H133 . 0.950
N3 . C20 . 1.453(4)	C14 . C18 . 1.388(6)
N3 . C23 . 1.310(4)	C14 . H141 . 0.950
N3 . C24 . 1.485(4)	C15 . C18 . 1.379(5)
O4 . C8 . 1.361(4)	C15 . H151 . 0.950
O4 . C13 . 1.432(4)	C16 . C24 . 1.514(5)
C5 . C9 . 1.400(5)	C16 . H162 . 0.950
C5 . C22 . 1.396(5)	C16 . H161 . 0.950
C5 . H51 . 0.950	C17 . H171 . 0.950
C6 . C9 . 1.381(5)	C17 . H173 . 0.950
C6 . C12 . 1.386(5)	C17 . H172 . 0.950
C6 . H61 . 0.950	C18 . H181 . 0.950
C7 . C16 . 1.510(5)	C19 . H192 . 0.950
C7 . H71 . 0.950	C19 . H191 . 0.950
C7 . H72 . 0.950	C19 . H193 . 0.950
C8 . C10 . 1.405(5)	C20 . C22 . 1.389(5)
C8 . C11 . 1.394(5)	C21 . C22 . 1.501(5)
C9 . C17 . 1.506(5)	C21 . H212 . 0.950
C10 . C15 . 1.391(5)	C21 . H211 . 0.950
C11 . C14 . 1.387(6)	C21 . H213 . 0.950
C11 . H111 . 0.950	C23 . H231 . 0.950
C12 . C19 . 1.502(5)	C24 . H241 . 0.950
C12 . C20 . 1.408(5)	C24 . H242 . 0.950

Table B. 3: Bond angles (°) for (6-o-MeOPh-Mes).

C7 . N2 . C10 . 120.4(3)	C18 . C15 . H151 . 120.2
C7 . N2 . C23 . 119.7(3)	C7 . C16 . C24 . 109.1(3)
C10 . N2 . C23 . 119.9(3)	C7 . C16 . H162 . 110.2
C20 . N3 . C23 . 120.1(3)	C24 . C16 . H162 . 109.9
C20 . N3 . C24 . 119.1(3)	C7 . C16 . H161 . 108.7
C23 . N3 . C24 . 120.6(3)	C24 . C16 . H161 . 109.4
C8 . O4 . C13 . 116.6(3)	H162 . C16 . H161 . 109.5
C9 . C5 . C22 . 121.6(3)	C9 . C17 . H171 . 109.1
C9 . C5 . H51 . 119.1	C9 . C17 . H173 . 109.2
C22 . C5 . H51 . 119.3	H171 . C17 . H173 . 109.5
C9 . C6 . C12 . 123.0(3)	C9 . C17 . H172 . 110.1
C9 . C6 . H61 . 118.8	H171 . C17 . H172 . 109.5
C12 . C6 . H61 . 118.2	H173 . C17 . H172 . 109.5
N2 . C7 . C16 . 109.9(3)	C14 . C18 . C15 . 119.9(4)
N2 . C7 . H71 . 109.9	C14 . C18 . H181 . 120.1
C16 . C7 . H71 . 110.0	C15 . C18 . H181 . 120.0
N2 . C7 . H72 . 109.0	C12 . C19 . H192 . 109.8
C16 . C7 . H72 . 108.6	C12 . C19 . H191 . 109.5
H71 . C7 . H72 . 109.5	H192 . C19 . H191 . 109.5
O4 . C8 . C10 . 116.0(3)	C12 . C19 . H193 . 109.1

Appendix 2. Tables of Bond Distances and Angles

O4 . C8 . C11 . 124.5(3)	H192 . C19 . H193 . 109.5
C10 . C8 . C11 . 119.5(3)	H191 . C19 . H193 . 109.5
C5 . C9 . C6 . 118.0(3)	N3 . C20 . C12 . 118.6(3)
C5 . C9 . C17 . 119.7(3)	N3 . C20 . C22 . 119.2(3)
C6 . C9 . C17 . 122.3(3)	C12 . C20 . C22 . 122.3(3)
N2 . C10 . C8 . 120.4(3)	C22 . C21 . H212 . 109.7
N2 . C10 . C15 . 119.5(3)	C22 . C21 . H211 . 109.9
C8 . C10 . C15 . 120.1(3)	H212 . C21 . H211 . 109.5
C8 . C11 . C14 . 119.4(4)	C22 . C21 . H213 . 108.8
C8 . C11 . H111 . 120.3	H212 . C21 . H213 . 109.5
C14 . C11 . H111 . 120.3	H211 . C21 . H213 . 109.5
C6 . C12 . C19 . 121.5(3)	C21 . C22 . C5 . 119.8(3)
C6 . C12 . C20 . 117.0(3)	C21 . C22 . C20 . 122.3(3)
C19 . C12 . C20 . 121.4(3)	C5 . C22 . C20 . 118.0(3)
O4 . C13 . H131 . 109.7	N2 . C23 . N3 . 124.7(3)
O4 . C13 . H132 . 109.1	N2 . C23 . H231 . 117.8
H131 . C13 . H132 . 109.5	N3 . C23 . H231 . 117.5
O4 . C13 . H133 . 109.6	C16 . C24 . N3 . 108.8(3)
H131 . C13 . H133 . 109.5	C16 . C24 . H241 . 109.9
H132 . C13 . H133 . 109.5	N3 . C24 . H241 . 109.1
C11 . C14 . C18 . 121.0(4)	C16 . C24 . H242 . 109.5
C11 . C14 . H141 . 119.5	N3 . C24 . H242 . 110.1
C18 . C14 . H141 . 119.5	H241 . C24 . H242 . 109.5
C10 . C15 . C18 . 120.0(4)	C10 . C15 . H151 . 119.8

**Table C.1:** Crystal data and structure refinement for (6-*o*-MeOPh-DIPP).

Identification code	kjc0749	
Empirical formula	C ₂₃ H ₃₁ Br N ₂ O	
Formula weight	431.41	
Temperature	150(2) K	
Wavelength	0.71073 Å	
Crystal system	Monoclinic	
Space group	P2 ₁ /n	
Unit cell dimensions	a = 9.0984(2) Å	a = 90°.
	b = 14.4997(3) Å	β = 99.2480(10)°.
	c = 16.9676(4) Å	γ = 90°.
Volume	2209.34(8) Å ³	
Z	4	
Density (calculated)	1.297 Mg/m ³	
Absorption coefficient	1.875 mm ⁻¹	
F(000)	904	
Crystal size	0.20 x 0.20 x 0.10 mm ³	
Theta range for data collection	1.86 to 27.49°.	
Index ranges	-11 ≤ h ≤ 11, -18 ≤ k ≤ 18, -	
	22 ≤ l ≤ 22	
Reflections collected	34696	
Independent reflections	5060 [R(int) = 0.1843]	
Completeness to theta = 27.49°	99.8 %	
Max. and min. transmission	0.8347 and 0.7055	
Refinement method	Full-matrix least-squares on F ²	
Data / restraints / parameters	5060 / 0 / 249	
Goodness-of-fit on F ²	1.179	
Final R indices [I > 2σ(I)]	R1 = 0.0764, wR2 = 0.1974	
R indices (all data)	R1 = 0.1005, wR2 = 0.2188	

Largest diff. peak and hole

1.411 and -0.870 e.Å⁻³**Table C. 2:** Bond lengths (Å) for (6-*o*-MeOPh-DIPP).

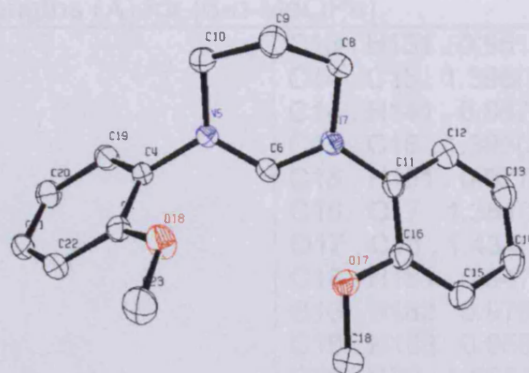
O3 . C4 . 1.322(7)	C17 . H173 . 0.940
O3 . C29 . 1.451(7)	C17 . H172 . 0.960
C4 . C5 . 1.383(8)	C18 . C19 . 1.539(8)
C4 . C27 . 1.375(7)	C18 . C20 . 1.523(8)
C5 . N6 . 1.457(7)	C18 . H181 . 0.972
C5 . C24 . 1.368(8)	C19 . H192 . 0.959
N6 . C7 . 1.316(6)	C19 . H191 . 0.970
N6 . C23 . 1.477(6)	C19 . H193 . 0.971
C7 . N8 . 1.347(6)	C20 . H201 . 0.964
C7 . H71 . 0.933	C20 . H202 . 0.957
N8 . C9 . 1.442(6)	C20 . H203 . 0.967
N8 . C21 . 1.472(6)	C21 . C22 . 1.529(7)
C9 . C10 . 1.408(6)	C21 . H211 . 0.969
C9 . C14 . 1.394(7)	C21 . H212 . 0.983
C10 . C11 . 1.398(7)	C22 . C23 . 1.557(7)
C10 . C18 . 1.525(7)	C22 . H222 . 0.969
C11 . C12 . 1.371(7)	C22 . H221 . 0.976
C11 . H111 . 0.936	C23 . H231 . 0.980
C12 . C13 . 1.395(7)	C23 . H232 . 0.962
C12 . H121 . 0.937	C24 . C25 . 1.389(8)
C13 . C14 . 1.390(7)	C24 . H241 . 0.933
C13 . H131 . 0.932	C25 . C26 . 1.341(10)
C14 . C15 . 1.520(7)	C25 . H251 . 0.932
C15 . C16 . 1.531(7)	C26 . C27 . 1.378(9)
C15 . C17 . 1.516(8)	C26 . H261 . 0.925
C15 . H151 . 0.964	C27 . H271 . 0.927
C16 . H162 . 0.948	C29 . H291 . 0.963
C16 . H161 . 0.961	C29 . H292 . 0.956
C16 . H163 . 0.956	C29 . H293 . 0.965
C17 . H171 . 0.962	

Table C. 3: Bond angles (°) for (6-*o*-MeOPh-DIPP).

C4 . O3 . C29 . 117.1(5)	C20 . C18 . H181 . 107.4
O3 . C4 . C5 . 116.9(5)	C18 . C19 . H192 . 111.2
O3 . C4 . C27 . 124.8(5)	C18 . C19 . H191 . 109.5
C5 . C4 . C27 . 118.3(6)	H192 . C19 . H191 . 108.4
C4 . C5 . N6 . 117.6(5)	C18 . C19 . H193 . 109.9
C4 . C5 . C24 . 122.3(5)	H192 . C19 . H193 . 109.1
N6 . C5 . C24 . 120.1(5)	H191 . C19 . H193 . 108.7
C5 . N6 . C7 . 120.1(4)	C18 . C20 . H201 . 109.2
C5 . N6 . C23 . 118.6(4)	C18 . C20 . H202 . 111.7
C7 . N6 . C23 . 121.0(4)	H201 . C20 . H202 . 108.6
N6 . C7 . N8 . 123.1(4)	C18 . C20 . H203 . 109.1
N6 . C7 . H71 . 117.9	H201 . C20 . H203 . 109.4
N8 . C7 . H71 . 119.0	H202 . C20 . H203 . 108.9
C7 . N8 . C9 . 120.3(4)	N8 . C21 . C22 . 109.4(4)
C7 . N8 . C21 . 122.9(4)	N8 . C21 . H211 . 111.3
C9 . N8 . C21 . 116.7(4)	C22 . C21 . H211 . 110.4
N8 . C9 . C10 . 119.0(4)	N8 . C21 . H212 . 108.1

Appendix 2. Tables of Bond Distances and Angles

N8 . C9 . C14 . 118.4(4)	C22 . C21 . H212 . 109.2
C10 . C9 . C14 . 122.4(4)	H211 . C21 . H212 . 108.4
C9 . C10 . C11 . 116.9(5)	C21 . C22 . C23 . 110.0(4)
C9 . C10 . C18 . 123.1(4)	C21 . C22 . H222 . 109.4
C11 . C10 . C18 . 120.0(4)	C23 . C22 . H222 . 111.4
C10 . C11 . C12 . 121.7(5)	C21 . C22 . H221 . 108.0
C10 . C11 . H111 . 119.3	C23 . C22 . H221 . 109.3
C12 . C11 . H111 . 119.0	H222 . C22 . H221 . 108.6
C11 . C12 . C13 . 120.4(5)	C22 . C23 . N6 . 108.6(4)
C11 . C12 . H121 . 121.1	C22 . C23 . H231 . 109.1
C13 . C12 . H121 . 118.5	N6 . C23 . H231 . 108.4
C12 . C13 . C14 . 120.1(5)	C22 . C23 . H232 . 111.0
C12 . C13 . H131 . 119.9	N6 . C23 . H232 . 110.7
C14 . C13 . H131 . 119.9	H231 . C23 . H232 . 108.9
C9 . C14 . C13 . 118.5(4)	C5 . C24 . C25 . 119.2(6)
C9 . C14 . C15 . 122.3(4)	C5 . C24 . H241 . 120.5
C13 . C14 . C15 . 119.1(4)	C25 . C24 . H241 . 120.3
C14 . C15 . C16 . 111.3(4)	C24 . C25 . C26 . 117.8(6)
C14 . C15 . C17 . 110.4(4)	C24 . C25 . H251 . 120.6
C16 . C15 . C17 . 111.4(5)	C26 . C25 . H251 . 121.6
C14 . C15 . H151 . 107.7	C25 . C26 . C27 . 124.3(6)
C16 . C15 . H151 . 107.0	C25 . C26 . H261 . 117.2
C17 . C15 . H151 . 108.8	C27 . C26 . H261 . 118.4
C15 . C16 . H162 . 108.7	C26 . C27 . C4 . 118.1(6)
C15 . C16 . H161 . 109.2	C26 . C27 . H271 . 120.9
H162 . C16 . H161 . 109.5	C4 . C27 . H271 . 121.0
C15 . C16 . H163 . 108.7	O3 . C29 . H291 . 109.4
H162 . C16 . H163 . 110.9	O3 . C29 . H292 . 110.0
H161 . C16 . H163 . 109.8	H291 . C29 . H292 . 108.7
C15 . C17 . H171 . 108.1	O3 . C29 . H293 . 109.9
C15 . C17 . H173 . 111.5	H291 . C29 . H293 . 109.3
H171 . C17 . H173 . 109.9	H292 . C29 . H293 . 109.6
C15 . C17 . H172 . 108.1	C10 . C18 . C20 . 109.6(5)
H171 . C17 . H172 . 109.1	C19 . C18 . C20 . 111.3(5)
H173 . C17 . H172 . 110.0	C10 . C18 . H181 . 108.4
C10 . C18 . C19 . 111.5(4)	C19 . C18 . H181 . 108.4

**Table D.1:** Crystal data and structure refinement for (6-*o*-MeOPh).

Identification code	kjc0727
Empirical formula	C ₁₈ H ₂₃ Br N ₂ O ₃
Formula weight	395.29
Temperature	150(2) K
Wavelength	0.71073 Å
Crystal system	Triclinic
Space group	P-1
Unit cell dimensions	a = 7.50160(10) Å a = 71.6920(10)° b = 10.2088(2) Å β = 82.8260(10)° c = 13.3104(3) Å γ = 74.2070(10)°
Volume	930.35(3) Å ³
Z	2
Density (calculated)	1.411 Mg/m ³
Absorption coefficient	2.227 mm ⁻¹
F(000)	408
Crystal size	0.35 x 0.20 x 0.12 mm ³
Theta range for data collection	3.06 to 30.24°.
Index ranges	-10 ≤ h ≤ 9, -14 ≤ k ≤ 14, -18 ≤ l ≤ 18
Reflections collected	16175
Independent reflections	5426 [R(int) = 0.1078]
Completeness to theta = 30.24°	97.7 %
Absorption correction	Empirical
Max. and min. transmission	0.7760 and 0.5095
Refinement method	Full-matrix least-squares on F ²
Data / restraints / parameters	5426 / 0 / 227
Goodness-of-fit on F ²	1.055
Final R indices [I > 2σ(I)]	R1 = 0.0388, wR2 = 0.1004
R indices (all data)	R1 = 0.0472, wR2 = 0.1052
Largest diff. peak and hole	0.565 and -0.760 e.Å ⁻³

Table D. 2: Bond lengths (Å) for (6-*o*-MeOPh).

O18 . C3 . 1.363(2)	C13 . H131 . 0.951
O18 . C23 . 1.423(3)	C14 . C15 . 1.396(3)
C3 . C4 . 1.398(3)	C14 . H141 . 0.947
C3 . C22 . 1.396(3)	C15 . C16 . 1.395(3)
C4 . N5 . 1.438(2)	C15 . H151 . 0.977
C4 . C19 . 1.389(3)	C16 . O17 . 1.361(2)
N5 . C6 . 1.310(2)	O17 . C18 . 1.434(3)
N5 . C10 . 1.476(2)	C18 . H181 . 0.947
C6 . N7 . 1.317(2)	C18 . H182 . 0.978
C6 . H61 . 0.941	C18 . H183 . 0.958
N7 . C8 . 1.479(2)	C19 . C20 . 1.391(3)
N7 . C11 . 1.427(2)	C19 . H191 . 0.932
C8 . C9 . 1.515(3)	C20 . C21 . 1.384(3)
C8 . H81 . 0.940	C20 . H201 . 0.944
C8 . H82 . 0.982	C21 . C22 . 1.387(3)
C9 . C10 . 1.520(3)	C21 . H211 . 0.936
C9 . H91 . 0.993	C22 . H221 . 0.959
C9 . H92 . 0.975	C23 . H233 . 0.941
C10 . H101 . 0.971	C23 . H232 . 0.932
C10 . H102 . 0.987	C23 . H231 . 0.940
C11 . C12 . 1.391(3)	O2 . H21 . 0.832
C11 . C16 . 1.403(3)	O2 . H22 . 0.828
C12 . C13 . 1.388(3)	C12 . H121 . 0.916
	C13 . C14 . 1.384(4)

Table D. 3: Bond angles (°) for (6-*o*-MeOPh).

C3 . O18 . C23 . 117.46(18)	C11 . C12 . H121 . 118.8
O18 . C3 . C4 . 115.24(17)	C13 . C12 . H121 . 121.1
O18 . C3 . C22 . 125.56(19)	C12 . C13 . C14 . 119.9(2)
C4 . C3 . C22 . 119.20(18)	C12 . C13 . H131 . 120.0
C3 . C4 . N5 . 118.45(16)	C14 . C13 . H131 . 120.1
C3 . C4 . C19 . 121.13(17)	C13 . C14 . C15 . 120.8(2)
N5 . C4 . C19 . 120.42(17)	C13 . C14 . H141 . 122.0
C4 . N5 . C6 . 118.08(16)	C15 . C14 . H141 . 117.3
C4 . N5 . C10 . 119.65(16)	C14 . C15 . C16 . 119.5(2)
C6 . N5 . C10 . 122.22(16)	C14 . C15 . H151 . 118.0
N5 . C6 . N7 . 124.67(18)	C16 . C15 . H151 . 122.5
N5 . C6 . H61 . 118.3	C11 . C16 . C15 . 119.59(19)
N7 . C6 . H61 . 117.0	C11 . C16 . O17 . 115.89(17)
C6 . N7 . C8 . 119.77(16)	C15 . C16 . O17 . 124.51(19)
C6 . N7 . C11 . 119.74(16)	C16 . O17 . C18 . 117.69(17)
C8 . N7 . C11 . 120.31(15)	O17 . C18 . H181 . 106.8
N7 . C8 . C9 . 108.94(17)	O17 . C18 . H182 . 109.9
N7 . C8 . H81 . 109.0	H181 . C18 . H182 . 109.4
C9 . C8 . H81 . 112.0	O17 . C18 . H183 . 109.6
N7 . C8 . H82 . 110.0	H181 . C18 . H183 . 111.7
C9 . C8 . H82 . 109.2	H182 . C18 . H183 . 109.5
H81 . C8 . H82 . 107.7	C4 . C19 . C20 . 119.28(19)
C8 . C9 . C10 . 110.97(18)	C4 . C19 . H191 . 118.0
C8 . C9 . H91 . 107.9	C20 . C19 . H191 . 122.7
C10 . C9 . H91 . 108.4	C19 . C20 . C21 . 119.67(19)

Appendix 2. Tables of Bond Distances and Angles

C8 . C9 . H92 . 107.9	C19 . C20 . H201 . 119.7
C10 . C9 . H92 . 111.2	C21 . C20 . H201 . 120.7
H91 . C9 . H92 . 110.5	C20 . C21 . C22 . 121.48(19)
C9 . C10 . N5 . 108.77(17)	C20 . C21 . H211 . 120.0
C9 . C10 . H101 . 112.7	C22 . C21 . H211 . 118.5
N5 . C10 . H101 . 108.0	C3 . C22 . C21 . 119.2(2)
C9 . C10 . H102 . 111.1	C3 . C22 . H221 . 121.2
N5 . C10 . H102 . 109.2	C21 . C22 . H221 . 119.5
H101 . C10 . H102 . 107.0	O18 . C23 . H233 . 107.6
N7 . C11 . C12 . 119.55(18)	O18 . C23 . H232 . 110.7
N7 . C11 . C16 . 120.32(17)	H233 . C23 . H232 . 109.1
C12 . C11 . C16 . 120.11(19)	O18 . C23 . H231 . 110.2
C11 . C12 . C13 . 120.1(2)	H233 . C23 . H231 . 109.4
H21 . O2 . H22 . 103.2	H232 . C23 . H231 . 109.7

Appendix 2. Tables of Bond Distances and Angles

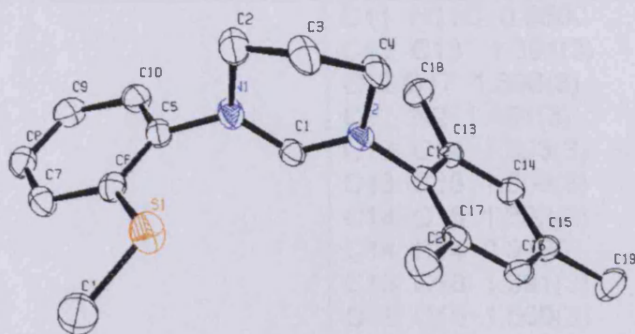


Table E.1: Crystal data and structure refinement for (6-*o*-MeSPH-Mes).

Identification code	kjc0819
Empirical formula	C ₂₀ H ₂₅ B F ₄ N ₂ S
Formula weight	412.29
Temperature	293(2) K
Wavelength	0.71073 Å
Crystal system	Monoclinic
Space group	P21/c
Unit cell dimensions	a = 8.0040(2) Å a = 90°. b = 16.1800(4) Å β = 102.2990(10)°. c = 16.1990(5) Å γ = 90°.
Volume	2049.70(10) Å ³
Z	4
Density (calculated)	1.336 Mg/m ³
Absorption coefficient	0.201 mm ⁻¹
F(000)	864
Crystal size	0.20 x 0.20 x 0.11 mm ³
Theta range for data collection	3.48 to 27.49°.
Index ranges	-10 ≤ h ≤ 10, -20 ≤ k ≤ 20, -
	20 ≤ l ≤ 20
Reflections collected	20675
Independent reflections	4659 [R(int) = 0.1194]
Completeness to theta = 27.49°	99.0 %
Refinement method	Full-matrix least-squares on F ²
Data / restraints / parameters	4659 / 0 / 257
Goodness-of-fit on F ²	1.038
Final R indices [I > 2σ(I)]	R1 = 0.0563, wR2 = 0.1273
R indices (all data)	R1 = 0.0846, wR2 = 0.1412
Largest diff. peak and hole	0.257 and -0.432 e.Å ⁻³

Table E. 2: Bond lengths(Å) for (6-*o*-MeSPh-Mes).

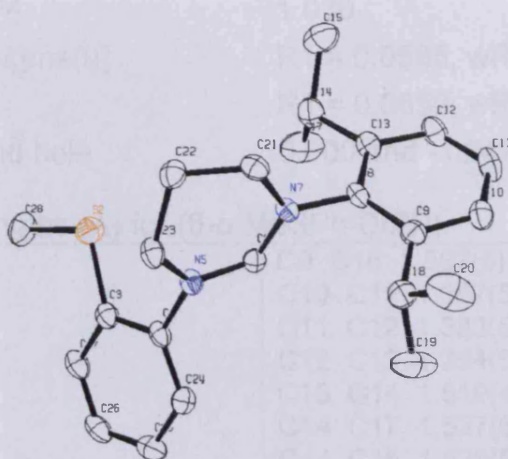
C1 N2 1.307(3)	C11 H11C 0.9600
C1 N1 1.320(3)	C12 C13 1.391(3)
C1 H1 0.9300	C12 C17 1.398(3)
C2 N1 1.475(3)	C12 N2 1.451(3)
C2 C3 1.510(3)	C13 C14 1.393(3)
C2 H2A 0.9700	C13 C18 1.509(3)
C2 H2B 0.9700	C14 C15 1.392(3)
C3 C4 1.512(3)	C14 H14 0.9300
C3 H3A 0.9700	C15 C16 1.391(3)
C3 H3B 0.9700	C15 C19 1.509(3)
C4 N2 1.480(3)	C16 C17 1.382(3)
C4 H4A 0.9700	C16 H16 0.9300
C4 H4B 0.9700	C17 C20 1.513(3)
C5 C10 1.372(3)	C18 H18A 0.9600
C5 C6 1.400(3)	C18 H18B 0.9600
C5 N1 1.441(3)	C18 H18C 0.9600
C6 C7 1.391(3)	C19 H19A 0.9600
C6 S1 1.768(2)	C19 H19B 0.9600
C7 C8 1.391(3)	C19 H19C 0.9600
C7 H7 0.9300	C20 H20A 0.9600
C8 C9 1.380(3)	C20 H20B 0.9600
C8 H8 0.9300	C20 H20C 0.9600
C9 C10 1.382(3)	B1 F3 1.379(3)
C9 H9 0.9300	B1 F2 1.385(3)
C10 H10 0.9300	B1 F5 1.386(3)
C11 S1 1.794(3)	B1 F4 1.403(3)
C11 H11A 0.9600	C11 H11B 0.9600

Table E. 3: Bond angles (°) for (6-*o*-MeSPh-Mes).

N2 C1 N1 123.76(18)	C12 C13 C14 117.75(17)
N2 C1 H1 118.1	C12 C13 C18 121.65(18)
N1 C1 H1 118.1	C14 C13 C18 120.55(18)
N1 C2 C3 109.61(19)	C15 C14 C13 121.81(19)
N1 C2 H2A 109.7	C15 C14 H14 119.1
C3 C2 H2A 109.7	C13 C14 H14 119.1
N1 C2 H2B 109.7	C16 C15 C14 118.10(19)
C3 C2 H2B 109.7	C16 C15 C19 120.82(19)
H2A C2 H2B 108.2	C14 C15 C19 121.1(2)
C2 C3 C4 110.22(19)	C17 C16 C15 122.44(18)
C2 C3 H3A 109.6	C17 C16 H16 118.8
C4 C3 H3A 109.6	C15 C16 H16 118.8
C2 C3 H3B 109.6	C16 C17 C12 117.51(19)
C4 C3 H3B 109.6	C16 C17 C20 121.67(19)
H3A C3 H3B 108.1	C12 C17 C20 120.8(2)
N2 C4 C3 109.34(16)	C13 C18 H18A 109.5
N2 C4 H4A 109.8	C13 C18 H18B 109.5
C3 C4 H4A 109.8	H18A C18 H18B 109.5
N2 C4 H4B 109.8	C13 C18 H18C 109.5
C3 C4 H4B 109.8	H18A C18 H18C 109.5
H4A C4 H4B 108.3	H18B C18 H18C 109.5
C10 C5 C6 121.05(19)	C15 C19 H19A 109.5

Appendix 2. Tables of Bond Distances and Angles

C10 C5 N1 119.54(18)	C15 C19 H19B 109.5
C6 C5 N1 119.34(18)	H19A C19 H19B 109.5
C7 C6 C5 118.03(18)	C15 C19 H19C 109.5
C7 C6 S1 124.60(16)	H19A C19 H19C 109.5
C5 C6 S1 117.35(15)	H19B C19 H19C 109.5
C8 C7 C6 120.06(19)	C17 C20 H20A 109.5
C8 C7 H7 120.0	C17 C20 H20B 109.5
C6 C7 H7 120.0	H20A C20 H20B 109.5
C9 C8 C7 121.4(2)	C17 C20 H20C 109.5
C9 C8 H8 119.3	H20A C20 H20C 109.5
C7 C8 H8 119.3	H20B C20 H20C 109.5
C8 C9 C10 118.4(2)	C1 N1 C5 121.09(17)
C8 C9 H9 120.8	C1 N1 C2 121.11(17)
C10 C9 H9 120.8	C5 N1 C2 117.79(17)
C5 C10 C9 121.0(2)	C1 N2 C12 120.58(16)
C5 C10 H10 119.5	C1 N2 C4 121.39(17)
C9 C10 H10 119.5	C12 N2 C4 118.00(15)
S1 C11 H11A 109.5	C6 S 1 C11 103.08(11)
S1 C11 H11B 109.5	F3 B1 F2 110.8(2)
H11A C11 H11B 109.5	F3 B1 F5 110.76(19)
S1 C11 H11C 109.5	F2 B1 F5 109.66(19)
H11A C11 H11C 109.5	F3 B1 F4 108.53(18)
H11B C11 H11C 109.5	F2 B1 F4 108.71(19)
C13 C12 C17 122.38(19)	F5 B1 F4 108.3(2)
C13 C12 N2 118.73(16)	C17 C12 N2 118.77(18)

**Table F. 1:** Crystal data and structure refinement for (6-*o*-MeSPH-DIPP).

Identification code	kjc0810	
Empirical formula	C ₂₃ H ₃₁ Br N ₂ S	
Formula weight	447.47	
Temperature	150(2) K	
Wavelength	0.71073 Å	
Crystal system	Monoclinic	
Space group	P2 ₁ /n	
Unit cell dimensions	a = 9.00230(10) Å	a = 90°.
	b = 14.4043(2) Å	β = 97.7(10)°.
	c = 17.6548(3) Å	γ = 90°.
Volume	2268.69(6) Å ³	
Z	4	
Density (calculated)	1.310 Mg/m ³	
Absorption coefficient	1.914 mm ⁻¹	
F(000)	936	
Crystal size	0.20 x 0.20 x 0.10 mm ³	
Theta range for data collection	3.05 to 27.54°.	
Index ranges	-11 ≤ h ≤ 11, -18 ≤ k ≤ 18, -	
	22 ≤ l ≤ 22	
Reflections collected	37229	
Independent reflections	5195 [R(int) = 0.2138]	
Completeness to theta = 27.54°	99.3 %	
Max. and min. transmission	0.8317 and 0.7008	
Refinement method	Full-matrix least-squares on F ²	
Data / restraints / parameters	5195 / 0 / 249	

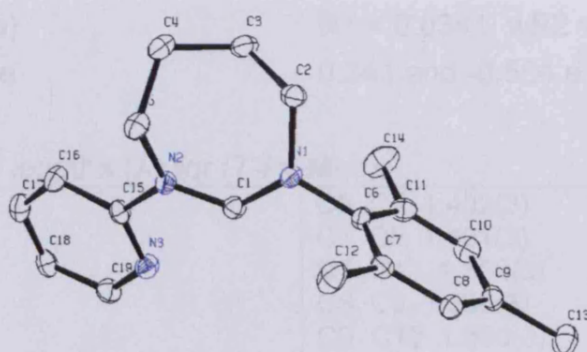
Goodness-of-fit on F^2	1.030
Final R indices [$I > 2\sigma(I)$]	R1 = 0.0585, wR2 = 0.1346
R indices (all data)	R1 = 0.0859, wR2 = 0.1498
Largest diff. peak and hole	0.800 and -1.247 e.Å ⁻³

Table F. 2: Bond lengths (Å) for (6-*o*-MeSPh-DIPP).

S2 C3 1.759(3)	C9 C18 1.507(5)
S2 C28 1.802(4)	C10 C11 1.367(5)
C3 C27 1.393(5)	C11 C12 1.383(5)
C3 C4 1.406(5)	C12 C13 1.394(5)
C4 C24 1.380(5)	C13 C14 1.519(4)
C4 N5 1.434(4)	C14 C17 1.527(6)
N5 C6 1.325(4)	C14 C15 1.528(5)
N5 C23 1.484(4)	C18 C20 1.507(5)
C6 N7 1.310(4)	C18 C19 1.528(5)
N7 C8 1.446(4)	C21 C22 1.512(4)
N7 C21 1.480(4)	C22 C23 1.512(5)
C8 C13 1.399(4)	C24 C25 1.389(5)
C8 C9 1.405(4)	C25 C26 1.389(5)
C9 C10 1.398(5)	C26 C27 1.387(5)

Table F. 3: Bond angles (°) for (6-*o*-MeSPh-DIPP).

C3 S2 C28 103.81(18)	C8 C9 C18 122.5(3)
C27 C3 C4 117.9(3)	C11 C10 C9 121.5(3)
C27 C3 S2 125.7(3)	C10 C11 C12 120.8(3)
C4 C3 S2 116.3(3)	C11 C12 C13 120.8(3)
C24 C4 C3 121.2(3)	C12 C13 C8 117.1(3)
C24 C4 N5 120.2(3)	C12 C13 C14 121.0(3)
C3 C4 N5 118.6(3)	C8 C13 C14 121.8(3)
C6 N5 C4 120.4(3)	C13 C14 C17 110.5(3)
C6 N5 C23 120.0(3)	C13 C14 C15 112.3(3)
C4 N5 C23 119.5(2)	C17 C14 C15 110.3(3)
N7 C6 N5 123.5(3)	C9 C18 C20 113.7(3)
C6 N7 C8 120.4(3)	C9 C18 C19 110.3(3)
C6 N7 C21 122.2(3)	C20 C18 C19 110.1(3)
C8 N7 C21 117.2(2)	N7 C21 C22 110.4(3)
C13 C8 C9 123.2(3)	C21 C22 C23 110.1(3)
C13 C8 N7 118.7(3)	N5 C23 C22 109.3(3)
C9 C8 N7 118.1(3)	C4 C24 C25 120.4(3)
C10 C9 C8 116.5(3)	C26 C25 C24 118.7(3)
C10 C9 C18 121.0(3)	C27 C26 C25 121.2(3)
	C26 C27 C3 120.5(3)

**Table G.1:** Crystal data and structure refinement for (7-Py-Mes).

Identification code	asKJC40
Empirical formula	C ₁₉ H ₂₄ I N ₃
Formula weight	421.31
Temperature	150(2) K
Wavelength	0.71073 Å
Crystal system	Monoclinic
Space group	P2(1)/c
Unit cell dimensions	a = 13.432(3) Å a = 90°. b = 17.575(4) Å β = 104.21(3)°. c = 7.9907(16) Å γ = 90°.
Volume	1828.6(6) Å ³
Z	4
Density (calculated)	1.530 Mg/m ³
Absorption coefficient	1.755 mm ⁻¹
F(000)	848
Crystal size	0.40 x 0.30 x 0.20 mm ³
Theta range for data collection	2.95 to 27.00°.
Index ranges	-17 ≤ h ≤ 17, -22 ≤ k ≤ 22, -
	10 ≤ l ≤ 10
Reflections collected	6579
Independent reflections	3964 [R(int) = 0.0278]
Completeness to theta = 27.00°	99.2 %
Absorption correction	Empirical
Max. and min. transmission	0.753 and 0.404
Refinement method	Full-matrix least-squares on F ²
Data / restraints / parameters	3964 / 0 / 211
Goodness-of-fit on F ²	1.038

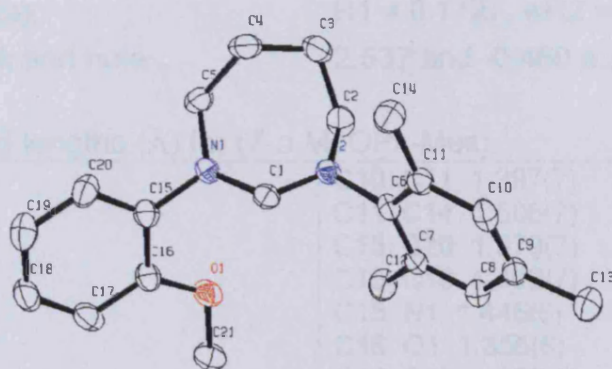
Final R indices [$I > 2\sigma(I)$] R1 = 0.0269, wR2 = 0.0566
 R indices (all data) R1 = 0.0341, wR2 = 0.0591 Largest
 diff. peak and hole 0.341 and -0.564 e.Å⁻³

Table G. 2: Bond lengths (Å) for (7-Py-Mes).

N1 C1 1.312(3)	C6 C7 1.402(3)
N1 C6 1.459(3)	C7 C8 1.401(3)
N1 C2 1.501(3)	C7 C12 1.502(3)
C1 N2 1.325(3)	C8 C9 1.386(3)
N2 C15 1.447(3)	C9 C10 1.390(3)
N2 C5 1.483(3)	C9 C13 1.511(3)
C2 C3 1.521(3)	C10 C11 1.394(3)
N3 C15 1.329(3)	C11 C14 1.509(3)
N3 C19 1.346(3)	C15 C16 1.382(3)
C3 C4 1.528(4)	C16 C17 1.392(3)
C4 C5 1.517(3)	C17 C18 1.379(3)
C6 C11 1.390(3)	C18 C19 1.379(3)

Table G. 3: Bond angles (°) for (7-Py-Mes).

C1 N1 C6 116.68(18)	C8 C7 C12 121.3(2)
C1 N1 C2 125.11(19)	C6 C7 C12 122.0(2)
C6 N1 C2 117.34(18)	C9 C8 C7 122.3(2)
N1 C1 N2 126.6(2)	C8 C9 C10 118.7(2)
C1 N2 C15 118.17(19)	C8 C9 C13 121.7(2)
C1 N2 C5 120.61(19)	C10 C9 C13 119.6(2)
C15 N2 C5 121.19(19)	C9 C10 C11 121.7(2)
N1 C2 C3 112.14(18)	C6 C11 C10 117.7(2)
C15 N3 C19 116.8(2)	C6 C11 C14 122.5(2)
C2 C3 C4 113.5(2)	C10 C11 C14 119.8(2)
C5 C4 C3 111.0(2)	N3 C15 C16 125.0(2)
N2 C5 C4 112.3(2)	N3 C15 N2 114.80(19)
C11 C6 C7 122.9(2)	C16 C15 N2 120.2(2)
C11 C6 N1 118.7(2)	C15 C16 C17 116.8(2)
C7 C6 N1 118.4(2)	C18 C17 C16 119.9(2)
C8 C7 C6 116.7(2)	C19 C18 C17 118.4(2)
	N3 C19 C18 123.3(2)

**Table H.1:** Crystal data and structure refinement for (7-o-MeOPh-Mes).

Identification code	kjc0818c	
Empirical formula	C ₂₁ H ₂₇ B F ₄ N ₂ O	
Formula weight	410.26	
Temperature	150(2) K	
Wavelength	0.71073 Å	
Crystal system	Monoclinic	
Space group	P21/a	
Unit cell dimensions	a = 8.978 Å	a = 90°.
	b = 16.022 Å	β = 104.31°.
	c = 14.812 Å	γ = 90°.
Volume	2064.5 Å ³	
Z	4	
Density (calculated)	1.320 Mg/m ³	
Absorption coefficient	0.105 mm ⁻¹	
F(000)	864	
Crystal size	0.25 x 0.05 x 0.05 mm ³	
Theta range for data collection	3.51 to 27.28°.	
Index ranges	-11 ≤ h ≤ 11, -20 ≤ k ≤ 20, -	
	19 ≤ l ≤ 18	
Reflections collected	33214	
Independent reflections	4552 [R(int) = 0.1960]	
Completeness to theta = 27.28°	98.1 %	
Max. and min. transmission	0.9948 and 0.9742	
Refinement method	Full-matrix least-squares on F ²	
Data / restraints / parameters	4552 / 1 / 261	
Goodness-of-fit on F ²	1.076	
Final R indices [I > 2σ(I)]	R1 = 0.1270, wR2 = 0.3184	

R indices (all data)

R1 = 0.1727, wR2 = 0.3471

Largest diff. peak and hole

2.537 and -0.460 e.Å⁻³**Table H. 2:** Bond lengths (Å) for (7-*o*-MeOPh-Mes).

C1 N2 1.307(6)	C10 C11 1.397(7)
C1 N1 1.330(6)	C11 C14 1.506(7)
C2 N2 1.485(6)	C15 C20 1.370(7)
C2 C3 1.514(8)	C15 C16 1.402(7)
C3 C4 1.515(8)	C15 N1 1.446(6)
C4 C5 1.526(7)	C16 O1 1.355(6)
C5 N1 1.489(6)	C16 C17 1.399(7)
C6 C7 1.393(7)	C17 C18 1.387(8)
C6 C11 1.397(6)	C18 C19 1.385(8)
C6 N2 1.459(6)	C19 C20 1.389(8)
C7 C8 1.400(7)	C21 O1 1.438(6)
C7 C12 1.497(7)	F1 B1 1.302(5)
C8 C9 1.378(7)	F2 B1 1.399(5)
C9 C10 1.388(7)	F3 B1 1.392(5)
C9 C13 1.513(7)	F4 B1 1.467(4)

Table H. 3: Bond angles (°) for (7-*o*-MeOPh-Mes).

N2 C1 N1 126.2(5)	O1 C16 C17 124.5(5)
N2 C2 C3 113.3(4)	O1 C16 C15 116.7(4)
C4 C3 C2 112.3(4)	C17 C16 C15 118.8(5)
C3 C4 C5 113.1(5)	C18 C17 C16 119.7(5)
N1 C5 C4 112.1(4)	C17 C18 C19 121.1(5)
C7 C6 C11 122.8(4)	C20 C19 C18 118.9(5)
C7 C6 N2 117.8(4)	C15 C20 C19 120.9(5)
C11 C6 N2 119.2(4)	C1 N1 C15 116.7(4)
C6 C7 C8 116.9(4)	C1 N1 C5 125.3(4)
C6 C7 C12 121.9(4)	C15 N1 C5 117.9(4)
C8 C7 C12 121.2(4)	C1 N2 C6 119.0(4)
C9 C8 C7 122.7(5)	C1 N2 C2 122.2(4)
C8 C9 C10 118.0(4)	C6 N2 C2 117.3(4)
C8 C9 C13 121.5(5)	C16 O1 C21 117.2(4)
C10 C9 C13 120.4(5)	F1 B1 F3 115.7(4)
C9 C10 C11 122.4(4)	F1 B1 F2 113.2(4)
C6 C11 C10 117.0(4)	F3 B1 F2 108.4(3)
C6 C11 C14 122.5(4)	F1 B1 F4 108.3(3)
C10 C11 C14 120.4(4)	F3 B1 F4 105.2(3)
C20 C15 C16 120.6(5)	F2 B1 F4 105.2(3)
C20 C15 N1 120.4(4)	C16 C15 N1 119.0(4)

Appendix 2. Tables of Bond Distances and Angles

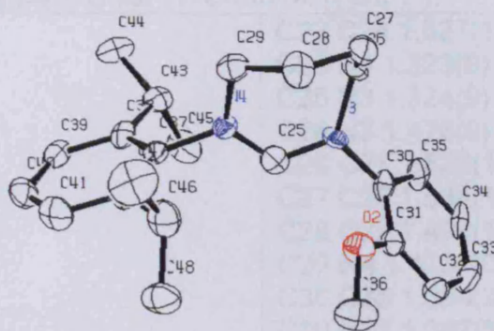


Table I. 1: Crystal data and structure refinement for (7-o-MeOPh-DIPP).

Identification code	kjc0839b	
Empirical formula	C ₂₄ H ₃₀ I N ₂ O	
Formula weight	489.40	
Temperature	150(2) K	
Wavelength	0.71073 Å	
Crystal system	Monoclinic	
Space group	P2 ₁ /n	
Unit cell dimensions	a = 10.4370(3) Å	a = 90°.
	b = 19.2770(7) Å	β = 91.811(2)°.
	c = 23.4090(8) Å	γ = 90°.
Volume	4707.4(3) Å ³	
Z	8	
Density (calculated)	1.381 Mg/m ³	
Absorption coefficient	1.376 mm ⁻¹	
F(000)	1992	
Crystal size	0.31 x 0.08 x 0.06 mm ³	
Theta range for data collection	1.37 to 27.47°.	
Index ranges	-13 ≤ h ≤ 13, -25 ≤ k ≤ 23, -	
	30 ≤ l ≤ 30	
Reflections collected	17345	
Independent reflections	10448 [R(int) = 0.1598]	
Completeness to theta = 27.47°	96.9 %	
Max. and min. transmission	0.9220 and 0.6750	
Refinement method	Full-matrix least-squares on F ²	
Data / restraints / parameters	10448 / 0 / 515	
Goodness-of-fit on F ²	0.892	
Final R indices [I > 2σ(I)]	R1 = 0.0739, wR2 = 0.1109	
R indices (all data)	R1 = 0.2458, wR2 = 0.1549	
Largest diff. peak and hole	0.654 and -0.749 e.Å ⁻³	

Table I. 2: Bond lengths (Å) for (7-*o*-MeOPh-DIPP).

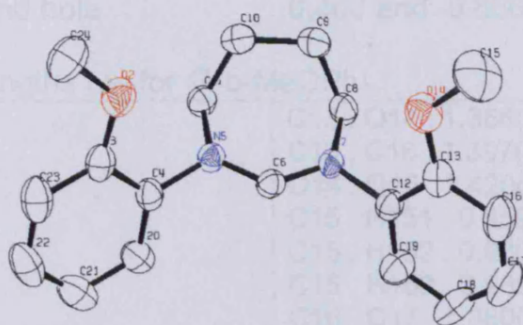
C36 O2 1.438(9)	C22 C24 1.527(10)
C1 N1 1.301(9)	C25 N4 1.323(9)
C1 N2 1.327(9)	C25 N3 1.324(9)
C2 N1 1.488(10)	C26 N3 1.476(9)
C2 C3 1.506(10)	C26 C27 1.522(10)
C3 C4 1.547(10)	C27 C28 1.544(10)
C4 C5 1.524(10)	C28 C29 1.499(10)
C5 N2 1.487(10)	C29 N4 1.473(10)
C6 C11 1.364(10)	C30 C35 1.384(9)
C6 C7 1.405(11)	C30 C31 1.387(10)
C6 N1 1.438(9)	C30 N3 1.449(9)
C7 O1 1.365(8)	C31 O2 1.357(9)
C7 C8 1.393(10)	C31 C32 1.408(10)
C8 C9 1.374(11)	C32 C33 1.371(10)
C9 C10 1.364(12)	C33 C34 1.363(11)
C10 C11 1.382(10)	C34 C35 1.388(11)
C12 O1 1.432(9)	C37 C38 1.395(10)
C13 C14 1.381(10)	C37 C42 1.395(10)
C13 C18 1.401(10)	C37 N4 1.467(10)
C13 N2 1.467(9)	C38 C39 1.380(10)
C14 C15 1.388(11)	C38 C43 1.523(10)
C14 C19 1.509(10)	C39 C40 1.397(11)
C15 C16 1.392(11)	C40 C41 1.382(11)
C16 C17 1.369(10)	C41 C42 1.399(11)
C17 C18 1.400(10)	C42 C46 1.513(10)
C18 C22 1.507(10)	C43 C45 1.531(10)
C19 C21 1.528(9)	C43 C44 1.533(9)
C19 C20 1.532(10)	C46 C48 1.536(12)
C22 C23 1.516(11)	C46 C47 1.560(11)

Table I. 3: Bond angles (°) for (7-*o*-MeOPh-DIPP).

N1 C1 N2 126.8(8)	C35 C30 C31 121.5(7)
N1 C2 C3 112.3(6)	C35 C30 N3 120.2(7)
C2 C3 C4 112.0(7)	C31 C30 N3 118.3(7)
C5 C4 C3 114.4(6)	O2 C31 C30 116.5(7)
N2 C5 C4 112.9(6)	O2 C31 C32 125.8(7)
C11 C6 C7 120.8(8)	C30 C31 C32 117.7(8)
C11 C6 N1 121.4(8)	C33 C32 C31 120.6(8)
C7 C6 N1 117.8(7)	C34 C33 C32 120.6(8)
O1 C7 C8 125.6(8)	C33 C34 C35 120.5(8)
O1 C7 C6 115.7(7)	C30 C35 C34 119.0(8)
C8 C7 C6 118.7(8)	C38 C37 C42 124.0(8)
C9 C8 C7 119.0(9)	C38 C37 N4 117.7(7)
C10 C9 C8 121.6(8)	C42 C37 N4 118.3(7)
C9 C10 C11 120.0(8)	C39 C38 C37 117.2(8)
C6 C11 C10 119.5(9)	C39 C38 C43 119.5(7)
C14 C13 C18 125.2(7)	C37 C38 C43 123.1(7)
C14 C13 N2 116.9(7)	C38 C39 C40 120.6(7)
C18 C13 N2 117.8(6)	C41 C40 C39 120.8(8)
C13 C14 C15 116.4(8)	C40 C41 C42 120.6(8)
C13 C14 C19 123.1(7)	C37 C42 C41 116.6(7)
C15 C14 C19 120.3(7)	C37 C42 C46 123.8(7)

Appendix 2. Tables of Bond Distances and Angles

C16 C15 C14 121.0(7)	C41 C42 C46 119.6(8)
C17 C16 C15 120.4(8)	C38 C43 C45 110.1(7)
C16 C17 C18 121.5(8)	C38 C43 C44 114.3(6)
C13 C18 C17 115.5(7)	C45 C43 C44 110.5(7)
C13 C18 C22 124.4(7)	C42 C46 C48 110.6(8)
C17 C18 C22 120.0(7)	C42 C46 C47 111.4(6)
C14 C19 C21 113.8(6)	C48 C46 C47 111.7(7)
C14 C19 C20 109.3(7)	C7 O1 C12 117.2(6)
C21 C19 C20 110.4(7)	C31 O2 C36 116.8(6)
C18 C22 C23 112.1(7)	C1 N1 C6 117.8(7)
C18 C22 C24 110.3(6)	C1 N1 C2 122.6(7)
C23 C22 C24 111.1(7)	C6 N1 C2 119.4(6)
N4 C25 N3 125.6(8)	C1 N2 C13 118.5(7)
N3 C26 C27 112.2(6)	C1 N2 C5 125.0(7)
C26 C27 C28 111.2(7)	C13 N2 C5 116.3(6)
C29 C28 C27 114.9(7)	C25 N3 C30 116.9(7)
C25 N4 C29 125.3(7)	C25 N3 C26 123.5(7)
C37 N4 C29 117.1(6)	C30 N3 C26 119.6(6)
N4 C29 C28 112.9(6)	C25 N4 C37 117.4(7)


Table J.1: Crystal data and structure refinement for (7-*o*-MeOPh).

Identification code	kjc0729
Empirical formula	C ₁₉ H ₂₃ I N ₂ O ₂
Formula weight	438.29
Temperature	296(2) K
Wavelength	0.71073 Å
Crystal system	Triclinic
Space group	P-1
Unit cell dimensions	$a = 7.89000(10)$ Å $a = 106.1680(10)^\circ$. $b = 10.2100(2)$ Å $\beta = 94.4780(10)^\circ$. $c = 12.9030(3)$ Å $\gamma = 104.8850(10)^\circ$.
Volume	$952.20(3)$ Å ³
Z	2
Density (calculated)	1.529 Mg/m ³
Absorption coefficient	1.694 mm ⁻¹
F(000)	440
Crystal size	0.20 x 0.08 x 0.04 mm ³
Theta range for data collection	1.66 to 27.49°.
Index ranges	-10 ≤ h ≤ 10, -13 ≤ k ≤ 13, -
	16 ≤ l ≤ 16
Reflections collected	8036
Independent reflections	4344 [R(int) = 0.0349]
Completeness to theta = 27.49°	99.3 %
Absorption correction	Empirical
Max. and min. transmission	0.9353 and 0.7281
Refinement method	Full-matrix least-squares on F ²
Data / restraints / parameters	4344 / 0 / 219
Goodness-of-fit on F ²	1.060
Final R indices [I > 2σ(I)]	R1 = 0.0370, wR2 = 0.1104
R indices (all data)	R1 = 0.0538, wR2 = 0.1405

Largest diff. peak and hole

0.460 and -0.666 e.Å⁻³**Table J. 2:** Bond lengths (Å) for (7-*o*-MeOPh).

O2 . C3 . 1.358(4)	C13 . O14 . 1.358(4)
O2 . C24 . 1.432(4)	C13 . C16 . 1.397(5)
C3 . C4 . 1.400(4)	O14 . C15 . 1.420(5)
C3 . C23 . 1.392(5)	C15 . H151 . 0.959
C4 . N5 . 1.445(4)	C15 . H152 . 0.980
C4 . C20 . 1.370(4)	C15 . H153 . 0.985
N5 . C6 . 1.310(4)	C16 . C17 . 1.380(6)
N5 . C11 . 1.487(4)	C16 . H161 . 0.928
C6 . N7 . 1.309(4)	C17 . C18 . 1.364(6)
C6 . H61 . 0.936	C17 . H171 . 0.938
N7 . C8 . 1.492(4)	C18 . C19 . 1.381(5)
N7 . C12 . 1.451(4)	C18 . H181 . 0.923
C8 . C9 . 1.506(4)	C19 . H191 . 0.959
C8 . H81 . 0.955	C20 . C21 . 1.392(5)
C8 . H82 . 0.978	C20 . H201 . 0.960
C9 . C10 . 1.519(5)	C21 . C22 . 1.372(5)
C9 . H91 . 0.979	C21 . H211 . 0.935
C9 . H92 . 0.970	C22 . C23 . 1.370(5)
C10 . C11 . 1.502(4)	C22 . H221 . 0.926
C10 . H101 . 0.968	C23 . H231 . 0.943
C10 . H102 . 0.973	C24 . H241 . 0.980
C11 . H111 . 0.983	C24 . H242 . 1.004
C11 . H112 . 0.984	C24 . H243 . 0.989
C12 . C13 . 1.382(5)	C12 . C19 . 1.378(5)

Table J. 3: Bond angles (°) for (7-*o*-MeOPh).

C3 . O2 . C24 . 118.0(3)	C12 . C13 . O14 . 115.8(3)
O2 . C3 . C4 . 115.8(3)	C12 . C13 . C16 . 118.3(3)
O2 . C3 . C23 . 125.8(3)	O14 . C13 . C16 . 125.9(3)
C4 . C3 . C23 . 118.4(3)	C13 . O14 . C15 . 118.1(3)
C3 . C4 . N5 . 118.4(3)	O14 . C15 . H151 . 107.6
C3 . C4 . C20 . 121.2(3)	O14 . C15 . H152 . 106.4
N5 . C4 . C20 . 120.4(3)	H151 . C15 . H152 . 110.0
C4 . N5 . C6 . 117.0(2)	O14 . C15 . H153 . 109.9
C4 . N5 . C11 . 117.6(2)	H151 . C15 . H153 . 110.7
C6 . N5 . C11 . 124.9(2)	H152 . C15 . H153 . 112.0
N5 . C6 . N7 . 129.3(3)	C13 . C16 . C17 . 119.2(4)
N5 . C6 . H61 . 116.5	C13 . C16 . H161 . 119.1
N7 . C6 . H61 . 114.2	C17 . C16 . H161 . 121.7
C6 . N7 . C8 . 125.2(2)	C16 . C17 . C18 . 121.8(4)
C6 . N7 . C12 . 117.7(2)	C16 . C17 . H171 . 121.1
C8 . N7 . C12 . 116.7(2)	C18 . C17 . H171 . 117.1
N7 . C8 . C9 . 113.4(3)	C17 . C18 . C19 . 119.7(4)
N7 . C8 . H81 . 107.8	C17 . C18 . H181 . 118.0
C9 . C8 . H81 . 109.1	C19 . C18 . H181 . 122.2
N7 . C8 . H82 . 108.9	C18 . C19 . C12 . 119.0(4)
C9 . C8 . H82 . 110.8	C18 . C19 . H191 . 122.1
H81 . C8 . H82 . 106.4	C12 . C19 . H191 . 118.8
C8 . C9 . C10 . 116.4(3)	C4 . C20 . C21 . 119.5(3)
C8 . C9 . H91 . 106.3	C4 . C20 . H201 . 117.7

Appendix 2. Tables of Bond Distances and Angles

C10 . C9 . H91 . 112.1	C21 . C20 . H201 . 122.8
C8 . C9 . H92 . 106.7	C20 . C21 . C22 . 119.6(4)
C10 . C9 . H92 . 106.1	C20 . C21 . H211 . 121.3
H91 . C9 . H92 . 108.8	C22 . C21 . H211 . 119.1
C9 . C10 . C11 . 116.9(3)	C21 . C22 . C23 . 121.3(3)
C9 . C10 . H101 . 108.4	C21 . C22 . H221 . 119.0
C11 . C10 . H101 . 104.9	C23 . C22 . H221 . 119.7
C9 . C10 . H102 . 109.0	C3 . C23 . C22 . 120.1(3)
C11 . C10 . H102 . 109.5	C3 . C23 . H231 . 119.2
H101 . C10 . H102 . 107.7	C22 . C23 . H231 . 120.7
C10 . C11 . N5 . 113.2(3)	O2 . C24 . H241 . 108.0
C10 . C11 . H111 . 110.5	O2 . C24 . H242 . 111.7
N5 . C11 . H111 . 107.9	H241 . C24 . H242 . 109.6
C10 . C11 . H112 . 107.5	O2 . C24 . H243 . 109.2
N5 . C11 . H112 . 107.6	H241 . C24 . H243 . 111.0
H111 . C11 . H112 . 110.1	H242 . C24 . H243 . 107.4
N7 . C12 . C13 . 118.6(3)	C13 . C12 . C19 . 122.0(3)
N7 . C12 . C19 . 119.5(3)	

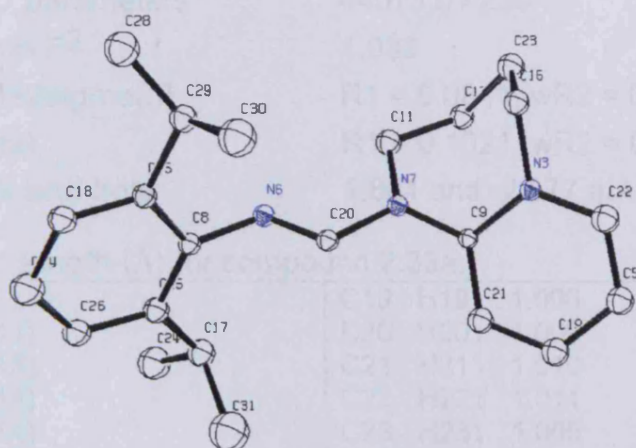


Table K.1: Crystal data and structure refinement for compound 2.33a (see chapter two).

Identification code	kjc0707
Empirical formula	C ₂₂ H ₃₀ I N ₃
Formula weight	463.39
Temperature	150(2) K
Wavelength	0.71073 Å
Crystal system	Monoclinic
Space group	P21/c
Unit cell dimensions	a = 8.47200(10) Å a = 90°. b = 33.8750(6) Å β = 116.8380(10)°. c = 8.3760(2) Å γ = 90°.
Volume	2144.90(7) Å ³
Z	4
Density (calculated)	1.435 Mg/m ³
Absorption coefficient	1.503 mm ⁻¹
F(000)	944
Crystal size	0.20 x 0.20 x 0.10 mm ³
Theta range for data collection	2.95 to 27.49°.
Index ranges	-11 ≤ h ≤ 10, -32 ≤ k ≤ 43, -7 ≤ l ≤ 10
Reflections collected	11030
Independent reflections	4407 [R(int) = 0.1177]
Completeness to theta = 27.49°	89.7 %
Absorption correction	Empirical
Max. and min. transmission	0.8642 and 0.7531
Refinement method	Full-matrix least-squares on F ²

Data / restraints / parameters	4407 / 0 / 239
Goodness-of-fit on F ²	1.033
Final R indices [$I > 2\sigma(I)$]	R1 = 0.0811, wR2 = 0.2183
R indices (all data)	R1 = 0.1021, wR2 = 0.2361
Largest diff. peak and hole	1.861 and -2.577 e.Å ⁻³

Table k. 2: Bond length (Å) for compound 2.33a.

N3 . C9 . 1.378(11)	C19 . H191 . 1.006
N3 . C16 . 1.475(11)	C20 . H201 . 1.009
N3 . C22 . 1.354(13)	C21 . H211 . 1.010
C5 . C19 . 1.393(14)	C22 . H221 . 1.011
C5 . C22 . 1.385(14)	C23 . H231 . 1.006
C5 . H51 . 1.013 no	C23 . H232 . 1.007
N6 . C8 . 1.419(11)	C24 . H241 . 1.002
N6 . C20 . 1.266(12)	C24 . H242 . 1.003
N7 . C9 . 1.368(12)	C24 . H243 . 1.006
N7 . C11 . 1.500(12)	C25 . C26 . 1.403(13)
N7 . C20 . 1.399(11)	C26 . H261 . 1.012
C8 . C15 . 1.415(12)	C28 . C29 . 1.508(15)
C8 . C25 . 1.419(13)	C28 . H281 . 1.007
C9 . C21 . 1.401(12)	C28 . H282 . 1.004
C11 . C12 . 1.512(13)	C28 . H283 . 1.006
C11 . H111 . 1.006	C29 . C30 . 1.551(17)
C11 . H112 . 1.005	C29 . H291 . 1.011
C12 . C23 . 1.540(14)	C30 . H301 . 1.005
C12 . H121 . 1.002	C30 . H302 . 1.001
C12 . H122 . 1.009	C30 . H303 . 1.012
C14 . C18 . 1.384(15)	C31 . H311 . 1.008
C14 . C26 . 1.387(14)	C31 . H312 . 1.003
C14 . H141 . 1.010	C31 . H313 . 1.000
C15 . C18 . 1.374(13)	C17 . C24 . 1.529(17)
C15 . C29 . 1.514(13)	C17 . C25 . 1.509(13)
C16 . C23 . 1.531(14)	C17 . C31 . 1.530(18)
C16 . H161 . 1.009	C17 . H171 . 1.013
C16 . H162 . 1.006	C18 . H181 . 1.012
	C19 . C21 . 1.394(14)

Table K.3: Bond angles (°) for compound 2.33a.

C9 . N3 . C16 . 119.7(8)	C9 . C21 . C19 . 120.2(9)
C9 . N3 . C22 . 121.7(8)	C9 . C21 . H211 . 119.8
C16 . N3 . C22 . 118.6(8)	C19 . C21 . H211 . 120.0
C19 . C5 . C22 . 118.8(10)	C5 . C22 . N3 . 120.9(9)
C19 . C5 . H51 . 120.5	C5 . C22 . H221 . 120.0
C22 . C5 . H51 . 120.7	N3 . C22 . H221 . 119.2
C8 . N6 . C20 . 120.0(8)	C12 . C23 . C16 . 110.6(8)
C9 . N7 . C11 . 124.3(7)	C12 . C23 . H231 . 109.4
C9 . N7 . C20 . 119.4(7)	C16 . C23 . H231 . 109.6
C11 . N7 . C20 . 115.4(8)	C12 . C23 . H232 . 108.7
N6 . C8 . C15 . 117.0(8)	C16 . C23 . H232 . 110.0
N6 . C8 . C25 . 120.8(8)	H231 . C23 . H232 . 108.5

Appendix 2. Tables of Bond Distances and Angles

C15 . C8 . C25 . 121.7(8)	C17 . C24 . H241 . 110.5
N3 . C9 . N7 . 118.5(7)	C17 . C24 . H242 . 110.2
N3 . C9 . C21 . 118.0(8)	H241 . C24 . H242 . 109.0
N7 . C9 . C21 . 123.4(8)	C17 . C24 . H243 . 109.4
N7 . C11 . C12 . 113.3(8)	H241 . C24 . H243 . 108.8
N7 . C11 . H111 . 108.7	H242 . C24 . H243 . 108.8
C12 . C11 . H111 . 108.9	C17 . C25 . C8 . 120.9(8)
N7 . C11 . H112 . 108.8	C17 . C25 . C26 . 122.2(9)
C12 . C11 . H112 . 108.5	C8 . C25 . C26 . 116.9(9)
H111 . C11 . H112 . 108.6	C25 . C26 . C14 . 121.4(10)
C11 . C12 . C23 . 113.0(8)	C25 . C26 . H261 . 119.1
C11 . C12 . H121 . 109.5	C14 . C26 . H261 . 119.4
C23 . C12 . H121 . 109.1	C29 . C28 . H281 . 110.6
C11 . C12 . H122 . 108.5	C29 . C28 . H282 . 110.5
C23 . C12 . H122 . 108.1	H281 . C28 . H282 . 108.6
H121 . C12 . H122 . 108.6	C29 . C28 . H283 . 109.9
C18 . C14 . C26 . 120.0(10)	H281 . C28 . H283 . 108.5
C18 . C14 . H141 . 119.9	H282 . C28 . H283 . 108.7
C26 . C14 . H141 . 120.1	C15 . C29 . C28 . 114.3(9)
C8 . C15 . C18 . 118.2(9)	C15 . C29 . C30 . 109.3(8)
C8 . C15 . C29 . 118.9(8)	C28 . C29 . C30 . 109.4(9)
C18 . C15 . C29 . 122.9(8)	C15 . C29 . H291 . 108.1
N3 . C16 . C23 . 112.1(8)	C28 . C29 . H291 . 107.8
N3 . C16 . H161 . 109.0	C30 . C29 . H291 . 107.8
C23 . C16 . H161 . 109.2	C29 . C30 . H301 . 110.7
N3 . C16 . H162 . 109.1	C29 . C30 . H302 . 110.3
C23 . C16 . H162 . 109.1	H301 . C30 . H302 . 109.0
H161 . C16 . H162 . 108.2	C29 . C30 . H303 . 110.2
C24 . C17 . C25 . 111.2(9)	H301 . C30 . H303 . 108.1
C24 . C17 . C31 . 109.0(10)	H302 . C30 . H303 . 108.4
C25 . C17 . C31 . 111.9(9)	C17 . C31 . H311 . 109.8
C24 . C17 . H171 . 107.7	C17 . C31 . H312 . 110.6
C25 . C17 . H171 . 108.5	H311 . C31 . H312 . 108.6
C31 . C17 . H171 . 108.3	C17 . C31 . H313 . 109.8
C14 . C18 . C15 . 121.6(9)	H311 . C31 . H313 . 108.8
C14 . C18 . H181 . 119.0	H312 . C31 . H313 . 109.3
C15 . C18 . H181 . 119.4	C21 . C19 . H191 . 120.0
C5 . C19 . C21 . 119.8(9)	N7 . C20 . N6 . 119.5(8)
C5 . C19 . H191 . 120.2	N7 . C20 . H201 . 119.8
	N6 . C20 . H201 . 120.7

Appendix 2. Tables of Bond Distances and Angles

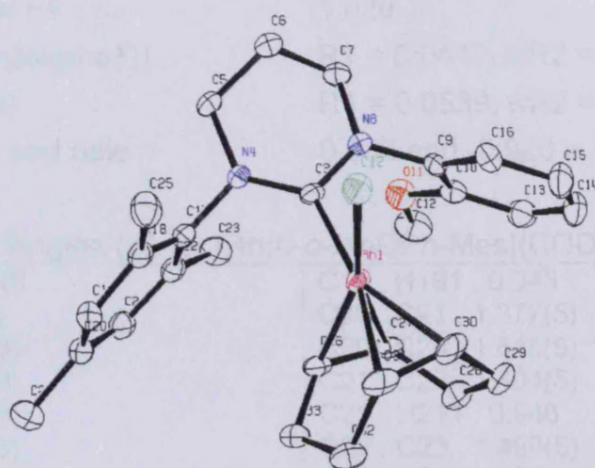


Table L.1: Crystal data and structure refinement for [Rh(6-*o*-MeOPh-Mes)(COD)Cl].

Identification code	kjc0757_2	
Empirical formula	C ₂₉ H ₃₈ Cl ₁ N ₂ O ₂ Rh	
Formula weight	639.87	
Temperature	150(2) K	
Wavelength	0.71073 Å	
Crystal system	Triclinic	
Space group	P-1	
Unit cell dimensions	a = 9.7164(2) Å	a = 86.629(2)°.
	b = 11.4614(4) Å	β = 78.935(2)°.
	c = 13.2888(4) Å	γ = 82.3150(10)°.
Volume	1438.50(7) Å ³	
Z	2	
Density (calculated)	1.477 Mg/m ³	
Absorption coefficient	0.897 mm ⁻¹	
F(000)	660	
Crystal size	0.20 x 0.20 x 0.10 mm ³	
Theta range for data collection	2.97 to 27.49°.	
Index ranges	-12 ≤ h ≤ 12, -14 ≤ k ≤ 14, -	
	17 ≤ l ≤ 16	
Reflections collected	22407	
Independent reflections	6485 [R(int) = 0.1097]	
Completeness to theta = 27.49°	98.4 %	
Max. and min. transmission	0.9156 and 0.8410	
Refinement method	Full-matrix least-squares on F ²	
Data / restraints / parameters	6485 / 0 / 329	

Goodness-of-fit on F ²	1.029
Final R indices [$I > 2\sigma(I)$]	R1 = 0.0417, wR2 = 0.0982
R indices (all data)	R1 = 0.0539, wR2 = 0.1048
Largest diff. peak and hole	0.605 and -0.920 e.Å ⁻³

Table L. 2: Bond lengths (Å) for [Rh(6-*o*-MeOPh-Mes)(COD)Cl].

Rh1 . Cl2 . 2.4052(8)	C19 . H191 . 0.945
Rh1 . C3 . 2.057(3)	C20 . C21 . 1.377(5)
Rh1 . C26 . 2.099(3)	C20 . C24 . 1.515(5)
Rh1 . C27 . 2.119(3)	C21 . C22 . 1.404(5)
Rh1 . C30 . 2.176(3)	C21 . H211 . 0.946
Rh1 . C31 . 2.206(3)	C22 . C23 . 1.498(5)
C3 . N4 . 1.349(4)	C23 . H233 . 0.956
C3 . N8 . 1.341(4)	C23 . H232 . 0.971
N4 . C5 . 1.474(4)	C23 . H231 . 0.946
N4 . C17 . 1.451(4)	C24 . H243 . 0.949
C5 . C6 . 1.518(4)	C24 . H242 . 0.948
C5 . H51 . 0.967	C24 . H241 . 0.952
C5 . H52 . 0.953	C25 . H251 . 0.974
C6 . C7 . 1.505(5)	C25 . H252 . 0.967
C6 . H61 . 0.970	C25 . H253 . 0.958
C6 . H62 . 0.963	C26 . C27 . 1.382(4)
C7 . N8 . 1.470(4)	C26 . C33 . 1.505(4)
C7 . H71 . 0.968	C26 . H261 . 0.973
C7 . H72 . 0.965	C27 . C28 . 1.531(4)
N8 . C9 . 1.445(4)	C27 . H271 . 0.961
C9 . C10 . 1.393(5)	C28 . C29 . 1.528(5)
C9 . C16 . 1.377(5)	C28 . H281 . 0.980
C10 . O11 . 1.370(4)	C28 . H282 . 0.976
C10 . C13 . 1.398(5)	C29 . C30 . 1.514(5)
O11 . C12 . 1.424(4)	C29 . H291 . 0.972
C12 . H121 . 0.956	C29 . H292 . 0.972
C12 . H122 . 0.963	C30 . C31 . 1.378(5)
C12 . H123 . 0.971	C30 . H301 . 0.970
C13 . C14 . 1.382(5)	C31 . C32 . 1.519(5)
C13 . H131 . 0.935	C31 . H311 . 0.985
C14 . C15 . 1.381(5)	C32 . C33 . 1.531(5)
C14 . H141 . 0.926	C32 . H321 . 0.979
C15 . C16 . 1.390(5)	C32 . H322 . 0.982
C15 . H151 . 0.931	C33 . H331 . 0.970
C16 . H161 . 0.948	C33 . H332 . 0.966
C17 . C18 . 1.390(5)	Cl34 . C35 . 1.747(4)
C17 . C22 . 1.398(4)	C35 . Cl36 . 1.750(4)
C18 . C19 . 1.400(4)	C35 . H351 . 0.970
C18 . C25 . 1.503(5)	C35 . H352 . 0.982
C19 . C20 . 1.390(5)	

Table L. 3: Bond angles (°) for [Rh(6-*o*-MeOPh-Mes)(COD)Cl].

Cl2 . Rh1 . C3 . 84.88(8)	C21 . C20 . C24 . 120.5(3)
Cl2 . Rh1 . C26 . 156.44(9)	C20 . C21 . C22 . 122.1(3)
C3 . Rh1 . C26 . 97.19(12)	C20 . C21 . H211 . 118.6
Cl2 . Rh1 . C27 . 164.84(9)	C22 . C21 . H211 . 119.2
C3 . Rh1 . C27 . 98.00(12)	C21 . C22 . C17 . 117.6(3)
C26 . Rh1 . C27 . 38.25(12)	C21 . C22 . C23 . 119.9(3)
Cl2 . Rh1 . C30 . 89.10(10)	C17 . C22 . C23 . 122.5(3)
C3 . Rh1 . C30 . 156.22(13)	C22 . C23 . H233 . 109.9
C26 . Rh1 . C30 . 97.46(13)	C22 . C23 . H232 . 108.3
C27 . Rh1 . C30 . 82.29(13)	H233 . C23 . H232 . 108.4
Cl2 . Rh1 . C31 . 90.74(9)	C22 . C23 . H231 . 111.9
C3 . Rh1 . C31 . 165.76(12)	H233 . C23 . H231 . 109.1
C26 . Rh1 . C31 . 81.52(13)	H232 . C23 . H231 . 109.3
C27 . Rh1 . C31 . 89.75(13)	C20 . C24 . H243 . 111.4
C30 . Rh1 . C31 . 36.64(13)	C20 . C24 . H242 . 110.7
Rh1 . C3 . N4 . 124.7(2)	H243 . C24 . H242 . 109.2
Rh1 . C3 . N8 . 116.7(2)	C20 . C24 . H241 . 111.2
N4 . C3 . N8 . 117.1(3)	H243 . C24 . H241 . 107.5
C3 . N4 . C5 . 124.9(3)	H242 . C24 . H241 . 106.7
C3 . N4 . C17 . 119.2(2)	C18 . C25 . H251 . 110.7
C5 . N4 . C17 . 114.8(2)	C18 . C25 . H252 . 110.5
N4 . C5 . C6 . 110.1(3)	H251 . C25 . H252 . 107.9
N4 . C5 . H51 . 107.1	C18 . C25 . H253 . 111.3
C6 . C5 . H51 . 110.8	H251 . C25 . H253 . 107.9
N4 . C5 . H52 . 110.5	H252 . C25 . H253 . 108.4
C6 . C5 . H52 . 109.0	Rh1 . C26 . C27 . 71.66(17)
H51 . C5 . H52 . 109.3	Rh1 . C26 . C33 . 110.7(2)
C5 . C6 . C7 . 109.2(3)	C27 . C26 . C33 . 126.3(3)
C5 . C6 . H61 . 110.8	Rh1 . C26 . H261 . 109.8
C7 . C6 . H61 . 109.3	C27 . C26 . H261 . 116.0
C5 . C6 . H62 . 109.5	C33 . C26 . H261 . 112.9
C7 . C6 . H62 . 109.5	C26 . C27 . Rh1 . 70.08(17)
H61 . C6 . H62 . 108.4	C26 . C27 . C28 . 124.0(3)
C6 . C7 . N8 . 108.4(3)	Rh1 . C27 . C28 . 112.8(2)
C6 . C7 . H71 . 111.3	C26 . C27 . H271 . 115.5
N8 . C7 . H71 . 110.1	Rh1 . C27 . H271 . 110.3
C6 . C7 . H72 . 110.3	C28 . C27 . H271 . 114.7
N8 . C7 . H72 . 110.3	C27 . C28 . C29 . 113.4(3)
H71 . C7 . H72 . 106.6	C27 . C28 . H281 . 108.7
C7 . N8 . C3 . 124.2(3)	C29 . C28 . H281 . 109.5
C7 . N8 . C9 . 116.6(2)	C27 . C28 . H282 . 108.4
C3 . N8 . C9 . 118.4(2)	C29 . C28 . H282 . 107.9
N8 . C9 . C10 . 117.8(3)	H281 . C28 . H282 . 108.9
N8 . C9 . C16 . 121.9(3)	C28 . C29 . C30 . 113.3(3)
C10 . C9 . C16 . 120.3(3)	C28 . C29 . H291 . 110.0
C9 . C10 . O11 . 115.2(3)	C30 . C29 . H291 . 108.9
C9 . C10 . C13 . 120.1(3)	C28 . C29 . H292 . 106.7
O11 . C10 . C13 . 124.7(3)	C30 . C29 . H292 . 109.2
C10 . O11 . C12 . 118.1(3)	H291 . C29 . H292 . 108.5
O11 . C12 . H121 . 106.7	C29 . C30 . Rh1 . 108.8(2)
O11 . C12 . H122 . 109.1	C29 . C30 . C31 . 125.2(3)
H121 . C12 . H122 . 110.9	Rh1 . C30 . C31 . 72.87(18)
O11 . C12 . H123 . 110.5	C29 . C30 . H301 . 114.8

Appendix 2. Tables of Bond Distances and Angles

H121 . C12 . H123 . 110.2	Rh1 . C30 . H301 . 109.3
H122 . C12 . H123 . 109.4	C31 . C30 . H301 . 115.6
C10 . C13 . C14 . 118.8(3)	Rh1 . C31 . C30 . 70.49(19)
C10 . C13 . H131 . 121.4	Rh1 . C31 . C32 . 111.4(2)
C14 . C13 . H131 . 119.8	C30 . C31 . C32 . 124.1(3)
C13 . C14 . C15 . 121.1(3)	Rh1 . C31 . H311 . 109.0
C13 . C14 . H141 . 119.9	C30 . C31 . H311 . 117.4
C15 . C14 . H141 . 119.0	C32 . C31 . H311 . 114.1
C14 . C15 . C16 . 119.9(3)	C31 . C32 . C33 . 111.7(3)
C14 . C15 . H151 . 120.6	C31 . C32 . H321 . 110.1
C16 . C15 . H151 . 119.5	C33 . C32 . H321 . 108.8
C15 . C16 . C9 . 119.8(3)	C31 . C32 . H322 . 109.6
C15 . C16 . H161 . 121.1	C33 . C32 . H322 . 109.2
C9 . C16 . H161 . 119.0	H321 . C32 . H322 . 107.4
N4 . C17 . C18 . 121.3(3)	C32 . C33 . C26 . 113.8(3)
N4 . C17 . C22 . 116.9(3)	C32 . C33 . H331 . 110.0
C18 . C17 . C22 . 121.7(3)	C26 . C33 . H331 . 109.7
C17 . C18 . C19 . 118.4(3)	C32 . C33 . H332 . 108.1
C17 . C18 . C25 . 121.6(3)	C26 . C33 . H332 . 106.4
C19 . C18 . C25 . 120.0(3)	H331 . C33 . H332 . 108.7
C18 . C19 . C20 . 121.3(3)	Cl34 . C35 . Cl36 . 112.2(2)
C18 . C19 . H191 . 119.5	Cl34 . C35 . H351 . 109.0
C20 . C19 . H191 . 119.2	Cl36 . C35 . H351 . 107.3
C19 . C20 . C21 . 118.8(3)	Cl34 . C35 . H352 . 109.8
C19 . C20 . C24 . 120.7(3)	Cl36 . C35 . H352 . 108.8
	H351 . C35 . H352 . 109.8

Appendix 2. Tables of Bond Distances and Angles

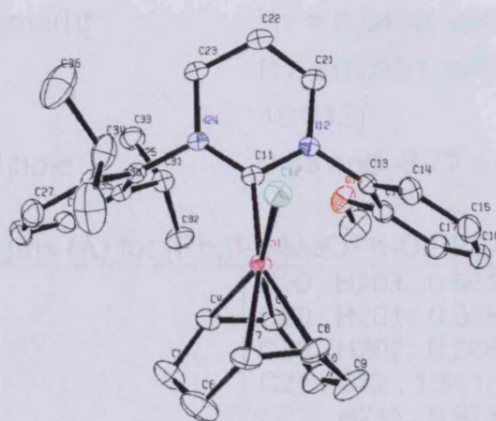


Table M.1: Crystal data and structure refinement for [Rh(6-o-MeOPh-DIPP)(COD)Cl].

Identification code	kjc0807	
Empirical formula	C ₃₁ H ₄₂ Cl ₁ N ₂ O ₁ Rh ₁	
Formula weight	597.05	
Temperature	150 K	
Wavelength	0.71073 Å	
Crystal system	Monoclinic	
Space group	P 1 21/n 1	
Unit cell dimensions	a = 17.4487(3) Å	a = 90°.
	b = 10.4263(2) Å	β = 116.8549(9)°.
	c = 17.7256(4) Å	γ = 90°.
Volume	2876.96(10) Å ³	
Z	4	
Density (calculated)	1.378 Mg/m ³	
Absorption coefficient	0.712 mm ⁻¹	
F(000)	1248	
Crystal size	0.20 x 0.20 x 0.08 mm ³	
Theta range for data collection	2.951 to 27.472°.	
Index ranges	-22 ≤ h ≤ 22, -13 ≤ k ≤ 13, -23 ≤ l ≤ 23	
Reflections collected	47505	
Independent reflections	12657 [R(int) = 0.075]	
Completeness to theta = 27.472°	99.5 %	
Absorption correction	Semi-empirical from equivalents	
Max. and min. transmission	0.94 and 0.87	
Refinement method	Full-matrix least-squares on F ²	
Data / restraints / parameters	12657 / 0 / 326	
Goodness-of-fit on F ²	0.9621	

Final R indices [$I > 2\sigma(I)$]	R1 = 0.0470, wR2 = 0.0874
R indices (all data)	R1 = 0.0721, wR2 = 0.0974
Extinction coefficient	181(12)
Largest diff. peak and hole	0.88 and -0.77 e.Å ⁻³

Table M. 2: Bond lengths (Å) for [Rh(6-o-MeOPh-DIPP)(COD)Cl].

Rh1 . C12 . 2.4010(6)	C20 . H203 . 0.961
Rh1 . C3 . 2.121(2)	C20 . H201 . 0.968
Rh1 . C4 . 2.102(2)	C20 . H202 . 0.966
Rh1 . C7 . 2.202(2)	C21 . C22 . 1.511(4)
Rh1 . C8 . 2.175(2)	C21 . H211 . 0.978
Rh1 . C11 . 2.049(2)	C21 . H212 . 0.982
C3 . C4 . 1.402(3)	C22 . C23 . 1.505(4)
C3 . C10 . 1.522(3)	C22 . H221 . 0.973
C3 . H31 . 0.993	C22 . H222 . 0.976
C4 . C5 . 1.507(3)	C23 . N24 . 1.480(3)
C4 . H41 . 0.991	C23 . H231 . 0.981
C5 . C6 . 1.495(4)	C23 . H232 . 0.986
C5 . H51 . 0.962	N24 . C25 . 1.450(3)
C5 . H52 . 0.990	C25 . C26 . 1.405(3)
C6 . C7 . 1.511(4)	C25 . C30 . 1.403(3)
C6 . H61 . 0.996	C26 . C27 . 1.393(4)
C6 . H62 . 0.965	C26 . C34 . 1.518(4)
C7 . C8 . 1.369(4)	C27 . C28 . 1.375(4)
C7 . H71 . 0.972	C27 . H271 . 0.947
C8 . C9 . 1.518(4)	C28 . C29 . 1.384(4)
C8 . H81 . 0.993	C28 . H281 . 0.936
C9 . C10 . 1.488(4)	C29 . C30 . 1.395(3)
C9 . H92 . 0.964	C29 . H291 . 0.943
C9 . H91 . 1.000	C30 . C31 . 1.522(3)
C10 . H101 . 0.975	C31 . C32 . 1.534(3)
C10 . H102 . 0.993	C31 . C33 . 1.538(3)
C11 . N12 . 1.349(3)	C31 . H311 . 0.978
C11 . N24 . 1.349(3)	C32 . H322 . 0.972
N12 . C13 . 1.436(3)	C32 . H321 . 0.970
N12 . C21 . 1.465(3)	C32 . H323 . 0.973
C13 . C14 . 1.383(3)	C33 . H333 . 0.965
C13 . C18 . 1.401(3)	C33 . H331 . 0.967
C14 . C15 . 1.391(4)	C33 . H332 . 0.966
C14 . H141 . 0.935	C34 . C35 . 1.534(4)
C15 . C16 . 1.372(4)	C34 . C36 . 1.538(4)
C15 . H151 . 0.947	C34 . H341 . 0.976
C16 . C17 . 1.384(4)	C35 . H351 . 0.953
C16 . H161 . 0.946	C35 . H353 . 0.975
C17 . C18 . 1.393(3)	C35 . H352 . 0.969
C17 . H171 . 0.935	C36 . H362 . 0.963
C18 . O19 . 1.367(3)	C36 . H361 . 0.971
O19 . C20 . 1.425(3)	C36 . H363 . 0.969

Table M. 3: Bond angles ($^{\circ}$) for [Rh(6-*o*-MeOPh-DIPP)(COD)Cl].

Cl2 . Rh1 . C3 . 164.75(7)	C13 . C18 . O19 . 115.6(2)
Cl2 . Rh1 . C4 . 156.16(7)	C17 . C18 . O19 . 124.9(2)
C3 . Rh1 . C4 . 38.78(9)	C18 . O19 . C20 . 117.7(2)
Cl2 . Rh1 . C7 . 90.44(7)	O19 . C20 . H203 . 107.2
C3 . Rh1 . C7 . 91.19(9)	O19 . C20 . H201 . 109.1
C4 . Rh1 . C7 . 81.38(9)	H203 . C20 . H201 . 110.6
Cl2 . Rh1 . C8 . 90.32(7)	O19 . C20 . H202 . 108.7
C3 . Rh1 . C8 . 82.07(9)	H203 . C20 . H202 . 109.6
C4 . Rh1 . C8 . 95.99(10)	H201 . C20 . H202 . 111.6
C7 . Rh1 . C8 . 36.43(10)	N12 . C21 . C22 . 108.5(2)
Cl2 . Rh1 . C11 . 84.60(6)	N12 . C21 . H211 . 109.1
C3 . Rh1 . C11 . 96.81(9)	C22 . C21 . H211 . 110.3
C4 . Rh1 . C11 . 98.35(9)	N12 . C21 . H212 . 110.3
C7 . Rh1 . C11 . 166.80(10)	C22 . C21 . H212 . 108.7
C8 . Rh1 . C11 . 155.33(10)	H211 . C21 . H212 . 109.8
Rh1 . C3 . C4 . 69.88(13)	C21 . C22 . C23 . 109.0(2)
Rh1 . C3 . C10 . 112.65(16)	C21 . C22 . H221 . 109.8
C4 . C3 . C10 . 122.8(2)	C23 . C22 . H221 . 109.6
Rh1 . C3 . H31 . 111.8	C21 . C22 . H222 . 109.5
C4 . C3 . H31 . 116.3	C23 . C22 . H222 . 109.1
C10 . C3 . H31 . 114.5	H221 . C22 . H222 . 109.9
C3 . C4 . Rh1 . 71.34(13)	C22 . C23 . N24 . 110.3(2)
C3 . C4 . C5 . 126.5(2)	C22 . C23 . H231 . 110.8
Rh1 . C4 . C5 . 111.12(16)	N24 . C23 . H231 . 109.5
C3 . C4 . H41 . 114.8	C22 . C23 . H232 . 108.2
Rh1 . C4 . H41 . 112.0	N24 . C23 . H232 . 108.1
C5 . C4 . H41 . 112.9	H231 . C23 . H232 . 109.9
C4 . C5 . C6 . 115.1(2)	C23 . N24 . C11 . 124.39(19)
C4 . C5 . H51 . 109.6	C23 . N24 . C25 . 114.60(18)
C6 . C5 . H51 . 109.8	C11 . N24 . C25 . 120.37(19)
C4 . C5 . H52 . 107.9	N24 . C25 . C26 . 120.3(2)
C6 . C5 . H52 . 104.5	N24 . C25 . C30 . 117.5(2)
H51 . C5 . H52 . 109.6	C26 . C25 . C30 . 122.2(2)
C5 . C6 . C7 . 113.6(2)	C25 . C26 . C27 . 117.4(2)
C5 . C6 . H61 . 107.1	C25 . C26 . C34 . 122.8(2)
C7 . C6 . H61 . 108.4	C27 . C26 . C34 . 119.8(2)
C5 . C6 . H62 . 109.2	C26 . C27 . C28 . 121.5(2)
C7 . C6 . H62 . 109.8	C26 . C27 . H271 . 118.9
H61 . C6 . H62 . 108.7	C28 . C27 . H271 . 119.6
C6 . C7 . Rh1 . 111.24(16)	C27 . C28 . C29 . 120.3(2)
C6 . C7 . C8 . 123.3(3)	C27 . C28 . H281 . 119.9
Rh1 . C7 . C8 . 70.71(14)	C29 . C28 . H281 . 119.7
C6 . C7 . H71 . 114.3	C28 . C29 . C30 . 120.9(2)
Rh1 . C7 . H71 . 109.3	C28 . C29 . H291 . 119.7
C8 . C7 . H71 . 117.7	C30 . C29 . H291 . 119.4
Rh1 . C8 . C7 . 72.86(14)	C25 . C30 . C29 . 117.7(2)
Rh1 . C8 . C9 . 108.30(16)	C25 . C30 . C31 . 123.2(2)
C7 . C8 . C9 . 126.7(3)	C29 . C30 . C31 . 119.1(2)
Rh1 . C8 . H81 . 109.5	C30 . C31 . C32 . 112.3(2)
C7 . C8 . H81 . 115.4	C30 . C31 . C33 . 110.6(2)
C9 . C8 . H81 . 113.8	C32 . C31 . C33 . 109.5(2)
C8 . C9 . C10 . 114.8(2)	C30 . C31 . H311 . 108.8
C8 . C9 . H92 . 108.6	C32 . C31 . H311 . 107.6

Appendix 2. Tables of Bond Distances and Angles

C10 . C9 . H92 . 110.5	C33 . C31 . H311 . 107.8
C8 . C9 . H91 . 107.3	C31 . C32 . H322 . 108.9
C10 . C9 . H91 . 106.0	C31 . C32 . H321 . 109.8
H92 . C9 . H91 . 109.6	H322 . C32 . H321 . 110.1
C3 . C10 . C9 . 114.3(2)	C31 . C32 . H323 . 108.3
C3 . C10 . H101 . 109.1	H322 . C32 . H323 . 110.2
C9 . C10 . H101 . 110.6	H321 . C32 . H323 . 109.5
C3 . C10 . H102 . 108.0	C31 . C33 . H333 . 110.3
C9 . C10 . H102 . 106.5	C31 . C33 . H331 . 109.8
H101 . C10 . H102 . 108.1	H333 . C33 . H331 . 108.7
Rh1 . C11 . N12 . 115.85(16)	C31 . C33 . H332 . 109.9
Rh1 . C11 . N24 . 125.86(17)	H333 . C33 . H332 . 109.3
N12 . C11 . N24 . 116.8(2)	H331 . C33 . H332 . 108.8
C11 . N12 . C13 . 118.99(19)	C26 . C34 . C35 . 112.2(3)
C11 . N12 . C21 . 124.4(2)	C26 . C34 . C36 . 110.3(2)
C13 . N12 . C21 . 116.35(19)	C35 . C34 . C36 . 110.8(3)
N12 . C13 . C14 . 121.8(2)	C26 . C34 . H341 . 107.6
N12 . C13 . C18 . 118.2(2)	C35 . C34 . H341 . 107.5
C14 . C13 . C18 . 119.9(2)	C36 . C34 . H341 . 108.3
C13 . C14 . C15 . 120.0(2)	C34 . C35 . H351 . 108.9
C13 . C14 . H141 . 120.1	C34 . C35 . H353 . 109.4
C15 . C14 . H141 . 119.9	H351 . C35 . H353 . 109.0
C14 . C15 . C16 . 119.8(2)	C34 . C35 . H352 . 109.2
C14 . C15 . H151 . 120.2	H351 . C35 . H352 . 109.9
C16 . C15 . H151 . 119.9	H353 . C35 . H352 . 110.4
C15 . C16 . C17 . 121.1(2)	C34 . C36 . H362 . 109.8
C15 . C16 . H161 . 118.8	C34 . C36 . H361 . 109.3
C17 . C16 . H161 . 120.1	H362 . C36 . H361 . 110.0
C16 . C17 . C18 . 119.5(2)	C34 . C36 . H363 . 108.6
C16 . C17 . H171 . 120.3	H362 . C36 . H363 . 110.0
C18 . C17 . H171 . 120.2	H361 . C36 . H363 . 109.1
C13 . C18 . C17 . 119.6(2)	

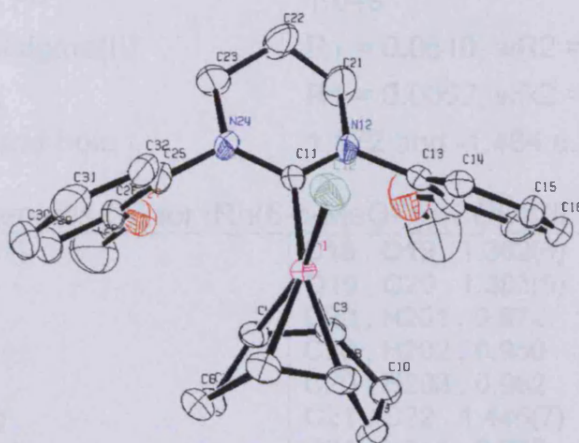


Table N.1: Crystal data and structure refinement for [Rh(6-*o*-MeOPh)(COD)Cl].

Identification code	kjc0801	
Empirical formula	C ₂₉ H ₃₉ Cl N ₂ O ₂ Rh	
Formula weight	585.98	
Temperature	293(2) K	
Wavelength	0.71073 Å	
Crystal system	Monoclinic	
Space group	P21/n	
Unit cell dimensions	a = 9.7607(2) Å	a = 90°.
	b = 18.7624(3) Å	β = 98.0190(10)°.
	c = 14.8596(3) Å	γ = 90°.
Volume	2694.69(9) Å ³	
Z	4	
Density (calculated)	1.444 Mg/m ³	
Absorption coefficient	0.762 mm ⁻¹	
F(000)	1220	
Crystal size	0.40 x 0.10 x 0.10 mm ³	
Theta range for data collection	2.97 to 27.42°.	
Index ranges	-12 ≤ h ≤ 12, -24 ≤ k ≤ 24, -	
	19 ≤ l ≤ 19	
Reflections collected	44792	
Independent reflections	6122 [R(int) = 0.1671]	
Completeness to theta = 27.42°	99.5 %	
Absorption correction	Empirical	
Max. and min. transmission	0.9277 and 0.7504	
Refinement method	Full-matrix least-squares on F ²	
Data / restraints / parameters	6122 / 5 / 318	

Goodness-of-fit on F^2	1.049
Final R indices [$I > 2\sigma(I)$]	R1 = 0.0610, wR2 = 0.1392
R indices (all data)	R1 = 0.0892, wR2 = 0.1535
Largest diff. peak and hole	1.172 and -1.464 e.Å ⁻³

Table N. 2: Bond lengths (Å) for [Rh(6-o-MeOPh)(COD)Cl].

Rh1 . Cl2 . 2.4195(11)	C18 . O19 . 1.362(6)
Rh1 . C3 . 2.099(4)	O19 . C20 . 1.383(9)
Rh1 . C4 . 2.111(4)	C20 . H201 . 0.972
Rh1 . C7 . 2.174(4)	C20 . H202 . 0.950
Rh1 . C8 . 2.213(4)	C20 . H203 . 0.962
Rh1 . C11 . 2.030(4)	C21 . C22 . 1.446(7)
C3 . C4 . 1.401(6)	C21 . H211 . 0.979
C3 . C10 . 1.511(6)	C21 . H212 . 0.989
C3 . H31 . 0.998	C22 . C23 . 1.466(7)
C4 . C5 . 1.524(6)	C22 . H221 . 0.975
C4 . H41 . 0.992	C22 . H222 . 1.021
C5 . C6 . 1.521(7)	C23 . N24 . 1.483(6)
C5 . H51 . 0.965	C23 . H231 . 0.954
C5 . H52 . 0.955	C23 . H232 . 0.969
C6 . C7 . 1.505(6)	N24 . C25 . 1.426(6)
C6 . H61 . 0.981	C25 . C26 . 1.430(9)
C6 . H62 . 0.974	C25 . C32 . 1.366(9)
C7 . C8 . 1.380(6)	C26 . O27 . 1.348(9)
C7 . H71 . 1.006	C26 . C29 . 1.384(9)
C8 . C9 . 1.514(6)	O27 . C28 . 1.429(8)
C8 . H81 . 0.990	C28 . H281 . 0.975
C9 . C10 . 1.520(7)	C28 . H283 . 0.965
C9 . H91 . 0.959	C28 . H282 . 0.976
C9 . H92 . 0.976	C29 . C30 . 1.344(13)
C10 . H101 . 0.987	C29 . H291 . 0.909
C10 . H102 . 0.961	C30 . C31 . 1.388(12)
C11 . N12 . 1.333(5)	C30 . H301 . 0.918
C11 . N24 . 1.357(5)	C31 . C32 . 1.409(8)
N12 . C13 . 1.430(5)	C31 . H311 . 0.922
N12 . C21 . 1.493(6)	C32 . H321 . 0.948
C13 . C14 . 1.364(6)	C33 . C33_2_766 . 1.641(18)
C13 . C18 . 1.400(6)	C33 . C34 . 1.206(11)
C14 . C15 . 1.392(6)	C33 . H331 . 0.950
C14 . H141 . 0.943	C33 . H332 . 0.950
C15 . C16 . 1.361(7)	C34 . C35 . 1.621(13)
C15 . H151 . 0.975	C34 . H341 . 0.950
C16 . C17 . 1.359(7)	C34 . H342 . 0.950
C16 . H161 . 0.942	C35 . H352 . 0.978
C17 . C18 . 1.412(7)	C35 . H351 . 0.974
C17 . H171 . 0.927	C35 . H353 . 0.951

Table N.3: Bond angles (°) for [Rh(6-o-MeOPh)(COD)Cl].

Cl2 . Rh1 . C3 . 155.89(11)	C15 . C16 . H161 . 118.8
Cl2 . Rh1 . C4 . 164.91(12)	C17 . C16 . H161 . 120.8
C3 . Rh1 . C4 . 38.88(15)	C16 . C17 . C18 . 120.2(4)
Cl2 . Rh1 . C7 . 89.65(13)	C16 . C17 . H171 . 121.4

Appendix 2. Tables of Bond Distances and Angles

C3 . Rh1 . C7 . 97.97(17)	C18 . C17 . H171 . 118.4
C4 . Rh1 . C7 . 81.99(17)	C17 . C18 . C13 . 119.1(4)
Cl2 . Rh1 . C8 . 92.01(12)	C17 . C18 . O19 . 123.4(5)
C3 . Rh1 . C8 . 81.07(16)	C13 . C18 . O19 . 117.5(4)
C4 . Rh1 . C8 . 88.75(15)	C18 . O19 . C20 . 117.8(6)
C7 . Rh1 . C8 . 36.65(16)	O19 . C20 . H201 . 108.1
Cl2 . Rh1 . C11 . 90.85(12)	O19 . C20 . H202 . 107.7
C3 . Rh1 . C11 . 90.91(17)	H201 . C20 . H202 . 111.6
C4 . Rh1 . C11 . 91.96(16)	O19 . C20 . H203 . 107.3
C7 . Rh1 . C11 . 156.83(16)	H201 . C20 . H203 . 111.6
C8 . Rh1 . C11 . 166.28(16)	H202 . C20 . H203 . 110.2
Rh1 . C3 . C4 . 71.0(2)	N12 . C21 . C22 . 110.3(4)
Rh1 . C3 . C10 . 110.3(3)	N12 . C21 . H211 . 110.5
C4 . C3 . C10 . 126.0(4)	C22 . C21 . H211 . 106.5
Rh1 . C3 . H31 . 108.7	N12 . C21 . H212 . 109.0
C4 . C3 . H31 . 116.4	C22 . C21 . H212 . 109.6
C10 . C3 . H31 . 113.6	H211 . C21 . H212 . 110.9
C3 . C4 . Rh1 . 70.1(2)	C21 . C22 . C23 . 114.3(5)
C3 . C4 . C5 . 125.1(4)	C21 . C22 . H221 . 110.1
Rh1 . C4 . C5 . 113.2(3)	C23 . C22 . H221 . 108.3
C3 . C4 . H41 . 114.1	C21 . C22 . H222 . 106.7
Rh1 . C4 . H41 . 111.1	C23 . C22 . H222 . 109.4
C5 . C4 . H41 . 114.5	H221 . C22 . H222 . 107.8
C4 . C5 . C6 . 112.4(3)	C22 . C23 . N24 . 110.6(4)
C4 . C5 . H51 . 111.7	C22 . C23 . H231 . 108.2
C6 . C5 . H51 . 109.9	N24 . C23 . H231 . 108.4
C4 . C5 . H52 . 106.8	C22 . C23 . H232 . 112.0
C6 . C5 . H52 . 105.2	N24 . C23 . H232 . 108.0
H51 . C5 . H52 . 110.6	H231 . C23 . H232 . 109.6
C5 . C6 . C7 . 113.6(4)	C23 . N24 . C11 . 124.8(4)
C5 . C6 . H61 . 110.2	C23 . N24 . C25 . 115.6(4)
C7 . C6 . H61 . 108.7	C11 . N24 . C25 . 119.6(3)
C5 . C6 . H62 . 105.4	N24 . C25 . C26 . 117.7(6)
C7 . C6 . H62 . 110.0	N24 . C25 . C32 . 120.3(5)
H61 . C6 . H62 . 108.8	C26 . C25 . C32 . 121.9(5)
C6 . C7 . Rh1 . 107.8(3)	C25 . C26 . O27 . 116.0(5)
C6 . C7 . C8 . 125.1(4)	C25 . C26 . C29 . 117.5(8)
Rh1 . C7 . C8 . 73.2(2)	O27 . C26 . C29 . 126.4(7)
C6 . C7 . H71 . 116.2	C26 . O27 . C28 . 116.6(6)
Rh1 . C7 . H71 . 109.3	O27 . C28 . H281 . 109.4
C8 . C7 . H71 . 114.4	O27 . C28 . H283 . 108.2
Rh1 . C8 . C7 . 70.1(2)	H281 . C28 . H283 . 110.8
Rh1 . C8 . C9 . 111.1(3)	O27 . C28 . H282 . 110.9
C7 . C8 . C9 . 124.6(4)	H281 . C28 . H282 . 109.1
Rh1 . C8 . H81 . 110.9	H283 . C28 . H282 . 108.5
C7 . C8 . H81 . 115.7	C26 . C29 . C30 . 121.1(8)
C9 . C8 . H81 . 114.6	C26 . C29 . H291 . 120.9
C8 . C9 . C10 . 111.6(3)	C30 . C29 . H291 . 118.0
C8 . C9 . H91 . 106.1	C29 . C30 . C31 . 121.7(6)
C10 . C9 . H91 . 109.3	C29 . C30 . H301 . 119.4
C8 . C9 . H92 . 107.2	C31 . C30 . H301 . 118.9
C10 . C9 . H92 . 112.4	C30 . C31 . C32 . 119.6(8)
H91 . C9 . H92 . 110.0	C30 . C31 . H311 . 119.0
C9 . C10 . C3 . 112.8(4)	C32 . C31 . H311 . 121.4

Appendix 2. Tables of Bond Distances and Angles

C9 . C10 . H101 . 106.5	C31 . C32 . C25 . 118.2(7)
C3 . C10 . H101 . 109.6	C31 . C32 . H321 . 120.9
C9 . C10 . H102 . 110.3	C25 . C32 . H321 . 120.8
C3 . C10 . H102 . 109.0	C33 2_766 C33 . C34 . 126.0(11)
H101 . C10 . H102 . 108.6	C33 2_766 C33 . H331 . 106.7
Rh1 . C11 . N12 . 124.7(3)	C34 . C33 . H331 . 104.0
Rh1 . C11 . N24 . 118.8(3)	C33 2_766 C33 . H332 . 105.7
N12 . C11 . N24 . 116.5(4)	C34 . C33 . H332 . 104.4
C11 . N12 . C13 . 120.2(3)	H331 . C33 . H332 . 109.5
C11 . N12 . C21 . 124.8(3)	C33 . C34 . C35 . 126.5(9)
C13 . N12 . C21 . 115.0(3)	C33 . C34 . H341 . 104.9
N12 . C13 . C14 . 122.2(4)	C35 . C34 . H341 . 105.9
N12 . C13 . C18 . 118.5(4)	C33 . C34 . H342 . 103.9
C14 . C13 . C18 . 119.3(4)	C35 . C34 . H342 . 105.6
C13 . C14 . C15 . 120.5(4)	H341 . C34 . H342 . 109.5
C13 . C14 . H141 . 119.8	C34 . C35 . H352 . 111.2
C15 . C14 . H141 . 119.6	C34 . C35 . H351 . 108.0
C14 . C15 . C16 . 120.5(4)	H352 . C35 . H351 . 109.8
C14 . C15 . H151 . 120.4	C34 . C35 . H353 . 107.4
C16 . C15 . H151 . 119.1	H352 . C35 . H353 . 111.3
C15 . C16 . C17 . 120.4(4)	H351 . C35 . H353 . 109.1

Appendix 2. Tables of Bond Distances and Angles

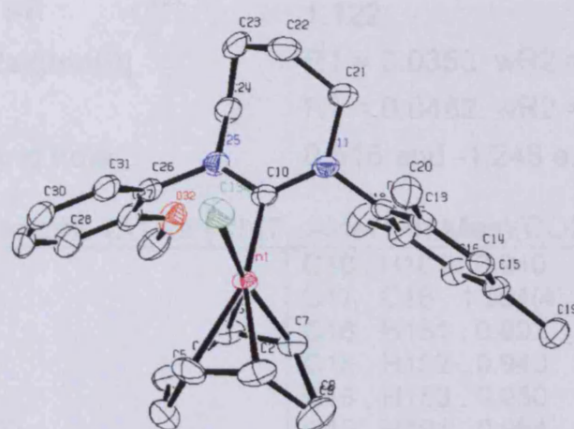


Table O.1: Crystal data and structure refinement for [Rh(7-*o*-MeOPh-Mes)(COD)Cl].

Identification code	kjc0746
Empirical formula	C ₂₉ H ₃₈ Cl N ₂ O Rh
Formula weight	568.97
Temperature	274(2) K
Wavelength	0.71073 Å
Crystal system	Monoclinic
Space group	P21/n
Unit cell dimensions	$a = 9.34140(10)$ Å $a = 90^\circ$. $b = 18.7565(2)$ Å $\beta = 104.9340(10)^\circ$. $c = 15.3054(2)$ Å $\gamma = 90^\circ$.
Volume	$2591.11(5)$ Å ³
Z	4
Density (calculated)	1.459 Mg/m ³
Absorption coefficient	0.787 mm ⁻¹
F(000)	1184
Crystal size	0.50 x 0.50 x 0.50 mm ³
Theta range for data collection	1.75 to 27.48°.
Index ranges	-12 ≤ h ≤ 12, -24 ≤ k ≤ 24, -19 ≤ l ≤ 19
Reflections collected	42261
Independent reflections	5934 [R(int) = 0.1206]
Completeness to theta = 27.48°	99.9 %
Absorption correction	Empirical
Max. and min. transmission	0.6944 and 0.6944
Refinement method	Full-matrix least-squares on F ²
Data / restraints / parameters	5934 / 0 / 311

Goodness-of-fit on F^2	1.122
Final R indices [$I > 2\sigma(I)$]	$R_1 = 0.0353$, $wR_2 = 0.0903$
R indices (all data)	$R_1 = 0.0482$, $wR_2 = 0.0971$
Largest diff. peak and hole	0.516 and -1.248 e.Å ⁻³

Table O. 2: Bond lengths (Å) for [Rh(7-*o*-MeOPh-Mes)(COD)Cl].

Rh1 . C2 . 2.192(3)	C16 . H161 . 0.940
Rh1 . C3 . 2.204(2)	C17 . C18 . 1.504(4)
Rh1 . C6 . 2.100(3)	C18 . H181 . 0.992
Rh1 . C7 . 2.110(2)	C18 . H182 . 0.940
Rh1 . C10 . 2.051(2)	C18 . H183 . 0.950
Rh1 . Cl34 . 2.4238(7)	C19 . H191 . 0.954
C2 . C3 . 1.360(4)	C19 . H192 . 0.936
C2 . C9 . 1.508(4)	C19 . H193 . 0.957
C2 . H21 . 0.984	C20 . H201 . 0.956
C3 . C4 . 1.503(4)	C20 . H202 . 0.974
C3 . H31 . 0.985	C20 . H203 . 0.949
C4 . C5 . 1.531(4)	C21 . C22 . 1.527(4)
C4 . H41 . 0.979	C21 . H211 . 0.964
C4 . H42 . 0.997	C21 . H212 . 0.986
C5 . C6 . 1.514(4)	C22 . C23 . 1.519(4)
C5 . H51 . 0.963	C22 . H221 . 0.961
C5 . H52 . 0.990	C22 . H222 . 0.966
C6 . C7 . 1.390(4)	C23 . C24 . 1.513(4)
C6 . H61 . 0.985	C23 . H231 . 0.972
C7 . C8 . 1.522(3)	C23 . H232 . 0.972
C7 . H71 . 0.989	C24 . N25 . 1.486(3)
C8 . C9 . 1.520(4)	C24 . H241 . 0.973
C8 . H81 . 0.983	C24 . H242 . 0.947
C8 . H82 . 0.979	N25 . C26 . 1.448(3)
C9 . H91 . 0.994	C26 . C27 . 1.393(4)
C9 . H92 . 0.976	C26 . C31 . 1.383(4)
C10 . N11 . 1.363(3)	C27 . C28 . 1.393(4)
C10 . N25 . 1.347(3)	C27 . O32 . 1.363(3)
N11 . C12 . 1.456(3)	C28 . C29 . 1.387(5)
N11 . C21 . 1.486(3)	C28 . H281 . 0.943
C12 . C13 . 1.394(3)	C29 . C30 . 1.367(5)
C12 . C17 . 1.401(3)	C29 . H291 . 0.915
C13 . C14 . 1.398(4)	C30 . C31 . 1.400(4)
C13 . C20 . 1.499(4)	C30 . H301 . 0.948
C14 . C15 . 1.381(4)	C31 . H311 . 0.951
C14 . H141 . 0.919	O32 . C33 . 1.414(4)
C15 . C16 . 1.392(4)	C33 . H331 . 0.969
C15 . C19 . 1.508(4)	C33 . H332 . 0.952
C16 . C17 . 1.387(4)	C33 . H333 . 0.978

Table O.3: Bond angles (°) for [Rh(7-*o*-MeOPh-Mes)(COD)Cl].

C2 . Rh1 . C3 . 36.04(11)	C14 . C15 . C19 . 121.9(2)
C2 . Rh1 . C6 . 96.72(10)	C16 . C15 . C19 . 119.9(2)
C3 . Rh1 . C6 . 81.43(11)	C15 . C16 . C17 . 121.6(2)
C2 . Rh1 . C7 . 81.16(10)	C15 . C16 . H161 . 118.9
C3 . Rh1 . C7 . 89.10(10)	C17 . C16 . H161 . 119.5

Appendix 2. Tables of Bond Distances and Angles

C6 . Rh1 . C7 . 38.56(11)	C12 . C17 . C16 . 118.6(2)
C2 . Rh1 . C10 . 161.58(11)	C12 . C17 . C18 . 121.4(2)
C3 . Rh1 . C10 . 162.16(10)	C16 . C17 . C18 . 119.9(2)
C6 . Rh1 . C10 . 92.89(10)	C17 . C18 . H181 . 106.2
C7 . Rh1 . C10 . 96.99(10)	C17 . C18 . H182 . 111.8
C2 . Rh1 . C134 . 87.70(8)	H181 . C18 . H182 . 107.8
C3 . Rh1 . C134 . 89.95(8)	C17 . C18 . H183 . 112.2
C6 . Rh1 . C134 . 158.05(8)	H181 . C18 . H183 . 106.0
C7 . Rh1 . C134 . 162.28(7)	H182 . C18 . H183 . 112.5
C10 . Rh1 . C134 . 89.23(7)	C15 . C19 . H191 . 110.8
Rh1 . C2 . C3 . 72.43(15)	C15 . C19 . H192 . 112.7
Rh1 . C2 . C9 . 108.62(18)	H191 . C19 . H192 . 109.0
C3 . C2 . C9 . 126.5(3)	C15 . C19 . H193 . 108.8
Rh1 . C2 . H21 . 113.0	H191 . C19 . H193 . 107.7
C3 . C2 . H21 . 115.0	H192 . C19 . H193 . 107.6
C9 . C2 . H21 . 113.0	C13 . C20 . H201 . 114.3
Rh1 . C3 . C2 . 71.53(15)	C13 . C20 . H202 . 110.4
Rh1 . C3 . C4 . 111.70(19)	H201 . C20 . H202 . 104.4
C2 . C3 . C4 . 122.8(3)	C13 . C20 . H203 . 114.7
Rh1 . C3 . H31 . 113.8	H201 . C20 . H203 . 107.3
C2 . C3 . H31 . 116.5	H202 . C20 . H203 . 104.8
C4 . C3 . H31 . 113.2	N11 . C21 . C22 . 113.4(2)
C3 . C4 . C5 . 111.9(2)	N11 . C21 . H211 . 113.4
C3 . C4 . H41 . 112.1	C22 . C21 . H211 . 107.5
C5 . C4 . H41 . 107.9	N11 . C21 . H212 . 108.9
C3 . C4 . H42 . 109.9	C22 . C21 . H212 . 105.6
C5 . C4 . H42 . 108.0	H211 . C21 . H212 . 107.7
H41 . C4 . H42 . 106.8	C21 . C22 . C23 . 112.8(3)
C4 . C5 . C6 . 113.3(2)	C21 . C22 . H221 . 107.9
C4 . C5 . H51 . 110.9	C23 . C22 . H221 . 107.7
C6 . C5 . H51 . 112.6	C21 . C22 . H222 . 110.2
C4 . C5 . H52 . 106.7	C23 . C22 . H222 . 109.5
C6 . C5 . H52 . 106.4	H221 . C22 . H222 . 108.5
H51 . C5 . H52 . 106.5	C22 . C23 . C24 . 111.1(2)
C5 . C6 . Rh1 . 110.38(19)	C22 . C23 . H231 . 108.2
C5 . C6 . C7 . 125.4(2)	C24 . C23 . H231 . 109.9
Rh1 . C6 . C7 . 71.12(14)	C22 . C23 . H232 . 108.8
C5 . C6 . H61 . 112.5	C24 . C23 . H232 . 111.2
Rh1 . C6 . H61 . 119.9	H231 . C23 . H232 . 107.6
C7 . C6 . H61 . 112.1	C23 . C24 . N25 . 112.4(2)
C6 . C7 . Rh1 . 70.32(14)	C23 . C24 . H241 . 104.0
C6 . C7 . C8 . 124.8(2)	N25 . C24 . H241 . 110.1
Rh1 . C7 . C8 . 114.22(17)	C23 . C24 . H242 . 107.2
C6 . C7 . H71 . 113.5	N25 . C24 . H242 . 111.3
Rh1 . C7 . H71 . 118.0	H241 . C24 . H242 . 111.6
C8 . C7 . H71 . 110.8	C24 . N25 . C10 . 124.2(2)
C7 . C8 . C9 . 112.7(2)	C24 . N25 . C26 . 115.7(2)
C7 . C8 . H81 . 108.9	C10 . N25 . C26 . 119.2(2)
C9 . C8 . H81 . 108.6	N25 . C26 . C27 . 118.6(2)
C7 . C8 . H82 . 109.5	N25 . C26 . C31 . 120.6(3)
C9 . C8 . H82 . 109.7	C27 . C26 . C31 . 120.7(3)
H81 . C8 . H82 . 107.2	C26 . C27 . C28 . 119.2(3)
C8 . C9 . C2 . 113.5(2)	C26 . C27 . O32 . 117.1(2)
C8 . C9 . H91 . 105.4	C28 . C27 . O32 . 123.7(3)

Appendix 2. Tables of Bond Distances and Angles

C2 . C9 . H91 . 109.1	C27 . C28 . C29 . 119.8(3)
C8 . C9 . H92 . 107.4	C27 . C28 . H281 . 120.7
C2 . C9 . H92 . 113.4	C29 . C28 . H281 . 119.5
H91 . C9 . H92 . 107.5	C28 . C29 . C30 . 121.0(3)
Rh1 . C10 . N11 . 120.63(18)	C28 . C29 . H291 . 120.7
Rh1 . C10 . N25 . 121.36(17)	C30 . C29 . H291 . 118.3
N11 . C10 . N25 . 117.6(2)	C29 . C30 . C31 . 120.0(3)
C10 . N11 . C12 . 118.03(19)	C29 . C30 . H301 . 120.1
C10 . N11 . C21 . 128.8(2)	C31 . C30 . H301 . 119.9
C12 . N11 . C21 . 113.08(19)	C30 . C31 . C26 . 119.4(3)
N11 . C12 . C13 . 121.2(2)	C30 . C31 . H311 . 119.4
N11 . C12 . C17 . 117.2(2)	C26 . C31 . H311 . 121.1
C13 . C12 . C17 . 121.5(2)	C27 . O32 . C33 . 118.1(2)
C12 . C13 . C14 . 117.3(2)	O32 . C33 . H331 . 112.6
C12 . C13 . C20 . 123.1(2)	O32 . C33 . H332 . 113.9
C14 . C13 . C20 . 119.5(2)	H331 . C33 . H332 . 107.6
C13 . C14 . C15 . 122.8(2)	O32 . C33 . H333 . 110.0
C13 . C14 . H141 . 119.3	H331 . C33 . H333 . 105.6
C15 . C14 . H141 . 117.9	H332 . C33 . H333 . 106.5
C14 . C15 . C16 . 118.1(2)	

Appendix 2. Tables of Bond Distances and Angles

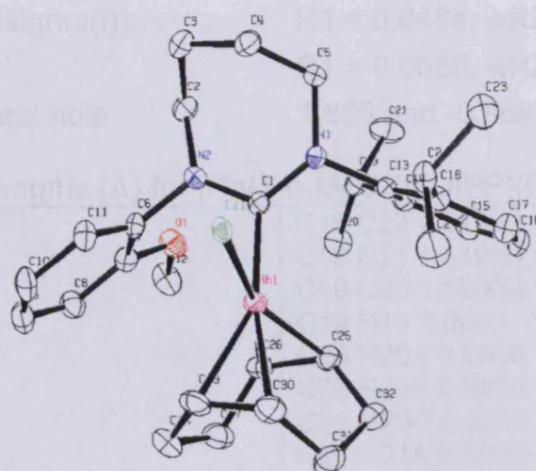


Table P.1: Crystal data and structure refinement for [Rh(7-o-MeOPh-DIPP)(COD)Cl].

Identification code	kjc0827
Empirical formula	C ₃₂ H ₄₄ Cl N ₂ O Rh
Formula weight	611.05
Temperature	150(2) K
Wavelength	0.71073 Å
Crystal system	Monoclinic
Space group	P2 ₁ /n
Unit cell dimensions	a = 10.1760(2) Å a = 90°. b = 16.5830(3) Å β = 92.8630(10)°. c = 17.0760(4) Å γ = 90°.
Volume	2877.95(10) Å ³
Z	4
Density (calculated)	1.410 Mg/m ³
Absorption coefficient	0.714 mm ⁻¹
F(000)	1280
Crystal size	0.23 x 0.20 x 0.10 mm ³
Theta range for data collection	2.59 to 27.47°.
Index ranges	-13 ≤ h ≤ 13, -21 ≤ k ≤ 16, -22 ≤ l ≤ 22
Reflections collected	11968
Independent reflections	6546 [R(int) = 0.0408]
Completeness to theta = 27.47°	99.4 %
Max. and min. transmission	0.9321 and 0.8530
Refinement method	Full-matrix least-squares on F ²
Data / restraints / parameters	6546 / 0 / 339
Goodness-of-fit on F ²	1.034

Final R indices [$I > 2\sigma(I)$]	R1 = 0.0484, wR2 = 0.1198
R indices (all data)	R1 = 0.0680, wR2 = 0.1301
Largest diff. peak and hole	1.528 and -0.868 e.Å ⁻³

Table P. 2: Bond lengths (Å) for [Rh(7-*o*-MeOPh-DIPP)(COD)Cl].

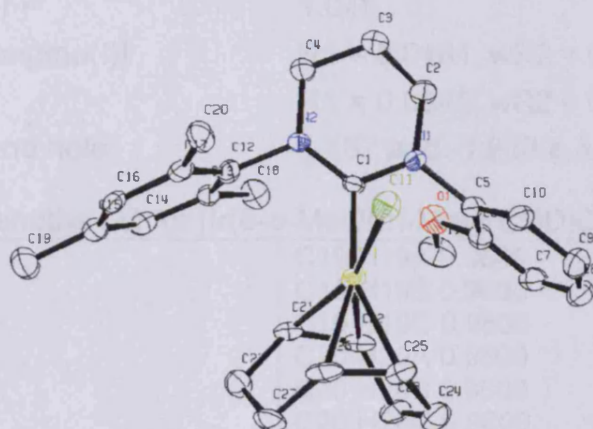
C1 N2 1.348(5)	C18 C22 1.513(5)
C1 N1 1.359(4)	C19 C21 1.519(6)
C1 Rh1 2.052(4)	C19 C20 1.520(6)
C2 N2 1.486(5)	C19 H19 1.0000
C2 C3 1.510(6)	C20 H20A 0.9800
C2 H2A 0.9900	C20 H20B 0.9800
C2 H2B 0.9900	C20 H20C 0.9800
C3 C4 1.532(6)	C21 H21A 0.9800
C3 H3A 0.9900	C21 H21B 0.9800
C3 H3B 0.9900	C21 H21C 0.9800
C4 C5 1.507(5)	C22 C24 1.526(6)
C4 H4A 0.9900	C22 C23 1.539(5)
C4 H4B 0.9900	C22 H22 1.0000
C5 N1 1.495(5)	C23 H23A 0.9800
C5 H5A 0.9900	C23 H23B 0.9800
C5 H5B 0.9900	C23 H23C 0.9800
C6 C11 1.373(5)	C24 H24A 0.9800
C6 C7 1.412(5)	C24 H24B 0.9800
C6 N2 1.446(5)	C24 H24C 0.9800
C7 O1 1.369(5)	C25 C26 1.399(6)
C7 C8 1.385(5)	C25 C32 1.515(6)
C8 C9 1.393(6)	C25 Rh1 2.104(4)
C8 H8 0.9500	C25 H25 0.9500
C9 C10 1.373(6)	C26 C27 1.525(5)
C9 H9 0.9500	C26 Rh1 2.130(4)
C10 C11 1.407(6)	C26 H26 0.9500
C10 H10 0.9500	C27 C28 1.539(6)
C11 H11 0.9500	C27 H27A 0.9900
C12 O1 1.427(5)	C27 H27B 0.9900
C12 H12A 0.9800	C28 C29 1.511(6)
C12 H12B 0.9800	C28 H28A 0.9900
C12 H12C 0.9800	C28 H28B 0.9900
C13 C18 1.403(5)	C29 C30 1.386(6)
C13 C14 1.409(5)	C29 Rh1 2.179(4)
C13 N1 1.452(4)	C29 H29 0.9500
C14 C15 1.393(5)	C30 C31 1.512(6)
C14 C19 1.522(6)	C30 Rh1 2.216(4)
C15 C16 1.382(6)	C30 H30 0.9500
C15 H15 0.9500	C31 C32 1.542(6)
C16 C17 1.383(6)	C31 H31A 0.9900
C16 H16 0.9500	C31 H31B 0.9900
C17 C18 1.400(6)	C32 H32A 0.9900
C17 H17 0.9500	C32 H32B 0.9900
	Rh1 Cl1 2.4628(8)

Table P. 3: Bond angles (°) for [Rh(7-*o*-MeOPh-DIPP)(COD)Cl].

N2 C1 N1 117.8(3)	C18 C22 C23 110.1(3)
N2 C1 Rh1 115.3(2)	C24 C22 C23 109.5(3)
N1 C1 Rh1 125.2(3)	C18 C22 H22 108.4
N2 C2 C3 112.1(3)	C24 C22 H22 108.4
N2 C2 H2A 109.2	C23 C22 H22 108.4
C3 C2 H2A 109.2	C22 C23 H23A 109.5
N2 C2 H2B 109.2	C22 C23 H23B 109.5
C3 C2 H2B 109.2	H23A C23 H23B 109.5
H2A C2 H2B 107.9	C22 C23 H23C 109.5
C2 C3 C4 110.8(3)	H23A C23 H23C 109.5
C2 C3 H3A 109.5	H23B C23 H23C 109.5
C4 C3 H3A 109.5	C22 C24 H24A 109.5
C2 C3 H3B 109.5	C22 C24 H24B 109.5
C4 C3 H3B 109.5	H24A C24 H24B 109.5
H3A C3 H3B 108.1	C22 C24 H24C 109.5
C5 C4 C3 112.8(3)	H24A C24 H24C 109.5
C5 C4 H4A 109.0	H24B C24 H24C 109.5
C3 C4 H4A 109.0	C26 C25 C32 125.3(4)
C5 C4 H4B 109.0	C26 C25 Rh1 71.7(2)
C3 C4 H4B 109.0	C32 C25 Rh1 111.0(3)
H4A C4 H4B 107.8	C26 C25 H25 117.4
N1 C5 C4 113.0(3)	C32 C25 H25 117.4
N1 C5 H5A 109.0	Rh1 C25 H25 87.3
C4 C5 H5A 109.0	C25 C26 C27 124.2(4)
N1 C5 H5B 109.0	C25 C26 Rh1 69.7(2)
C4 C5 H5B 109.0	C27 C26 Rh1 113.8(3)
H5A C5 H5B 107.8	C25 C26 H26 117.9
C11 C6 C7 120.5(3)	C27 C26 H26 117.9
C11 C6 N2 121.7(3)	Rh1 C26 H26 86.5
C7 C6 N2 117.7(3)	C26 C27 C28 112.1(3)
O1 C7 C8 124.4(4)	C26 C27 H27A 109.2
O1 C7 C6 115.9(3)	C28 C27 H27A 109.2
C8 C7 C6 119.6(4)	C26 C27 H27B 109.2
C7 C8 C9 119.2(4)	C28 C27 H27B 109.2
C7 C8 H8 120.4	H27A C27 H27B 107.9
C9 C8 H8 120.4	C29 C28 C27 114.2(3)
C10 C9 C8 121.5(4)	C29 C28 H28A 108.7
C10 C9 H9 119.3	C27 C28 H28A 108.7
C8 C9 H9 119.3	C29 C28 H28B 108.7
C9 C10 C11 119.5(4)	C27 C28 H28B 108.7
C9 C10 H10 120.2	H28A C28 H28B 107.6
C11 C10 H10 120.2	C30 C29 C28 124.9(4)
C6 C11 C10 119.6(4)	C30 C29 Rh1 73.1(2)
C6 C11 H11 120.2	C28 C29 Rh1 108.6(3)
C10 C11 H11 120.2	C30 C29 H29 117.5
O1 C12 H12A 109.5	C28 C29 H29 117.5
O1 C12 H12B 109.5	Rh1 C29 H29 88.3
H12A C12 H12B 109.5	C29 C30 C31 123.5(4)
O1 C12 H12C 109.5	C29 C30 Rh1 70.1(2)
H12A C12 H12C 109.5	C31 C30 Rh1 111.6(3)
H12B C12 H12C 109.5	C29 C30 H30 118.3
C18 C13 C14 121.6(3)	C31 C30 H30 118.3
C18 C13 N1 120.6(3)	Rh1 C30 H30 88.3

Appendix 2. Tables of Bond Distances and Angles

C14 C13 N1 117.6(3)	C30 C31 C32 112.1(3)
C15 C14 C13 118.1(4)	C30 C31 H31A 109.2
C15 C14 C19 119.2(3)	C32 C31 H31A 109.2
C13 C14 C19 122.7(3)	C30 C31 H31B 109.2
C16 C15 C14 121.3(4)	C32 C31 H31B 109.2
C16 C15 H15 119.3	H31A C31 H31B 107.9
C14 C15 H15 119.3	C25 C32 C31 113.4(3)
C15 C16 C17 119.6(4)	C25 C32 H32A 108.9
C15 C16 H16 120.2	C31 C32 H32A 108.9
C17 C16 H16 120.2	C25 C32 H32B 108.9
C16 C17 C18 121.6(4)	C31 C32 H32B 108.9
C16 C17 H17 119.2	H32A C32 H32B 107.7
C18 C17 H17 119.2	C1 N1 C13 118.2(3)
C17 C18 C13 117.5(4)	C1 N1 C5 128.0(3)
C17 C18 C22 118.9(4)	C13 N1 C5 113.7(3)
C13 C18 C22 123.5(3)	C1 N2 C6 118.7(3)
C21 C19 C20 110.0(3)	C1 N2 C2 125.3(3)
C21 C19 C14 111.5(3)	C6 N2 C2 115.2(3)
C20 C19 C14 112.7(3)	C7 O1 C12 115.9(3)
C21 C19 H19 107.4	C1 Rh1 C25 99.07(14)
C20 C19 H19 107.4	C1 Rh1 C26 98.62(14)
C14 C19 H19 107.4	C25 Rh1 C26 38.58(15)
C19 C20 H20A 109.5	C1 Rh1 C29 153.58(16)
C19 C20 H20B 109.5	C25 Rh1 C29 97.52(16)
H20A C20 H20B 109.5	C26 Rh1 C29 81.93(15)
C19 C20 H20C 109.5	C1 Rh1 C30 167.57(15)
H20A C20 H20C 109.5	C25 Rh1 C30 81.51(15)
H20B C20 H20C 109.5	C26 Rh1 C30 89.57(15)
C19 C21 H21A 109.5	C29 Rh1 C30 36.76(16)
C19 C21 H21B 109.5	C1 Rh1 Cl1 85.12(9)
H21A C21 H21B 109.5	C25 Rh1 Cl1 151.25(11)
C19 C21 H21C 109.5	C26 Rh1 Cl1 169.02(10)
H21A C21 H21C 109.5	C29 Rh1 Cl1 90.14(11)
H21B C21 H21C 109.5	C30 Rh1 Cl1 88.56(11)
C18 C22 C24 111.9(4)	


Table Q.1: Crystal data and structure refinement for [Ir(6-o-MeOPh-Mes)(COD)Cl].

Identification code	kjc0903	
Empirical formula	C ₃₂ H ₄₄ Cl Ir N ₂ O ₂	
Formula weight	716.34	
Temperature	150(2) K	
Wavelength	0.71073 Å	
Crystal system	Triclinic	
Space group	P-1	
Unit cell dimensions	a = 9.6970(5) Å	a = 85.593(2)°.
	b = 11.1510(6) Å	β = 79.370(2)°.
	c = 13.9060(11) Å	γ = 81.103(4)°.
Volume	1458.28(16) Å ³	
Z	2	
Density (calculated)	1.631 Mg/m ³	
Absorption coefficient	4.701 mm ⁻¹	
F(000)	720	
Crystal size	0.15 x 0.15 x 0.02 mm ³	
Theta range for data collection	1.49 to 27.50°.	
Index ranges	-12 ≤ h ≤ 12, -14 ≤ k ≤ 14, -	
	17 ≤ l ≤ 18	
Reflections collected	9737	
Independent reflections	6473 [R(int) = 0.0517]	
Completeness to theta = 27.50°	96.5 %	
Max. and min. transmission	0.9118 and 0.5390	
Refinement method	Full-matrix least-squares on F ²	

Data / restraints / parameters	6473 / 0 / 347
Goodness-of-fit on F ²	1.048
Final R indices [I>2sigma(I)]	R1 = 0.0481, wR2 = 0.0946
R indices (all data)	R1 = 0.0645, wR2 = 0.1008
Largest diff. peak and hole	1.187 and -1.830 e.Å ⁻³

Table Q. 2: Bond lengths (Å) for [Ir(6-*o*-MeOPh-Mes)(COD)Cl].

C1 N2 1.335(7)	C19 H19A 0.9800
C1 N1 1.342(7)	C19 H19B 0.9800
C1 Ir1 2.074(5)	C19 H19C 0.9800
C2 N1 1.480(7)	C20 H20A 0.9800
C2 C3 1.513(10)	C20 H20B 0.9800
C2 H2A 0.9900	C20 H20C 0.9800
C2 H2B 0.9900	C21 C22 1.422(9)
C3 C4 1.503(8)	C21 C28 1.512(8)
C3 H3A 0.9900	C21 Ir1 2.091(6)
C3 H3B 0.9900	C21 H21 0.9500
C4 N2 1.464(7)	C22 C23 1.523(9)
C4 H4A 0.9900	C22 Ir1 2.112(7)
C4 H4B 0.9900	C22 H22 0.9500
C5 C10 1.363(9)	C23 C24 1.539(10)
C5 C6 1.418(9)	C23 H23A 0.9900
C5 N1 1.454(7)	C23 H23B 0.9900
C6 O1 1.367(7)	C24 C25 1.501(11)
C6 C7 1.384(9)	C24 H24A 0.9900
C7 C8 1.386(10)	C24 H24B 0.9900
C7 H7 0.9500	C25 C26 1.402(9)
C8 C9 1.372(11)	C25 Ir1 2.160(6)
C8 H8 0.9500	C25 H25 0.9500
C9 C10 1.403(9)	C26 C27 1.518(10)
C9 H9 0.9500	C26 Ir1 2.187(6)
C10 H10 0.9500	C26 H26 0.9500
C11 O1 1.435(9)	C27 C28 1.514(9)
C11 H11A 0.9800	C27 H27A 0.9900
C11 H11B 0.9800	C27 H27B 0.9900
C11 H11C 0.9800	C28 H28A 0.9900
C12 C13 1.387(9)	C28 H28B 0.9900
C12 C17 1.405(9)	C29 O2 1.414(9)
C12 N2 1.463(7)	C29 C30 1.509(12)
C13 C14 1.397(8)	C29 H29A 0.9900
C13 C18 1.516(9)	C29 H29B 0.9900
C14 C15 1.396(9)	C30 C31 1.520(12)
C14 H14 0.9500	C30 H30A 0.9900
C15 C16 1.387(10)	C30 H30B 0.9900
C15 C19 1.513(8)	C31 C32 1.499(10)
C16 C17 1.397(8)	C31 H31A 0.9900
C16 H16 0.9500	C31 H31B 0.9900
C17 C20 1.499(9)	C32 O2 1.424(9)
C18 H18A 0.9800	C32 H32A 0.9900
C18 H18B 0.9800	C32 H32B 0.9900
C18 H18C 0.9800	Ir1 Cl1 2.3842(17)

Table Q.3: Bond angles (°) for [Ir(6-*o*-MeOPh-Mes)(COD)Cl].

N2 C1 N1 117.3(5)	C21 C22 Ir1 69.4(4)
N2 C1 Ir1 124.0(4)	C23 C22 Ir1 114.4(5)
N1 C1 Ir1 117.7(4)	C21 C22 H22 118.9
N1 C2 C3 107.7(5)	C23 C22 H22 118.9
N1 C2 H2A 110.2	Ir1 C22 H22 86.4
C3 C2 H2A 110.2	C22 C23 C24 111.7(6)
N1 C2 H2B 110.2	C22 C23 H23A 109.3
C3 C2 H2B 110.2	C24 C23 H23A 109.3
H2A C2 H2B 108.5	C22 C23 H23B 109.3
C4 C3 C2 108.9(6)	C24 C23 H23B 109.3
C4 C3 H3A 109.9	H23A C23 H23B 107.9
C2 C3 H3A 109.9	C25 C24 C23 112.9(5)
C4 C3 H3B 109.9	C25 C24 H24A 109.0
C2 C3 H3B 109.9	C23 C24 H24A 109.0
H3A C3 H3B 108.3	C25 C24 H24B 109.0
N2 C4 C3 110.7(5)	C23 C24 H24B 109.0
N2 C4 H4A 109.5	H24A C24 H24B 107.8
C3 C4 H4A 109.5	C26 C25 C24 125.6(7)
N2 C4 H4B 109.5	C26 C25 Ir1 72.2(3)
C3 C4 H4B 109.5	C24 C25 Ir1 110.1(5)
H4A C4 H4B 108.1	C26 C25 H25 117.2
C10 C5 C6 121.3(6)	C24 C25 H25 117.2
C10 C5 N1 122.0(6)	Ir1 C25 H25 87.6
C6 C5 N1 116.6(5)	C25 C26 C27 123.4(7)
O1 C6 C7 126.1(6)	C25 C26 Ir1 70.2(3)
O1 C6 C5 115.3(6)	C27 C26 Ir1 112.2(4)
C7 C6 C5 118.6(6)	C25 C26 H26 118.3
C6 C7 C8 120.0(7)	C27 C26 H26 118.3
C6 C7 H7 120.0	Ir1 C26 H26 87.6
C8 C7 H7 120.0	C28 C27 C26 112.9(5)
C9 C8 C7 120.6(6)	C28 C27 H27A 109.0
C9 C8 H8 119.7	C26 C27 H27A 109.0
C7 C8 H8 119.7	C28 C27 H27B 109.0
C8 C9 C10 120.5(7)	C26 C27 H27B 109.0
C8 C9 H9 119.7	H27A C27 H27B 107.8
C10 C9 H9 119.7	C21 C28 C27 112.3(5)
C5 C10 C9 118.8(7)	C21 C28 H28A 109.1
C5 C10 H10 120.6	C27 C28 H28A 109.1
C9 C10 H10 120.6	C21 C28 H28B 109.1
O1 C11 H11A 109.5	C27 C28 H28B 109.1
O1 C11 H11B 109.5	H28A C28 H28B 107.9
H11A C11 H11B 109.5	O2 C29 C30 107.9(7)
O1 C11 H11C 109.5	O2 C29 H29A 110.1
H11A C11 H11C 109.5	C30 C29 H29A 110.1
H11B C11 H11C 109.5	O2 C29 H29B 110.1
C13 C12 C17 121.6(5)	C30 C29 H29B 110.1
C13 C12 N2 117.4(5)	H29A C29 H29B 108.4
C17 C12 N2 120.8(6)	C29 C30 C31 105.1(6)
C12 C13 C14 118.6(6)	C29 C30 H30A 110.7
C12 C13 C18 121.7(5)	C31 C30 H30A 110.7
C14 C13 C18 119.6(6)	C29 C30 H30B 110.7

Appendix 2. Tables of Bond Distances and Angles

C15 C14 C13 121.9(6)	C31 C30 H30B 110.7
C15 C14 H14 119.1	H30A C30 H30B 108.8
C13 C14 H14 119.1	C32 C31 C30 102.0(7)
C16 C15 C14 117.4(5)	C32 C31 H31A 111.4
C16 C15 C19 121.8(6)	C30 C31 H31A 111.4
C14 C15 C19 120.8(6)	C32 C31 H31B 111.4
C15 C16 C17 123.2(6)	C30 C31 H31B 111.4
C15 C16 H16 118.4	H31A C31 H31B 109.2
C17 C16 H16 118.4	O2 C32 C31 106.7(6)
C16 C17 C12 117.1(6)	O2 C32 H32A 110.4
C16 C17 C20 120.9(6)	C31 C32 H32A 110.4
C12 C17 C20 122.0(5)	O2 C32 H32B 110.4
C13 C18 H18A 109.5	C31 C32 H32B 110.4
C13 C18 H18B 109.5	H32A C32 H32B 108.6
H18A C18 H18B 109.5	C1 N1 C5 119.3(5)
C13 C18 H18C 109.5	C1 N1 C2 123.6(5)
H18A C18 H18C 109.5	C5 N1 C2 116.6(4)
H18B C18 H18C 109.5	C1 N2 C12 119.0(5)
C15 C19 H19A 109.5	C1 N2 C4 125.0(5)
C15 C19 H19B 109.5	C12 N2 C4 115.0(4)
H19A C19 H19B 109.5	C1 Ir1 C21 97.8(2)
C15 C19 H19C 109.5	C1 Ir1 C22 98.6(2)
H19A C19 H19C 109.5	C21 Ir1 C22 39.6(2)
H19B C19 H19C 109.5	C1 Ir1 C25 156.1(2)
C17 C20 H20A 109.5	C21 Ir1 C25 97.0(3)
C17 C20 H20B 109.5	C22 Ir1 C25 81.4(3)
H20A C20 H20B 109.5	C1 Ir1 C26 164.8(2)
C17 C20 H20C 109.5	C21 Ir1 C26 80.7(3)
H20A C20 H20C 109.5	C22 Ir1 C26 89.8(3)
H20B C20 H20C 109.5	C25 Ir1 C26 37.6(2)
C22 C21 C28 125.6(6)	C1 Ir1 Cl1 84.82(17)
C22 C21 Ir1 71.0(4)	C21 Ir1 Cl1 157.46(18)
C28 C21 Ir1 113.1(4)	C22 Ir1 Cl1 162.36(18)
C22 C21 H21 117.2	C25 Ir1 Cl1 88.6(2)
C28 C21 H21 117.2	C26 Ir1 Cl1 91.0(2)
Ir1 C21 H21 85.8	C6 O1 C11 116.7(6)
C21 C22 C23 122.2(5)	C29 O2 C32 107.7(6)

Appendix 2. Tables of Bond Distances and Angles

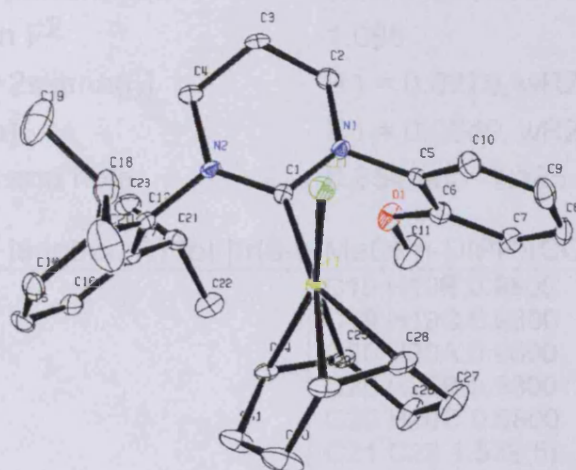


Table R.1: Crystal data and structure refinement for [Ir(6-o-MeOPh-DIPP)(COD)Cl].

Identification code	kjc0846
Empirical formula	C ₃₁ H ₄₂ Cl Ir N ₂ O
Formula weight	686.32
Temperature	150(2) K
Wavelength	0.71073 Å
Crystal system	Monoclinic
Space group	P21/n
Unit cell dimensions	a = 17.4350(3) Å a = 90°. b = 10.4170(2) Å β = 116.7360(10)°. c = 17.6770(4) Å γ = 90°.
Volume	2867.26(10) Å ³
Z	4
Density (calculated)	1.590 Mg/m ³
Absorption coefficient	4.776 mm ⁻¹
F(000)	1376
Crystal size	0.20 x 0.20 x 0.18 mm ³
Theta range for data collection	2.34 to 27.46°.
Index ranges	-22 ≤ h ≤ 22, -13 ≤ k ≤ 12, -
	22 ≤ l ≤ 22
Reflections collected	10761
Independent reflections	6537 [R(int) = 0.0268]
Completeness to theta = 27.46°	99.5 %
Max. and min. transmission	0.4802 and 0.4485
Refinement method	Full-matrix least-squares on F ²

Appendix 2. Tables of Bond Distances and Angles

Data / restraints / parameters	6537 / 0 / 330
Goodness-of-fit on F ²	1.068
Final R indices [$I > 2\sigma(I)$]	R1 = 0.0279, wR2 = 0.0583
R indices (all data)	R1 = 0.0349, wR2 = 0.0611
Largest diff. peak and hole	0.854 and -1.185 e.Å ⁻³

Table R. 2: Bond lengths (Å) for [Ir(6-*o*-MeOPh-DIPP)(COD)Cl].

C1 N1 1.346(4)	C19 H19B 0.9800
C1 N2 1.348(4)	C19 H19C 0.9800
C1 Ir1 2.060(3)	C20 H20A 0.9800
C2 N1 1.467(4)	C20 H20B 0.9800
C2 C3 1.506(5)	C20 H20C 0.9800
C2 H2A 0.9900	C21 C23 1.539(5)
C2 H2B 0.9900	C21 C22 1.542(5)
C3 C4 1.516(5)	C21 H21 1.0000
C3 H3A 0.9900	C22 H22A 0.9800
C3 H3B 0.9900	C22 H22B 0.9800
C4 N2 1.478(4)	C22 H22C 0.9800
C4 H4A 0.9900	C23 H23A 0.9800
C4 H4B 0.9900	C23 H23B 0.9800
C5 C10 1.391(5)	C23 H23C 0.9800
C5 C6 1.393(5)	C24 C25 1.417(5)
C5 N1 1.442(4)	C24 C31 1.503(5)
C6 O1 1.373(4)	C24 Ir1 2.104(3)
C6 C7 1.393(5)	C24 H24 0.9500
C7 C8 1.400(5)	C25 C26 1.525(5)
C7 H7 0.9500	C25 Ir1 2.120(3)
C8 C9 1.380(5)	C25 H25 0.9500
C8 H8 0.9500	C26 C27 1.498(5)
C9 C10 1.387(5)	C26 H26A 0.9900
C9 H9 0.9500	C26 H26B 0.9900
C10 H10 0.9500	C27 C28 1.524(5)
C11 O1 1.423(4)	C27 H27A 0.9900
C11 H11A 0.9800	C27 H27B 0.9900
C11 H11B 0.9800	C28 C29 1.386(5)
C11 H11C 0.9800	C28 Ir1 2.164(3)
C12 C13 1.403(5)	C28 H28 0.9500
C12 C17 1.410(5)	C29 C30 1.511(5)
C12 N2 1.449(4)	C29 Ir1 2.191(3)
C13 C14 1.396(5)	C29 H29 0.9500
C13 C18 1.522(5)	C30 C31 1.505(5)
C14 C15 1.382(5)	C30 H30A 0.9900
C14 H14 0.9500	C30 H30B 0.9900
C15 C16 1.392(5)	C31 H31A 0.9900
C15 H15 0.9500	C31 H31B 0.9900
C16 C17 1.389(5)	Cl1 Ir1 2.3867(8)
C16 H16 0.9500	C18 C19 1.533(6)
C17 C21 1.523(5)	C18 H18 1.0000
C18 C20 1.530(6)	C19 H19A 0.9800

Table R.3: Bond angles (°) for [Ir(6-*o*-MeOPh-DIPP)(COD)Cl].

N1 C1 N2 117.2(3)	C22 C21 H21 108.1
N1 C1 Ir1 116.2(2)	C21 C22 H22A 109.5
N2 C1 Ir1 125.4(2)	C21 C22 H22B 109.5
N1 C2 C3 108.4(3)	H22A C22 H22B 109.5
N1 C2 H2A 110.0	C21 C22 H22C 109.5
C3 C2 H2A 110.0	H22A C22 H22C 109.5
N1 C2 H2B 110.0	H22B C22 H22C 109.5
C3 C2 H2B 110.0	C21 C23 H23A 109.5
H2A C2 H2B 108.4	C21 C23 H23B 109.5
C2 C3 C4 108.5(3)	H23A C23 H23B 109.5
C2 C3 H3A 110.0	C21 C23 H23C 109.5
C4 C3 H3A 110.0	H23A C23 H23C 109.5
C2 C3 H3B 110.0	H23B C23 H23C 109.5
C4 C3 H3B 110.0	C25 C24 C31 125.5(3)
H3A C3 H3B 108.4	C25 C24 Ir1 70.99(19)
N2 C4 C3 109.8(3)	C31 C24 Ir1 112.2(2)
N2 C4 H4A 109.7	C25 C24 H24 117.3
C3 C4 H4A 109.7	C31 C24 H24 117.3
N2 C4 H4B 109.7	Ir1 C24 H24 86.7
C3 C4 H4B 109.7	C24 C25 C26 122.9(3)
H4A C4 H4B 108.2	C24 C25 Ir1 69.82(18)
C10 C5 C6 120.1(3)	C26 C25 Ir1 113.7(2)
C10 C5 N1 121.2(3)	C24 C25 H25 118.6
C6 C5 N1 118.6(3)	C26 C25 H25 118.6
O1 C6 C7 124.2(3)	Ir1 C25 H25 86.6
O1 C6 C5 115.6(3)	C27 C26 C25 113.5(3)
C7 C6 C5 120.2(3)	C27 C26 H26A 108.9
C6 C7 C8 118.9(3)	C25 C26 H26A 108.9
C6 C7 H7 120.6	C27 C26 H26B 108.9
C8 C7 H7 120.6	C25 C26 H26B 108.9
C9 C8 C7 120.8(3)	H26A C26 H26B 107.7
C9 C8 H8 119.6	C26 C27 C28 113.9(3)
C7 C8 H8 119.6	C26 C27 H27A 108.8
C8 C9 C10 120.2(3)	C28 C27 H27A 108.8
C8 C9 H9 119.9	C26 C27 H27B 108.8
C10 C9 H9 119.9	C28 C27 H27B 108.8
C9 C10 C5 119.7(3)	H27A C27 H27B 107.7
C9 C10 H10 120.1	C29 C28 C27 126.6(4)
C5 C10 H10 120.1	C29 C28 Ir1 72.5(2)
O1 C11 H11A 109.5	C27 C28 Ir1 109.6(2)
O1 C11 H11B 109.5	C29 C28 H28 116.7
H11A C11 H11B 109.5	C27 C28 H28 116.7
O1 C11 H11C 109.5	Ir1 C28 H28 87.8
H11A C11 H11C 109.5	C28 C29 C30 122.9(4)
H11B C11 H11C 109.5	C28 C29 Ir1 70.40(19)
C13 C12 C17 121.8(3)	C30 C29 Ir1 112.1(2)
C13 C12 N2 120.6(3)	C28 C29 H29 118.5
C17 C12 N2 117.6(3)	C30 C29 H29 118.5
C14 C13 C12 117.7(3)	Ir1 C29 H29 87.6
C14 C13 C18 119.7(3)	C31 C30 C29 113.4(3)
C12 C13 C18 122.6(3)	C31 C30 H30A 108.9
C15 C14 C13 121.6(3)	C29 C30 H30A 108.9
C15 C14 H14 119.2	C31 C30 H30B 108.9

Appendix 2. Tables of Bond Distances and Angles

C13 C14 H14 119.2	C29 C30 H30B 108.9
C14 C15 C16 119.7(3)	H30A C30 H30B 107.7
C14 C15 H15 120.2	C24 C31 C30 114.3(3)
C16 C15 H15 120.2	C24 C31 H31A 108.7
C17 C16 C15 121.1(3)	C30 C31 H31A 108.7
C17 C16 H16 119.4	C24 C31 H31B 108.7
C15 C16 H16 119.4	C30 C31 H31B 108.7
C16 C17 C12 118.1(3)	H31A C31 H31B 107.6
C16 C17 C21 119.1(3)	C1 N1 C5 119.4(3)
C12 C17 C21 122.8(3)	C1 N1 C2 123.8(3)
C13 C18 C20 112.0(3)	C5 N1 C2 116.3(3)
C13 C18 C19 110.2(3)	C1 N2 C12 120.5(3)
C20 C18 C19 110.7(4)	C1 N2 C4 124.6(3)
C13 C18 H18 108.0	C12 N2 C4 114.1(3)
C20 C18 H18 108.0	C6 O1 C11 117.7(3)
C19 C18 H18 108.0	C1 Ir1 C24 98.65(13)
C18 C19 H19A 109.5	C1 Ir1 C25 97.30(13)
C18 C19 H19B 109.5	C24 Ir1 C25 39.19(13)
H19A C19 H19B 109.5	C1 Ir1 C28 154.75(14)
C18 C19 H19C 109.5	C24 Ir1 C28 96.08(14)
H19A C19 H19C 109.5	C25 Ir1 C28 81.46(13)
H19B C19 H19C 109.5	C1 Ir1 C29 166.73(14)
C18 C20 H20A 109.5	C24 Ir1 C29 80.99(13)
C18 C20 H20B 109.5	C25 Ir1 C29 90.76(13)
H20A C20 H20B 109.5	C28 Ir1 C29 37.10(14)
C18 C20 H20C 109.5	C1 Ir1 Cl1 85.02(9)
H20A C20 H20C 109.5	C24 Ir1 Cl1 156.26(10)
H20B C20 H20C 109.5	C25 Ir1 Cl1 163.99(10)
C17 C21 C23 111.0(3)	C28 Ir1 Cl1 89.70(10)
C17 C21 C22 112.2(3)	C29 Ir1 Cl1 90.14(9)
C23 C21 C22 109.3(3)	C17 C21 H21 108.1
	C23 C21 H21 108.1

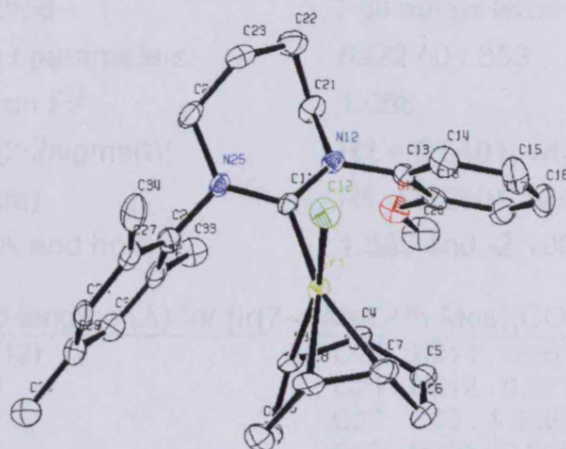


Table S.1: Crystal data and structure refinement for [Ir(7-*o*-MeOPh-Mes)(COD)Cl].

Identification code	kjc0802	
Empirical formula	C ₃₃ H ₄₆ Cl Ir N ₂ O ₂	
Formula weight	730.37	
Temperature	150(2) K	
Wavelength	0.71073 Å	
Crystal system	Triclinic	
Space group	P-1	
Unit cell dimensions	a = 9.5131(2) Å	a = 80.8690(10)°.
	b = 11.5515(2) Å	β = 82.8800(10)°.
	c = 14.2948(2) Å	γ = 82.0440(10)°.
Volume	1527.65(5) Å ³	
Z	2	
Density (calculated)	1.588 Mg/m ³	
Absorption coefficient	4.489 mm ⁻¹	
F(000)	736	
Crystal size	0.30 x 0.20 x 0.10 mm ³	
Theta range for data collection	2.99 to 27.51°.	
Index ranges	-11 ≤ h ≤ 12, -14 ≤ k ≤ 14, -	
	17 ≤ l ≤ 18	
Reflections collected	25944	
Independent reflections	6922 [R(int) = 0.0955]	
Completeness to theta = 27.51°	98.5 %	
Absorption correction	Empirical	

Max. and min. transmission	0.6624 and 0.3461
Refinement method	Full-matrix least-squares on F ²
Data / restraints / parameters	6922 / 0 / 356
Goodness-of-fit on F ²	1.068
Final R indices [$I > 2\sigma(I)$]	R1 = 0.0401, wR2 = 0.0940
R indices (all data)	R1 = 0.0501, wR2 = 0.0999
Largest diff. peak and hole	1.395 and -2.100 e.Å ⁻³

Table S.2: Bond lengths (Å) for [Ir(7-*o*-MeOPh-Mes)(COD)Cl].

Ir1 . Cl2 . 2.3846(12)	C21 . H211 . 0.961
Ir1 . C3 . 2.114(4)	C21 . H212 . 0.971
Ir1 . C4 . 2.096(5)	C22 . C23 . 1.536(8)
Ir1 . C7 . 2.187(5)	C22 . H221 . 0.969
Ir1 . C8 . 2.164(4)	C22 . H222 . 0.999
Ir1 . C11 . 2.041(5)	C23 . C24 . 1.522(8)
C3 . C4 . 1.424(7)	C23 . H231 . 0.965
C3 . C10 . 1.515(7)	C23 . H232 . 0.967
C3 . H31 . 0.986	C24 . N25 . 1.479(6)
C4 . C5 . 1.511(8)	C24 . H241 . 0.970
C4 . H41 . 0.987	C24 . H242 . 0.982
C5 . C6 . 1.531(8)	N25 . C26 . 1.443(6)
C5 . H51 . 0.971	C26 . C27 . 1.398(7)
C5 . H52 . 0.973	C26 . C32 . 1.399(7)
C6 . C7 . 1.516(8)	C27 . C28 . 1.405(8)
C6 . H61 . 0.975	C27 . C34 . 1.489(8)
C6 . H62 . 0.962	C28 . C29 . 1.387(9)
C7 . C8 . 1.404(8)	C28 . H281 . 0.934
C7 . H71 . 0.994	C29 . C30 . 1.506(8)
C8 . C9 . 1.504(7)	C29 . C31 . 1.386(8)
C8 . H81 . 0.991	C30 . H301 . 0.964
C9 . C10 . 1.532(7)	C30 . H302 . 0.955
C9 . H91 . 0.981	C30 . H303 . 0.969
C9 . H92 . 0.970	C31 . C32 . 1.383(8)
C10 . H101 . 0.973	C31 . H311 . 0.933
C10 . H102 . 0.950	C32 . C33 . 1.515(7)
C11 . N12 . 1.357(6)	C33 . H331 . 0.927
C11 . N25 . 1.370(6)	C33 . H332 . 0.966
N12 . C13 . 1.425(6)	C33 . H333 . 0.961
N12 . C21 . 1.482(6)	C34 . H343 . 0.949
C13 . C14 . 1.383(7)	C34 . H342 . 0.955
C13 . C18 . 1.403(7)	C34 . H341 . 0.971
C14 . C15 . 1.389(8)	C35 . C36 . 1.474(10)
C14 . H141 . 0.940	C35 . C39 . 1.465(11)
C15 . C16 . 1.367(9)	C35 . H351 . 0.985
C15 . H151 . 0.920	C35 . H352 . 0.981
C16 . C17 . 1.375(8)	C36 . C37 . 1.497(10)
C16 . H161 . 0.933	C36 . H361 . 0.965
C17 . C18 . 1.399(8)	C36 . H362 . 0.973
C17 . H171 . 0.939	C37 . O38 . 1.421(8)
C18 . O19 . 1.366(6)	C37 . H371 . 0.964
O19 . C20 . 1.419(7)	C37 . H372 . 0.963

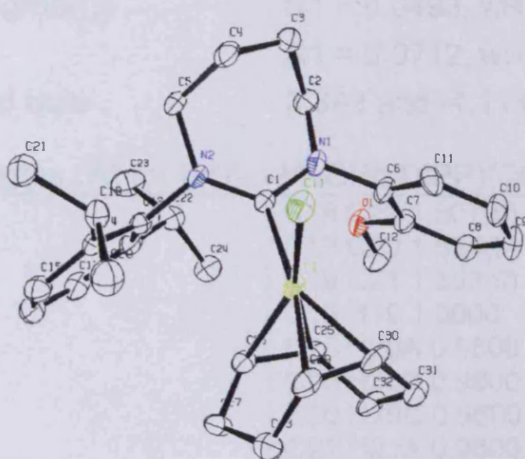
C20 . H201 . 0.975	O38 . C39 . 1.422(8)
C20 . H202 . 0.957	C39 . H391 . 0.971
C20 . H203 . 0.951	C39 . H392 . 0.975
C21 . C22 . 1.509(8)	

Table S. 3: Bond angles (°) for [Ir(7-*o*-MeOPh-Mes)(COD)Cl].

Cl2 . Ir1 . C3 . 164.23(14)	O19 . C20 . H203 . 110.5
Cl2 . Ir1 . C4 . 155.13(15)	H201 . C20 . H203 . 109.3
C3 . Ir1 . C4 . 39.53(19)	H202 . C20 . H203 . 110.5
Cl2 . Ir1 . C7 . 89.72(15)	N12 . C21 . C22 . 112.1(4)
C3 . Ir1 . C7 . 88.97(19)	N12 . C21 . H211 . 108.3
C4 . Ir1 . C7 . 81.1(2)	C22 . C21 . H211 . 108.4
Cl2 . Ir1 . C8 . 88.19(14)	N12 . C21 . H212 . 108.7
C3 . Ir1 . C8 . 81.21(19)	C22 . C21 . H212 . 109.1
C4 . Ir1 . C8 . 98.08(19)	H211 . C21 . H212 . 110.3
C7 . Ir1 . C8 . 37.6(2)	C21 . C22 . C23 . 110.1(4)
Cl2 . Ir1 . C11 . 88.09(13)	C21 . C22 . H221 . 108.0
C3 . Ir1 . C11 . 97.33(18)	C23 . C22 . H221 . 110.0
C4 . Ir1 . C11 . 94.41(19)	C21 . C22 . H222 . 110.2
C7 . Ir1 . C11 . 164.06(19)	C23 . C22 . H222 . 108.7
C8 . Ir1 . C11 . 157.9(2)	H221 . C22 . H222 . 109.8
Ir1 . C3 . C4 . 69.6(3)	C22 . C23 . C24 . 112.1(5)
Ir1 . C3 . C10 . 113.8(3)	C22 . C23 . H231 . 109.5
C4 . C3 . C10 . 125.1(5)	C24 . C23 . H231 . 110.1
Ir1 . C3 . H31 . 113.6	C22 . C23 . H232 . 108.8
C4 . C3 . H31 . 114.4	C24 . C23 . H232 . 107.7
C10 . C3 . H31 . 112.9	H231 . C23 . H232 . 108.5
Ir1 . C4 . C3 . 70.9(3)	C23 . C24 . N25 . 113.6(4)
Ir1 . C4 . C5 . 111.0(4)	C23 . C24 . H241 . 109.4
C3 . C4 . C5 . 125.1(4)	N25 . C24 . H241 . 108.8
Ir1 . C4 . H41 . 115.6	C23 . C24 . H242 . 108.4
C3 . C4 . H41 . 112.8	N25 . C24 . H242 . 106.3
C5 . C4 . H41 . 114.1	H241 . C24 . H242 . 110.3
C4 . C5 . C6 . 112.7(4)	C24 . N25 . C11 . 127.9(4)
C4 . C5 . H51 . 110.7	C24 . N25 . C26 . 115.1(4)
C6 . C5 . H51 . 108.5	C11 . N25 . C26 . 117.0(4)
C4 . C5 . H52 . 107.8	N25 . C26 . C27 . 121.0(4)
C6 . C5 . H52 . 106.2	N25 . C26 . C32 . 117.6(4)
H51 . C5 . H52 . 110.8	C27 . C26 . C32 . 121.4(5)
C5 . C6 . C7 . 110.9(4)	C26 . C27 . C28 . 117.5(5)
C5 . C6 . H61 . 108.4	C26 . C27 . C34 . 123.3(5)
C7 . C6 . H61 . 109.1	C28 . C27 . C34 . 119.2(5)
C5 . C6 . H62 . 108.1	C27 . C28 . C29 . 121.9(5)
C7 . C6 . H62 . 110.7	C27 . C28 . H281 . 119.1
H61 . C6 . H62 . 109.6	C29 . C28 . H281 . 118.9
Ir1 . C7 . C6 . 112.4(4)	C28 . C29 . C30 . 120.9(6)
Ir1 . C7 . C8 . 70.3(3)	C28 . C29 . C31 . 118.2(5)
C6 . C7 . C8 . 123.5(5)	C30 . C29 . C31 . 120.9(6)
Ir1 . C7 . H71 . 109.7	C29 . C30 . H301 . 109.9
C6 . C7 . H71 . 113.7	C29 . C30 . H302 . 108.9
C8 . C7 . H71 . 117.7	H301 . C30 . H302 . 107.0
Ir1 . C8 . C7 . 72.1(3)	C29 . C30 . H303 . 111.2
Ir1 . C8 . C9 . 109.9(3)	H301 . C30 . H303 . 110.0

Appendix 2. Tables of Bond Distances and Angles

C7 . C8 . C9 . 125.9(5)	H302 . C30 . H303 . 109.7
Ir1 . C8 . H81 . 110.2	C29 . C31 . C32 . 122.2(6)
C7 . C8 . H81 . 117.0	C29 . C31 . H311 . 118.9
C9 . C8 . H81 . 112.5	C32 . C31 . H311 . 118.9
C8 . C9 . C10 . 111.9(4)	C26 . C32 . C31 . 118.3(5)
C8 . C9 . H91 . 110.1	C26 . C32 . C33 . 120.6(5)
C10 . C9 . H91 . 109.5	C31 . C32 . C33 . 121.0(5)
C8 . C9 . H92 . 108.8	C32 . C33 . H331 . 110.0
C10 . C9 . H92 . 108.3	C32 . C33 . H332 . 109.4
H91 . C9 . H92 . 108.2	H331 . C33 . H332 . 109.3
C9 . C10 . C3 . 112.9(4)	C32 . C33 . H333 . 109.6
C9 . C10 . H101 . 108.4	H331 . C33 . H333 . 109.6
C3 . C10 . H101 . 109.4	H332 . C33 . H333 . 109.0
C9 . C10 . H102 . 107.7	C27 . C34 . H343 . 109.9
C3 . C10 . H102 . 108.7	C27 . C34 . H342 . 111.2
H101 . C10 . H102 . 109.8	H343 . C34 . H342 . 108.9
Ir1 . C11 . N12 . 122.6(3)	C27 . C34 . H341 . 108.9
Ir1 . C11 . N25 . 120.0(3)	H343 . C34 . H341 . 108.3
N12 . C11 . N25 . 117.1(4)	H342 . C34 . H341 . 109.7
C11 . N12 . C13 . 120.1(4)	C36 . C35 . C39 . 104.5(7)
C11 . N12 . C21 . 123.9(4)	C36 . C35 . H351 . 111.1
C13 . N12 . C21 . 115.8(4)	C39 . C35 . H351 . 111.7
N12 . C13 . C14 . 121.6(4)	C36 . C35 . H352 . 109.9
N12 . C13 . C18 . 118.8(4)	C39 . C35 . H352 . 110.1
C14 . C13 . C18 . 119.5(5)	H351 . C35 . H352 . 109.5
C13 . C14 . C15 . 119.9(5)	C35 . C36 . C37 . 104.0(6)
C13 . C14 . H141 . 118.7	C35 . C36 . H361 . 112.1
C15 . C14 . H141 . 121.4	C37 . C36 . H361 . 111.9
C14 . C15 . C16 . 120.6(5)	C35 . C36 . H362 . 109.8
C14 . C15 . H151 . 118.8	C37 . C36 . H362 . 110.0
C16 . C15 . H151 . 120.6	H361 . C36 . H362 . 109.0
C15 . C16 . C17 . 120.7(5)	C36 . C37 . O38 . 106.9(5)
C15 . C16 . H161 . 119.4	C36 . C37 . H371 . 112.2
C17 . C16 . H161 . 119.9	O38 . C37 . H371 . 110.4
C16 . C17 . C18 . 119.7(5)	C36 . C37 . H372 . 107.8
C16 . C17 . H171 . 119.9	O38 . C37 . H372 . 108.7
C18 . C17 . H171 . 120.4	H371 . C37 . H372 . 110.6
C13 . C18 . C17 . 119.6(5)	C37 . O38 . C39 . 107.4(5)
C13 . C18 . O19 . 116.2(5)	C35 . C39 . O38 . 109.6(6)
C17 . C18 . O19 . 124.2(5)	C35 . C39 . H391 . 109.8
C18 . O19 . C20 . 118.7(5)	O38 . C39 . H391 . 108.9
O19 . C20 . H201 . 106.8	C35 . C39 . H392 . 109.9
O19 . C20 . H202 . 109.6	O38 . C39 . H392 . 109.4
H201 . C20 . H202 . 110.1	H391 . C39 . H392 . 109.3


Table T.1: Crystal data and structure refinement for [Ir(7-o-MeOPh-DIPP)(COD)Cl].

Identification code	kjc0814
Empirical formula	C ₃₂ H ₄₄ Cl Ir N ₂ O
Formula weight	700.34
Temperature	150(2) K
Wavelength	0.71073 Å
Crystal system	Monoclinic
Space group	P21/c
Unit cell dimensions	a = 10.1870(2) Å a = 90°. b = 16.5340(3) Å β = 118.7510(10)°. c = 19.4270(3) Å γ = 90°.
Volume	2868.73(9) Å ³
Z	4
Density (calculated)	1.622 Mg/m ³
Absorption coefficient	4.775 mm ⁻¹
F(000)	1408
Crystal size	0.38 x 0.08 x 0.05 mm ³
Theta range for data collection	3.18 to 27.47°.
Index ranges	-13 ≤ h ≤ 11, -21 ≤ k ≤ 21, -
	25 ≤ l ≤ 25
Reflections collected	46665
Independent reflections	6540 [R(int) = 0.1803]
Completeness to theta = 27.47°	99.5 %
Refinement method	Full-matrix least-squares on F ²
Data / restraints / parameters	6540 / 0 / 339
Goodness-of-fit on F ²	1.068

Appendix 2. Tables of Bond Distances and Angles

Final R indices [$I > 2\sigma(I)$] R1 = 0.0493, wR2 = 0.1140
 R indices (all data) R1 = 0.0712, wR2 = 0.1267
 Largest diff. peak and hole 3.392 and -4.113 e.Å⁻³

Table T. 2: Bond lengths (Å) for [Ir(7-*o*-MeOPh-DIPP)(COD)Cl].

C1 N1 1.343(8)	C18 C22 1.507(9)
C1 N2 1.364(7)	C19 C20 1.534(9)
C1 Ir1 2.062(6)	C19 C21 1.553(9)
C2 N1 1.484(8)	C19 H19 1.0000
C2 C3 1.526(9)	C20 H20A 0.9800
C2 H2A 0.9900	C20 H20B 0.9800
C2 H2B 0.9900	C20 H20C 0.9800
C3 C4 1.531(10)	C21 H21A 0.9800
C3 H3A 0.9900	C21 H21B 0.9800
C3 H3B 0.9900	C21 H21C 0.9800
C4 C5 1.515(9)	C22 C24 1.524(9)
C4 H4A 0.9900	C22 C23 1.536(9)
C4 H4B 0.9900	C22 H22 1.0000
C5 N2 1.507(8)	C23 H23A 0.9800
C5 H5A 0.9900	C23 H23B 0.9800
C5 H5B 0.9900	C23 H23C 0.9800
C6 C11 1.381(9)	C24 H24A 0.9800
C6 C7 1.402(8)	C24 H24B 0.9800
C6 N1 1.444(8)	C24 H24C 0.9800
C7 O1 1.378(7)	C25 C26 1.412(9)
C7 C8 1.384(8)	C25 C32 1.546(8)
C8 C9 1.396(9)	C25 Ir1 2.116(5)
C8 H8 0.9500	C25 H25 0.9500
C9 C10 1.380(10)	C26 C27 1.514(9)
C9 H9 0.9500	C26 Ir1 2.106(6)
C10 C11 1.382(10)	C26 H26 0.9500
C10 H10 0.9500	C27 C28 1.545(9)
C11 H11 0.9500	C27 H27A 0.9900
C12 O1 1.432(7)	C27 H27B 0.9900
C12 H12A 0.9800	C28 C29 1.498(10)
C12 H12B 0.9800	C28 H28A 0.9900
C12 H12C 0.9800	C28 H28B 0.9900
C13 C14 1.396(9)	C29 C30 1.394(11)
C13 C18 1.418(8)	C29 Ir1 2.207(7)
C13 N2 1.445(8)	C29 H29 0.9500
C14 C15 1.401(9)	C30 C31 1.511(9)
C14 C19 1.519(8)	C30 Ir1 2.162(6)
C15 C16 1.373(9)	C30 H30 0.9500
C15 H15 0.9500	C31 C32 1.533(9)
C16 C17 1.380(10)	C31 H31A 0.9900
C16 H16 0.9500	C31 H31B 0.9900
C17 C18 1.403(9)	C32 H32A 0.9900
C17 H17 0.9500	C32 H32B 0.9900
	Ir1 Cl1 2.3911(15)

Table T.3: Bond angles (°) for [Ir(7-*o*-MeOPh-DIPP)(COD)Cl].

N1 C1 N2 119.0(5)	C18 C22 C24 112.5(5)
N1 C1 Ir1 116.2(4)	C18 C22 C23 110.9(6)
N2 C1 Ir1 123.5(5)	C24 C22 C23 109.3(5)
N1 C2 C3 111.8(5)	C18 C22 H22 108.0
N1 C2 H2A 109.3	C24 C22 H22 108.0
C3 C2 H2A 109.3	C23 C22 H22 108.0
N1 C2 H2B 109.3	C22 C23 H23A 109.5
C3 C2 H2B 109.3	C22 C23 H23B 109.5
H2A C2 H2B 107.9	H23A C23 H23B 109.5
C2 C3 C4 110.5(5)	C22 C23 H23C 109.5
C2 C3 H3A 109.5	H23A C23 H23C 109.5
C4 C3 H3A 109.5	H23B C23 H23C 109.5
C2 C3 H3B 109.5	C22 C24 H24A 109.5
C4 C3 H3B 109.5	C22 C24 H24B 109.5
H3A C3 H3B 108.1	H24A C24 H24B 109.5
C5 C4 C3 112.5(5)	C22 C24 H24C 109.5
C5 C4 H4A 109.1	H24A C24 H24C 109.5
C3 C4 H4A 109.1	H24B C24 H24C 109.5
C5 C4 H4B 109.1	C26 C25 C32 123.3(6)
C3 C4 H4B 109.1	C26 C25 Ir1 70.1(3)
H4A C4 H4B 107.8	C32 C25 Ir1 114.1(4)
N2 C5 C4 113.1(5)	C26 C25 H25 118.4
N2 C5 H5A 109.0	C32 C25 H25 118.4
C4 C5 H5A 109.0	Ir1 C25 H25 86.0
N2 C5 H5B 109.0	C25 C26 C27 125.5(5)
C4 C5 H5B 109.0	C25 C26 Ir1 70.8(3)
H5A C5 H5B 107.8	C27 C26 Ir1 112.7(4)
C11 C6 C7 119.9(6)	C25 C26 H26 117.3
C11 C6 N1 122.0(5)	C27 C26 H26 117.3
C7 C6 N1 118.1(5)	Ir1 C26 H26 86.4
O1 C7 C8 123.9(5)	C26 C27 C28 112.1(5)
O1 C7 C6 115.9(5)	C26 C27 H27A 109.2
C8 C7 C6 120.2(6)	C28 C27 H27A 109.2
C7 C8 C9 118.5(6)	C26 C27 H27B 109.2
C7 C8 H8 120.8	C28 C27 H27B 109.2
C9 C8 H8 120.8	H27A C27 H27B 107.9
C10 C9 C8 121.6(6)	C29 C28 C27 113.1(5)
C10 C9 H9 119.2	C29 C28 H28A 109.0
C8 C9 H9 119.2	C27 C28 H28A 109.0
C9 C10 C11 119.4(6)	C29 C28 H28B 109.0
C9 C10 H10 120.3	C27 C28 H28B 109.0
C11 C10 H10 120.3	H28A C28 H28B 107.8
C6 C11 C10 120.3(6)	C30 C29 C28 123.5(6)
C6 C11 H11 119.9	C30 C29 Ir1 69.6(4)
C10 C11 H11 119.9	C28 C29 Ir1 112.4(4)
O1 C12 H12A 109.5	C30 C29 H29 118.2
O1 C12 H12B 109.5	C28 C29 H29 118.2
H12A C12 H12B 109.5	Ir1 C29 H29 88.0
O1 C12 H12C 109.5	C29 C30 C31 125.1(6)
H12A C12 H12C 109.5	C29 C30 Ir1 73.2(4)
H12B C12 H12C 109.5	C31 C30 Ir1 110.1(4)
C14 C13 C18 122.0(6)	C29 C30 H30 117.4
C14 C13 N2 120.9(5)	C31 C30 H30 117.4

Appendix 2. Tables of Bond Distances and Angles

C18 C13 N2 117.0(5)	Ir1 C30 H30 86.6
C13 C14 C15 117.7(6)	C30 C31 C32 113.4(5)
C13 C14 C19 123.1(6)	C30 C31 H31A 108.9
C15 C14 C19 119.2(6)	C32 C31 H31A 108.9
C16 C15 C14 121.6(7)	C30 C31 H31B 108.9
C16 C15 H15 119.2	C32 C31 H31B 108.9
C14 C15 H15 119.2	H31A C31 H31B 107.7
C15 C16 C17 120.0(7)	C31 C32 C25 111.8(5)
C15 C16 H16 120.0	C31 C32 H32A 109.3
C17 C16 H16 120.0	C25 C32 H32A 109.3
C16 C17 C18 121.4(6)	C31 C32 H32B 109.3
C16 C17 H17 119.3	C25 C32 H32B 109.3
C18 C17 H17 119.3	H32A C32 H32B 107.9
C17 C18 C13 117.1(6)	C1 N1 C6 118.6(5)
C17 C18 C22 120.3(5)	C1 N1 C2 124.5(5)
C13 C18 C22 122.5(6)	C6 N1 C2 115.9(6)
C14 C19 C20 111.5(6)	C1 N2 C13 119.6(5)
C14 C19 C21 110.1(5)	C1 N2 C5 126.7(5)
C20 C19 C21 109.0(6)	C13 N2 C5 113.7(4)
C14 C19 H19 108.7	C7 O1 C12 115.6(5)
C20 C19 H19 108.7	C1 Ir1 C26 100.0(2)
C21 C19 H19 108.7	C1 Ir1 C25 98.6(2)
C19 C20 H20A 109.5	C26 Ir1 C25 39.1(2)
C19 C20 H20B 109.5	C1 Ir1 C30 152.9(3)
H20A C20 H20B 109.5	C26 Ir1 C30 97.0(2)
C19 C20 H20C 109.5	C25 Ir1 C30 81.6(2)
H20A C20 H20C 109.5	C1 Ir1 C29 167.9(2)
H20B C20 H20C 109.5	C26 Ir1 C29 80.7(2)
C19 C21 H21A 109.5	C25 Ir1 C29 89.6(2)
C19 C21 H21B 109.5	C30 Ir1 C29 37.2(3)
H21A C21 H21B 109.5	C1 Ir1 Cl1 84.49(15)
C19 C21 H21C 109.5	C26 Ir1 Cl1 152.15(18)
H21A C21 H21C 109.5	C25 Ir1 Cl1 167.85(18)
H21B C21 H21C 109.5	C30 Ir1 Cl1 90.29(17)
	C29 Ir1 Cl1 89.38(17)

Appendix 2. Tables of Bond Distances and Angles

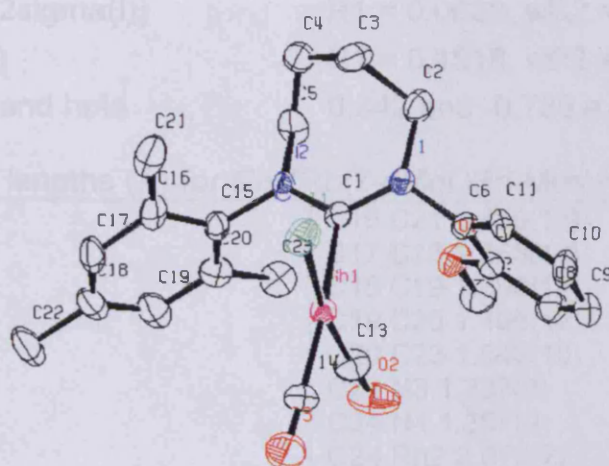


Table W.1: Crystal data and structure refinement for *Cis*-[Rh(7-oMeOPh-Mes)(CO)₂I].

Identification code	kjc0829	
Empirical formula	C ₂₃ H ₂₆ I N ₂ O ₃ Rh	
Formula weight	608.27	
Temperature	150(2) K	
Wavelength	0.71073 Å	
Crystal system	Monoclinic	
Space group	P2 ₁ /c	
Unit cell dimensions	a = 9.151 Å	a = 90°.
	b = 16.091 Å	β = 92.40°.
	c = 32.325 Å	γ = 90°.
Volume	4755.6 Å ³	
Z	8	
Density (calculated)	1.699 Mg/m ³	
Absorption coefficient	2.042 mm ⁻¹	
F(000)	2400	
Crystal size	0.22 x 0.10 x 0.08 mm ³	
Theta range for data collection	1.26 to 27.49°.	
Index ranges	-11 ≤ h ≤ 11, -20 ≤ k ≤ 19, -	
	41 ≤ l ≤ 41	
Reflections collected	17033	
Independent reflections	10607 [R(int) = 0.0996]	
Completeness to theta = 27.49°	97.4 %	
Max. and min. transmission	0.8537 and 0.6622	
Refinement method	Full-matrix least-squares on F ²	
Data / restraints / parameters	10607 / 0 / 549	
Goodness-of-fit on F ²	0.992	

Appendix 2. Tables of Bond Distances and Angles

Final R indices [$I > 2\sigma(I)$]	R1 = 0.0628, wR2 = 0.1055
R indices (all data)	R1 = 0.1518, wR2 = 0.1307
Largest diff. peak and hole	0.842 and -0.739 e.Å ⁻³

Table W. 2: Bond lengths (Å) for *Cis*-[Rh(7-oMeOPh-Mes)(CO)₂].

C3 C4 1.508(11)	C16 C21 1.459(13)
C3 C2 1.533(10)	C17 C18 1.363(14)
C8 C7 1.389(10)	C18 C19 1.396(12)
C8 C9 1.397(12)	C19 C20 1.408(12)
C12 O1 1.415(10)	C20 C23 1.540(10)
C22 C18 1.485(12)	C24 N3 1.337(8)
C35 O4 1.438(11)	C24 N4 1.357(9)
C39 C40 1.389(11)	C24 Rh2 2.079(7)
C39 C38 1.415(12)	C25 N3 1.483(9)
C39 C44 1.476(11)	C25 C26 1.489(11)
C40 C41 1.405(12)	C26 C27 1.525(10)
C45 C41 1.531(11)	C27 C28 1.512(10)
C1 N2 1.340(8)	C28 N4 1.489(10)
C1 N1 1.350(9)	C29 C30 1.391(12)
C1 Rh1 2.096(7)	C29 C34 1.398(12)
C2 N1 1.478(10)	C29 N4 1.433(9)
C4 C5 1.487(12)	C30 O4 1.352(10)
C5 N2 1.493(9)	C30 C31 1.372(10)
C6 C11 1.374(11)	C31 C32 1.389(13)
C6 C7 1.400(11)	C32 C33 1.357(14)
C6 N1 1.449(8)	C33 C34 1.392(11)
C7 O1 1.358(9)	C36 O5 1.129(9)
C9 C10 1.369(13)	C36 Rh2 1.904(9)
C10 C11 1.400(9)	C37 O6 1.132(11)
C13 O2 1.106(10)	C37 Rh2 1.849(11)
C13 Rh1 1.869(10)	C38 C43 1.390(10)
C14 O3 1.125(9)	C38 N3 1.458(9)
C14 Rh1 1.898(9)	C41 C42 1.371(12)
C15 C20 1.364(12)	C42 C43 1.394(11)
C15 C16 1.417(10)	C43 C46 1.492(12)
C15 N2 1.453(10)	Rh1 I1 2.6656(9)
C16 C17 1.415(12)	Rh2 I2 2.6739(9)

Table W. 3: Bond angles (°) for *Cis*-[Rh(7-oMeOPh-Mes)(CO)₂].

C4 C3 C2 113.1(7)	C34 C29 N4 121.5(8)
C7 C8 C9 119.4(8)	O4 C30 C31 123.7(9)
C40 C39 C38 117.3(8)	O4 C30 C29 115.4(6)
C40 C39 C44 120.5(8)	C31 C30 C29 121.0(9)
C38 C39 C44 122.1(7)	C30 C31 C32 118.8(9)
C39 C40 C41 121.1(9)	C33 C32 C31 121.5(8)
N2 C1 N1 119.6(6)	C32 C33 C34 120.1(9)
N2 C1 Rh1 120.6(5)	C33 C34 C29 119.3(9)
N1 C1 Rh1 119.6(5)	O5 C36 Rh2 179.4(10)
N1 C2 C3 112.3(6)	O6 C37 Rh2 174.2(8)
C5 C4 C3 111.6(6)	C43 C38 C39 122.6(7)
C4 C5 N2 114.2(7)	C43 C38 N3 119.8(8)
C11 C6 C7 120.5(6)	C39 C38 N3 117.4(6)

Appendix 2. Tables of Bond Distances and Angles

C11 C6 N1 121.8(7)	C42 C41 C40 119.2(8)
C7 C6 N1 117.6(7)	C42 C41 C45 121.0(8)
O1 C7 C8 124.4(8)	C40 C41 C45 119.7(9)
O1 C7 C6 116.0(6)	C41 C42 C43 122.3(8)
C8 C7 C6 119.5(8)	C38 C43 C42 117.3(9)
C10 C9 C8 120.9(7)	C38 C43 C46 122.7(7)
C9 C10 C11 119.8(9)	C42 C43 C46 119.9(7)
C6 C11 C10 119.8(8)	C1 N1 C6 115.8(6)
O2 C13 Rh1 172.0(8)	C1 N1 C2 129.8(5)
O3 C14 Rh1 177.7(8)	C6 N1 C2 114.5(5)
C20 C15 C16 121.8(8)	C1 N2 C15 118.1(6)
C20 C15 N2 118.6(7)	C1 N2 C5 123.2(6)
C16 C15 N2 119.4(8)	C15 N2 C5 116.2(6)
C17 C16 C15 115.2(9)	C24 N3 C38 118.4(6)
C17 C16 C21 122.2(8)	C24 N3 C25 123.1(5)
C15 C16 C21 122.7(8)	C38 N3 C25 116.5(5)
C18 C17 C16 125.0(8)	C24 N4 C29 117.5(6)
C17 C18 C19 117.0(8)	C24 N4 C28 128.0(5)
C17 C18 C22 122.1(9)	C29 N4 C28 114.4(5)
C19 C18 C22 120.9(10)	C7 O1 C12 117.9(6)
C18 C19 C20 121.0(10)	C30 O4 C35 118.3(6)
C15 C20 C19 119.7(8)	C13 Rh1 C14 90.6(4)
C15 C20 C23 122.4(7)	C13 Rh1 C1 93.6(3)
C19 C20 C23 117.8(9)	C14 Rh1 C1 174.9(3)
N3 C24 N4 118.4(6)	C13 Rh1 I1 169.8(2)
N3 C24 Rh2 122.9(5)	C14 Rh1 I1 86.8(3)
N4 C24 Rh2 118.6(4)	C1 Rh1 I1 89.5(2)
N3 C25 C26 114.0(7)	C37 Rh2 C36 90.6(4)
C25 C26 C27 109.5(6)	C37 Rh2 C24 91.8(3)
C28 C27 C26 111.8(7)	C36 Rh2 C24 176.9(3)
N4 C28 C27 113.1(6)	C37 Rh2 I2 171.3(2)
C30 C29 C34 119.2(7)	C36 Rh2 I2 87.3(3)
C30 C29 N4 119.2(8)	C24 Rh2 I2 90.7(2)

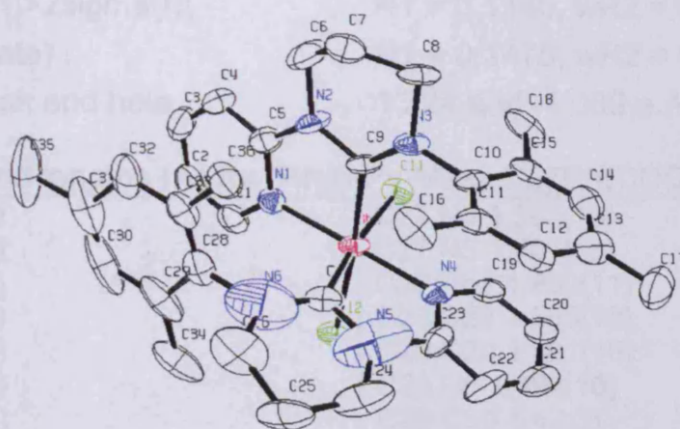


Table Y.1: Crystal data and structure refinement for $[\text{Rh}(\text{6-Py-Mes})_2\text{Cl}_2][\text{Rh}(\text{COD})\text{Cl}_2]$.

Identification code	kjc0843	
Empirical formula	$\text{C}_{45} \text{H}_{56} \text{Cl}_6 \text{N}_8 \text{Rh}_2$	
Formula weight	1127.50	
Temperature	150(2) K	
Wavelength	0.71073 Å	
Crystal system	Orthorhombic	
Space group	Pbca	
Unit cell dimensions	$a = 18.65700(10)$ Å	$a = 90^\circ$.
	$b = 14.5440(2)$ Å	$\beta = 90^\circ$.
	$c = 34.2020(4)$ Å	$\gamma = 90^\circ$.
Volume	$9280.62(17)$ Å ³	
Z	8	
Density (calculated)	1.614 Mg/m ³	
Absorption coefficient	1.100 mm ⁻¹	
F(000)	4592	
Crystal size	0.40 x 0.30 x 0.08 mm ³	
Theta range for data collection	1.87 to 27.51°.	
Index ranges	-23 ≤ h ≤ 24, -18 ≤ k ≤ 18, -	
	44 ≤ l ≤ 43	
Reflections collected	44612	
Independent reflections	10603 [R(int) = 0.0685]	
Completeness to theta = 27.51°	99.4 %	
Max. and min. transmission	0.9172 and 0.6674	
Refinement method	Full-matrix least-squares on F ²	
Data / restraints / parameters	10603 / 53 / 595	
Goodness-of-fit on F ²	1.155	

Appendix 2. Tables of Bond Distances and Angles

Final R indices [$I > 2\sigma(I)$]	R1 = 0.1140, wR2 = 0.2327
R indices (all data)	R1 = 0.1470, wR2 = 0.2459
Largest diff. peak and hole	1.224 and -1.389 e.Å ⁻³

Table Y. 2: Bond lengths (Å) for [Rh(6-Py-Mes)₂Cl₂][Rh(COD)Cl₂].

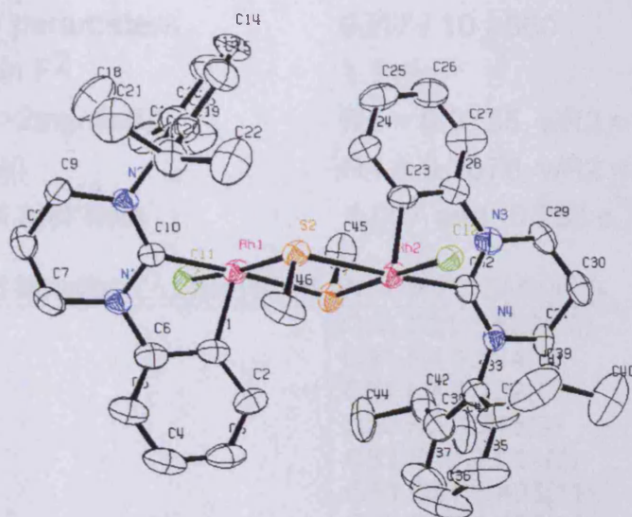
C1 N1 1.348(14)	C27 N6 1.363(15)
C1 C2 1.356(16)	C27 N5 1.401(15)
C2 C3 1.365(18)	C27 Rh1 1.950(11)
C3 C4 1.387(18)	C28 C33 1.355(18)
C4 C5 1.370(15)	C28 C29 1.391(18)
C5 N1 1.360(13)	C28 N6 1.492(16)
C5 N2 1.389(14)	C29 C30 1.43(3)
C6 N2 1.490(14)	C29 C34 1.46(2)
C6 C7 1.541(5)	C30 C31 1.34(3)
C7 C8 1.540(5)	C31 C32 1.41(2)
C8 N3 1.506(16)	C31 C35 1.52(2)
C9 N3 1.288(13)	C32 C33 1.375(18)
C9 N2 1.380(13)	C33 C36 1.525(17)
C9 Rh1 2.031(9)	C37 C38 1.300(5)
C10 C11 1.403(14)	C37 C44 1.537(5)
C10 C15 1.409(16)	C37 Rh2 2.081(14)
C10 N3 1.448(13)	C38 C39 1.541(5)
C11 C12 1.383(16)	C38 Rh2 2.119(18)
C11 C16 1.504(17)	C39 C40 1.539(5)
C12 C13 1.402(18)	C40 C41 1.537(5)
C13 C14 1.394(18)	C41 C42 1.299(5)
C13 C17 1.480(18)	C41 Rh2 2.120(16)
C14 C15 1.374(17)	C42 C43 1.534(5)
C15 C18 1.507(15)	C42 Rh2 2.091(14)
C19 N4 1.308(15)	C43 C44 1.535(5)
C19 C20 1.383(17)	N1 Rh1 2.031(8)
C20 C21 1.43(2)	N4 Rh1 2.036(9)
C21 C22 1.33(2)	Cl1 Rh1 2.412(3)
C22 C23 1.361(16)	Cl2 Rh1 2.418(2)
C23 N4 1.314(16)	Cl3 Rh2 2.396(4)
C23 N5 1.464(17)	Cl4 Rh2 2.359(5)
C24 N5 1.532(16)	C46 Cl5 1.75(3)
C24 C25 1.540(5)	C46 Cl6 1.75(4)
C25 C26 1.535(5)	C46A Cl5A 1.60(7)
C26 N6 1.510(16)	C46A Cl6A 1.72(10)
	C7A C8A 1.540(5)

Table Y. 3: Bond angles (°) for [Rh(6-Py-Mes)₂Cl₂][Rh(COD)Cl₂].

N1 C1 C2 122.8(11)	C41 C40 C39 110(2)
C1 C2 C3 119.5(12)	C42 C41 C40 127(2)
C2 C3 C4 119.4(11)	C42 C41 Rh2 70.8(9)
C5 C4 C3 118.4(11)	C40 C41 Rh2 114.3(17)
N1 C5 C4 122.3(11)	C41 C42 C43 125.2(16)
N1 C5 N2 113.4(9)	C41 C42 Rh2 73.2(10)
C4 C5 N2 124.3(10)	C43 C42 Rh2 113.1(10)
N2 C6 C7 109.1(10)	C42 C43 C44 113.8(13)

Appendix 2. Tables of Bond Distances and Angles

C8 C7 C6 107.0(14)	C43 C44 C37 113.7(14)
N3 C8 C7 106.1(12)	C1 N1 C5 117.4(9)
N3 C9 N2 117.8(8)	C1 N1 Rh1 125.9(7)
N3 C9 Rh1 131.1(8)	C5 N1 Rh1 114.8(7)
N2 C9 Rh1 110.9(7)	C9 N2 C5 119.9(8)
C11 C10 C15 120.8(10)	C9 N2 C6 123.4(9)
C11 C10 N3 120.4(11)	C5 N2 C6 116.6(9)
C15 C10 N3 118.3(9)	C9 N3 C10 125.3(8)
C12 C11 C10 118.8(11)	C9 N3 C8 125.9(11)
C12 C11 C16 119.1(10)	C10 N3 C8 108.4(10)
C10 C11 C16 122.0(11)	C19 N4 C23 115.4(10)
C11 C12 C13 121.5(11)	C19 N4 Rh1 125.5(8)
C14 C13 C12 117.5(12)	C23 N4 Rh1 117.7(8)
C14 C13 C17 122.2(14)	C27 N5 C23 117.6(11)
C12 C13 C17 120.2(12)	C27 N5 C24 125.9(13)
C15 C14 C13 123.2(13)	C23 N5 C24 116.3(11)
C14 C15 C10 117.8(11)	C27 N6 C28 124.1(10)
C14 C15 C18 120.4(12)	C27 N6 C26 128.2(12)
C10 C15 C18 121.9(11)	C28 N6 C26 107.6(11)
N4 C19 C20 123.8(13)	C27 Rh1 C9 96.4(4)
C19 C20 C21 116.4(14)	C27 Rh1 N1 102.8(4)
C22 C21 C20 120.7(14)	C9 Rh1 N1 80.4(4)
C21 C22 C23 115.4(15)	C27 Rh1 N4 80.5(5)
N4 C23 C22 128.3(14)	C9 Rh1 N4 102.6(4)
N4 C23 N5 110.5(10)	N1 Rh1 N4 175.4(3)
C22 C23 N5 121.3(14)	C27 Rh1 Cl1 174.3(4)
N5 C24 C25 111.1(13)	C9 Rh1 Cl1 86.3(3)
C26 C25 C24 112.6(14)	N1 Rh1 Cl1 82.6(2)
N6 C26 C25 109.3(14)	N4 Rh1 Cl1 94.0(3)
N6 C27 N5 114.5(11)	C27 Rh1 Cl2 85.8(3)
N6 C27 Rh1 132.2(9)	C9 Rh1 Cl2 175.1(3)
N5 C27 Rh1 113.2(9)	N1 Rh1 Cl2 94.9(2)
C33 C28 C29 126.5(14)	N4 Rh1 Cl2 82.1(2)
C33 C28 N6 117.6(11)	Cl1 Rh1 Cl2 91.92(9)
C29 C28 N6 115.5(13)	C37 Rh2 C42 83.5(6)
C28 C29 C30 111.5(16)	C37 Rh2 C38 36.0(2)
C28 C29 C34 123.5(16)	C42 Rh2 C38 93.1(7)
C30 C29 C34 124.9(15)	C37 Rh2 C41 95.6(7)
C31 C30 C29 124.8(15)	C42 Rh2 C41 35.9(2)
C30 C31 C32 119.4(17)	C38 Rh2 C41 83.3(7)
C30 C31 C35 118.8(18)	C37 Rh2 Cl4 89.1(5)
C32 C31 C35 122(2)	C42 Rh2 Cl4 163.0(4)
C33 C32 C31 119.0(17)	C38 Rh2 Cl4 89.8(6)
C28 C33 C32 118.5(13)	C41 Rh2 Cl4 160.9(5)
C28 C33 C36 123.1(12)	C37 Rh2 Cl3 160.8(6)
C32 C33 C36 118.4(13)	C42 Rh2 Cl3 89.6(4)
C38 C37 C44 125(2)	C38 Rh2 Cl3 163.0(6)
C38 C37 Rh2 73.5(11)	C41 Rh2 Cl3 89.1(5)
C44 C37 Rh2 112.5(12)	Cl4 Rh2 Cl3 92.47(19)
C37 C38 C39 126(2)	Cl5 C46 Cl6 112.3(16)
C37 C38 Rh2 70.4(10)	Cl5A C46A Cl6A 121(5)
C39 C38 Rh2 109.8(16)	C40 C39 C38 119(2)


Table X.1: Crystal data and structure refinement for [Rh(6-Ph-DIPP)(SMe)Cl]₂.

Identification code	kjc0902	
Empirical formula	C ₅₄ H ₇₆ Cl ₂ N ₄ O ₂ Rh ₂ S ₂	
Formula weight	1154.03	
Temperature	150(2) K	
Wavelength	0.71073 Å	
Crystal system	Monoclinic	
Space group	C2/c	
Unit cell dimensions	a = 43.1080(3) Å	a = 90°.
	b = 14.0820(4) Å	β = 97.6640(10)°.
	c = 18.2190(6) Å	γ = 90°.
Volume	10961.0(5) Å ³	
Z	8	
Density (calculated)	1.399 Mg/m ³	
Absorption coefficient	0.818 mm ⁻¹	
F(000)	4800	
Crystal size	0.10 x 0.10 x 0.06 mm ³	
Theta range for data collection	2.03 to 24.70°.	
Index ranges	-42 ≤ h ≤ 50, -16 ≤ k ≤ 15, -	
	21 ≤ l ≤ 20	
Reflections collected	28680	
Independent reflections	9317 [R(int) = 0.0679]	
Completeness to theta = 24.70°	99.7 %	
Max. and min. transmission	0.9525 and 0.9226	

Refinement method	Full-matrix least-squares on F ²
Data / restraints / parameters	9317 / 10 / 560
Goodness-of-fit on F ²	1.119
Final R indices [$I > 2\sigma(I)$]	R1 = 0.0735, wR2 = 0.1485
R indices (all data)	R1 = 0.1076, wR2 = 0.1598
Largest diff. peak and hole	1.097 and -0.733 e.Å ⁻³

Table X. 2: Bond lengths (Å) for [Rh(6-Ph-DIPP)(SMe)Cl]₂.

C1 C2 1.386(10)	C30 C31 1.500(10)
C1 C6 1.399(11)	C31 N4 1.474(9)
C1 Rh1 1.971(7)	C32 N4 1.339(9)
C2 C3 1.394(11)	C32 N3 1.358(9)
C3 C4 1.372(12)	C32 Rh2 2.011(7)
C4 C5 1.369(12)	C33 C34 1.403(11)
C5 C6 1.369(11)	C33 C38 1.423(11)
C6 N1 1.412(9)	C33 N4 1.437(9)
C7 N1 1.478(9)	C34 C35 1.407(13)
C7 C8 1.505(11)	C34 C39 1.514(12)
C8 C9 1.491(10)	C35 C36 1.370(17)
C9 N2 1.478(9)	C36 C37 1.340(17)
C10 N1 1.334(8)	C37 C38 1.390(13)
C10 N2 1.345(8)	C38 C42 1.488(13)
C10 Rh1 1.996(7)	C39 C40 1.524(12)
C11 C12 1.388(11)	C39 C41 1.539(11)
C11 C16 1.401(11)	C42 C44 1.542(11)
C11 N2 1.452(9)	C42 C43 1.557(11)
C12 C13 1.416(12)	C45 S1 1.814(8)
C12 C17 1.520(12)	C46 S2 1.815(8)
C13 C14 1.346(15)	S1 Rh2 2.3084(19)
C14 C15 1.364(15)	S1 Rh1 2.4066(19)
C15 C16 1.405(12)	S2 Rh1 2.3028(19)
C16 C20 1.513(12)	S2 Rh2 2.4177(19)
C17 C19 1.532(12)	Cl1 Rh1 2.3624(19)
C17 C18 1.550(12)	Cl2 Rh2 2.3705(19)
C20 C22 1.533(11)	Rh2 Cl2A 2.387(13)
C20 C21 1.548(11)	C47 O1 1.434(10)
C23 C24 1.395(10)	C47 C48 1.511(10)
C23 C28 1.398(11)	C48 C49 1.538(10)
C23 Rh2 1.970(7)	C49 C50 1.521(9)
C24 C25 1.390(11)	C50 O1 1.416(9)
C25 C26 1.366(12)	C51 O2 1.448(10)
C26 C27 1.388(12)	C51 C52 1.531(10)
C27 C28 1.376(11)	C52 C53 1.529(10)
C28 N3 1.434(10)	C53 C54 1.524(10)
C29 N3 1.477(9)	C54 O2 1.453(10)
C29 C30 1.494(11)	

Table X.3: Bond angles (°) for [Rh(6-Ph-DIPP)(SMe)Cl]₂.

C2 C1 C6 119.1(7)	C33 C38 C42 122.6(8)
C2 C1 Rh1 127.6(6)	C34 C39 C40 111.3(7)
C6 C1 Rh1 113.3(5)	C34 C39 C41 113.5(8)
C1 C2 C3 119.4(8)	C40 C39 C41 109.7(8)
C4 C3 C2 121.0(8)	C38 C42 C44 114.1(9)
C5 C4 C3 119.1(8)	C38 C42 C43 109.5(8)
C4 C5 C6 121.4(9)	C44 C42 C43 107.7(7)
C5 C6 C1 119.9(7)	C10 N1 C6 114.4(6)
C5 C6 N1 124.9(8)	C10 N1 C7 125.2(6)
C1 C6 N1 115.1(6)	C6 N1 C7 120.4(6)
N1 C7 C8 108.0(6)	C10 N2 C11 120.2(6)
C9 C8 C7 110.3(6)	C10 N2 C9 122.7(6)
N2 C9 C8 109.1(6)	C11 N2 C9 116.5(5)
N1 C10 N2 118.0(6)	C32 N3 C28 114.7(6)
N1 C10 Rh1 114.9(5)	C32 N3 C29 126.0(6)
N2 C10 Rh1 126.9(5)	C28 N3 C29 119.2(6)
C12 C11 C16 122.3(7)	C32 N4 C33 122.2(6)
C12 C11 N2 119.6(7)	C32 N4 C31 121.9(6)
C16 C11 N2 118.0(7)	C33 N4 C31 115.9(6)
C11 C12 C13 116.8(8)	C45 S1 Rh2 112.6(3)
C11 C12 C17 123.0(7)	C45 S1 Rh1 108.8(3)
C13 C12 C17 120.1(8)	Rh2 S1 Rh1 97.58(7)
C14 C13 C12 121.5(10)	C46 S2 Rh1 111.9(3)
C13 C14 C15 121.2(9)	C46 S2 Rh2 108.7(3)
C14 C15 C16 120.6(9)	Rh1 S2 Rh2 97.42(7)
C11 C16 C15 117.5(9)	C1 Rh1 C10 80.4(3)
C11 C16 C20 124.1(7)	C1 Rh1 S2 95.2(2)
C15 C16 C20 118.3(8)	C10 Rh1 S2 97.90(19)
C12 C17 C19 112.8(9)	C1 Rh1 Cl1 92.3(2)
C12 C17 C18 108.7(8)	C10 Rh1 Cl1 88.26(19)
C19 C17 C18 110.7(8)	S2 Rh1 Cl1 171.02(7)
C16 C20 C22 113.9(8)	C1 Rh1 S1 96.2(2)
C16 C20 C21 109.4(7)	C10 Rh1 S1 176.6(2)
C22 C20 C21 107.7(7)	S2 Rh1 S1 82.60(6)
C24 C23 C28 117.6(7)	Cl1 Rh1 S1 91.65(7)
C24 C23 Rh2 127.8(6)	C23 Rh2 C32 81.0(3)
C28 C23 Rh2 114.6(5)	C23 Rh2 S1 91.3(2)
C25 C24 C23 120.5(8)	C32 Rh2 S1 94.8(2)
C26 C25 C24 121.0(8)	C23 Rh2 Cl2 94.7(2)
C25 C26 C27 119.5(8)	C32 Rh2 Cl2 92.6(2)
C28 C27 C26 119.9(9)	S1 Rh2 Cl2 171.10(7)
C27 C28 C23 121.5(8)	C23 Rh2 Cl2A 174.2(4)
C27 C28 N3 123.7(8)	C32 Rh2 Cl2A 102.7(4)
C23 C28 N3 114.6(7)	S1 Rh2 Cl2A 92.9(3)
N3 C29 C30 109.4(6)	Cl2 Rh2 Cl2A 80.7(3)
C29 C30 C31 108.8(6)	C23 Rh2 S2 95.3(2)
N4 C31 C30 109.6(6)	C32 Rh2 S2 175.2(2)
N4 C32 N3 116.8(6)	S1 Rh2 S2 82.24(6)
N4 C32 Rh2 128.5(5)	Cl2 Rh2 S2 90.67(7)
N3 C32 Rh2 114.7(5)	Cl2A Rh2 S2 81.2(3)
C34 C33 C38 121.9(8)	O1 C47 C48 95.7(14)
C34 C33 N4 119.8(7)	C47 C48 C49 115.7(16)
C38 C33 N4 118.1(7)	C50 C49 C48 90.7(14)

Appendix 2. Tables of Bond Distances and Angles

C33 C34 C35 117.3(9)	O1 C50 C49 104.5(14)
C33 C34 C39 122.3(7)	C50 O1 C47 110.0(14)
C35 C34 C39 120.3(9)	O2 C51 C52 94.9(18)
C36 C35 C34 120.1(11)	C53 C52 C51 104.0(19)
C37 C36 C35 122.4(11)	C54 C53 C52 90(2)
C36 C37 C38 121.4(11)	O2 C54 C53 86.8(19)
C37 C38 C33 116.9(10)	C51 O2 C54 105(2)
C37 C38 C42 120.1(9)	

